UNIVERSITY OF CALIFORNIA, DAVIS

DEPARTMENT OF CIVIL AND ENVIRONMENTAL ENGINEERING

Lecture notes and hand outs

ECI 146: Water Resources Simulation

Prepared by:

Prof. Fabián A. Bombardelli

Preface

This is a basic compilation of hand outs and class notes that I have been gathering and preparing during the years of teaching of ECI 146, since 2004, at the Department of Civil and Environmental Engineering of UC Davis. When I had to prepare the notes for the course for the first time (starting from zero), I soon realized that there was not a single book including all the needed material for a course on "Water Resources Simulation" (at least, not with the perspective that I consider useful and interesting for such a course). This assertion is unfortunately true even today, in my modest opinion.

Thus, these pages assemble some portions of text from very well-known books, in addition to notes I prepared for the course. The course initially review material from basic numerical analysis in order to place the application to water resources in the right context, and in the proper understanding of the source of the different schemes. I humbly consider this approach to be not common in usual books dealing with water resources. Immediately after the explanation of each numerical technique, the course emphasizes its application to solve problems in water resources engineering, ranging from flow in pipes to the flow in open channels and transport of pollutants.

This compilation is expected to be improved in quality of presentation, content, and number of notes prepared by myself. It was put together following some requests from the students in order to have a unique repository on paper for all handouts, provided up to now in electronic form in the course website.

I will particularly thank any comment, suggestion or direct collaboration to make this a better compilation for ECI 146.

Yours truly,

Fabián A. Bombardelli, Davis, CA
January

UNIVERSITY OF CALIFORNIA, DAVIS
DEPARTMENT OF CIVIL AND ENVIRONMENTAL ENGINEERING

COURSE: WATER RESOURCES SIMULATION (ECI 146)

INSTRUCTOR: ***Fabián A. Bombardelli (fabombardelli@ucdavis.edu, bmbrdll@yahoo.com, fabianbombardelli2@gmail.com)***
OFFICE: 3105, Engineering III building
Class: Tuesdays and Thursdays-1:40 PM to 3:00 PM (Hutch 115)
Computer lab: Fridays-11:00 AM to 11:50 PM (Chem 166)
READER: ***Mr. Carlos Zuritz (Ph.D. Student)***
TEACHING ASSISTANT: ***Mr. James Kohne (M.S. Student)***

COURSE DESCRIPTION

This course focuses on the development and application of numerical simulation techniques for the analysis, design and operation of surface water systems. The course especially addresses problems associated with surface run-off, water quality in streams and ponds, and management of reservoirs. The course possesses a strong emphasis on the theory conducive to the development of simple codes to analyze different cases of practical importance.

PREREQUISITES

ECI 141, ECI 145, and ECI 142.

TEXT

There is *no* formal text that covers what we cover in the course. Hand outs and supplemental reading material will therefore be provided, compiled in a book.

SOME REFERENCES

1. Chapra, S. C., and Canale, R. P. (2006). "*Numerical Methods for Engineers.*" Fifth Edition, McGraw Hill Higher Education Series. Only some chapters from this book will be used.
2. Mays, L. (2006). "*Water Resources Engineering.*" John Wiley and Sons. Only some chapters from this book will be used.
3. Mays, L., Ed. in Chief (2001). "*Stormwater Collection Systems Design Handbook.*" McGraw-Hill.
4. Chow, V. T., Mays, L., and Maidment, D. (1998). "*Applied Hydrology.*" McGraw-Hill.
5. Linsley, R. K., and Franzini, J. B. (1979). "*Water-Resources Engineering.*" McGraw-Hill.
6. Burden, R. L., and Faires, J. D. (2004). *"Numerical Analysis."* Brooks-Cole Publishing, Eighth Edition.
7. Isaacson, E., and Keller, H. B. (1966). *"Analysis of Numerical Methods."* Dover.

8. Abbott, M. B. (1979). *"Computational Hydraulics. Elements of the Theory of Free Surface Flows."* Pitman, UK.
9. Koutitas, C. G. (1983). *"Elements of Computational Hydraulics."* Pentech Press, UK.
10. Press, W. H., Teukolsky, S. A., Vetterling, W. T., and Flannery, B. P. (2007). *"Numerical Recipes in Fortran. The art of scientific computing."* Cambridge.

OFFICE HOURS

Tuesdays and Thursdays after class

Mondays and Fridays, 12:00 to 2:00 PM. Also, e-mail me to make special appointments (fabombardelli@ucdavis.edu or bmbrdll@yahoo.com
.or fabianbombardelli2@gmail.com)

GRADING

Assignments	10%
Computer problems	20%
1 hourly in class exam	20% **(individual effort)**
1 special project	20% **(individual effort)**
Final exam (2 hours)	30% **(individual effort)**

NUMERICAL TOOLS

The codes can be developed in Fortran, Basic, C, Pascal, Matlab, or Excel (if applicable).

ASSIGNMENT, COMPUTER PROBLEM, PROJECT, AND EXAM POLICIES

The purpose of homework is to contribute significantly to the learning process. Students are strongly encouraged to develop assignments and computer problems [redacted] in teams. The total number of team members should not exceed three (3). The composition of the team can be varied from homework to homework, but the students have to turn in just *one* solution to the homework. Team members receive the same grade. Based on this, it is mandatory that the students of the team share similar loads of work. It is not necessary to report the names of the team members to the instructor in advance. Just make a cover page with the names of the members when turning in the homework solution.

Normally, each assignment should be completed in 7 to 15 days. Assignments, computer problems and projects turned in one (1) week after the deadline will be penalized with 30 points out of 100. After two (2) weeks, assignments, computer problems or projects will not be accepted.

Examination *and project* solutions must represent the efforts of *individuals* only. It is strongly recommended that the students have a copy of the graded solution before the examination. Exams will be *closed notes, closed books*, and they may include the development of code flow charts.

IMPORTANT DATES

Midterm exam (in class): Tuesday, February 17, 2009
Final exam (in class): Saturday, March 21, 2009, 3:30 PM to 5:30 PM
Review session for the midterm: Thursday, February 12, 2009 (half hour)
Review session for the final: Thursday, March 12, 2009 (entire class)

Computer Problem 1: Iterative solution of the Colebrook-White Equation and of systems of non-linear equations for the design of pipes
Assigned: 01/08/09
Due with no penalization: 01/20/09
Due with 30% penalization: 01/27/09

Computer Problem 2: Solution of the water-quality problem in a lake by finite differences
Assigned: 01/29/09
Due with no penalization: 02/10/09
Due with 30% penalization: 02/17/09

Computer Problem 3: Solution of backwater curves using the explicit and implicit methods in finite differences **(after Midterm)**
Assigned: 02/26/09
Due with no penalization: 03/05/09
Due with 30% penalization: 03/12/09

Assignment 1
Assigned: 01/20/09
Due with no penalization: 01/29/09
Due with 30% penalization: 02/05/09

Assignment 2 (after Midterm)
Assigned: 02/19/09
Due with no penalization: 02/26/09
Due with 30% penalization: 03/05/09

Project
Assigned: 01/15/09
Due with no penalization: 03/12/09
Due with 30% penalization: 03/19/09

UNIVERSITY OF CALIFORNIA, DAVIS
DEPARTMENT OF CIVIL AND ENVIRONMENTAL ENGINEERING

COURSE: WATER RESOURCES SIMULATION (ECI 146)

INSTRUCTOR: *Fabián A. Bombardelli (fabombardelli@ucdavis.edu, bmbrdll@yahoo.com, fabianbombardelli2@gmail.com)*
OFFICE: 3105, Engineering III building
Class: Tuesdays and Thursdays-1:40 PM to 3:00 PM (Hutch 115)
Computer lab: Fridays-11:00 AM to 11:50 PM (Chem 166)
READER: *Mr. Carlos Zuritz (Ph.D. Student)*
TEACHING ASSISTANT: *Mr. James Kohne (M.S. Student)*

SYLLABUS OF ECI 146, WATER RESOURCES SIMULATION

1. **Introduction.**
   1.a) Importance of water resources (01/06/09).
   1.b) Definition of simulation. Evaluation of simulation of water resources as a tool for management (01/06/09).
   1.c) Classification of modeling approximations: 0D, 1D, 2D and 3D. Examples of water bodies in California (01/06-08/09).
   1.d) The Moody diagram (01/08/09).

2. **Basic concepts on numerical techniques. Part I.**
   2.a) Heuristic classification of equations (01/08/09).
   2.b) Iterative solution of non-linear equations by the methods of Newton-Raphson, bisection, Regula-Falsi, and iteration of a point (01/13-15/09).
   2.c) Advantages and disadvantages of each method (01/15/09).
   2.d) Iterative solutions of *systems* of non-linear equations applied to the solution of flow in pipes (01/15-20/09).
   2.e) Computation of normal-flow depth (01/20/09).

3. **Basic concepts on numerical techniques. Part II.**
   3.a) Introductory ideas on the solution of ordinary differential equations by finite-difference methods. Forward, backward or centered schemes (01/22/09).
   3.b) Approximation of first and higher-order derivatives by finite differences. Explicit and implicit solutions of Ordinary Differential Equations (ODEs) (01/22/09).
   3.c) Euler and Runge-Kutta methods (01/22/09).
   3.d) Consistency, convergence and stability of numerical solutions (01/27/09).
   3.e) Notions on the finite-element method (01/27/09).
   3.f) Computations of backwater curves by finite differences (01/27-29/09).

4. **Zero-order models for water-quality simulations in water bodies.**
   4.a) Phenomena associated with pollution in water bodies (01/29/09).
   4.b) Reactor models for the simulation of the time evolution of phosphorus and nitrogen in lakes. Lake model (02/03/09).
   4.c) A simple sedimentation-resuspension model for rivers (02/03/09).

5. **Simulation of water retention in ponds and reservoirs.**
   5.a) Methods for flood-wave routing in reservoirs and rivers (02/05/09).
   5.b) Hydrologic reservoir modeling (02/05/09).
   5.c) Reservoir flood management (02/05/09).

6. **One-dimensional hydrodynamic models.**
   6.a) *Hydrologic* river routing. Muskingum method (02/10/09).
   6.b) Derivation of the one-dimensional equations of fluid motion in rivers (02/10/09).
   6.c) *Hydraulic* river routing (02/12/09).
   6.d) Kinematic wave model. Kinematic wave model for overland flow (02/12/09).
   6.e) Different numerical schemes used to solve the flow equations (02/17/09).
   6.f) Muskingum-Cunge method (02/19/09).

7. **One-dimensional models of water quality in streams.**
   7.a) Basic equations of one-dimensional advection-diffusion (dispersion) of pollutants (02/19/09).
   7.b) Transport models including reactive terms (02/19/09).
   7.c) Transport models for organic matter in streams (02/24/09).
   7.d) Transport models for suspended sediment in streams (02/24/09).
   7.e) Transport models to assess pollution in water bodies (02/24/09).
   7.f) Numerical schemes to deal with transport equations of the advection-diffusion type (02/26/09).

8. **Introduction to two- and three-dimensional, flow and water-quality models.**
   8.a) Basic concepts and models most used in practice (03/05/09).
   8.b) Description of case studies (03/05/09).
   8.c) Shallow-water equations (03/05/09).

Note: Dates for each topic are subject to change.

HAND OUT 1: Importance of water resources (Chapter 1 of our syllabus)

ECI 146: Water Resources Simulation

Classes 1-2

Hand out 1

Review of concepts

Water resources

1) Water=life. Key to the development of civilization. Fresh water is very scarce (see table in Hand out 2)

2) "Resources" has two meanings:

   a) Something we can profit from (obtain benefits for irrigation, drinking water, power generation, navigation, recreation, etc.)

   b) Something we need to care about, because it is a finite resource. Sustainability of hydraulic designs

3) Water has an economic value:

   a) Water stored in reservoirs is valuable because it can generate energy and produce money

   b) Water is very expensive in some developing countries because it is scarce

Review of concepts

simulation

It is the analysis of a phenomenon under controlled conditions. The objective of the simulation is the study of the phenomenon and the prediction of its behavior.

Types of simulation

1. Experiments
   a) Full scale
   b) Small scale
2. Analog solutions
3. Theoretical-numerical solutions

Review of concepts

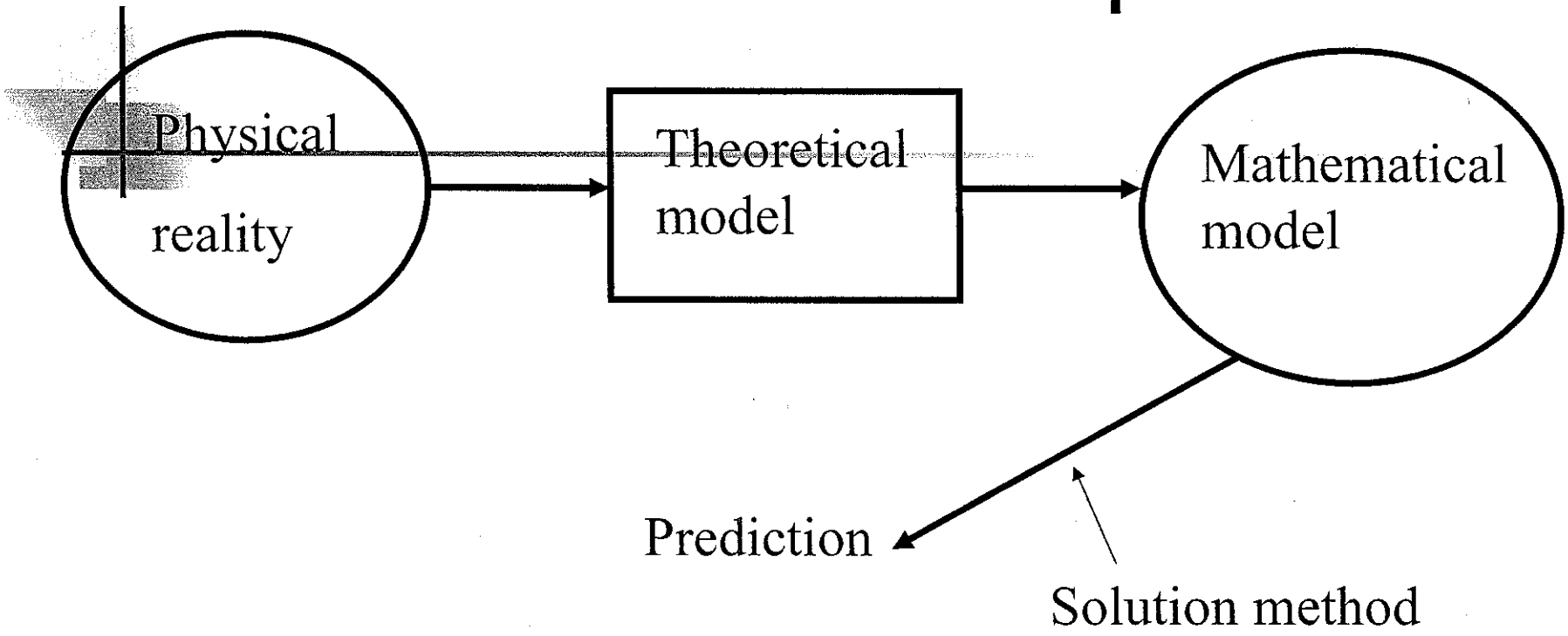

Solution method:

a) Analytical

b) Numerical

Problems with water resources

1) Rivers:
   a) Floods
   b) Release of heated discharges from power plants
   c) Dispersion of pollutants by currents and velocity gradients (water quality)
   d) Density currents in low-velocity environments
   e) Bed changes
   f) Dam removal
2) Lakes:
   a) Dispersion of pollutants by currents and velocity gradients (water quality)
   b) Stratification: water layers with different density
   c) Eutrophication: incorporation of nutrients to the water body
   d) Sediment resuspension

Problems with water resources

3) Aquifers:
   a) Dispersion of pollutants by currents and velocity gradients (water quality)
   b) Phreatic-level depletion due to pumping
4) Wetlands:
   a) Dispersion of pollutants by currents and velocity gradients (water quality)
   b) Sedimentation
   c) Sediment resuspension
5) Estuaries:
   a) Dispersion of pollutants by currents and velocity gradients (water quality)
   b) Sedimentation
   c) Sediment resuspension
6) Fjords
7) Seas and oceans

Rivers: Floods

Mississippi river

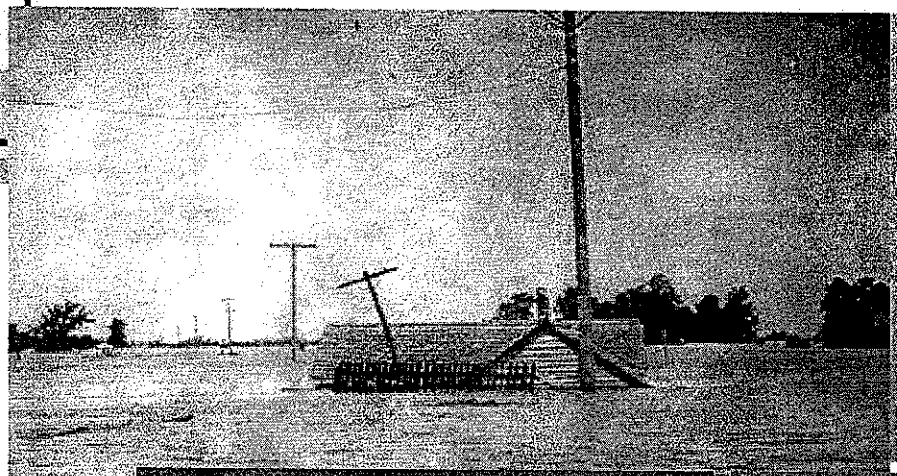

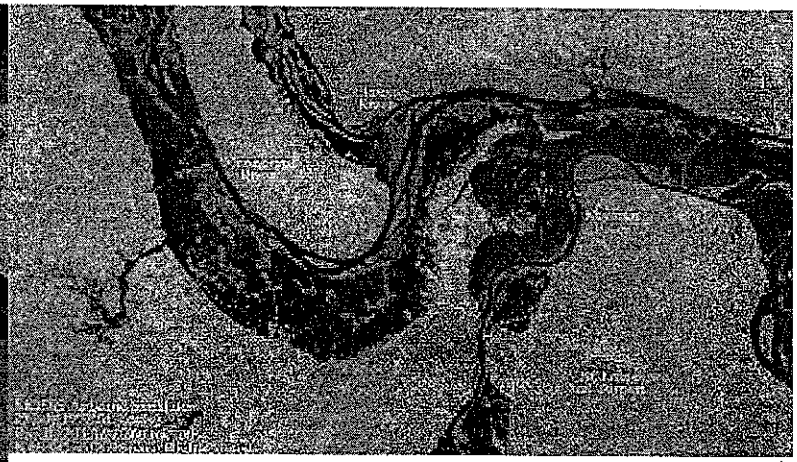

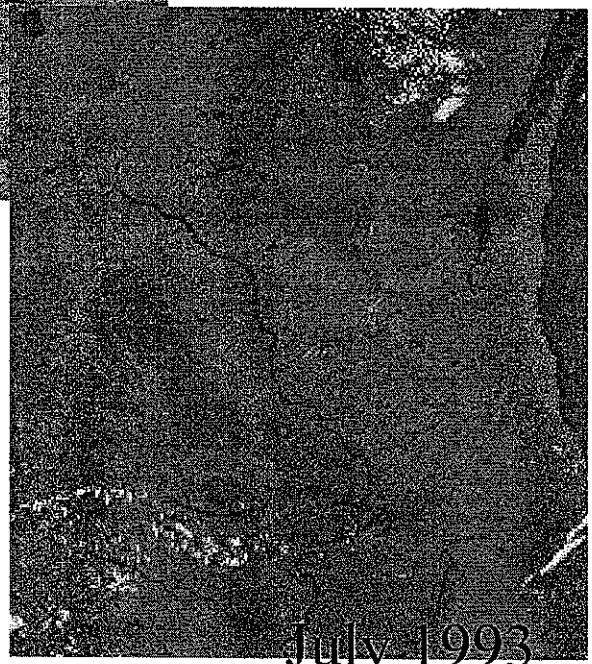

July 1992

July 1993

Rivers: Floods

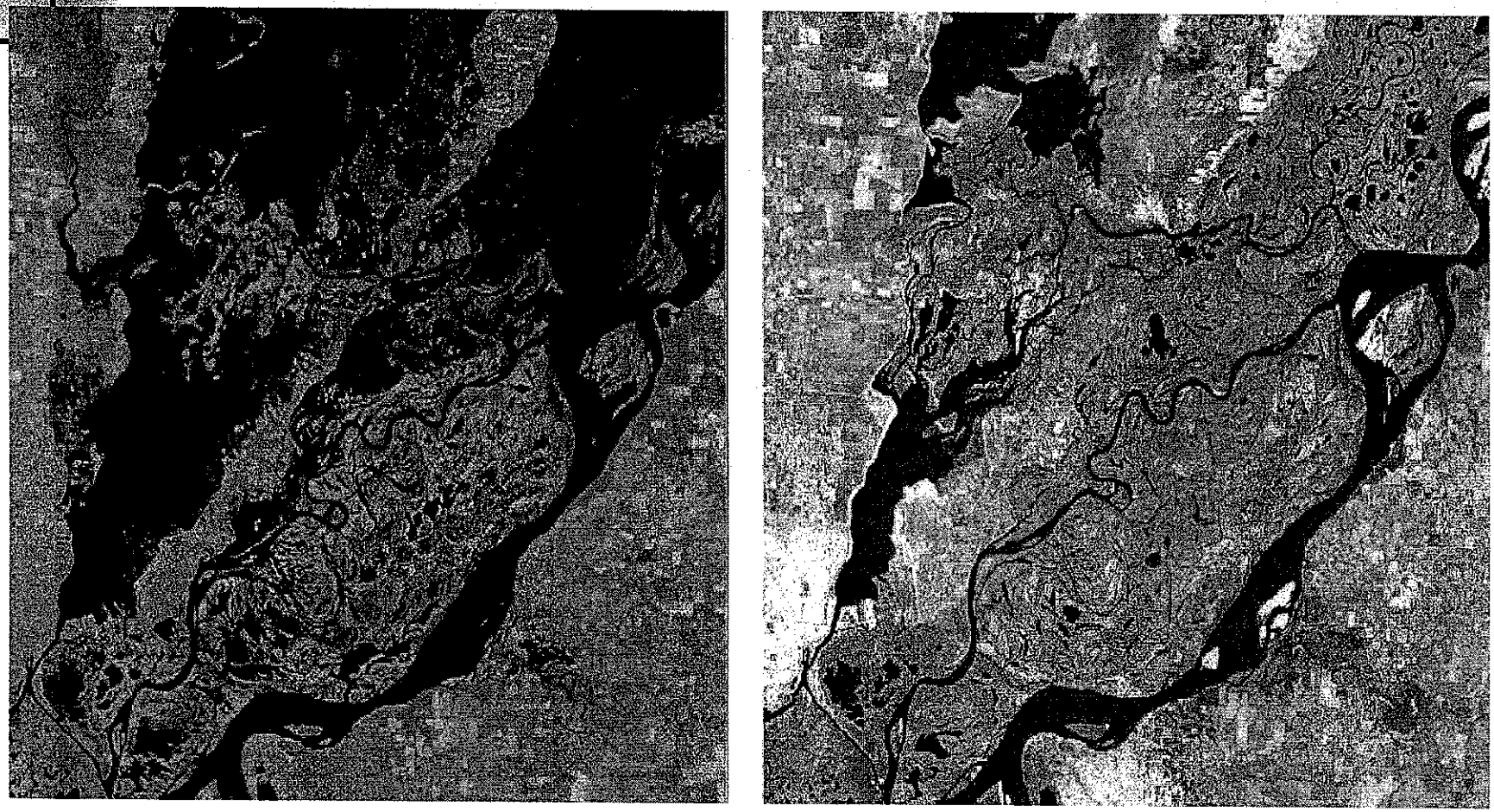

Paraná River, Argentina, South America

Rivers: Floods

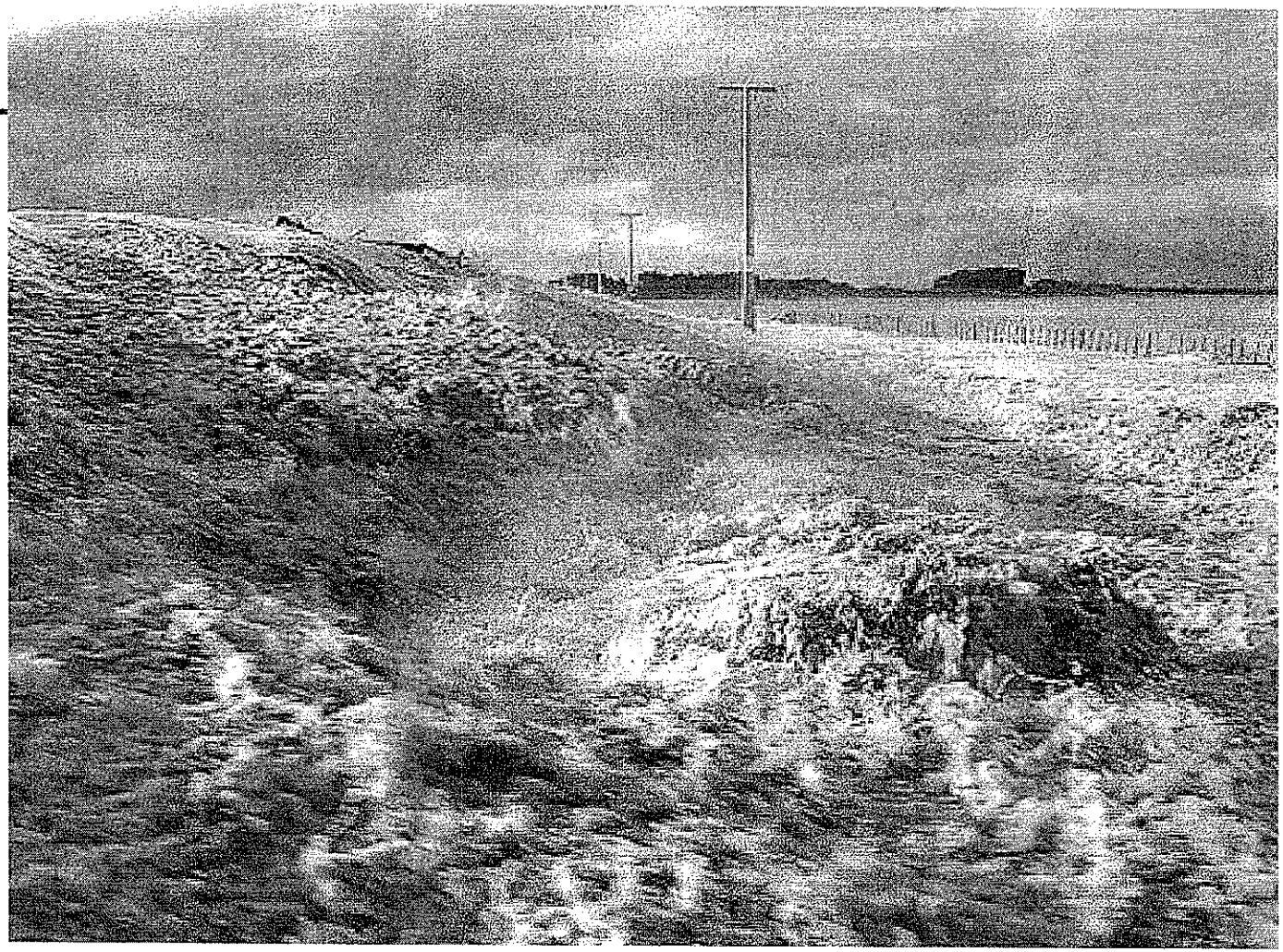

http://www.ourregion.co.nz/home.php - Manawatu, New Zealand

Bridges that work

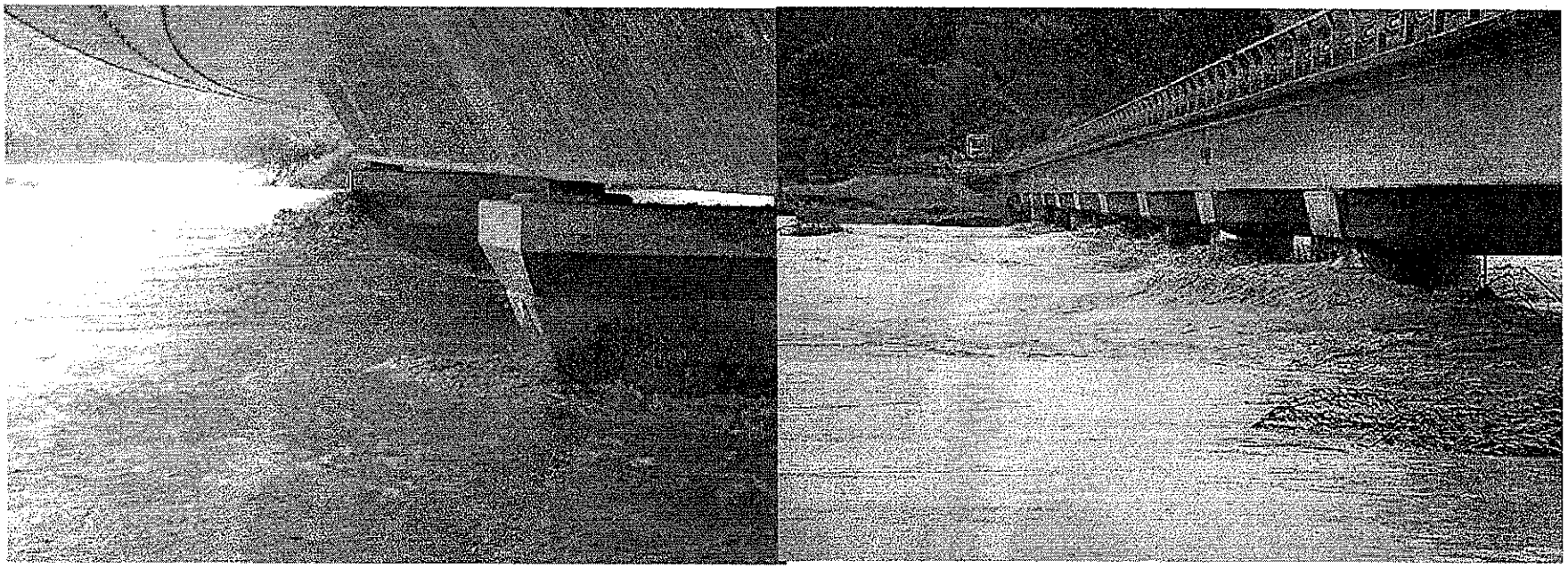

http://www.ourregion.co.nz/home.php - Source: Prof. Maidment (UT)

Bridges that don't work

Small bridge on a country road is washed away

http://www.ourregion.co.nz/home.php - Source: Prof. Maidment (UT)

Major highways in Houston during tropical storm Allison

I-10 West

I-45 South

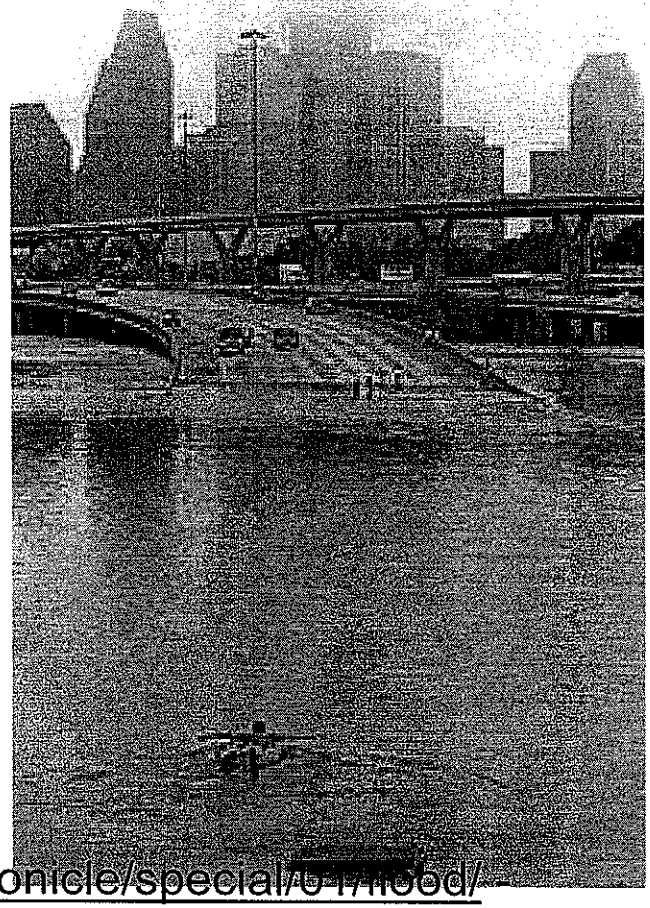

http://www.chron.com/content/chronicle/special/01/tx06d/

Source: Prof. Maidment (UT)

Kayaking on US 59, Houston (tropical storm Allison)

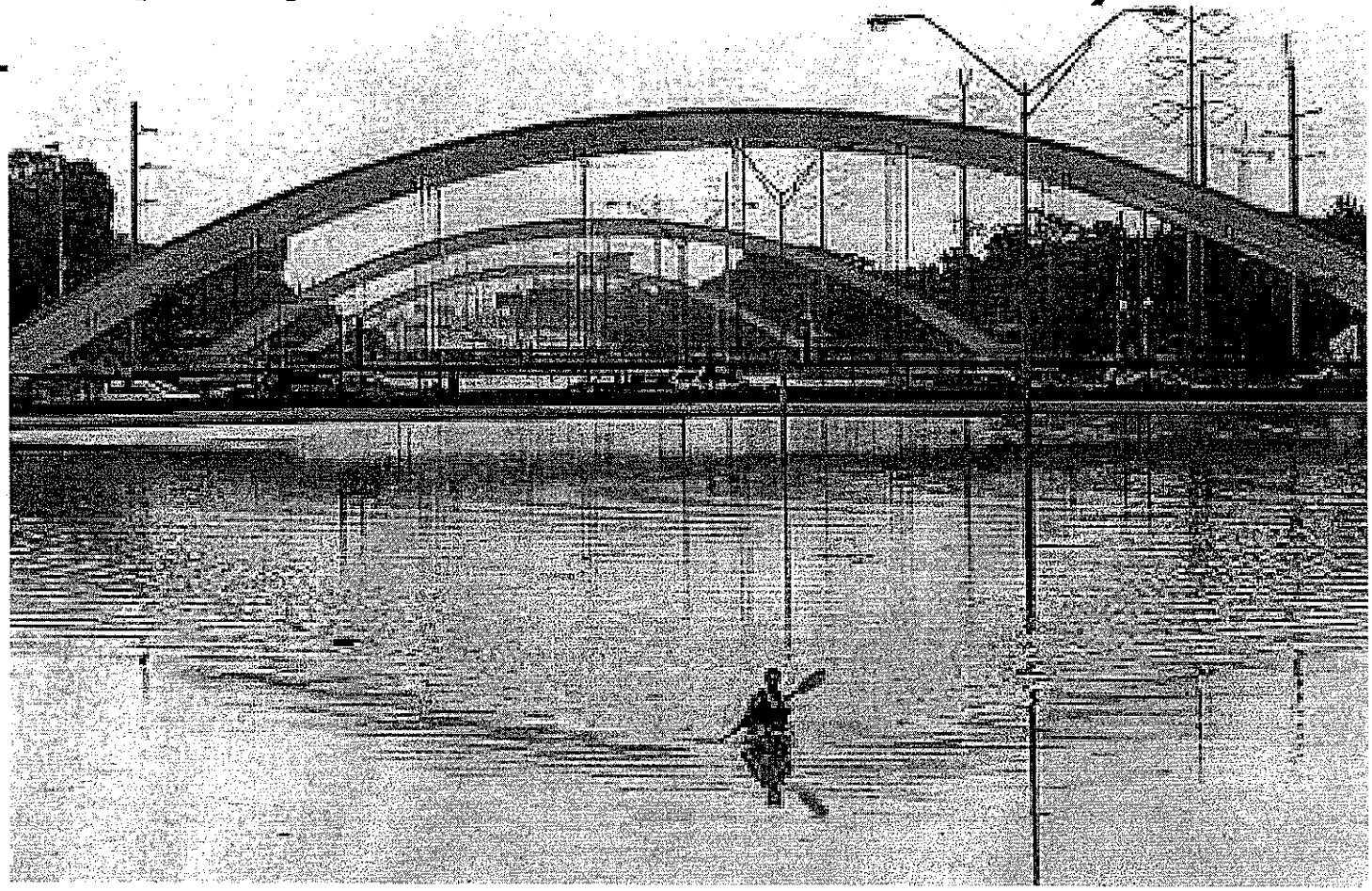

http://www.chron.com/content/chronicle/special/01/flood/ - Source: Prof. Maidment

Residential flooding in tropical storm Allison

http://www.chron.com/content/chronicle/special/01/flood/ - Source: Prof. Maidment (UT)

The human cost

Saving the wedding photos

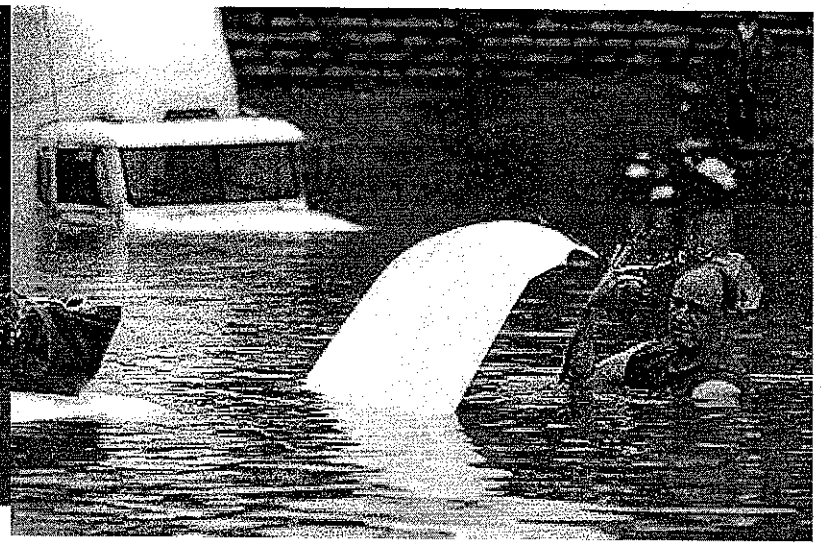

Cleaning out the car

http://www.chron.com/content/chronicle/special/01/flood/ -
Source: Prof. D. Maidment (UT)

Flood wave passes the reach in 2-3 minutes

Measures againts floods: Central Park wet pond (Austin)

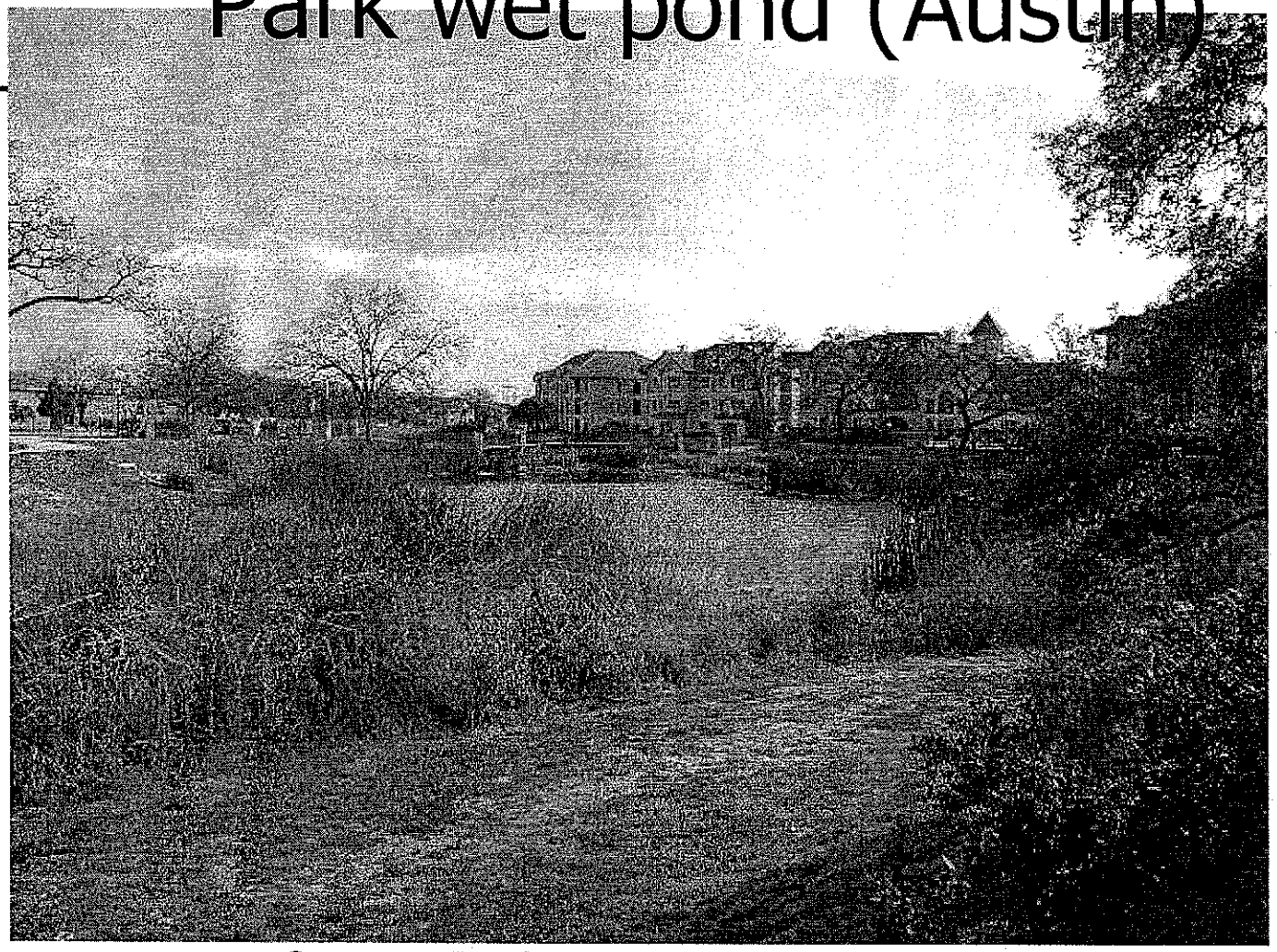

Source: Prof. D. Maidment (UT)

Extended detention basin

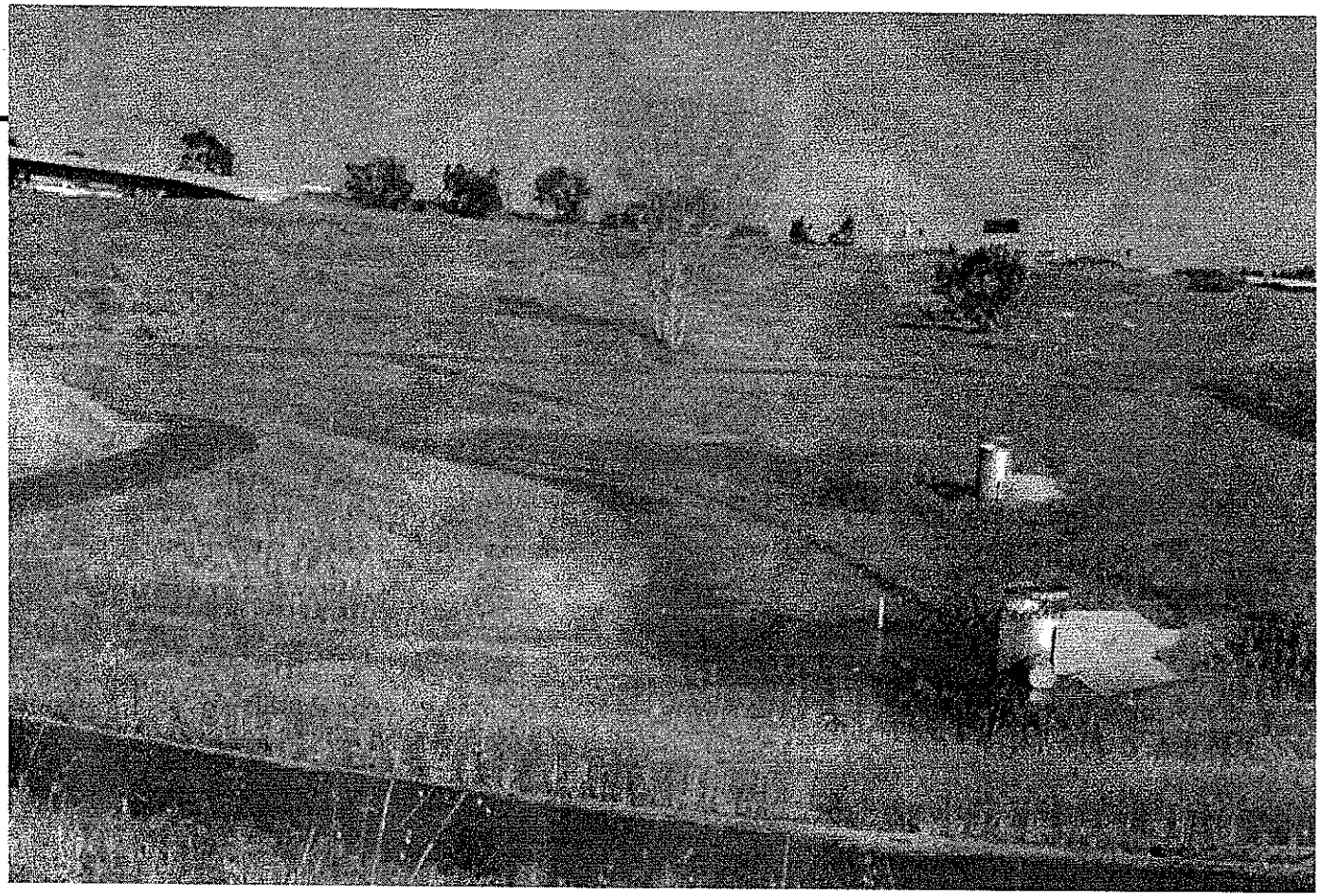

Source: Prof. D. Maidment (UT)

Rivers: Dam removal

Butte Creek, CA

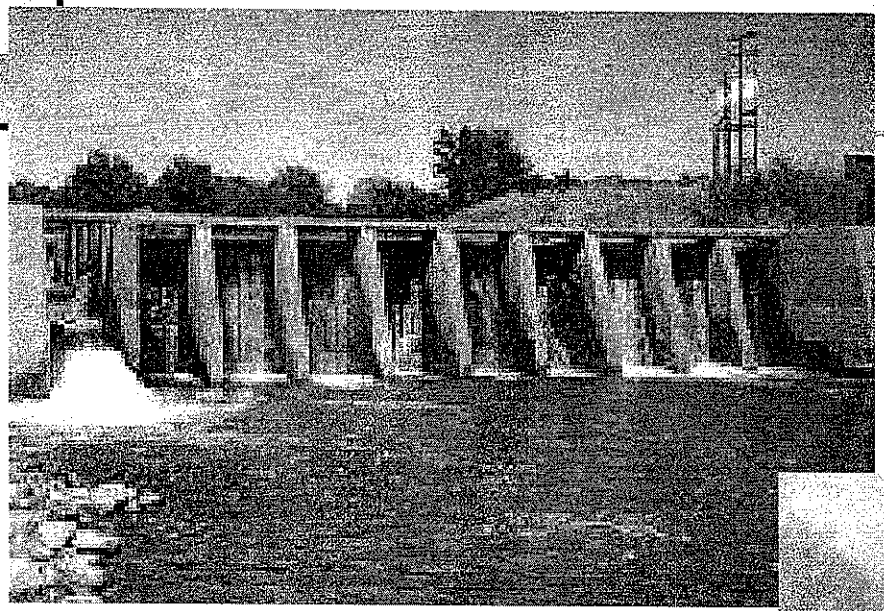

- 6 to 12 ft in height
- 100 ft in length
- Water diversion

- restored passage for the chinook salmon

Rivers: Discharge of heated water

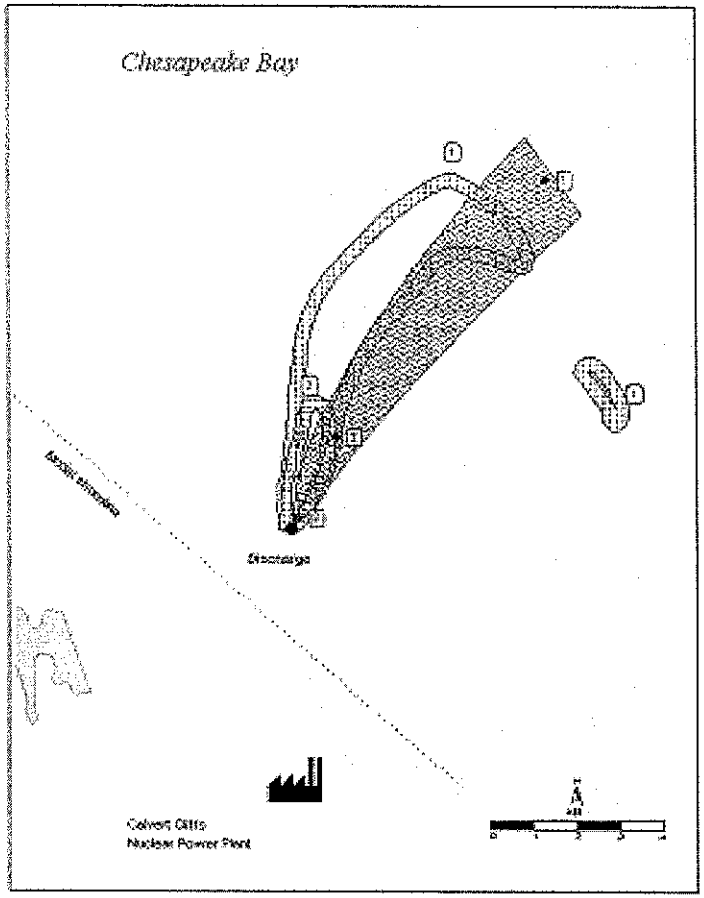

The plume at Calvert Cliffs Nuclear Power Plant during ebb tide on May 12, 1978. Blue lines are 1°C delta-T measured isotherms with a 0.2°C uncertainty band. The red region is the thermal plume predicted by CORMIX. 1°C, 2°C and 3°C delta-T values are plotted for comparison

Estuaries: density currents

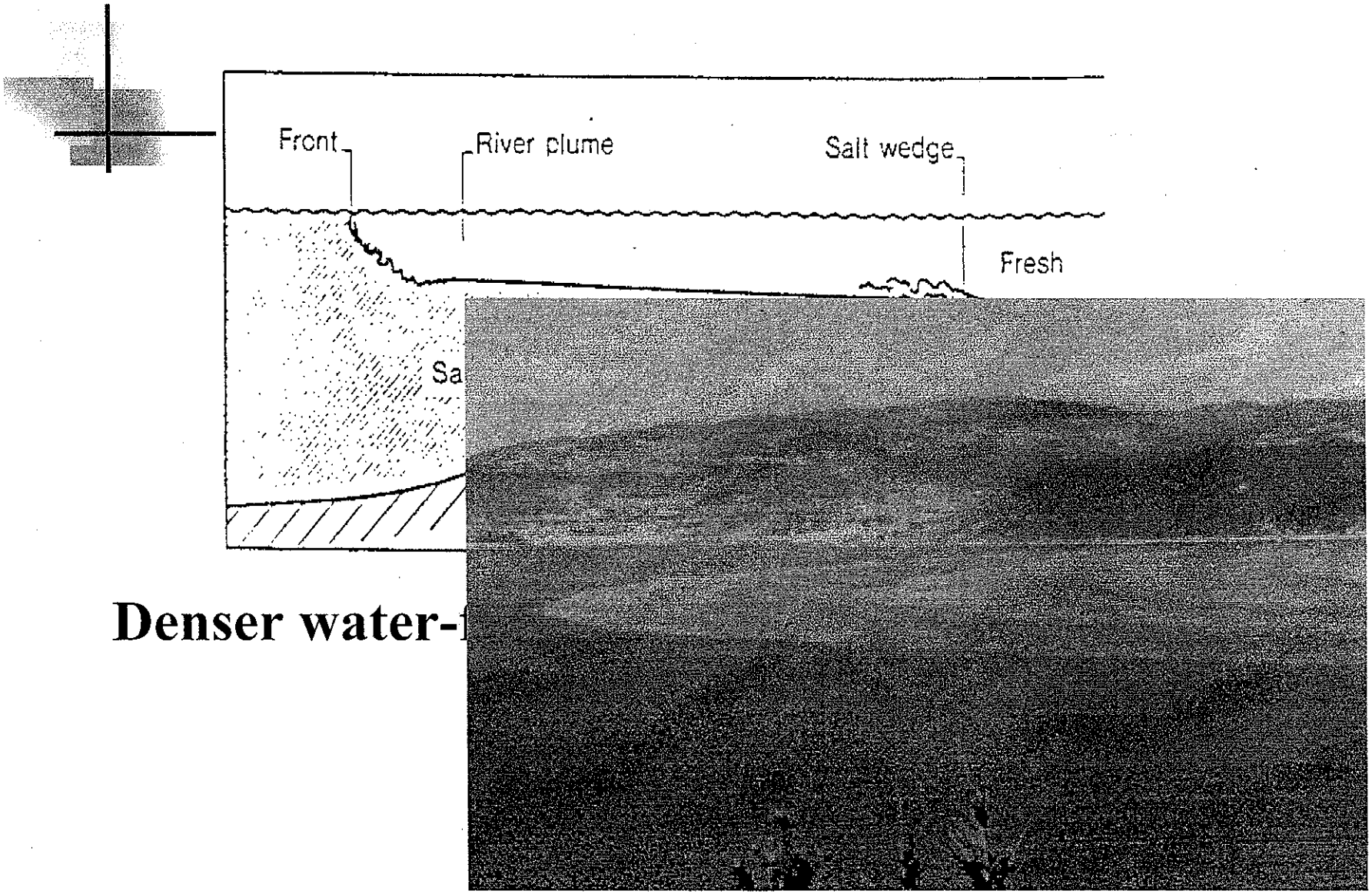

Denser water-

HAND OUT 2: Importance of water resources (Chapter 1 of our syllabus)
Source: Mays, L. (2006). *"Water resources engineering"* John Wiley and Sons

Chapter 1

Introduction

1.1 BACKGROUND

Water resources engineering (and management) as defined for the purposes of this book includes engineering for both *water supply management* and *water excess management* (see Figure 1.1.1). This book does not cover the *water quality management (or environmental restoration)* aspect of water resources engineering. The two major processes that are engineered are the *hydrologic processes* and the *hydraulic processes*. The common threads that relate to the explanation of the hydrologic and hydraulic processes are the fundamentals of fluid mechanics. The hydraulic processes include three types of flow: pipe (pressurized) flow, open-channel flow, and groundwater flow.

The broad topic of *water resources* includes areas of study in the biological sciences, engineering, physical sciences, and social sciences, as illustrated in Figure 1.1.1. The areas in biological sciences range from ecology to zoology, those in the physical sciences range from chemistry to meteorology to physics, and those in the social sciences range from economics to sociology. Water resources engineering as used in this book focuses on the engineering aspects of hydrology and hydraulics for water supply management and water excess management.

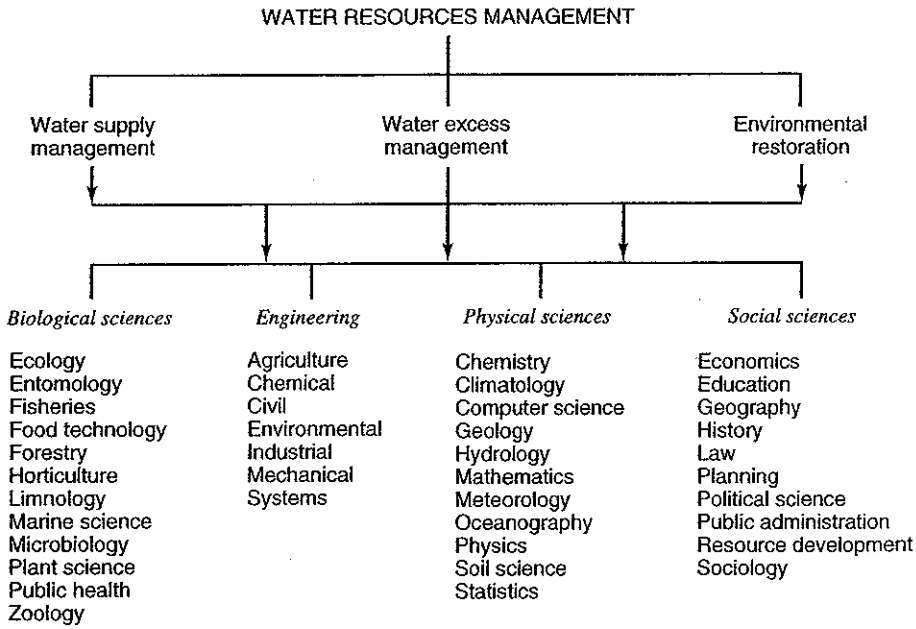

Figure 1.1.1 Ingredients of water resources management (from Mays (1996)).

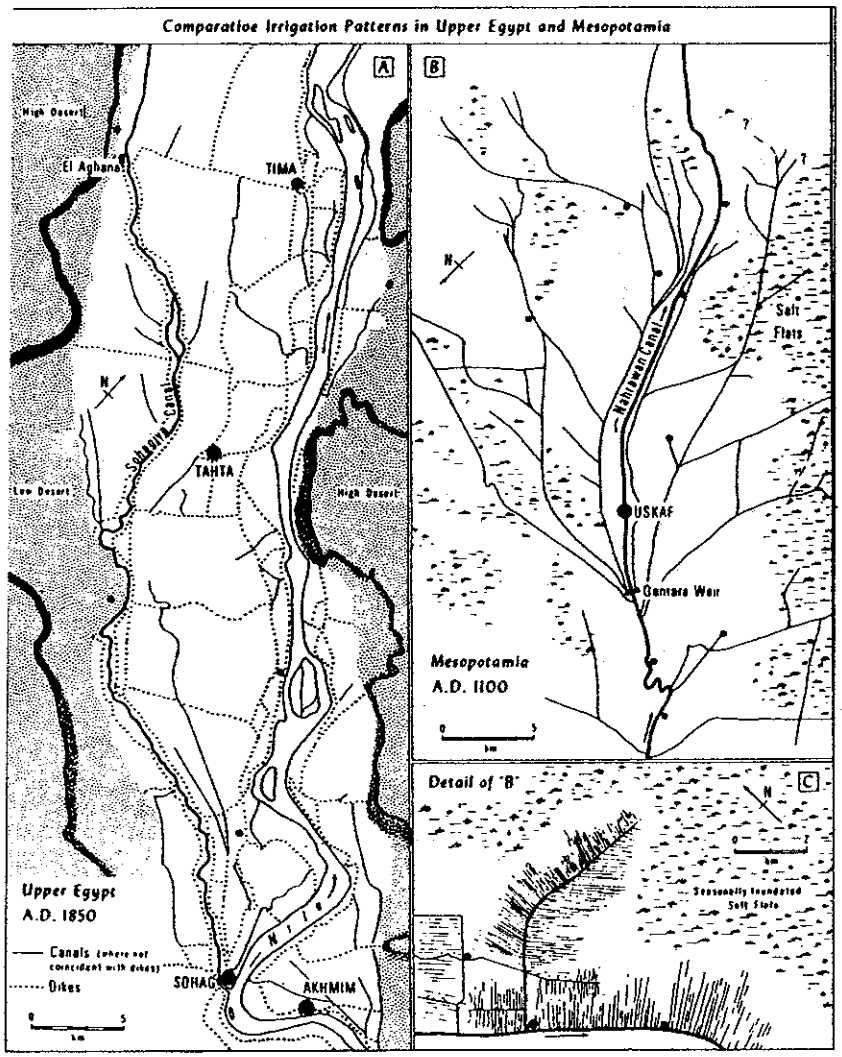

Figure 1.1.2 Comparative irrigation networks in Upper Egypt and Mesopotamia. (*a*) Example of linear, basin irrigation in Sohag province, ca. AD 1850; (*b*) Example of radial canalization system in the lower Nasharawan region southeast of Baghdad, Abbasid (A.D. 883–1150). (Modified from R. M. Adams (1965), Fig. 9. Same scale as Egyptian counterpart). (*c*) Detail of field canal layout in *b*. (Simplified from R. M. Adams (1965), Fig. 10. Figure as presented in Butzer (1976)).

Water resources engineering not only includes the analysis and synthesis of various water problems through the use of the many analytical tools in hydrologic engineering and hydraulic engineering but also extends to the design aspects.

Water resources engineering has evolved over the past 9,000 to 10,000 years as humans have developed the knowledge and techniques for building hydraulic structures to convey and store water. Early examples include irrigation networks built by the Egyptians and Mesopotamians (see Figure 1.1.2) and by the Hohokam in North America (see Figure 1.1.3). The world's oldest large dam was the Sadd-el-kafara dam built in Egypt between 2950 and 2690 B.C. The oldest known pressurized water distribution (approximately 2000 B.C.) was in the ancient city of Knossos on Crete (see Mays, 1999, 2000, for further details). There are many examples of ancient water systems throughout the world.

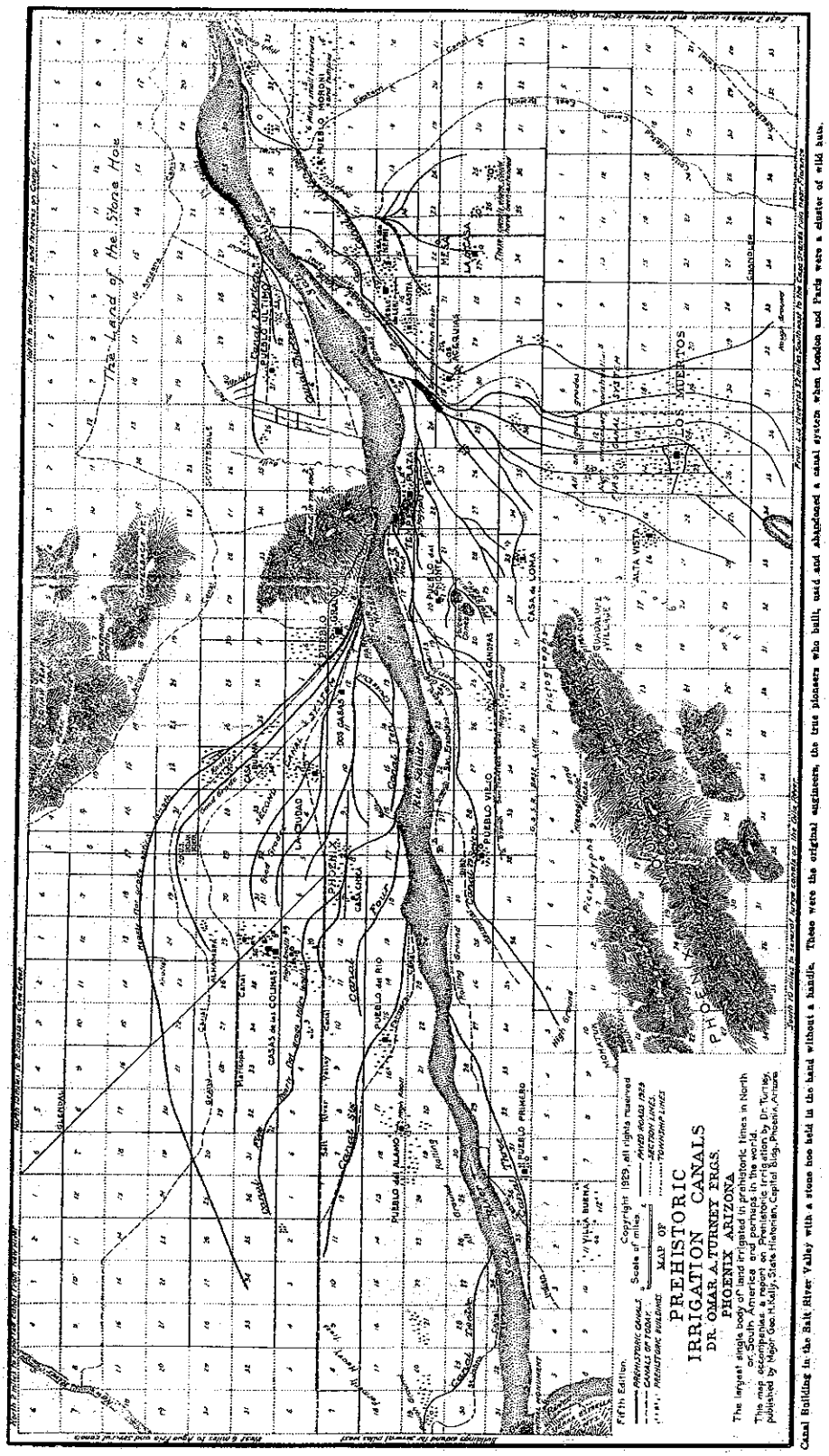

Figure 1.1.3 Canal building in the Salt River Valley with a stone hoe held in the hand without a handle. These were the original engineers, the true pioneers who built, used, and abandoned a canal system when London and Paris were clusters of wild huts (from Turney (1922)). (Courtesy of Salt River Project, Phoenix, Arizona.)

1.2 THE WORLD'S FRESHWATER RESOURCES

Among today's most acute and complex problems are water problems related to the rational use and protection of water resources (see Gleick, 1993). Associated with water problems is the need to supply humankind with adequate clean freshwater. Data collected on global water resources by Soviet scientists are listed in Table 1.2.1. These obviously are only approximations and should not be considered as accurate (Shiklomanov, 1993). Table 1.2.2 presents the dynamics of actual water availability in different regions of the world. Table 1.2.3 presents the dynamics of water use in the world by human activity. Table 1.2.4 presents the annual runoff and water consumption by continents and by physiographic and economic regions of the world.

Table 1.2.1 Water Reserves on the Earth

	Distribution area (10^3 km^2)	Volume (10^3 km^3)	Layer (m)	Percentage of global reserves	
				Of total water	Of freshwater
World ocean	361,300	1,338,000	3,700	96.5	—
Groundwater	134,800	23,400	174	1.7	—
Freshwater		10,530	78	0.76	30.1
Soil moisture		16.5	0.2	0.001	0.05
Glaciers and permanent snow cover	16,227	24,064	1,463	1.74	68.7
Antarctic	13,980	21,600	1,546	1.56	61.7
Greenland	1,802	2,340	1,298	0.17	6.68
Arctic islands	226	83.5	369	0.006	0.24
Mountainous regions	224	40.6	181	0.003	0.12
Ground ice/permafrost	21,000	300	14	0.022	0.86
Water reserves in lakes	2,058.7	176.4	85.7	0.013	—
Fresh	1,236.4	91	73.6	0.007	0.26
Saline	822.3	85.4	103.8	0.006	—
Swamp water	2,682.6	11.47	4.28	0.0008	0.03
River flows	148,800	2.12	0.014	0.0002	0.006
Biological water	510,000	1.12	0.002	0.0001	0.003
Atmospheric water	510,000	12.9	0.025	0.001	0.04
Total water reserves	510,000	1,385,984	2,718	100	—
Total freshwater reserves	148,800	35,029	235	2.53	100

Source: Shiklomanov (1993).

Table 1.2.2 Dynamics of Actual Water Availability in Different Regions of the World

Continent and region	Area (10^6 km^2)	Actual water availability (10^3 m^3 per year per capita)				
		1950	1960	1970	1980	2000
Europe	10.28	5.9	5.4	4.9	4.6	4.1
North	1.32	39.2	36.5	33.9	32.7	30.9
Central	1.86	3.0	2.8	2.6	2.4	2.3
South	1.76	3.8	3.5	3.1	2.8	2.5
European USSR (North)	1.82	33.8	29.2	26.3	24.1	20.9
European USSR (South)	3.52	4.4	4	3.6	3.2	2.4
North America	24.16	37.2	30.2	25.2	21.3	17.5
Canada and Alaska	13.67	384	294	246	219	189
United States	7.83	10.6	8.8	7.6	6.8	5.6
Central America	2.67	22.7	17.2	12.5	9.4	7.1

Table 1.2.2 Dynamics of Actual Water Availability in Different Regions of the World *(continued)*

Continent and region	Area (10^6 km^2)	Actual water availability (10^3 m^3 per year per capita)				
		1950	1960	1970	1980	2000
Africa	30.10	20.6	16.5	12.7	9.4	5.1
North	8.78	2.3	1.6	1.1	0.69	0.21
South	5.11	12.2	10.3	7.6	5.7	3.0
East	5.17	15.0	12	9.2	6.9	3.7
West	6.96	20.5	16.2	12.4	9.2	4.9
Central	4.08	92.7	79.5	59.1	46.0	25.4
Asia	44.56	9.6	7.9	6.1	5.1	3.3
North China and Mongolia	9.14	3.8	3.0	2.3	1.9	1.2
South	4.49	4.1	3.4	2.5	2.1	1.1
West	6.82	6.3	4.2	3.3	2.3	1.3
South-east	7.17	13.2	11.1	8.6	7.1	4.9
Central Asia and Kazakhstan	2.43	7.5	5.5	3.3	2.0	0.7
Siberia and Far East	14.32	124	112	102	96.2	95.3
Trans-Caucasus	0.19	8.8	6.9	5.4	4.5	3.0
South America	17.85	105	80.2	61.7	48.8	28.3
North	2.55	179	128	94.8	72.9	37.4
Brazil	8.51	115	86	64.5	50.3	32.2
West	2.33	97.9	77.1	58.6	45.8	25.7
Central	4.46	34	27	23.9	20.5	10.4
Australia and Oceania	8.59	112	91.3	74.6	64.0	50.0
Australia	7.62	35.7	28.4	23	19.8	15.0
Oceania	1.34	161	132	108	92.4	73.5

Source: Shiklomanov (1993).

Table 1.2.3 Dynamics of Water Use in the World by Human Activity

Water users[a]	1900 (km^3 per year)	1940 (km^3 per year)	1950 (km^3 per year)	1960 (km^3 per year)	1970 (km^3 per year)	1975 (km^3 per year)	1980		1990[b]		2000[b]	
							(km^3 per year)	(%)	(km^3 per year)	(%)	(km^3 per year)	(%)
Agriculture												
Withdrawal	525	893	1,130	1,550	1,850	2,050	2,290	69.0	2,680	64.9	3,250	62.6
Consumption	409	679	859	1,180	1,400	1,570	1,730	88.7	2,050	86.9	2,500	86.2
Industry												
Withdrawal	37.2	124	178	330	540	612	710	21.4	973	23.6	1,280	24.7
Consumption	3.5	9.7	14.5	24.9	38.0	47.2	61.9	3.2	88.5	3.8	117	4.0
Municipal supply												
Withdrawal	16.1	36.3	52.0	82.0	130	161	200	6.0	300	7.3	441	8.5
Consumption	4.0	9.0	14	20.3	29.2	34.3	41.1	2.1	52.4	2.2	64.5	2.2
Reservoirs												
Withdrawal	0.3	3.7	6.5	23.0	66.0	103	120	3.6	170	4.1	220	4.2
Consumption	0.3	3.7	6.5	23.0	66.0	103	120	6.2	170	7.2	220	7.6
Total (rounded off)												
Withdrawal	579	1,060	1,360	1,990	2,590	2,930	3,320	100	4,130	100	5,190	100
Consumption	417	701	894	1,250	1,540	1,760	1,950	100	2,360	100	2,900	100

[a] Total water withdrawal is shown in the first line of each category, consumptive use (irretrievable water loss) is shown in the second line.
[b] Estimated.

Source: Shiklomanov (1993).

Table 1.2.4 Annual Runoff and Water Consumption by Continents and by Physiographic and Economic Regions of the World

Continent and region	Mean annual runoff (mm)	Mean annual runoff (km^3 per year)	Aridity index (R/LP)	Water consumption (km^3 per year) 1980 Total	1980 Irretrievable	1990 Total	1990 Irretrievable	2000 Total	2000 Irretrievable
Europe	310	3,210	—	435	127	555	178	673	222
North	480	737	0.6	9.9	1.6	12	2.0	13	2.3
Central	380	705	0.7	141	22	176	28	205	33
South	320	564	1.4	132	51	184	64	226	73
European USSR (North)	330	601	0.7	18	2.1	24	3.4	29	5.2
European USSR (South)	150	525	1.5	134	50	159	81	200	108
North America	340	8,200	—	663	224	724	255	796	302
Canada and Alaska	390	5,300	0.8	41	8	57	11	97	15
United States	220	1,700	1.5	527	155	546	171	531	194
Central America	450	1,200	1.2	95	61	120	73	168	93
Africa	150	4,570	—	168	129	232	165	317	211
North	17	154	8.1	100	79	125	97	150	112
South	68	349	2.5	23	16	36	20	63	34
East	160	809	2.2	23	18	32	23	45	28
West	190	1,350	2.5	19	14	33	23	51	34
Central	470	1,909	0.8	2.8	1.3	4.8	2.1	8.4	3.4
Asia	330	14,410	—	1,910	1,380	2,440	1,660	3,140	2,020
North China and Mongolia	160	1,470	2.2	395	270	527	314	677	360
South	490	2,200	1.3	668	518	857	638	1,200	865
West	72	490	2.7	192	147	220	165	262	190
South-east	1,090	6,650	0.7	461	337	609	399	741	435
Central Asia and Kazakhstan	70	170	3.1	135	87	157	109	174	128
Siberia and Far East	230	3,350	0.9	34	11	40	17	49	25
Trans-Caucasus	410	77	1.2	24	14	26	18	33	21
South America	660	11,760	—	111	71	150	86	216	116
Northern area	1,230	3,126	0.6	15	11	23	16	33	20
Brazil	720	6,148	0.7	23	10	33	14	48	21
West	740	1,714	1.3	40	30	45	32	64	44
Central	170	812	2.0	33	20	48	24	70	31
Australia and Oceania	270	2,390		29	15	38	17	47	22
Australia	39	301	4.0	27	13	34	16	42	20
Oceania	1,560	2,090	0.6	2.4	1.5	3.3	1.8	4.5	2.3
Land area (rounded off)	—	44,500	—	3,320	1,450	4,130	2,360	5,190	2,900

Source: Shiklomanov (1993).

1.3 WATER USE IN THE UNITED STATES

Dziegielewski et al. (1996) define *water use* from a hydrologic perspective as all water flows that are a result of human intervention in the hydrologic cycle. The National Water Use Information Program (NWUI Program), conducted by the United States Geological Survey (USGS), used this perspective on water use in establishing a national system of water-use accounting. This accounting system distinguishes the following water-use flows: (1) water withdrawals for off-stream purposes, (2) water deliveries at point of use or quantities released after use, (3) consumptive use, (4) conveyance loss, (5) reclaimed wastewater, (6) return flow, and (7) in-stream flow (Solley et al., 1993). The relationships among these human-made flows at various points of measurement are illustrated in Figure 1.3.1. Figure 1.3.2 illustrates the estimated water use by tracking the sources,

HAND OUT 3: Algorithm for the Computer Problem 1

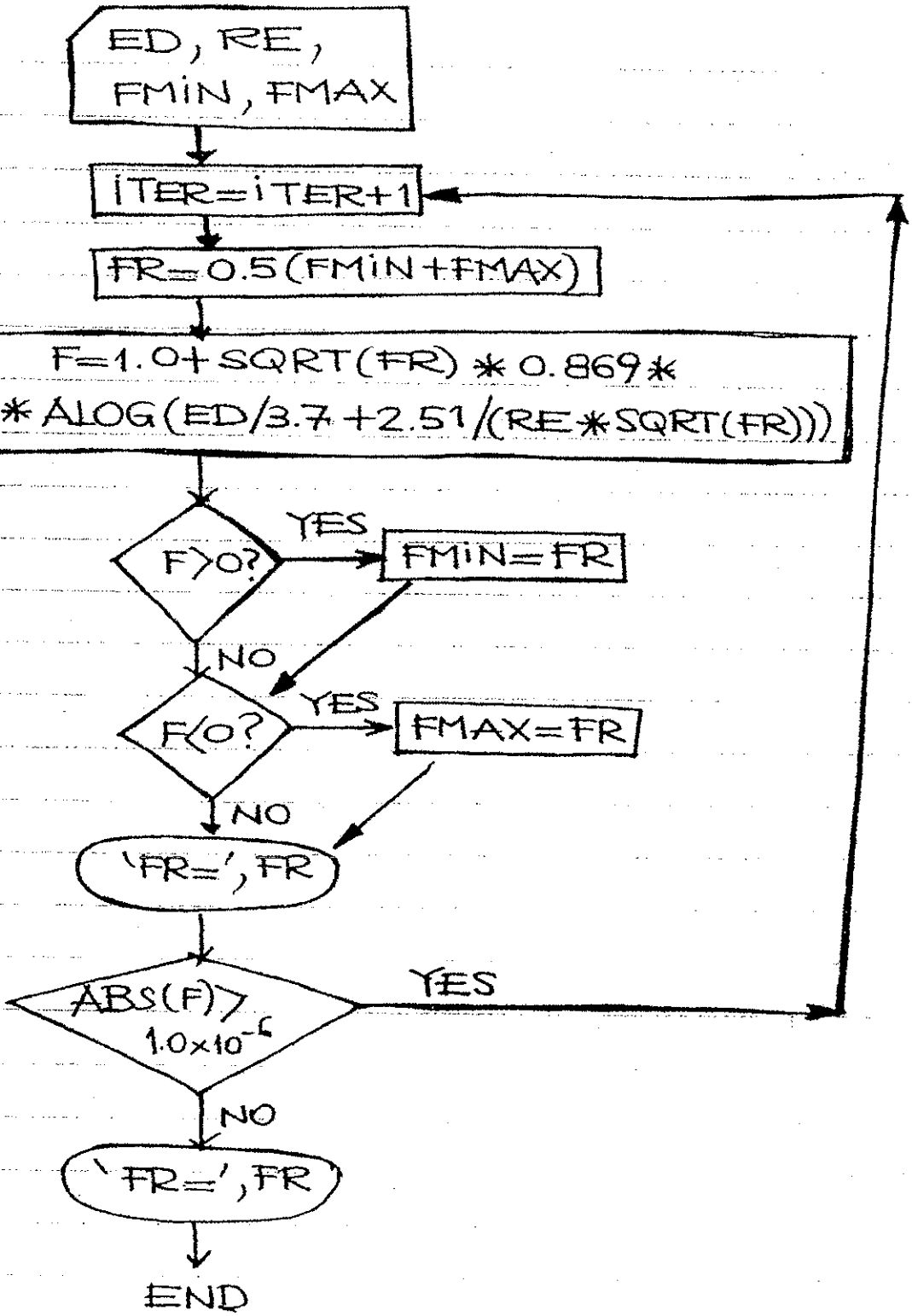
ED, RE,
FMIN, FMAX
ITER=ITER+1
FR=0.5(FMIN+FMAX)
F=1.0+SQRT(FR)*0.869*
*ALOG(ED/3.7+2.51/(RE*SQRT(FR)))
F>0?
YES
FMIN=FR
NO
F<0?
YES
FMAX=FR
NO
'FR=', FR
ABS(F)
1.0x10^-6
YES
NO
'FR=', FR
END

HAND OUT 4: Classification of modeling approximations (Chapter 1 of our syllabus)

Examples of modeling:

1) ESTUARIES:

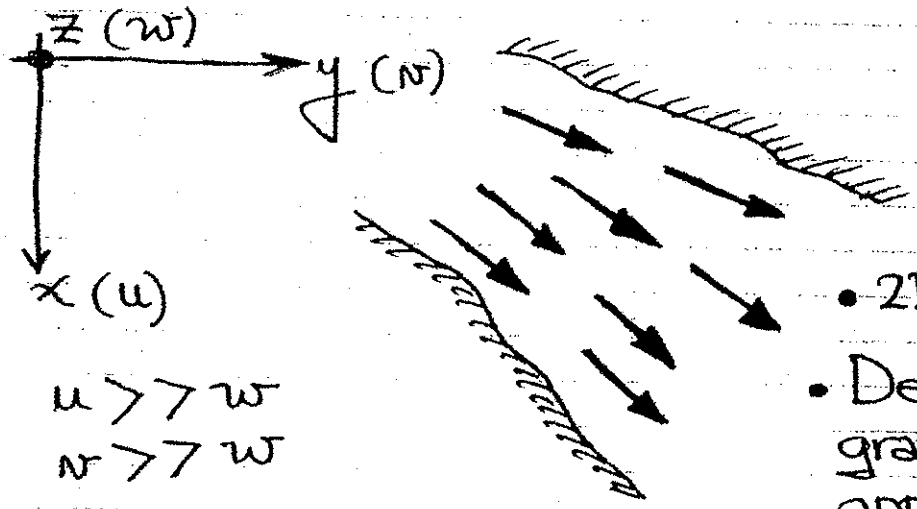

$u >> w$
$v >> w$

- 2D approx.
- Depth-integrated approaches

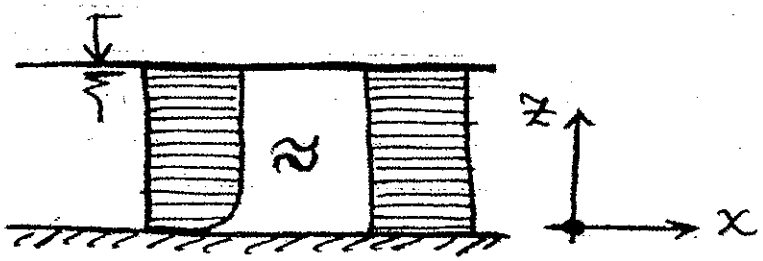

2) FJORDS:

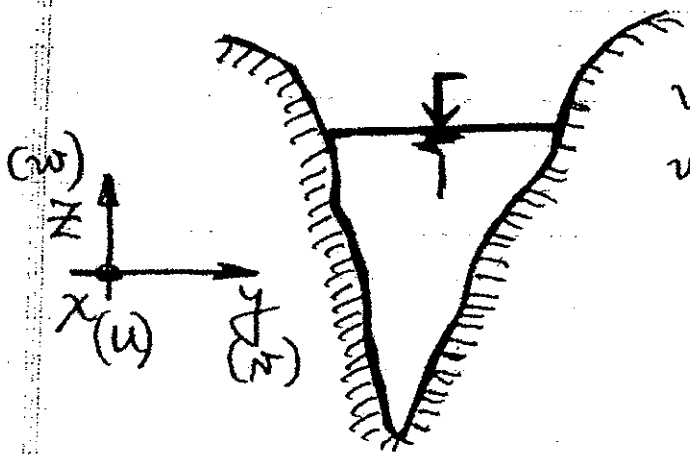

$w >> v$
$u >> v$

- 2D approx.
- Transversally integrated

3) RIVERS:

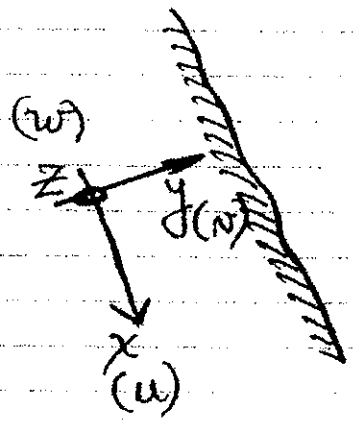

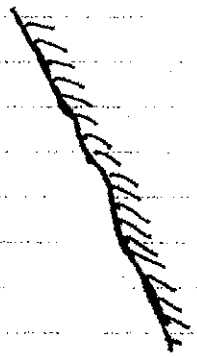

u ⊥ N

u ⊥ w

- 1D approx

HAND OUT 5: The Moody diagram (Chapter 1 of our syllabus)

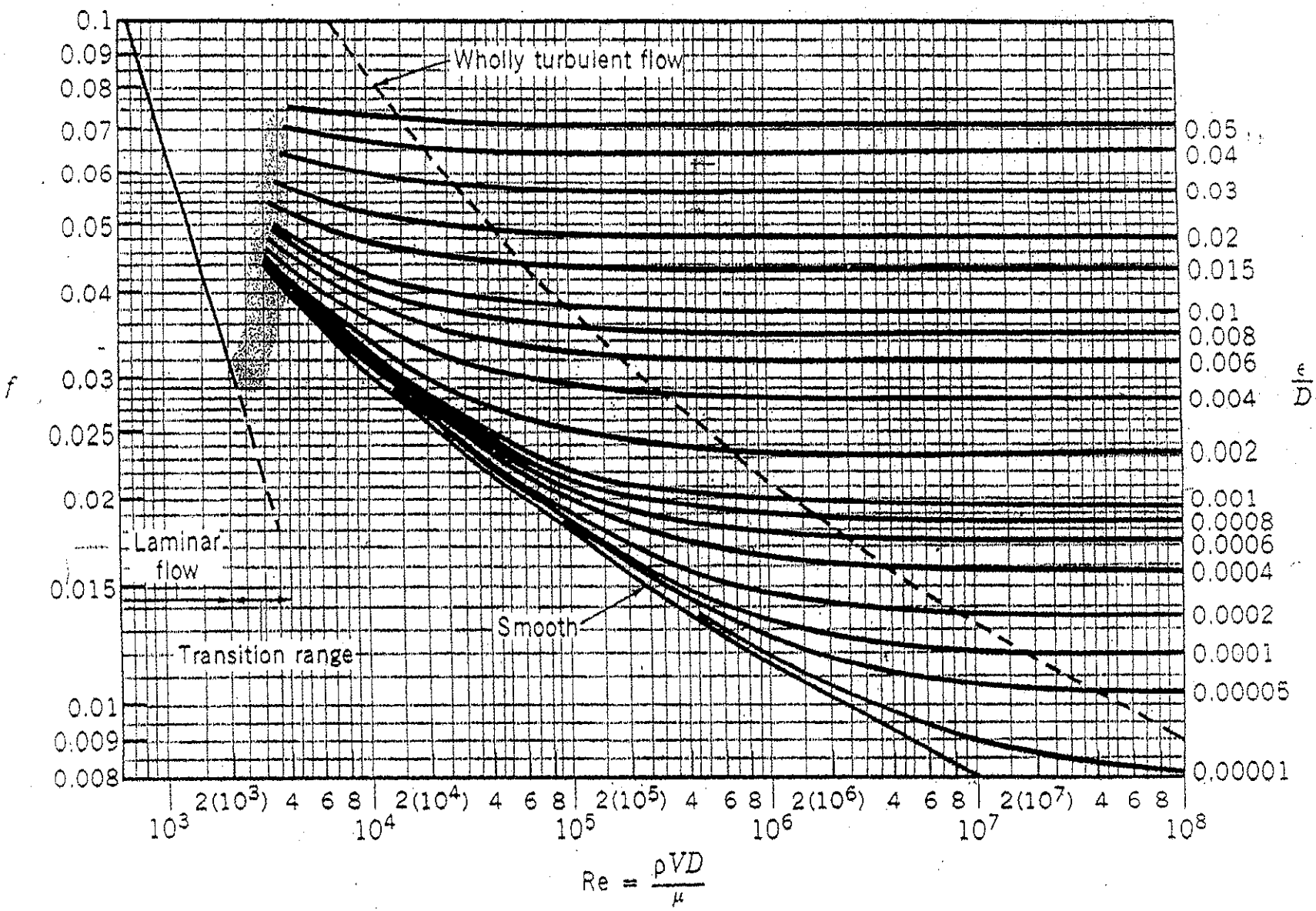

■ **FIGURE 8.23** Friction factor as a function of Reynolds number and relative roughness for round pipes—the Moody chart (Data from Ref. 7 with permission).

HAND OUT 6: Methods for obtaining roots of algebraic equations (Chapter 2 of our syllabus). Source: Alexandrou, A. (2001). *"Principles of fluid mechanics."* Prentice Hall

and ideas are developed in sufficient depth so that the techniques can be readily used in practical problems.

13.1 Algebraic Equations

As encountered in several cases, mathematical models often reduce to single algebraic equations whose solution must be obtained numerically by iteration. Recall, for instance, from Chapter 8 that the friction factor could be obtained by using the Colebrook formula

$$\frac{1}{\sqrt{f}} = -0.869 \ln\left(\frac{e/D}{3.7} + \frac{2.51}{Re\sqrt{f}}\right). \tag{13.1}$$

Since f appears in both sides of the equation, the solution must be obtained numerically.

Similarly, in Prandtl-Meyer expansion, when the flow turns through a total angle ν, the resulting Mach number M is a complicated function given by

$$\nu = \sqrt{\frac{\gamma+1}{\gamma-1}}\tan^{-1}\sqrt{\frac{\gamma-1}{\gamma+1}(M^2-1)} - \tan^{-1}\sqrt{M^2-1}. \tag{13.2}$$

The solution to this equation must also be obtained numerically.

Another example is the case of oblique shocks in which the geometry of the shock as a function of the incoming M is given by

$$\beta = \theta - \tan^{-1}\left[\frac{1}{\sin\theta\cos\theta}\left(\frac{\gamma-1}{\gamma+1}\sin^2\theta + \frac{2}{\gamma+1}\frac{1}{M_1^2}\right)\right]. \tag{13.3}$$

Given the complexity of the expression, the angle of the shock θ as a function of the Mach number M and deflection angle β must be found numerically.

13.1.1 Root of Equations

Consider a general algebraic equation of the form

$$y = f(x).$$

For most of such equations, the final objective is to find the root of the equation—that is, the value (or values) of the unknown x_i that satisfies

$$F = y - f(x_i) = 0. \tag{13.4}$$

The problem is shown schematically in Figure 13.3. As shown in the figure, depending on the order of F, the function F can have multiple solutions. An obvious choice to find the roots of Equation (13.4) is to start guessing values of x_i until we find those that satisfy $F(x_i) = 0$. However, this approach can be inefficient and lengthy. Fortunately, the search for the roots can be accelerated by using a number of numerical procedures. These methods can also be implemented easily in computer form. We review two such methods: (a) the *bisection method* and (b) the *Newton-Raphson method.*

Bisection Method

The bisection method formalizes the search for the root that lies in the range of (x_{min}, x_{max}), where x_{min}, and x_{max} are initial limits set by the user. During the iteration procedure,

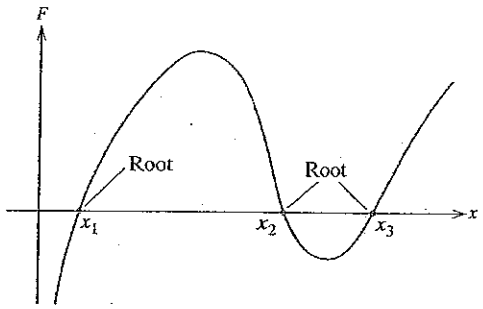

FIGURE 13.3 Multiple roots of a function.

the estimate for the root x_g is assumed to be the midpoint of the current range $x_g = \frac{x_{min} + x_{max}}{2}$, while the limits x_{min} and x_{max} are updated depending on the sign of $F(x_g)$ using

$$\text{If } F(x_g) > 0 \quad x_{min} = x_g,$$

and

$$\text{If } F(x_g) < 0 \quad x_{max} = x_g.$$

However, the above update is not unique and depends on the functional form of F. For instance, the proper update may be the opposite—that is,

$$\text{If } F(x_g) > 0 \quad x_{max} = x_g,$$

and

$$\text{If } F(x_g) < 0 \quad x_{min} = x_g.$$

The proper criterion for updating the range must be determined on a case-by-case basis, by keeping track of x_g: if x_g between iterations remains unchanged, the criterion must be reversed.

The procedure is terminated when $|F(x_g)| < \epsilon$, where ϵ is a predetermined small number typically of the same order as the machine accuracy. In general, the method works well and yields the root of the expression provided the range within which the solution lies is known.

EXAMPLE 13.1

Problem Statement Using the bisection method, find the friction factor by solving the Colebrook formula,

$$\frac{1}{\sqrt{f}} = -0.869 \ln\left(\frac{e/D}{3.7} + \frac{2.51}{Re\sqrt{f}}\right),$$

for flow through a pipe with $Re = 298{,}805$ and roughness ratio $e/D = 0.0004$.

SOLUTION For the solution procedure, the equation is expressed as

$$F = \frac{1}{\sqrt{f}} + 0.869 \ln\left(\frac{e/D}{3.7} + \frac{2.51}{Re\sqrt{f}}\right).$$

The root of $F(f)$ is the unknown friction factor f. Here we use $\epsilon = 10^{-6}$.

The method is implemented in the Fortran program found in Appendix D. Note the proper criterion for updating the limits f_{min} and f_{max}. For the given conditions with the limits initially at $f_{min} = 0$ and $f_{max} = 0.2$, the program gives the following intermediate estimates for the friction factor: 0.1, 0.05, 0.025, ... until it converges in 24 iterations to $f = 0.0176$.

Newton-Raphson Method

The Newton-Raphson method is based on Taylor's expansion series: if x_i is an estimate for the root x_r, the function expanded around x_i is then given as

$$F(x_r) = F(x_i) + F'(x_i)\,dx + F''(x_i)(dx)^2 + \cdots,$$

where primes such as F' denote differentiation with respect to x.

By definition, if x_r is the root of $F(x)$, then $F(x_r) = 0$. Therefore, by considering only the first two terms of the foregoing series, an appropriate correction $dx = x_{i+1} - x_i$ of the current estimate x_i is given as

$$dx = x_{i+1} - x_i = -\frac{F(x_i)}{F'(x_i)}.$$

As shown in Figure 13.4, geometrically the method is equivalent to approximating the function by a linear function using the local tangent. Formally, then, using an initial estimate of x_i, the iteration proceeds by correcting the estimate according to

$$x_{i+1} = x_i - \frac{F(x_i)}{F'(x_i)},$$

until $|x_{i+1} - x_i| < \epsilon$, where ϵ is again a small tolerance number (usually 10^{-6}).

In general, the method works very well having one of the fastest convergence rates (quadratic). However, the method has two limitations: (a) unless the initial guess is sufficiently close to the root, there is no guarantee that the procedure will converge; and (b) when $F' = 0$, the method breaks down.

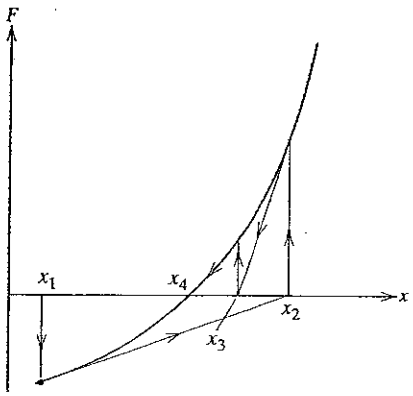

FIGURE 13.4 Geometric description of the Newton-Raphson method.

EXAMPLE 13.2

Problem Statement Using the Newton-Raphson method, find the friction factor by solving the Colebrook formula:

$$\frac{1}{\sqrt{f}} = -0.869 \ln\left(\frac{\varepsilon/D}{3.7} + \frac{2.51}{Re\sqrt{f}}\right)$$

for flow through a pipe with $Re = 298{,}805$ and roughness ratio $\varepsilon/D = 0.0004$.

SOLUTION For the solution procedure, the equation is again expressed as

$$f = \frac{1}{\sqrt{f}} + 0.869 \ln\left(\frac{\varepsilon/D}{3.7} + \frac{2.51}{Re\sqrt{f}}\right)$$

Again, the root of $F(f)$ is the unknown friction factor f. The tolerance is selected again as $\varepsilon = 10^{-6}$. This method is implemented in the Fortran program found in Appendix D. For the given conditions, and initial estimate (as discussed in Chapter 8) given by,

$$f_1 = 0.25\left[0.434 \ln\left(\frac{\varepsilon/D}{3.7} + \frac{5.74}{Re^{0.9}}\right)\right]^{-2}$$

the program after three (3) iterations converges to $f = 0.0176$. This example shows the faster convergence of the Newton-Raphson iteration procedure as compared with the bisection method.

13.1.2 Numerical Integration

In many fluid problems, the solution to the problem is the integral of a function $f(x)$ over a certain domain. For instance, in hydrostatics in order to determine the total force, we must integrate the pressure over submerged surfaces. Therefore, when the function $f(x)$ is complicated, the integral must be performed numerically. For a given function $f(x)$ the integral

$$A = \int_{x_1}^{x_2} f(x)\,dx$$

is the area under the graph, as shown in Figure 13.5.

An obvious approach is to subdivide the domain into smaller strips and add the area of each one of them. Indeed, numerical integration starts by dividing the range between x_1 and x_2 into n strips. Including the two ends, then, we have $n + 1$ points along the x-axis.

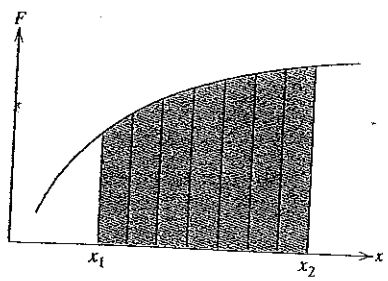

FIGURE 13.5 Schematic of numerical integration.

HAND OUT 7: Bracketing methods (Chapter 2 of our syllabus). Source: Chapra, S. C., and Canale, R. P. (2006). *"Numerical methods for engineers."* McGraw-Hill, fifth edition.

CHAPTER 5

Bracketing Methods

This chapter on roots of equations deals with methods that exploit the fact that a function typically changes sign in the vicinity of a root. These techniques are called *bracketing methods* because two initial guesses for the root are required. As the name implies, these guesses must "bracket," or be on either side of, the root. The particular methods described herein employ different strategies to systematically reduce the width of the bracket and, hence, home in on the correct answer.

As a prelude to these techniques, we will briefly discuss graphical methods for depicting functions and their roots. Beyond their utility for providing rough guesses, graphical techniques are also useful for visualizing the properties of the functions and the behavior of the various numerical methods.

5.1 GRAPHICAL METHODS

A simple method for obtaining an estimate of the root of the equation $f(x) = 0$ is to make a plot of the function and observe where it crosses the x axis. This point, which represents the x value for which $f(x) = 0$, provides a rough approximation of the root.

EXAMPLE 5.1 The Graphical Approach

Problem Statement. Use the graphical approach to determine the drag coefficient c needed for a parachutist of mass $m = 68.1$ kg to have a velocity of 40 m/s after free-falling for time $t = 10$ s. *Note:* The acceleration due to gravity is 9.8 m/s^2.

Solution. This problem can be solved by determining the root of Eq. (PT2.4) using the parameters $t = 10$, $g = 9.8$, $v = 40$, and $m = 68.1$:

$$f(c) = \frac{9.8(68.1)}{c}\left(1 - e^{-(c/68.1)10}\right) - 40$$

or

$$f(c) = \frac{667.38}{c}\left(1 - e^{-0.146843c}\right) - 40 \qquad \text{(E5.1.1)}$$

Various values of c can be substituted into the right-hand side of this equation to compute

c	f(c)
4	34.115
8	17.653
12	6.067
16	−2.269
20	−8.401

These points are plotted in Fig. 5.1. The resulting curve crosses the c axis between 12 and 16. Visual inspection of the plot provides a rough estimate of the root of 14.75. The validity of the graphical estimate can be checked by substituting it into Eq. (E5.1.1) to yield

$$f(14.75) = \frac{667.38}{14.75}\left(1 - e^{-0.146843(14.75)}\right) - 40 = 0.059$$

which is close to zero. It can also be checked by substituting it into Eq. (PT2.4) along with the parameter values from this example to give

$$v = \frac{9.8(68.1)}{14.75}\left(1 - e^{-(14.75/68.1)10}\right) = 40.059$$

which is very close to the desired fall velocity of 40 m/s.

FIGURE 5.1
The graphical approach for determining the roots of an equation.

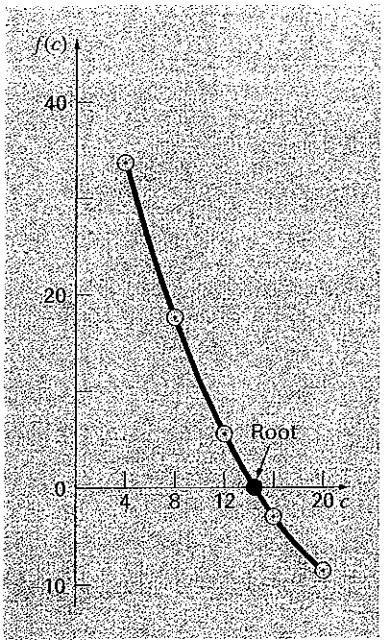

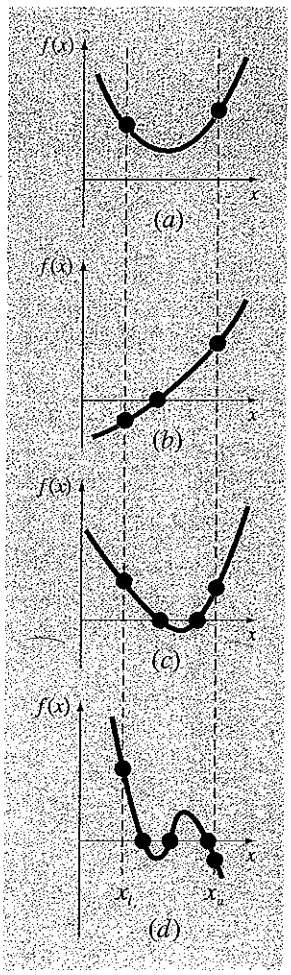

FIGURE 5.2
Illustration of a number of general ways that a root may occur in an interval prescribed by a lower bound x_l and an upper bound x_u. Parts (*a*) and (*c*) indicate that if both $f(x_l)$ and $f(x_u)$ have the same sign, either there will be no roots or there will be an even number of roots within the interval. Parts (*b*) and (*d*) indicate that if the function has different signs at the end points, there will be an odd number of roots in the interval.

Graphical techniques are of limited practical value because they are not precise. However, graphical methods can be utilized to obtain rough estimates of roots. These estimates can be employed as starting guesses for numerical methods discussed in this and the next chapter.

Aside from providing rough estimates of the root, graphical interpretations are important tools for understanding the properties of the functions and anticipating the pitfalls of the numerical methods. For example, Fig. 5.2 shows a number of ways in which roots can occur (or be absent) in an interval prescribed by a lower bound x_l and an upper bound x_u. Figure 5.2*b* depicts the case where a single root is bracketed by negative and positive values of $f(x)$. However, Fig. 5.2*d*, where $f(x_l)$ and $f(x_u)$ are also on opposite sides of the x axis, shows three roots occurring within the interval. In general, if $f(x_l)$ and $f(x_u)$ have opposite signs, there are an odd number of roots in the interval. As indicated by Fig. 5.2*a* and *c*, if $f(x_l)$ and $f(x_u)$ have the same sign, there are either no roots or an even number of roots between the values.

Although these generalizations are usually true, there are cases where they do not hold. For example, functions that are tangential to the x axis (Fig. 5.3*a*) and discontinuous functions (Fig. 5.3*b*) can violate these principles. An example of a function that is tangential to the axis is the cubic equation $f(x) = (x - 2)(x - 2)(x - 4)$. Notice that $x = 2$ makes two terms in this polynomial equal to zero. Mathematically, $x = 2$ is called a *multiple root*. At the end of Chap. 6, we will present techniques that are expressly designed to locate multiple roots.

The existence of cases of the type depicted in Fig. 5.3 makes it difficult to develop general computer algorithms guaranteed to locate all the roots in an interval. However, when used in conjunction with graphical approaches, the methods described in the following

FIGURE 5.3
Illustration of some exceptions to the general cases depicted in Fig. 5.2. (*a*) Multiple root that occurs when the function is tangential to the x axis. For this case, although the end points are of opposite signs, there are an even number of axis intersections for the interval. (*b*) Discontinuous function where end points of opposite sign bracket an even number of roots. Special strategies are required for determining the roots for these cases.

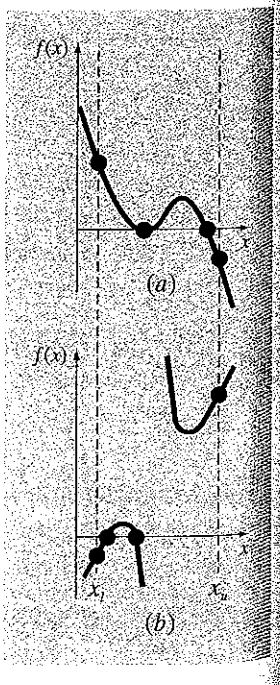

sections are extremely useful for solving many roots of equations problems confronted routinely by engineers and applied mathematicians.

EXAMPLE 5.2 Use of Computer Graphics to Locate Roots

Problem Statement. Computer graphics can expedite and improve your efforts to locate roots of equations. The function

$$f(x) = \sin 10x + \cos 3x$$

has several roots over the range $x = 0$ to $x = 5$. Use computer graphics to gain insight into the behavior of this function.

Solution. Packages such as Excel and MATLAB software can be used to generate plots. Figure 5.4*a* is a plot of $f(x)$ from $x = 0$ to $x = 5$. This plot suggests the presence of several roots, including a possible double root at about $x = 4.2$ where $f(x)$ appears to be tangent to

FIGURE 5.4
The progressive enlargement of $f(x) = \sin 10x + \cos 3x$ by the computer. Such interactive graphics permits the analyst to determine that two distinct roots exist between $x = 4.2$ and $x = 4.3$.

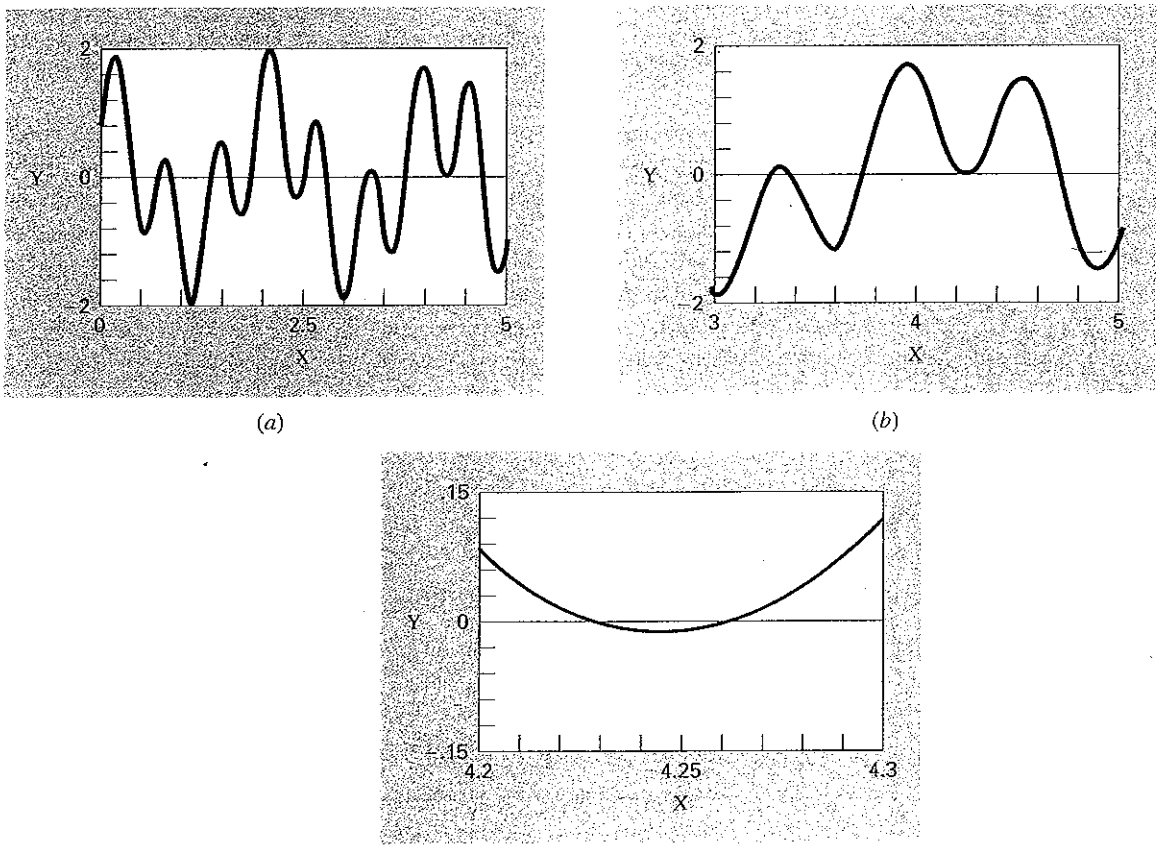

the x axis. A more detailed picture of the behavior of $f(x)$ is obtained by changing the plotting range from $x = 3$ to $x = 5$, as shown in Fig. 5.4*b*. Finally, in Fig. 5.4*c*, the vertical scale is narrowed further to $f(x) = -0.15$ to $f(x) = 0.15$ and the horizontal scale is narrowed to $x = 4.2$ to $x = 4.3$. This plot shows clearly that a double root does not exist in this region and that in fact there are two distinct roots at about $x = 4.23$ and $x = 4.26$.

Computer graphics will have great utility in your studies of numerical methods. This capability will also find many other applications in your other classes and professional activities as well.

5.2 THE BISECTION METHOD

When applying the graphical technique in Example 5.1, you have observed (Fig. 5.1) that $f(x)$ changed sign on opposite sides of the root. In general, if $f(x)$ is real and continuous in the interval from x_l to x_u and $f(x_l)$ and $f(x_u)$ have opposite signs, that is,

$$f(x_l)\, f(x_u) < 0 \tag{5.1}$$

then there is at least one real root between x_l and x_u.

Incremental search methods capitalize on this observation by locating an interval where the function changes sign. Then the location of the sign change (and consequently, the root) is identified more precisely by dividing the interval into a number of subintervals. Each of these subintervals is searched to locate the sign change. The process is repeated and the root estimate refined by dividing the subintervals into finer increments. We will return to the general topic of incremental searches in Sec. 5.4.

The *bisection method*, which is alternatively called binary chopping, interval halving, or Bolzano's method, is one type of incremental search method in which the interval is always divided in half. If a function changes sign over an interval, the function value at the midpoint is evaluated. The location of the root is then determined as lying at the midpoint of the subinterval within which the sign change occurs. The process is repeated to obtain refined estimates. A simple algorithm for the bisection calculation is listed in Fig. 5.5, and a graphical depiction of the method is provided in Fig. 5.6. The following example goes through the actual computations involved in the method.

FIGURE 5.5

Step 1: Choose lower x_l and upper x_u guesses for the root such that the function changes sign over the interval. This can be checked by ensuring that $f(x_l)f(x_u) < 0$.

Step 2: An estimate of the root x_r is determined by

$$x_r = \frac{x_l + x_u}{2}$$

Step 3: Make the following evaluations to determine in which subinterval the root lies:

(a) If $f(x_l)f(x_r) < 0$, the root lies in the lower subinterval. Therefore, set $x_u = x_r$ and return to step 2.

(b) If $f(x_l)f(x_r) > 0$, the root lies in the upper subinterval. Therefore, set $x_l = x_r$ and return to step 2.

(c) If $f(x_l)f(x_r) = 0$, the root equals x_r; terminate the computation.

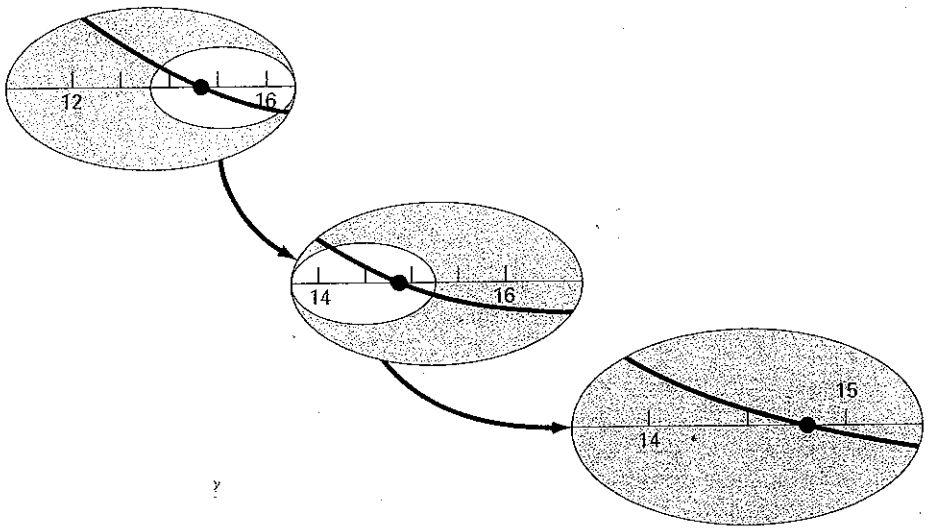

FIGURE 5.6
A graphical depiction of the bisection method. This plot conforms to the first three iterations from Example 5.3.

EXAMPLE 5.3 Bisection

Problem Statement. Use bisection to solve the same problem approached graphically in Example 5.1.

Solution. The first step in bisection is to guess two values of the unknown (in the present problem, c) that give values for $f(c)$ with different signs. From Fig. 5.1, we can see that the function changes sign between values of 12 and 16. Therefore, the initial estimate of the root x_r lies at the midpoint of the interval

$$x_r = \frac{12 + 16}{2} = 14$$

This estimate represents a true percent relative error of $\varepsilon_t = 5.3\%$ (note that the true value of the root is 14.7802). Next we compute the product of the function value at the lower bound and at the midpoint:

$$f(12)\,f(14) = 6.067(1.569) = 9.517$$

which is greater than zero, and hence no sign change occurs between the lower bound and the midpoint. Consequently, the root must be located between 14 and 16. Therefore, we create a new interval by redefining the lower bound as 14 and determining a revised root estimate as

$$x_r = \frac{14 + 16}{2} = 15$$

which represents a true percent error of $\varepsilon_t = 1.5\%$. The process can be repeated to obtain refined estimates. For example,

$$f(14)\,f(15) = 1.569(-0.425) = -0.666$$

Therefore, the root is between 14 and 15. The upper bound is redefined as 15, and the root estimate for the third iteration is calculated as

$$x_r = \frac{14 + 15}{2} = 14.5$$

which represents a percent relative error of $\varepsilon_t = 1.9\%$. The method can be repeated until the result is accurate enough to satisfy your needs.

In the previous example, you may have noticed that the true error does not decrease with each iteration. However, the interval within which the root is located is halved with each step in the process. As discussed in the next section, the interval width provides an exact estimate of the upper bound of the error for the bisection method.

5.2.1 Termination Criteria and Error Estimates

We ended Example 5.3 with the statement that the method could be continued to obtain a refined estimate of the root. We must now develop an objective criterion for deciding when to terminate the method.

An initial suggestion might be to end the calculation when the true error falls below some prespecified level. For instance, in Example 5.3, the relative error dropped from 5.3 to 1.9 percent during the course of the computation. We might decide that we should terminate when the error drops below, say, 0.1 percent. This strategy is flawed because the error estimates in the example were based on knowledge of the true root of the function. This would not be the case in an actual situation because there would be no point in using the method if we already knew the root.

Therefore, we require an error estimate that is not contingent on foreknowledge of the root. As developed previously in Sec. 3.3, an approximate percent relative error ε_a can be calculated, as in [recall Eq. (3.5)]

$$\varepsilon_a = \left| \frac{x_r^{\text{new}} - x_r^{\text{old}}}{x_r^{\text{new}}} \right| 100\% \tag{5.2}$$

where x_r^{new} is the root for the present iteration and x_r^{old} is the root from the previous iteration. The absolute value is used because we are usually concerned with the magnitude of ε_a rather than with its sign. When ε_a becomes less than a prespecified stopping criterion ε_s, the computation is terminated.

EXAMPLE 5.4 Error Estimates for Bisection

Problem Statement. Continue Example 5.3 until the approximate error falls below a stopping criterion of $\varepsilon_s = 0.5\%$. Use Eq. (5.2) to compute the errors.

Solution. The results of the first two iterations for Example 5.3 were 14 and 15. Substituting these values into Eq. (5.2) yields

$$|\varepsilon_a| = \left| \frac{15 - 14}{15} \right| 100\% = 6.667\%$$

Recall that the true percent relative error for the root estimate of 15 was 1.5%. Therefore, ε_a is greater than ε_t. This behavior is manifested for the other iterations:

Iteration	x_l	x_u	x_r	ε_a (%)	ε_t (%)
1	12	16	14		5.279
2	14	16	15	6.667	1.487
3	14	15	14.5	3.448	1.896
4	14.5	15	14.75	1.695	0.204
5	14.75	15	14.875	0.840	0.641
6	14.75	14.875	14.8125	0.422	0.219

Thus, after six iterations ε_a finally falls below $\varepsilon_s = 0.5\%$, and the computation can be terminated.

These results are summarized in Fig. 5.7. The "ragged" nature of the true error is due to the fact that, for bisection, the true root can lie anywhere within the bracketing interval. The true and approximate errors are far apart when the interval happens to be centered on the true root. They are close when the true root falls at either end of the interval.

Although the approximate error does not provide an exact estimate of the true error, Fig. 5.7 suggests that ε_a captures the general downward trend of ε_t. In addition, the plot exhibits the extremely attractive characteristic that ε_a is always greater than ε_t. Thus, when

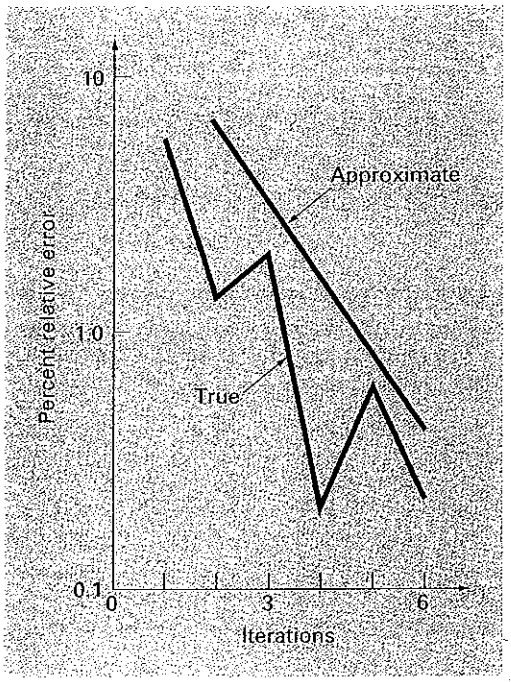

FIGURE 5.7
Errors for the bisection method. True and estimated errors are plotted versus the number of iterations.

ε_a falls below ε_s, the computation could be terminated with confidence that the root is known to be at least as accurate as the prespecified acceptable level.

Although it is always dangerous to draw general conclusions from a single example, it can be demonstrated that ε_a will always be greater than ε_t for the bisection method. This is because each time an approximate root is located using bisection as $x_r = (x_l + x_u)/2$, we know that the true root lies somewhere within an interval of $(x_u - x_l)/2 = \Delta x/2$. Therefore, the root must lie within $\pm\Delta x/2$ of our estimate (Fig. 5.8). For instance, when Example 5.3 was terminated, we could make the definitive statement that

$$x_r = 14.5 \pm 0.5$$

Because $\Delta x/2 = x_r^{\text{new}} - x_r^{\text{old}}$ (Fig. 5.9), Eq. (5.2) provides an exact upper bound on the true error. For this bound to be exceeded, the true root would have to fall outside the bracketing interval, which, by definition, could never occur for the bisection method. As illustrated in a subsequent example (Example 5.7), other root-locating techniques do not always behave as nicely. Although bisection is generally slower than other methods, the

FIGURE 5.8
Three ways in which the interval may bracket the root. In (*a*) the true value lies at the center of the interval, whereas in (*b*) and (*c*) the true value lies near the extreme. Notice that the discrepancy between the true value and the midpoint of the interval never exceeds half the interval length, or $\Delta x/2$.

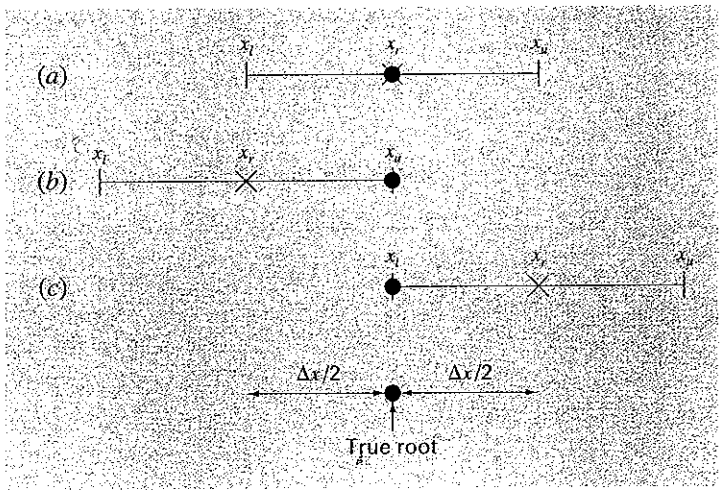

FIGURE 5.9
Graphical depiction of why the error estimate for bisection ($\Delta x/2$) is equivalent to the root estimate for the present iteration (x_r^{new}) minus the root estimate for the previous iteration (x_r^{old}).

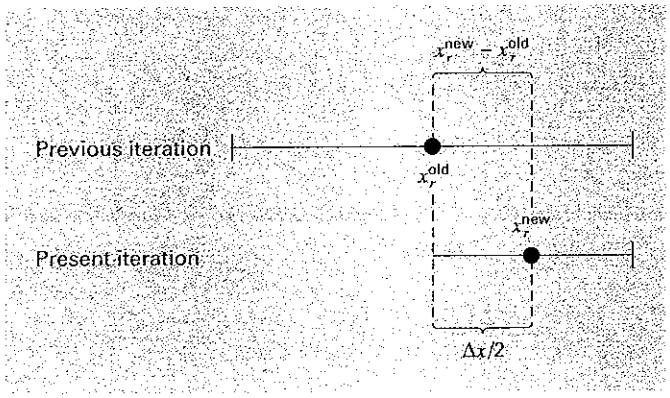

neatness of its error analysis is certainly a positive aspect that could make it attractive for certain engineering applications.

Before proceeding to the computer program for bisection, we should note that the relationships (Fig. 5.9)

$$x_r^{\text{new}} - x_r^{\text{old}} = \frac{x_u - x_l}{2}$$

and

$$x_r^{\text{new}} = \frac{x_l + x_u}{2}$$

can be substituted into Eq. (5.2) to develop an alternative formulation for the approximate percent relative error

$$\varepsilon_a = \left| \frac{x_u - x_l}{x_u + x_l} \right| 100\% \tag{5.3}$$

This equation yields identical results to Eq. (5.2) for bisection. In addition, it allows us to calculate an error estimate on the basis of our initial guesses—that is, on our first iteration. For instance, on the first iteration of Example 5.2, an approximate error can be computed as

$$\varepsilon_a = \left| \frac{16 - 12}{16 + 12} \right| 100\% = 14.29\%$$

Another benefit of the bisection method is that the number of iterations required to attain an absolute error can be computed *a priori*—that is, before starting the iterations. This can be seen by recognizing that before starting the technique, the absolute error is

$$E_a^0 = x_u^0 - x_l^0 = \Delta x^0$$

where the superscript designates the iteration. Hence, before starting the method, we are at the "zero iteration." After the first iteration, the error becomes

$$E_a^1 = \frac{\Delta x^0}{2}$$

Because each succeeding iteration halves the error, a general formula relating the error and the number of iterations, n, is

$$E_a^n = \frac{\Delta x^0}{2^n} \tag{5.4}$$

If $E_{a,d}$ is the desired error, this equation can be solved for

$$n = \frac{\log\left(\Delta x^0 / E_{a,d}\right)}{\log 2} = \log_2\left(\frac{\Delta x^0}{E_{a,d}}\right) \tag{5.5}$$

Let us test the formula. For Example 5.4, the initial interval was $\Delta x_0 = 16 - 12 = 4$. After six iterations, the absolute error was

$$E_a = \frac{|14.875 - 14.75|}{2} = 0.0625$$

We can substitute these values into Eq. (5.5) to give

$$n = \frac{\log(4/0.0625)}{\log 2} = 6$$

Thus, if we knew beforehand that an error of less than 0.0625 was acceptable, the formula tells us that six iterations would yield the desired result.

Although we have emphasized the use of relative errors for obvious reasons, there will be cases where (usually through knowledge of the problem context) you will be able to specify an absolute error. For these cases, bisection along with Eq. (5.5) can provide a useful root-location algorithm. We will explore such applications in the end-of-chapter problems.

5.2.2 Bisection Algorithm

The algorithm in Fig. 5.5 can now be expanded to include the error check (Fig. 5.10). The algorithm employs user-defined functions to make root location and function evaluation more efficient. In addition, an upper limit is placed on the number of iterations. Finally, an error check is included to avoid division by zero during the error evaluation. Such would be the case when the bracketing interval is centered on zero. For this situation Eq. (5.2) becomes infinite. If this occurs, the program skips over the error evaluation for that iteration.

The algorithm in Fig. 5.10 is not user-friendly; it is designed strictly to come up with the answer. In Prob. 5.14 at the end of this chapter, you will have the task of making it easier to use and understand.

FIGURE 5.10
Pseudocode for function to implement bisection.

```
FUNCTION Bisect(xl, xu, es, imax, xr, iter, ea)
  iter = 0
  DO
    xrold = xr
    xr = (xl + xu) / 2
    iter = iter + 1
    IF xr ≠ 0 THEN
      ea = ABS((xr - xrold) / xr) * 100
    END IF
    test = f(xl) * f(xr)
    IF test < 0 THEN
      xu = xr
    ELSE IF test > 0 THEN
      xl = xr
    ELSE
      ea = 0
    END IF
    IF ea < es OR iter ≥ imax EXIT
  END DO
  Bisect = xr
END Bisect
```

5.2.3 Minimizing Function Evaluations

The bisection algorithm in Fig. 5.10 is just fine if you are performing a single root evaluation for a function that is easy to evaluate. However, there are many instances in engineering when this is not the case. For example, suppose that you develop a computer program that must locate a root numerous times. In such cases you could call the algorithm from Fig. 5.10 thousands and even millions of times in the course of a single run.

Further, in its most general sense, a univariate function is merely an entity that returns a single value in return for a single value you send to it. Perceived in this sense, functions are not always simple formulas like the one-line equations solved in the preceding examples in this chapter. For example, a function might consist of many lines of code that could take a significant amount of execution time to evaluate. In some cases, the function might even represent an independent computer program.

Because of both these factors, it is imperative that numerical algorithms minimize function evaluations. In this light, the algorithm from Fig. 5.10 is deficient. In particular, notice that in making two function evaluations per iteration, it recalculates one of the functions that was determined on the previous iteration.

Figure 5.11 provides a modified algorithm that does not have this deficiency. We have highlighted the lines that differ from Fig. 5.10. In this case, only the new function value at

FIGURE 5.11
Pseudocode for bisection subprogram which minimizes function evaluations.

```
FUNCTION Bisect(xl, xu, es, imax, xr, iter, ea)
  iter = 0
  fl = f(xl)
  DO
    xrold = xr
    xr = (xl + xu) / 2
    fr = f(xr)
    iter = iter + 1
    IF xr ≠ 0 THEN
      ea = ABS((xr - xrold) / xr) * 100
    END IF
    test = fl * fr
    IF test < 0 THEN
      xu = xr
    ELSE IF test > 0 THEN
      xl = xr
      fl = fr
    ELSE
      ea = 0
    END IF
    IF ea < es OR iter ≥ imax EXIT
  END DO
  Bisect = xr
END Bisect
```

the root estimate is calculated. Previously calculated values are saved and merely reassigned as the bracket shrinks. Thus, $n + 1$ function evaluations are performed, rather than $2n$.

5.3 THE FALSE-POSITION METHOD

Although bisection is a perfectly valid technique for determining roots, its "brute-force" approach is relatively inefficient. False position is an alternative based on a graphical insight.

A shortcoming of the bisection method is that, in dividing the interval from x_l to x_u into equal halves, no account is taken of the magnitudes of $f(x_l)$ and $f(x_u)$. For example, if $f(x_l)$ is much closer to zero than $f(x_u)$, it is likely that the root is closer to x_l than to x_u (Fig. 5.12). An alternative method that exploits this graphical insight is to join $f(x_l)$ and $f(x_u)$ by a straight line. The intersection of this line with the x axis represents an improved estimate of the root. The fact that the replacement of the curve by a straight line gives a "false position" of the root is the origin of the name, *method of false position,* or in Latin, *regula falsi.* It is also called the *linear interpolation method.*

Using similar triangles (Fig. 5.12), the intersection of the straight line with the x axis can be estimated as

$$\frac{f(x_l)}{x_r - x_l} = \frac{f(x_u)}{x_r - x_u} \tag{5.6}$$

which can be solved for (see Box 5.1 for details).

$$x_r = x_u - \frac{f(x_u)(x_l - x_u)}{f(x_l) - f(x_u)} \tag{5.7}$$

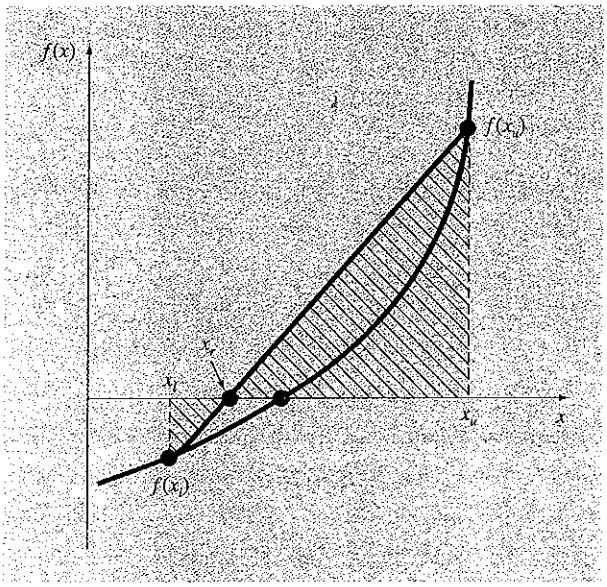

FIGURE 5.12
A graphical depiction of the method of false position. Similar triangles used to derive the formula for the method are shaded.

Box 5.1 Derivation of the Method of False Position

Cross-multiply Eq. (5.6) to yield

$$f(x_l)(x_r - x_u) = f(x_u)(x_r - x_l)$$

Collect terms and rearrange:

$$x_r[f(x_l) - f(x_u)] = x_u f(x_l) - x_l f(x_u)$$

Divide by $f(x_l) - f(x_u)$:

$$x_r = \frac{x_u f(x_l) - x_l f(x_u)}{f(x_l) - f(x_u)} \tag{B5.1.1}$$

This is one form of the method of false position. Note that it allows the computation of the root x_r as a function of the lower and upper guesses x_l and x_u. It can be put in an alternative form by expanding it:

$$x_r = \frac{x_u f(x_l)}{f(x_l) - f(x_u)} - \frac{x_l f(x_u)}{f(x_l) - f(x_u)}$$

then adding and subtracting x_u on the right-hand side:

$$x_r = x_u + \frac{x_u f(x_l)}{f(x_l) - f(x_u)} - x_u - \frac{x_l f(x_u)}{f(x_l) - f(x_u)}$$

Collecting terms yields

$$x_r = x_u + \frac{x_u f(x_u)}{f(x_l) - f(x_u)} - \frac{x_l f(x_u)}{f(x_l) - f(x_u)}$$

or

$$x_r = x_u - \frac{f(x_u)(x_l - x_u)}{f(x_l) - f(x_u)}$$

which is the same as Eq. (5.7). We use this form because it involves one less function evaluation and one less multiplication than Eq. (B5.1.1). In addition, it is directly comparable with the secant method which will be discussed in Chap. 6.

This is the *false-position formula*. The value of x_r computed with Eq. (5.7) then replaces whichever of the two initial guesses, x_l or x_u, yields a function value with the same sign as $f(x_r)$. In this way, the values of x_l and x_u always bracket the true root. The process is repeated until the root is estimated adequately. The algorithm is identical to the one for bisection (Fig. 5.5) with the exception that Eq. (5.7) is used for step 2. In addition, the same stopping criterion [Eq. (5.2)] is used to terminate the computation.

EXAMPLE 5.5 False Position

Problem Statement. Use the false-position method to determine the root of the same equation investigated in Example 5.1 [Eq. (E5.1.1)].

Solution. As in Example 5.3, initiate the computation with guesses of $x_l = 12$ and $x_u = 16$.

First iteration:

$$x_l = 12 \qquad f(x_l) = 6.0699$$
$$x_u = 16 \qquad f(x_u) = -2.2688$$
$$x_r = 16 - \frac{-2.2688(12 - 16)}{6.0669 - (-2.2688)} = 14.9113$$

which has a true relative error of 0.89 percent.

Second iteration:

$$f(x_l) f(x_r) = -1.5426$$

Therefore, the root lies in the first subinterval, and x_r becomes the upper limit for the next iteration, $x_u = 14.9113$:

$$x_l = 12 \qquad f(x_l) = 6.0699$$
$$x_u = 14.9113 \qquad f(x_u) = -0.2543$$
$$x_r = 14.9113 - \frac{-0.2543(12 - 14.9113)}{6.0669 - (-0.2543)} = 14.7942$$

which has true and approximate relative errors of 0.09 and 0.79 percent. Additional iterations can be performed to refine the estimate of the roots.

A feeling for the relative efficiency of the bisection and false-position methods can be appreciated by referring to Fig. 5.13, where we have plotted the true percent relative errors for Examples 5.4 and 5.5. Note how the error for false position decreases much faster than for bisection because of the more efficient scheme for root location in the false-position method.

Recall in the bisection method that the interval between x_l and x_u grew smaller during the course of a computation. The interval, as defined by $\Delta x/2 = |x_u - x_l|/2$ for the first iteration, therefore provided a measure of the error for this approach. This is not the case

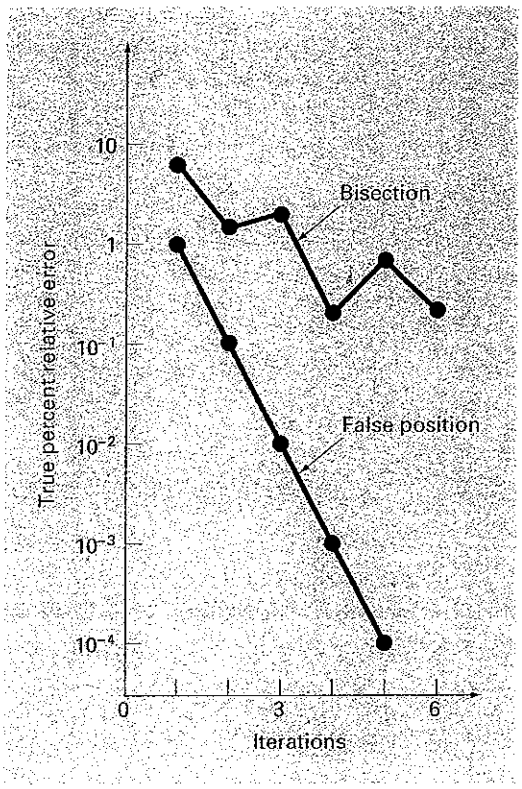

FIGURE 5.13
Comparison of the relative errors of the bisection and the false-position methods.

for the method of false position because one of the initial guesses may stay fixed throughout the computation as the other guess converges on the root. For instance, in Example 5.6 the lower guess x_l remained at 12 while x_u converged on the root. For such cases, the interval does not shrink but rather approaches a constant value.

Example 5.6 suggests that Eq. (5.2) represents a very conservative error criterion. In fact, Eq. (5.2) actually constitutes an approximation of the discrepancy of the previous iteration. This is because for a case such as Example 5.6, where the method is converging quickly (for example, the error is being reduced nearly an order of magnitude per iteration), the root for the present iteration x_r^{new} is a much better estimate of the true value than the result of the previous iteration x_r^{old}. Thus, the quantity in the numerator of Eq. (5.2) actually represents the discrepancy of the previous iteration. Consequently, we are assured that satisfaction of Eq. (5.2) ensures that the root will be known with greater accuracy than the prescribed tolerance. However, as described in the next section, there are cases where false position converges slowly. For these cases, Eq. (5.2) becomes unreliable, and an alternative stopping criterion must be developed.

5.3.1 Pitfalls of the False-Position Method

Although the false-position method would seem to always be the bracketing method of preference, there are cases where it performs poorly. In fact, as in the following example, there are certain cases where bisection yields superior results.

EXAMPLE 5.6 A Case Where Bisection Is Preferable to False Position

Problem Statement. Use bisection and false position to locate the root of

$$f(x) = x^{10} - 1$$

between $x = 0$ and 1.3.

Solution. Using bisection, the results can be summarized as

Iteration	x_l	x_u	x_r	ε_a (%)	ε_t (%)
1	0	1.3	0.65	100.0	35
2	0.65	1.3	0.975	33.3	2.5
3	0.975	1.3	1.1375	14.3	13.8
4	0.975	1.1375	1.05625	7.7	5.6
5	0.975	1.05625	1.015625	4.0	1.6

Thus, after five iterations, the true error is reduced to less than 2 percent. For false position, a very different outcome is obtained:

Iteration	x_l	x_u	x_r	ε_a (%)	ε_t (%)
1	0	1.3	0.09430		90.6
2	0.09430	1.3	0.18176	48.1	81.8
3	0.18176	1.3	0.26287	30.9	73.7
4	0.26287	1.3	0.33811	22.3	66.2
5	0.33811	1.3	0.40788	17.1	59.2

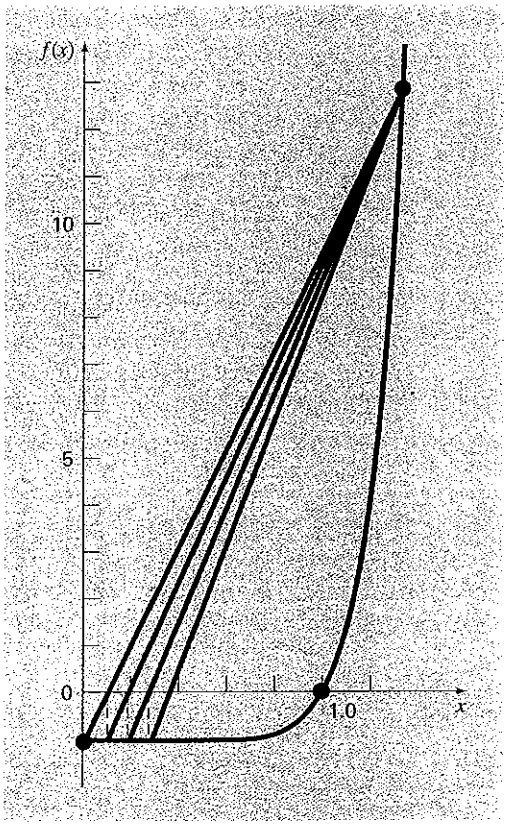

FIGURE 5.14
Plot of $f(x) = x^{10} - 1$, illustrating slow convergence of the false-position method.

After five iterations, the true error has only been reduced to about 59 percent. In addition, note that $\varepsilon_a < \varepsilon_t$. Thus, the approximate error is misleading. Insight into these results can be gained by examining a plot of the function. As in Fig. 5.14, the curve violates the premise upon which false position was based—that is, if $f(x_l)$ is much closer to zero than $f(x_u)$, then the root is closer to x_l than to x_u (recall Fig. 5.12). Because of the shape of the present function, the opposite is true.

The forgoing example illustrates that blanket generalizations regarding root-location methods are usually not possible. Although a method such as false position is often superior to bisection, there are invariably cases that violate this general conclusion. Therefore, in addition to using Eq. (5.2), the results should always be checked by substituting the root estimate into the original equation and determining whether the result is close to zero. Such a check should be incorporated into all computer programs for root location.

The example also illustrates a major weakness of the false-position method: its one-sidedness. That is, as iterations are proceeding, one of the bracketing points will tend to

stay fixed. This can lead to poor convergence, particularly for functions with significant curvature. The following section provides a remedy.

5.3.2 Modified False Position

One way to mitigate the "one-sided" nature of false position is to have the algorithm detect when one of the bounds is stuck. If this occurs, the function value at the stagnant bound can be divided in half. This is called the *modified false-position method.*

The algorithm in Fig. 5.15 implements this strategy. Notice how counters are used to determine when one of the bounds stays fixed for two iterations. If this occurs, the function value at this stagnant bound is halved.

The effectiveness of this algorithm can be demonstrated by applying it to Example 5.6. If a stopping criterion of 0.01% is used, the bisection and standard false-position methods

FIGURE 5.15
Pseudocode for the modified false-position method.

```
FUNCTION ModFalsePos(xl, xu, es, imax, xr, iter, ea)
  iter = 0
  fl = f(xl)
  fu = f(xu)
  DO
    xrold = xr
    xr = xu - fu * (xl - xu) / (fl - fu)
    fr = f(xr)
    iter = iter + 1
    IF xr <> 0 THEN
      ea = Abs((xr - xrold) / xr) * 100
    END IF
    test = fl * fr
    IF test < 0 THEN
      xu = xr
      fu = f(xu)
      iu = 0
      il = il + 1
      If il ≥ 2 THEN fl = fl / 2
    ELSE IF test > 0 THEN
      xl = xr
      fl = f(xl)
      il = 0
      iu = iu + 1
      IF iu ≥ 2 THEN fu = fu / 2
    ELSE
      ea = 0
    END IF
    IF ea < es OR iter ≥ imax THEN EXIT
  END DO
  ModFalsePos = xr
END ModFalsePos
```

would converge in 14 and 39 iterations, respectively. In contrast, the modified false-position method would converge in 12 iterations. Thus, for this example, it is somewhat more efficient than bisection and is vastly superior to the unmodified false-position method.

5.4 INCREMENTAL SEARCHES AND DETERMINING INITIAL GUESSES

Besides checking an individual answer, you must determine whether all possible roots have been located. As mentioned previously, a plot of the function is usually very useful in guiding you in this task. Another option is to incorporate an incremental search at the beginning of the computer program. This consists of starting at one end of the region of interest and then making function evaluations at small increments across the region. When the function changes sign, it is assumed that a root falls within the increment. The x values at the beginning and the end of the increment can then serve as the initial guesses for one of the bracketing techniques described in this chapter.

A potential problem with an incremental search is the choice of the increment length. If the length is too small, the search can be very time consuming. On the other hand, if the length is too great, there is a possibility that closely spaced roots might be missed (Fig. 5.16). The problem is compounded by the possible existence of multiple roots. A partial remedy for such cases is to compute the first derivative of the function $f'(x)$ at the beginning and the end of each interval. If the derivative changes sign, it suggests that a minimum or maximum may have occurred and that the interval should be examined more closely for the existence of a possible root.

Although such modifications or the employment of a very fine increment can alleviate the problem, it should be clear that brute-force methods such as incremental search are not foolproof. You would be wise to supplement such automatic techniques with any other information that provides insight into the location of the roots. Such information can be found in plotting and in understanding the physical problem from which the equation originated.

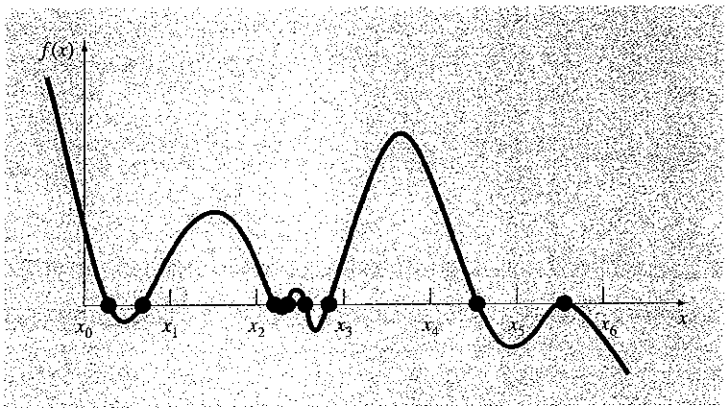

FIGURE 5.16
Cases where roots could be missed because the increment length of the search procedure is too large. Note that the last root on the right is multiple and would be missed regardless of increment length.

PROBLEMS

5.1 Determine the real roots of $f(x) = -0.5x^2 + 2.5x + 4.5$:
(a) Graphically.
(b) Using the quadratic formula.
(c) Using three iterations of the bisection method to determine the highest root. Employ initial guesses of $x_l = 5$ and $x_u = 10$. Compute the estimated error ε_a and the true error ε_t after each iteration.

5.2 Determine the real root of $f(x) = 5x^3 - 5x^2 + 6x - 2$:
(a) Graphically.
(b) Using bisection to locate the root. Employ initial guesses of $x_l = 0$ and $x_u = 1$ and iterate until the estimated error ε_a falls below a level of $\varepsilon_s = 10\%$.

5.3 Determine the real root of $f(x) = -25 + 82x - 90x^2 + 44x^3 - 8x^4 + 0.7x^5$:
(a) Graphically.
(b) Using bisection to determine the root to $\varepsilon_s = 10\%$. Employ initial guesses of $x_l = 0.5$ and $x_u = 1.0$.
(c) Perform the same computation as in **(b)** but use the false-position method and $\varepsilon_s = 0.2\ \%$.

5.4 **(a)** Determine the roots of $f(x) = -12 - 21x + 18x^2 - 2.75x^3$ graphically. In addition, determine the first root of the function with **(b)** bisection, and **(c)** false position. For **(b)** and **(c)** use initial guesses of $x_l = -1$ and $x_u = 0$, and a stopping criterion of 1%.

5.5 Locate the first nontrivial root of $\sin x = x^3$, where x is in radians. Use a graphical technique and bisection with the initial interval from 0.5 to 1. Perform the computation until ε_a is less than $\varepsilon_s = 2\%$. Also perform an error check by substituting your final answer into the original equation.

5.6 Determine the positive real root of $\ln(x^4) = 0.7$ **(a)** graphically, **(b)** using three iterations of the bisection method, with initial guesses of $x_l = 0.5$ and $x_u = 2$, and **(c)** using three iterations of the false-position method, with the same initial guesses as in **(b)**.

5.7 Determine the real root of $f(x) = (0.8 - 0.3x)/x$:
(a) Analytically.
(b) Graphically.
(c) Using three iterations of the false-position method and initial guesses of 1 and 3. Compute the approximate error ε_a and the true error ε_t after each iteration. Is there a problem with the result?

5.8 Find the positive square root of 18 using the false-position method to within $\varepsilon_s = 0.5\%$. Employ initial guesses of $x_l = 4$ and $x_u = 5$.

5.9 Find the smallest positive root of the function (x is in radians) $x^2|\cos\sqrt{x}| = 5$ using the false-position method. To locate the region in which the root lies, first plot this function for values of x between 0 and 5. Perform the computation until ε_a falls below $\varepsilon_s = 1\%$. Check your final answer by substituting it into the original function.

5.10 Find the positive real root of $f(x) = x^4 - 8x^3 - 35x^2 + 450x - 1001$ using the false-position method. Use initial guesses of $x_l = 4.5$ and $x_u = 6$ and performs five iterations. Compute both the true and approximate errors based on the fact that the root is 5.60979. Use a plot to explain your results and perform the computation to within $\varepsilon_s = 1.0\%$.

5.11 Determine the real root of $x^{3.5} = 80$: **(a)** analytically, and **(b)** with the false-position method to within $\varepsilon_s = 2.5\%$. Use initial guesses of 2.0 and 5.0.

5.12 Given

$$f(x) = -2x^6 - 1.5x^4 + 10x + 2$$

Use bisection to determine the *maximum* of this function. Employ initial guesses of $x_l = 0$ and $x_u = 1$, and perform iterations until the approximate relative error falls below 5%.

5.13 The velocity v of a falling parachutist is given by

$$v = \frac{gm}{c}\left(1 - e^{-(c/m)t}\right)$$

where $g = 9.8\ \text{m/s}^2$. For a parachutist with a drag coefficient $c = 15$ kg/s, compute the mass m so that the velocity is $v = 35$ m/s at $t = 9$ s. Use the false-position method to determine m to a level of $\varepsilon_s = 0.1\%$.

5.14 A beam is loaded as shown in Fig. P5.14. Use the bisection method to solve for the position inside the beam where there is no moment.

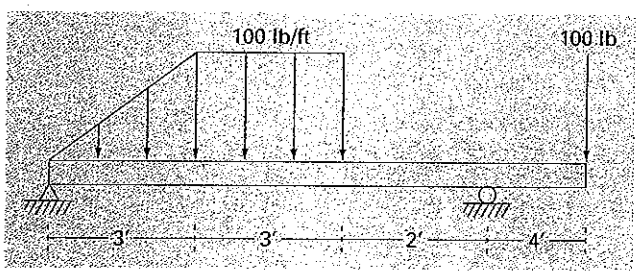

Figure P5.14

5.15 Water is flowing in a trapezoidal channel at a rate of $Q = 20\ \text{m}^3/\text{s}$. The critical depth y for such a channel must satisfy the equation

$$0 = 1 - \frac{Q^2}{gA_c^3}B$$

where $g = 9.81$ m/s^2, A_c = the cross-sectional area (m^2), and B = the width of the channel at the surface (m). For this case, the width and the cross-sectional area can be related to depth y by

$$B = 3 + y \qquad \text{and} \qquad A_c = 3y + \frac{y^2}{2}$$

Solve for the critical depth using **(a)** the graphical method, **(b)** bisection, and **(c)** false position. For **(b)** and **(c)** use initial guesses of $x_l = 0.5$ and $x_u = 2.5$, and iterate until the approximate error falls below 1% or the number of iterations exceeds 10. Discuss your results.

5.16 You are designing a spherical tank (Fig. P5.16) to hold water for a small village in a developing country. The volume of liquid it can hold can be computed as

$$V = \pi h^2 \frac{[3R - h]}{3} 2$$

where V = volume [m^3], h = depth of water in tank [m], and R = the tank radius [m].

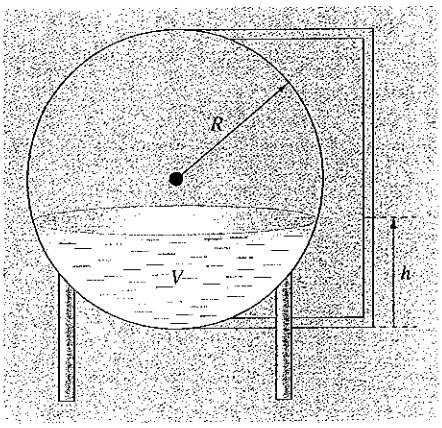

Figure P5.16

If $R = 3$ m, to what depth must the tank be filled so that it holds 30 m^3? Use three iterations of the false-position method to determine your answer. Determine the approximate relative error after each iteration.

5.17 The saturation concentration of dissolved oxygen in freshwater can be calculated with the equation (APHA, 1992)

$$\ln o_{sf} = -139.34411 + \frac{1.575701 \times 10^5}{T_a} - \frac{6.642308 \times 10^7}{T_a^2} + \frac{1.243800 \times 10^{10}}{T_a^3} - \frac{8.621949 \times 10^{11}}{T_a^4}$$

where o_{sf} = the saturation concentration of dissolved oxygen in freshwater at 1 atm (mg/L) and T_a = absolute temperature (K). Remember that $T_a = T + 273.15$, where T = temperature (°C). According to this equation, saturation decreases with increasing temperature. For typical natural waters in temperate climates, the equation can be used to determine that oxygen concentration ranges from 14.621 mg/L at 0°C to 6.413 mg/L at 40°C. Given a value of oxygen concentration, this formula and the bisection method can be used to solve for temperature in °C.

(a) If the initial guesses are set as 0 and 40°C, how many bisection iterations would be required to determine temperature to an absolute error of 0.05°C?

(b) Develop and test a bisection program to determine T as a function of a given oxygen concentration to a prespecified absolute error as in **(a)**. Given initial guesses of 0 and 40°C, test your program for an absolute error = 0.05°C and the following cases: $o_{sf} = 8$, 10 and 12 mg/L. Check your results.

5.18 Integrate the algorithm outlined in Fig. 5.10 into a complete, user-friendly bisection subprogram. Among other things:

(a) Place documentation statements throughout the subprogram to identify what each section is intended to accomplish.

(b) Label the input and output.

(c) Add an answer check that substitutes the root estimate into the original function to verify whether the final result is close to zero.

(d) Test the subprogram by duplicating the computations from Examples 5.3 and 5.4.

5.19 Develop a subprogram for the bisection method that minimizes function evaluations based on the pseudocode from Fig. 5.11. Determine the number of function evaluations (n) per total iterations. Test the program by duplicating Example 5.6.

5.20 Develop a user-friendly program for the false-position method. The structure of your program should be similar to the bisection algorithm outlined in Fig. 5.10. Test the program by duplicating Example 5.5.

5.21 Develop a subprogram for the false-position method that minimizes function evaluations in a fashion similar to Fig. 5.11. Determine the number of function evaluations (n) per total iterations. Test the program by duplicating Example 5.6.

5.22 Develop a user-friendly subprogram for the modified false-position method based on Fig. 5.15. Test the program by determining the root of the function described in Example 5.6. Perform a number of runs until the true percent relative error falls below 0.01%. Plot the true and approximate percent relative errors versus number of iterations on semilog paper. Interpret your results.

HAND OUT 8: Open methods (Chapter 2 of our syllabus). Source: Chapra, S. C., and Canale, R. P. (2006). *"Numerical methods for engineers."* McGraw-Hill, fifth edition.

CHAPTER 6

Open Methods

For the bracketing methods in the previous chapter, the root is located within an interval prescribed by a lower and an upper bound. Repeated application of these methods always results in closer estimates of the true value of the root. Such methods are said to be *convergent* because they move closer to the truth as the computation progresses (Fig. 6.1*a*).

In contrast, the *open methods* described in this chapter are based on formulas that require only a single starting value of x or two starting values that do not necessarily bracket

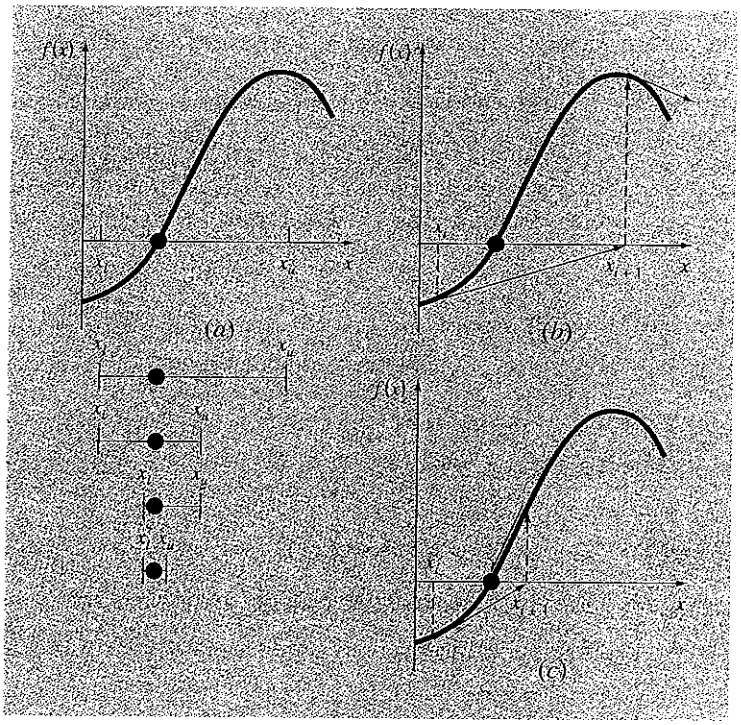

FIGURE 6.1
Graphical depiction of the fundamental difference between the (*a*) bracketing and (*b*) and (*c*) open methods for root location. In (*a*), which is the bisection method, the root is constrained within the interval prescribed by x_l and x_u. In contrast, for the open method depicted in (*b*) and (*c*), a formula is used to project from x_i to x_{i+1} in an iterative fashion. Thus, the method can either (*b*) diverge or (*c*) converge rapidly, depending on the value of the initial guess.

the root. As such, they sometimes *diverge* or move away from the true root as the computation progresses (Fig. 6.1*b*). However, when the open methods converge (Fig. 6.1*c*), they usually do so much more quickly than the bracketing methods. We will begin our discussion of open techniques with a simple version that is useful for illustrating their general form and also for demonstrating the concept of convergence.

6.1 SIMPLE FIXED-POINT ITERATION

As mentioned above, open methods employ a formula to predict the root. Such a formula can be developed for simple *fixed-point iteration* (or, as it is also called, one-point iteration or successive substitution) by rearranging the function $f(x) = 0$ so that x is on the left-hand side of the equation:

$$x = g(x) \tag{6.1}$$

This transformation can be accomplished either by algebraic manipulation or by simply adding x to both sides of the original equation. For example,

$$x^2 - 2x + 3 = 0$$

can be simply manipulated to yield

$$x = \frac{x^2 + 3}{2}$$

whereas $\sin x = 0$ could be put into the form of Eq. (6.1) by adding x to both sides to yield

$$x = \sin x + x$$

The utility of Eq. (6.1) is that it provides a formula to predict a new value of x as a function of an old value of x. Thus, given an initial guess at the root x_i, Eq. (6.1) can be used to compute a new estimate x_{i+1} as expressed by the iterative formula

$$x_{i+1} = g(x_i) \tag{6.2}$$

As with other iterative formulas in this book, the approximate error for this equation can be determined using the error estimator [Eq. (3.5)]:

$$\varepsilon_a = \left| \frac{x_{i+1} - x_i}{x_{i+1}} \right| 100\%$$

EXAMPLE 6.1 Simple Fixed-Point Iteration

Problem Statement. Use simple fixed-point iteration to locate the root of $f(x) = e^{-x} - x$.

Solution. The function can be separated directly and expressed in the form of Eq. (6.2) as

$$x_{i+1} = e^{-x_i}$$

Starting with an initial guess of $x_0 = 0$, this iterative equation can be applied to compute

i	x_i	ε_a (%)	ε_t (%)
0	0		100.0
1	1.000000	100.0	76.3
2	0.367879	171.8	35.1
3	0.692201	46.9	22.1
4	0.500473	38.3	11.8
5	0.606244	17.4	6.89
6	0.545396	11.2	3.83
7	0.579612	5.90	2.20
8	0.560115	3.48	1.24
9	0.571143	1.93	0.705
10	0.564879	1.11	0.399

Thus, each iteration brings the estimate closer to the true value of the root: 0.56714329.

6.1.1 Convergence

Notice that the true percent relative error for each iteration of Example 6.1 is roughly proportional (by a factor of about 0.5 to 0.6) to the error from the previous iteration. This property, called *linear convergence,* is characteristic of fixed-point iteration.

Aside from the "rate" of convergence, we must comment at this point about the "possibility" of convergence. The concepts of convergence and divergence can be depicted graphically. Recall that in Sec. 5.1, we graphed a function to visualize its structure and behavior (Example 5.1). Such an approach is employed in Fig. 6.2*a* for the function $f(x) = e^{-x} - x$. An alternative graphical approach is to separate the equation into two component parts, as in

$$f_1(x) = f_2(x)$$

Then the two equations

$$y_1 = f_1(x) \tag{6.3}$$

and

$$y_2 = f_2(x) \tag{6.4}$$

can be plotted separately (Fig. 6.2*b*). The x values corresponding to the intersections of these functions represent the roots of $f(x) = 0$.

EXAMPLE 6.2 The Two-Curve Graphical Method

Problem Statement. Separate the equation $e^{-x} - x = 0$ into two parts and determine its root graphically.

Solution. Reformulate the equation as $y_1 = x$ and $y_2 = e^{-x}$. The following values can be computed:

x	y_1	y_2
0.0	0.0	1.000
0.2	0.2	0.819
0.4	0.4	0.670
0.6	0.6	0.549
0.8	0.8	0.449
1.0	1.0	0.368

These points are plotted in Fig. 6.2*b*. The intersection of the two curves indicates a root estimate of approximately $x = 0.57$, which corresponds to the point where the single curve in Fig. 6.2*a* crosses the x axis.

FIGURE 6.2
Two alternative graphical methods for determining the root of $f(x) = e^{-x} - x$. (*a*) Root at the point where it crosses the x axis; (*b*) root at the intersection of the component functions.

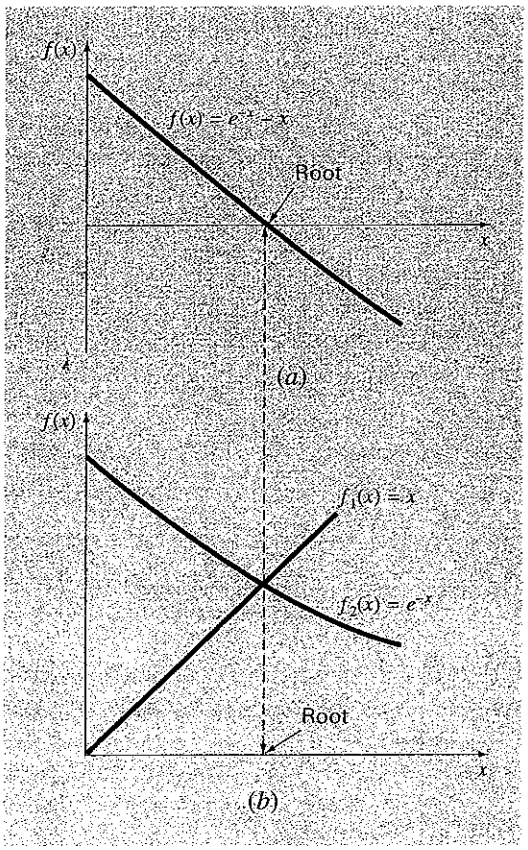

The two-curve method can now be used to illustrate the convergence and divergence of fixed-point iteration. First, Eq. (6.1) can be re-expressed as a pair of equations $y_1 = x$ and $y_2 = g(x)$. These two equations can then be plotted separately. As was the case with Eqs. (6.3) and (6.4), the roots of $f(x) = 0$ correspond to the abscissa value at the intersection of the two curves. The function $y_1 = x$ and four different shapes for $y_2 = g(x)$ are plotted in Fig. 6.3.

For the first case (Fig. 6.3*a*), the initial guess of x_0 is used to determine the corresponding point on the y_2 curve $[x_0, g(x_0)]$. The point (x_1, x_1) is located by moving left horizontally to the y_1 curve. These movements are equivalent to the first iteration in the fixed-point method:

$$x_1 = g(x_0)$$

Thus, in both the equation and in the plot, a starting value of x_0 is used to obtain an estimate of x_1. The next iteration consists of moving to $[x_1, g(x_1)]$ and then to (x_2, x_2). This iteration

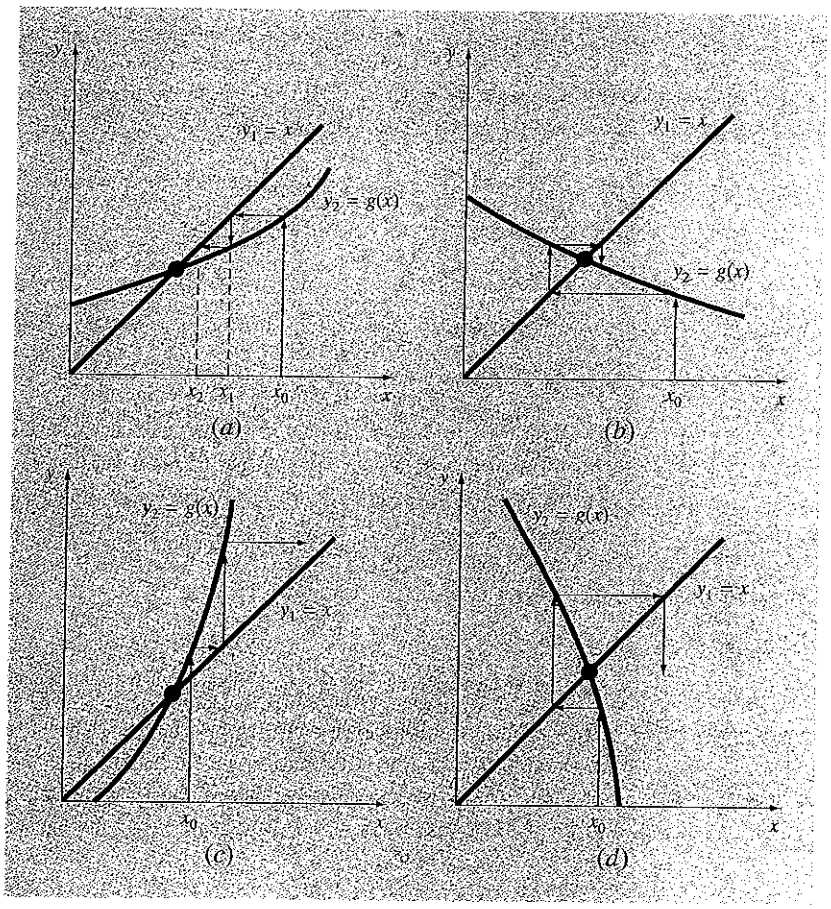

FIGURE 6.3
Graphical depiction of (*a*) and (*b*) convergence and (*c*) and (*d*) divergence of simple fixed-point iteration. Graphs (*a*) and (*c*) are called monotone patterns, whereas (*b*) and (*d*) are called oscillating or spiral patterns. Note that convergence occurs when $|g'(x)| < 1$.

Box 6.1 Convergence of Fixed-Point Iteration

From studying Fig. 6.3, it should be clear that fixed-point iteration converges if, in the region of interest, $|g'(x)| < 1$. In other words, convergence occurs if the magnitude of the slope of $g(x)$ is less than the slope of the line $f(x) = x$. This observation can be demonstrated theoretically. Recall that the iterative equation is

$$x_{i+1} = g(x_i)$$

Suppose that the true solution is

$$x_r = g(x_r)$$

Subtracting these equations yields

$$x_r - x_{i+1} = g(x_r) - g(x_i) \tag{B6.1.1}$$

The *derivative mean-value theorem* (recall Sec. 4.1.1) states that if a function $g(x)$ and its first derivative are continuous over an interval $a \le x \le b$, then there exists at least one value of $x = \xi$ within the interval such that

$$g'(\xi) = \frac{g(b) - g(a)}{b - a} \tag{B6.1.2}$$

The right-hand side of this equation is the slope of the line joining $g(a)$ and $g(b)$. Thus, the mean-value theorem states that there is at least one point between a and b that has a slope, designated by $g'(\xi)$, which is parallel to the line joining $g(a)$ and $g(b)$ (recall Fig. 4.3).

Now, if we let $a = x_i$ and $b = x_r$, the right-hand side of Eq. (B6.1.1) can be expressed as

$$g(x_r) - g(x_i) = (x_r - x_i)g'(\xi)$$

where ξ is somewhere between x_i and x_r. This result can then be substituted into Eq. (B6.1.1) to yield

$$x_r - x_{i+1} = (x_r - x_i)g'(\xi) \tag{B6.1.3}$$

If the true error for iteration i is defined as

$$E_{t,i} = x_r - x_i$$

then Eq. (B6.1.3) becomes

$$E_{t,i+1} = g'(\xi)E_{t,i}$$

Consequently, if $|g'(x)| < 1$, the errors decrease with each iteration. For $|g'(x)| > 1$, the errors grow. Notice also that if the derivative is positive, the errors will be positive, and hence, the iterative solution will be monotonic (Fig. 6.3*a* and *c*). If the derivative is negative, the errors will oscillate (Fig. 6.3*b* and *d*).

An offshoot of the analysis is that it also demonstrates that when the method converges, the error is roughly proportional to and less than the error of the previous step. For this reason, simple fixed-point iteration is said to be *linearly convergent*.

is equivalent to the equation

$$x_2 = g(x_1)$$

The solution in Fig. 6.3*a* is *convergent* because the estimates of x move closer to the root with each iteration. The same is true for Fig. 6.3*b*. However, this is not the case for Fig. 6.3*c* and *d*, where the iterations diverge from the root. Notice that convergence seems to occur only when the absolute value of the slope of $y_2 = g(x)$ is less than the slope of $y_1 = x$, that is, when $|g'(x)| < 1$. Box 6.1 provides a theoretical derivation of this result.

6.1.2 Algorithm for Fixed-Point Iteration

The computer algorithm for fixed-point iteration is extremely simple. It consists of a loop to iteratively compute new estimates until the termination criterion has been met. Figure 6.4 presents pseudocode for the algorithm. Other open methods can be programmed in a similar way, the major modification being to change the iterative formula that is used to compute the new root estimate.

```
FUNCTION Fixpt(x0, es, imax, iter, ea)
  xr = x0
  iter = 0
  DO
    xrold = xr
    xr = g(xrold)
    iter = iter + 1
    IF xr ≠ 0 THEN
      ea = |(xr - xrold)/xr| · 100
    END IF
    IF ea < es OR iter ≥ imax EXIT
  END DO
  Fixpt = xr
END Fixpt
```

FIGURE 6.4
Pseudocode for fixed-point iteration. Note that other open methods can be cast in this general format.

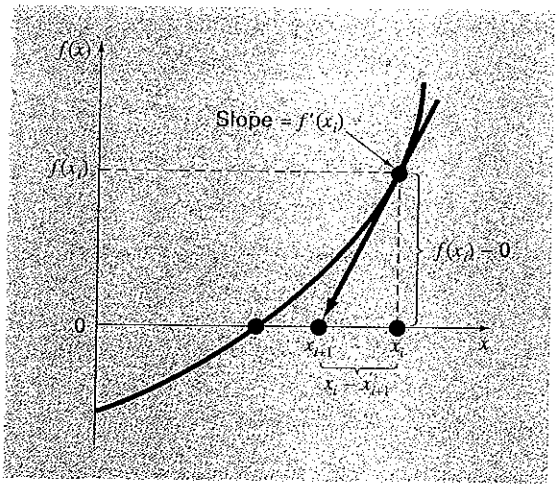

FIGURE 6.5
Graphical depiction of the Newton-Raphson method. A tangent to the function of x_i [that is, $f'(x_i)$] is extrapolated down to the x axis to provide an estimate of the root at x_{i+1}.

6.2 THE NEWTON-RAPHSON METHOD

Perhaps the most widely used of all root-locating formulas is the Newton-Raphson equation (Fig. 6.5). If the initial guess at the root is x_i, a tangent can be extended from the point $[x_i, f(x_i)]$. The point where this tangent crosses the x axis usually represents an improved estimate of the root.

The Newton-Raphson method can be derived on the basis of this geometrical interpretation (an alternative method based on the Taylor series is described in Box 6.2). As in Fig. 6.5, the first derivative at x is equivalent to the slope:

$$f'(x_i) = \frac{f(x_i) - 0}{x_i - x_{i+1}} \tag{6.5}$$

which can be rearranged to yield

$$x_{i+1} = x_i - \frac{f(x_i)}{f'(x_i)} \tag{6.6}$$

which is called the *Newton-Raphson formula.*

EXAMPLE 6.3 Newton-Raphson Method

Problem Statement. Use the Newton-Raphson method to estimate the root of $f(x) = e^{-x} - x$, employing an initial guess of $x_0 = 0$.

Solution. The first derivative of the function can be evaluated as

$$f'(x) = -e^{-x} - 1$$

which can be substituted along with the original function into Eq. (6.6) to give

$$x_{i+1} = x_i - \frac{e^{-x_i} - x_i}{-e^{-x_i} - 1}$$

Starting with an initial guess of $x_0 = 0$, this iterative equation can be applied to compute

i	x_i	ε_t (%)
0	0	100
1	0.500000000	11.8
2	0.566311003	0.147
3	0.567143165	0.0000220
4	0.567143290	$< 10^{-8}$

Thus, the approach rapidly converges on the true root. Notice that the true percent relative error at each iteration decreases much faster than it does in simple fixed-point iteration (compare with Example 6.1).

6.2.1 Termination Criteria and Error Estimates

As with other root-location methods, Eq. (3.5) can be used as a termination criterion. In addition, however, the Taylor series derivation of the method (Box 6.2) provides theoretical insight regarding the rate of convergence as expressed by $E_{i+1} = O(E_i^2)$. Thus the error should be roughly proportional to the square of the previous error. In other words, the

Box 6.2 Derivation and Error Analysis of the Newton-Raphson Method

Aside from the geometric derivation [Eqs. (6.5) and (6.6)], the Newton-Raphson method may also be developed from the Taylor series expansion. This alternative derivation is useful in that it also provides insight into the rate of convergence of the method.

Recall from Chap. 4 that the Taylor series expansion can be represented as

$$f(x_{i+1}) = f(x_i) + f'(x_i)(x_{i+1} - x_i) + \frac{f''(\xi)}{2!}(x_{i+1} - x_i)^2 \tag{B6.2.1}$$

where ξ lies somewhere in the interval from x_i to x_{i+1}. An approximate version is obtainable by truncating the series after the first derivative term:

$$f(x_{i+1}) \cong f(x_i) + f'(x_i)(x_{i+1} - x_i)$$

At the intersection with the x axis, $f(x_{i+1})$ would be equal to zero, or

$$0 = f(x_i) + f'(x_i)(x_{i+1} - x_i) \tag{B6.2.2}$$

which can be solved for

$$x_{i+1} = x_i - \frac{f(x_i)}{f'(x_i)}$$

which is identical to Eq. (6.6). Thus, we have derived the Newton-Raphson formula using a Taylor series.

Aside from the derivation, the Taylor series can also be used to estimate the error of the formula. This can be done by realizing that if the complete Taylor series were employed, an exact result would be obtained. For this situation $x_{i+1} = x_r$, where x is the true value of the root. Substituting this value along with $f(x_r) = 0$ into Eq. (B6.2.1) yields

$$0 = f(x_i) + f'(x_i)(x_r - x_i) + \frac{f''(\xi)}{2!}(x_r - x_i)^2 \tag{B6.2.3}$$

Equation (B6.2.2) can be subtracted from Eq. (B6.2.3) to give

$$0 = f'(x_i)(x_r - x_{i+1}) + \frac{f''(\xi)}{2!}(x_r - x_i)^2 \tag{B6.2.4}$$

Now, realize that the error is equal to the discrepancy between x_{i+1} and the true value x_r, as in

$$E_{t,i+1} = x_r - x_{i+1}$$

and Eq. (B6.2.4) can be expressed as

$$0 = f'(x_i)E_{t,i+1} + \frac{f''(\xi)}{2!}E_{t,i}^2 \tag{B6.2.5}$$

If we assume convergence, both x_i and ξ should eventually be approximated by the root x_r, and Eq. (B6.2.5) can be rearranged to yield

$$E_{t,i+1} = \frac{-f''(x_r)}{2f'(x_r)}E_{t,i}^2 \tag{B6.2.6}$$

According to Eq. (B6.2.6), the error is roughly proportional to the square of the previous error. This means that the number of correct decimal places approximately doubles with each iteration. Such behavior is referred to as *quadratic convergence*. Example 6.4 manifests this property.

number of significant figures of accuracy approximately doubles with each iteration. This behavior is examined in the following example.

EXAMPLE 6.4 Error Analysis of Newton-Raphson Method

Problem Statement. As derived in Box 6.2, the Newton-Raphson method is quadratically convergent. That is, the error is roughly proportional to the square of the previous error, as in

$$E_{t,i+1} \cong \frac{-f''(x_r)}{2f'(x_r)}E_{t,i}^2 \tag{E6.4.1}$$

Examine this formula and see if it applies to the results of Example 6.3.

Solution. The first derivative of $f(x) = e^{-x} - x$ is

$$f'(x) = -e^{-x} - 1$$

which can be evaluated at $x_r = 0.56714329$ as $f'(0.56714329) = -1.56714329$. The second derivative is

$$f''(x) = e^{-x}$$

which can be evaluated as $f''(0.56714329) = 0.56714329$. These results can be substituted into Eq. (E6.4.1) to yield

$$E_{t,i+1} \cong -\frac{0.56714329}{2(-1.56714329)} E_{t,i}^2 = 0.18095 E_{t,i}^2$$

From Example 6.3, the initial error was $E_{t,0} = 0.56714329$, which can be substituted into the error equation to predict

$$E_{t,1} \cong 0.18095(0.56714329)^2 = 0.0582$$

which is close to the true error of 0.06714329. For the next iteration,

$$E_{t,2} \cong 0.18095(0.06714329)^2 = 0.0008158$$

which also compares favorably with the true error of 0.0008323. For the third iteration,

$$E_{t,3} \cong 0.18095(0.0008323)^2 = 0.000000125$$

which is the error obtained in Example 6.3. The error estimate improves in this manner because, as we come closer to the root, x and ξ are better approximated by x_r [recall our assumption in going from Eq. (B6.2.5) to Eq. (B6.2.6) in Box 6.2]. Finally,

$$E_{t,4} \cong 0.18095(0.000000125)^2 = 2.83 \times 10^{-15}$$

Thus, this example illustrates that the error of the Newton-Raphson method for this case is, in fact, roughly proportional (by a factor of 0.18095) to the square of the error of the previous iteration.

6.2.2 Pitfalls of the Newton-Raphson Method

Although the Newton-Raphson method is often very efficient, there are situations where it performs poorly. A special case—multiple roots—will be addressed later in this chapter. However, even when dealing with simple roots, difficulties can also arise, as in the following example.

EXAMPLE 6.5 Example of a Slowly Converging Function with Newton-Raphson

Problem Statement. Determine the positive root of $f(x) = x^{10} - 1$ using the Newton-Raphson method and an initial guess of $x = 0.5$.

Solution. The Newton-Raphson formula for this case is

$$x_{i+1} = x_i - \frac{x_i^{10} - 1}{10x_i^9}$$

which can be used to compute

Iteration	x
0	0.5
1	51.65
2	46.485
3	41.8365
4	37.65285
5	33.887565
.	
.	
.	
∞	1.0000000

Thus, after the first poor prediction, the technique is converging on the true root of 1, but at a very slow rate.

Aside from slow convergence due to the nature of the function, other difficulties can arise, as illustrated in Fig. 6.6. For example, Fig. 6.6*a* depicts the case where an inflection point [that is, $f''(x) = 0$] occurs in the vicinity of a root. Notice that iterations beginning at x_0 progressively diverge from the root. Figure 6.6*b* illustrates the tendency of the Newton-Raphson technique to oscillate around a local maximum or minimum. Such oscillations may persist, or as in Fig. 6.6*b*, a near-zero slope is reached, whereupon the solution is sent far from the area of interest. Figure 6.6*c* shows how an initial guess that is close to one root can jump to a location several roots away. This tendency to move away from the area of interest is because near-zero slopes are encountered. Obviously, a zero slope [$f'(x) = 0$] is truly a disaster because it causes division by zero in the Newton-Raphson formula [Eq. (6.6)]. Graphically (see Fig 6.6*d*), it means that the solution shoots off horizontally and never hits the x axis.

Thus, there is no general convergence criterion for Newton-Raphson. Its convergence depends on the nature of the function and on the accuracy of the initial guess. The only remedy is to have an initial guess that is "sufficiently" close to the root. And for some functions, no guess will work! Good guesses are usually predicated on knowledge of the physical problem setting or on devices such as graphs that provide insight into the behavior of the solution. The lack of a general convergence criterion also suggests that good computer software should be designed to recognize slow convergence or divergence. The next section addresses some of these issues.

6.2.3 Algorithm for Newton-Raphson

An algorithm for the Newton-Raphson method is readily obtained by substituting Eq. (6.6) for the predictive formula [Eq. (6.2)] in Fig. 6.4. Note, however, that the program must also be modified to compute the first derivative. This can be simply accomplished by the inclusion of a user-defined function.

Additionally, in light of the foregoing discussion of potential problems of the Newton-Raphson method, the program would be improved by incorporating several additional features:

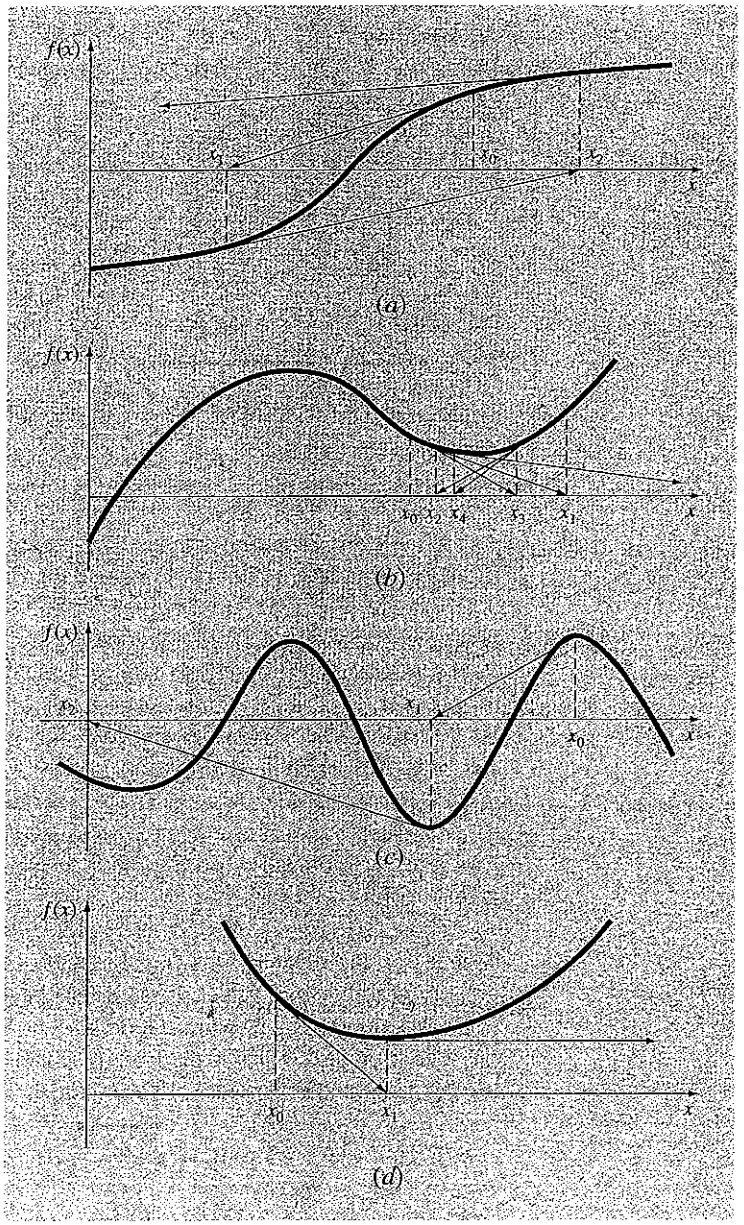

FIGURE 6.6
Four cases where the Newton-Raphson method exhibits poor convergence.

1. A plotting routine should be included in the program.
2. At the end of the computation, the final root estimate should always be substituted into the original function to compute whether the result is close to zero. This check partially guards against those cases where slow or oscillating convergence may lead to a small value of ε_a while the solution is still far from a root.
3. The program should always include an upper limit on the number of iterations to guard against oscillating, slowly convergent, or divergent solutions that could persist interminably.
4. The program should alert the user and take account of the possibility that $f'(x)$ might equal zero at any time during the computation.

6.3 THE SECANT METHOD

A potential problem in implementing the Newton-Raphson method is the evaluation of the derivative. Although this is not inconvenient for polynomials and many other functions, there are certain functions whose derivatives may be extremely difficult or inconvenient to evaluate. For these cases, the derivative can be approximated by a backward finite divided difference, as in (Fig. 6.7)

$$f'(x_i) \cong \frac{f(x_{i-1}) - f(x_i)}{x_{i-1} - x_i}$$

FIGURE 6.7
Graphical depiction of the secant method. This technique is similar to the Newton-Raphson technique (Fig. 6.5) in the sense that an estimate of the root is predicted by extrapolating a tangent of the function to the x axis. However, the secant method uses a difference rather than a derivative to estimate the slope.

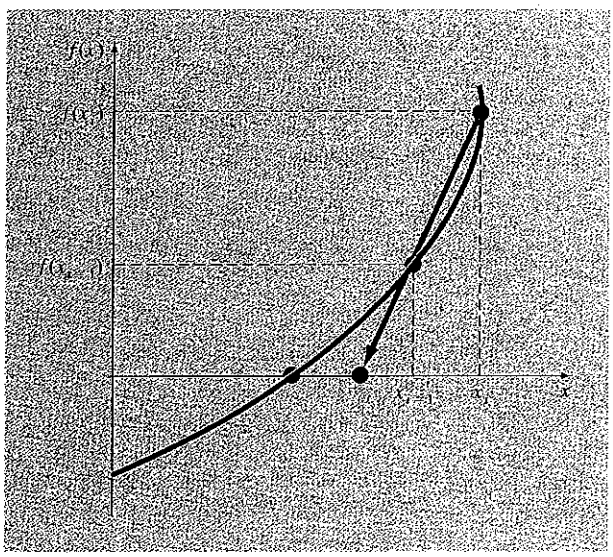

HAND OUT 9: Behavior of the Colebrook-White equation (Chapter 2 of our syllabus).

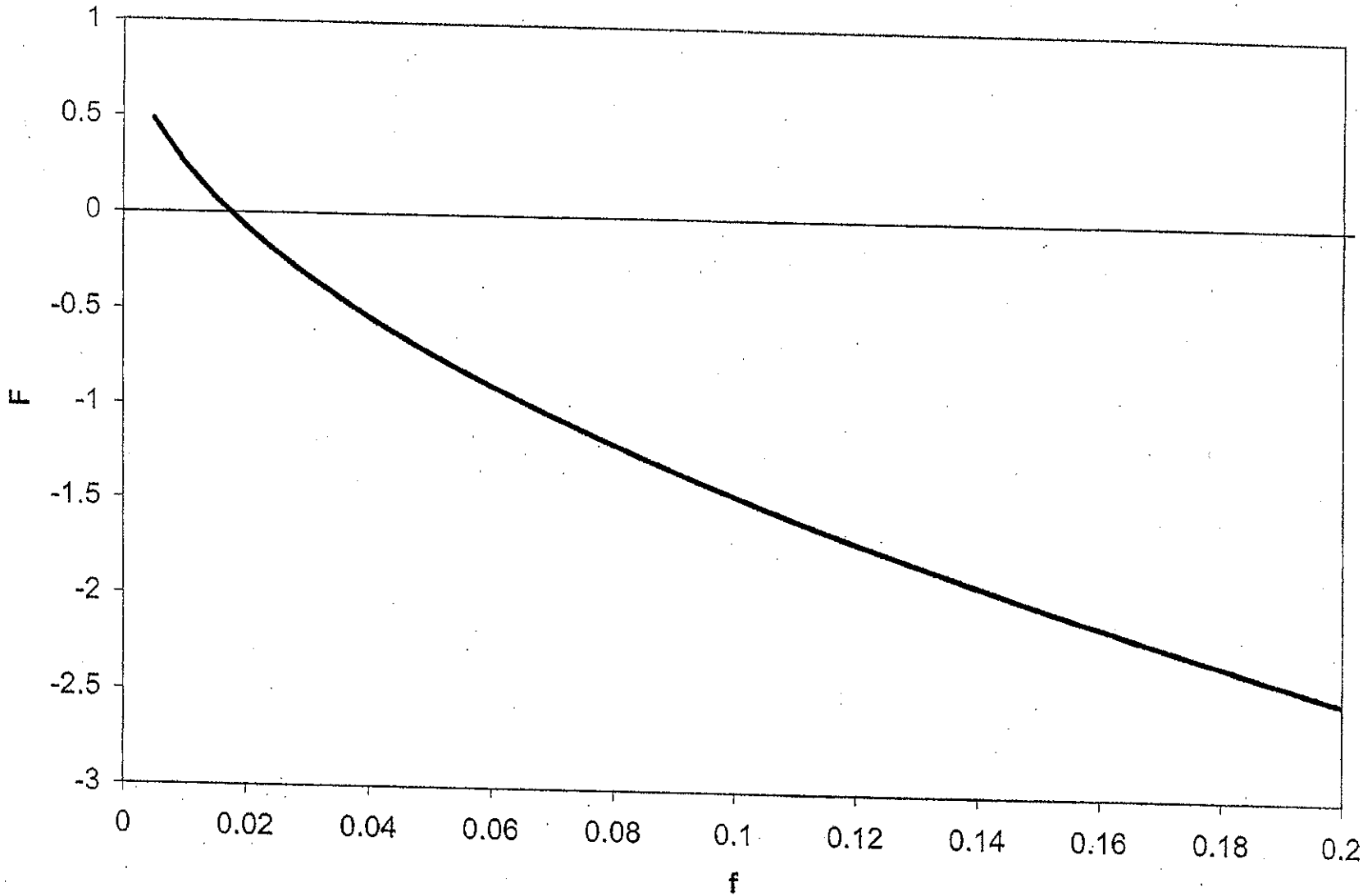
1
0.5
0
-0.5
-1
-1.5
-2
-2.5
-3
F
0
0.02
0.04
0.06
0.08
0.1
0.12
0.14
0.16
0.18
0.2
f

HAND OUT 10: Example of the behavior of the Iteration of a point method (Chapter 2 of our syllabus).

Example of point iteration:

$$F(x) = x^3 - x - 5 = 0$$

x	$F(x)$
1.9	−0.041
2.0	1.0

Alternatives:

(I) $x = x^3 - 5$

(II) $x = \dfrac{5}{x^2 - 1}$

(III) $x = \sqrt[3]{x+5}$

$$x_{k+1} = \varphi(x_k)$$

$$x_0 = 1.9$$

(I)	(II)	(III)
1.859	1.9157088	1.90378
1.42448	1.87270	1.90413
−2.10951	1.99441	1.90416
−14.38738	1.87916	1.90416
−2983.1451	1.635769	

↑

HAND OUT 11: Picture of flow in the Hayden-Rhodes Aqueduct, Central Arizona Project (Chapter 2 of our syllabus). Source: Mays, L. (2006). *"Water resources engineering."* John Wiley and Sons.

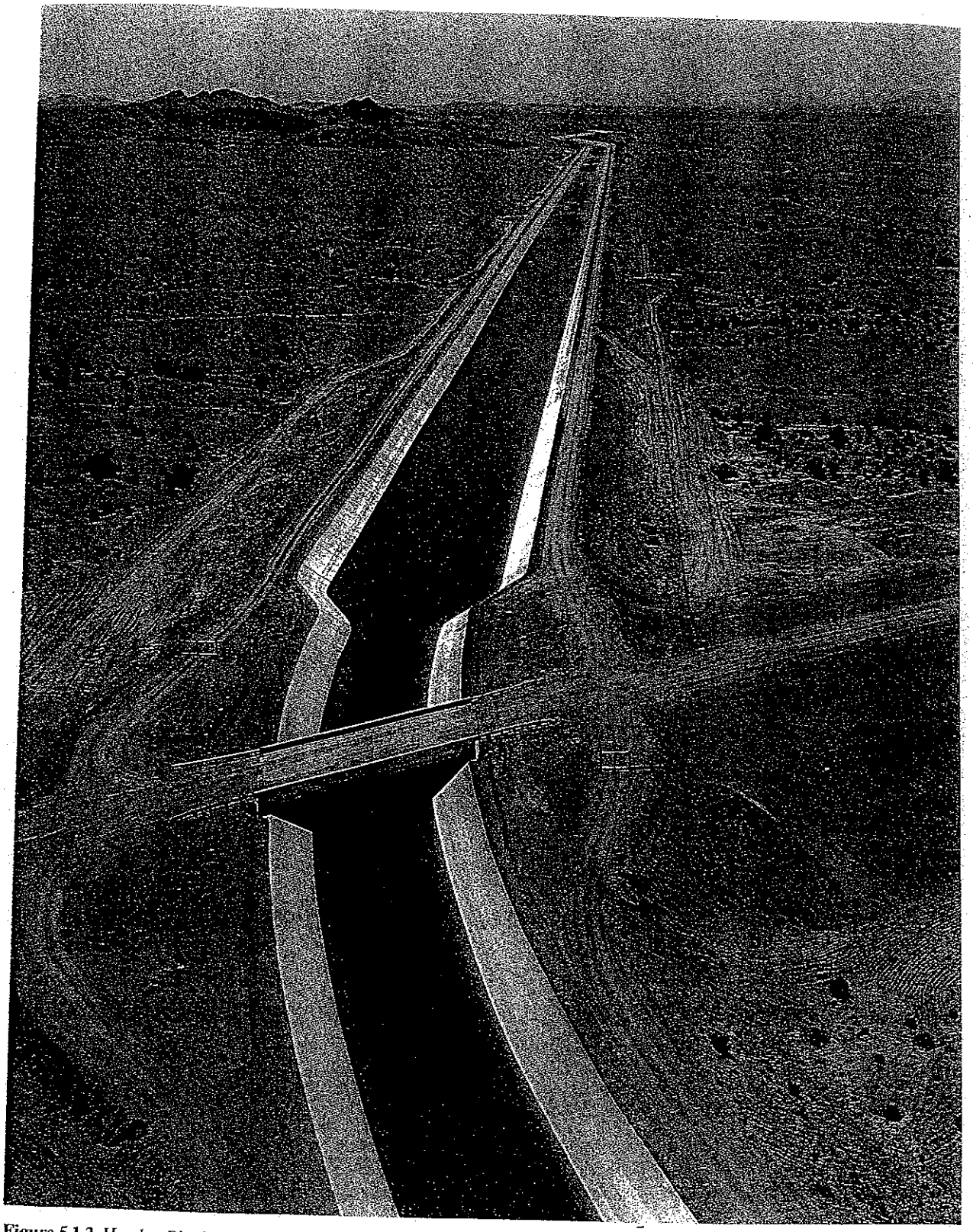

Figure 5.1.2 Hayden-Rhodes Aqueduct, Central Arizona Project. (Courtesy of the U.S. Bureau of Reclamation, (1985), photograph by Joe Madrigal Jr.)

HAND OUT 12: Picture of pollution (Chapter 4 of our syllabus). Source: Cover of the book by Altinakar, M., and Graf, W. (1998). *"Fluvial Hydraulics."* John Wiley and Sons.

HAND OUT 13: Description of the LAKE model (Chapter 4 of our syllabus).
Source: ILEC, International Lake Environment Committee.

Model description

Lake Model consists of a combination of two kinds of models: a causal dynamical model, and a set of associated empirical models. The dynamical model integrates the pools nitrogen and phosphorus in water and sediment in time as functions of the massflows. The empirical models are simple regressions made from data of simple physical and chemical characteristics of a number of lakes.

The dynamical model is a modification of the general model made by Vollenweider (1975). While Vollenweiders model was only concerned with phosphorus, which is the limiting nutrient in most freshwater bodies, *Lake Model* has included nitrogen as well. The conceptual diagram for *Lake Model* is shown below.

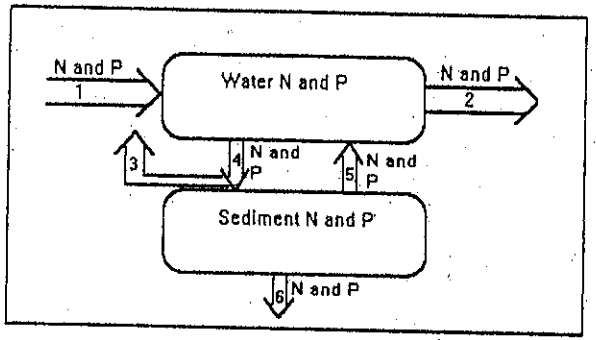

The nitrogen and the phosphorus submodels are almost identical. The only difference is the denitrification process included in the nitrogen submodel.

The mathematical formulation of the nitrogen submodel, referring to the numbers in the diagram:

1) Nload/z	(loading, mg/l/year)
2) (1/Wres) * Nwat * a	(hydraulic outwash, mg/l/year)
3) Denit/z	(denitrification, mg/l/year)
4) NWat * SedRate /z	(sedimentation, mg/l/year)
5) NSed * NRel/z	(sediment release, mg/l/year)
6) (1-NBound) * Nsed	(demobilization from sediment, g/m²/year)

These processes form the two differential equations :

$$\frac{dNwat}{dt} = \left((Nload - Denit) + Nrel * NSed\right)/z * (1/Wres) * Nwat * a - (1/z) * SedRate * Nwat$$

$$\frac{dNSed}{dt} = SedRate * Nwat * (1 - NBound) - Nrel * Nsed$$

where

NWat is total nitrogen (mg/l) in the water column.
Nsed is nitrogen (g/m²) in sediment.
Nload is the nitrogen input (g/m²/year) to the lake
Nrel is the sediment release rate (/year) of nitrogen.
Nbound is the ratio of immobilized sedimentated nitrogen.
z is mean depth (m) of the lake.
Wres is the mean residence time (year) of the water.
SedRate is the mean sedimentation rate. (m/year)
a is a correction factor of nutrient output due to thermocline formation.

Note that the units for the sediment pools are g/m² and mg/l for the water column pools. The denitrification is described by the empirical model:

$$Denit = NLoad \cdot 0.34 * Wres^{-0.16} * z^{0.17}$$

Except for the denitrification, the phosphorus submodel is formulated analogous to the nitrogen submodel. The equations are

$$\frac{dPWat}{dt} = (Pload + Prel * Psed) / z \cdot 1 / Wres * Pwat * a \cdot 1/z * SedRate * Pwat$$

$$\frac{dPSed}{dt} = SedRate * Pwat * (1 - PBound) - Prel * Psed$$

where

PWat is total nitrogen (mg/l) in the water column.
Psed is nitrogen (g/m²) in sediment.
Pload is the nitrogen input (g/m²/year) to the lake.
Prel is the sediment release rate (/year) of nitrogen.
Pbound is the immobilized ratio of sedimentated nitrogen.

The empirical models are a number af relations made from statistical regression analyses (Edmondson, 1986).

= 0.810 * (TP * 1000)^0.71

Average primary production (mg/l/day) = (10000 * TP - 79)/1000

Maximum primary production (mg/l/day) = (20000 * TP - 77)/1000

Average fish yield (mg ww/m^2/year) = 7.1 * TP

TP is the total phosphorus. *Lake Model* is supplied with an algorithm to decide if phosphorus and/or nitrogen are limiting nutrients to the phytoplankton growth. The algorithm is based on the knowledge about the mean internal cell ratios of nutrients in phytoplankton. The algorithm is based on the following rules:

If total N >= 10 * total P then P is the limiting nutrient

If total N <= 5 * total P then N is the limiting nutrient

If 5 < total N <10 * total P then P is the limiting nutrient

1159 *Limnol. Oceanogr.* 31(5).

Jensen, J. P., P. Kristensen and E. Jeppesen. 1990. Relationship betweer nitrogen loading and in-lake nitrogen concentrations in shallow Danisl lakes. Verh. Internat. Verein. Limn. 24 pp. 201-204

Vollenweider, R. A. 1975. Input-output models with special reference to the phosphorus loading concept in limnology. *Schweitz Z. Hydrol.*, 37 pp. 53 84

HAND OUT 14: Flood reservoir routing (Chapter 5 of our syllabus). Source: Adapted from classes from Prof. Bedient of Rice University.

Review of Flood Reservoir Routing

Modified from classes by Philip B. Bedient
Rice University

Mansfield Dam, Austin, Texas

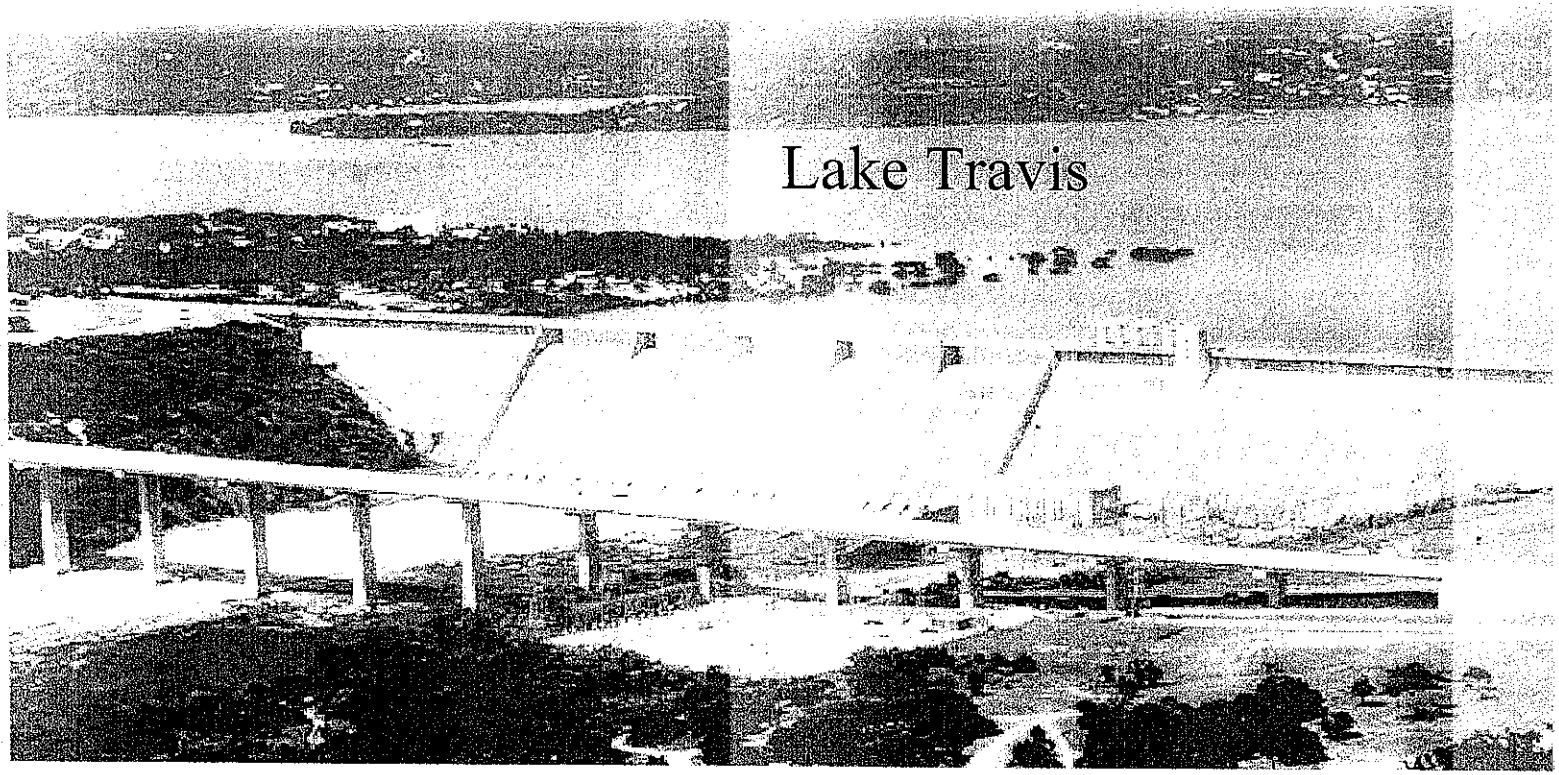

Mansfield Dam, Hill Country of Texas

Reservoir Routing

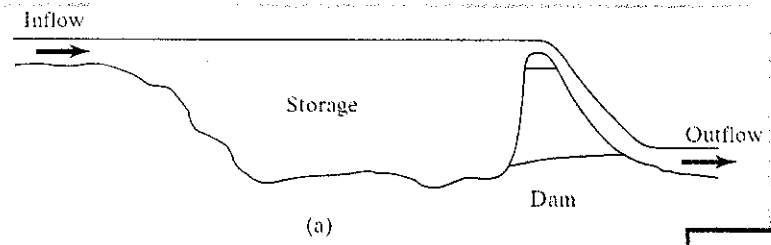

(a)

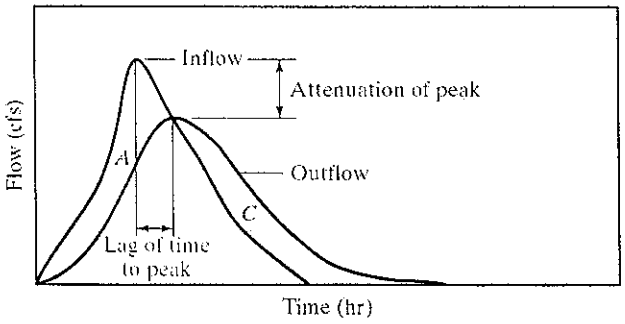

(b)

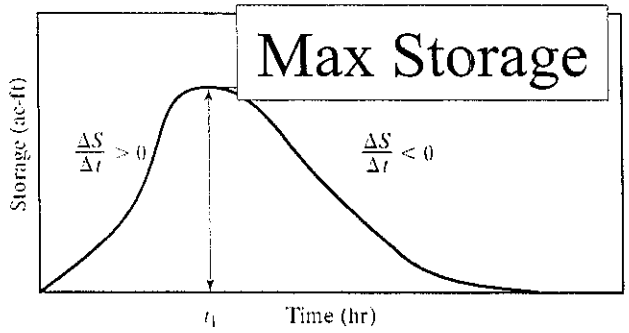

(c)

- **Reservoir acts storing water, and releasing it through the control structure with a certain delay**
- **Inflow hydrograph**
- **Outflow hydrograph**
- **Storage - Discharge Rel'n**
- **Outflow peaks are reduced**
- **Outflow timing is delayed**

Inflow and Outflow

$$I - Q = \frac{dS}{dt}$$

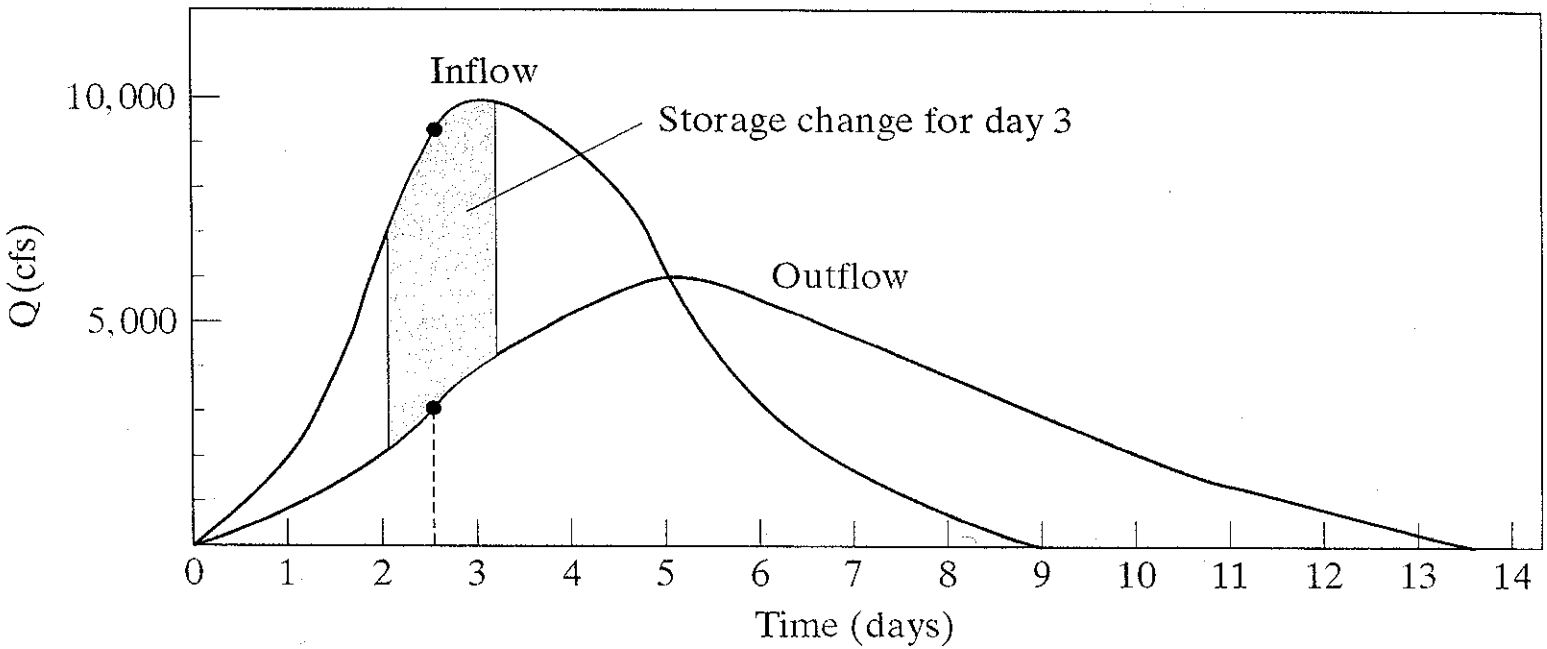

Figure E4.1(a)

Inflow and Outflow

= change in storage / time

$$(I_2 + I_3)/2 - (Q_2 + Q_3)/2 = \frac{S_3 - S_2}{dt}$$

Re Repeat for each day

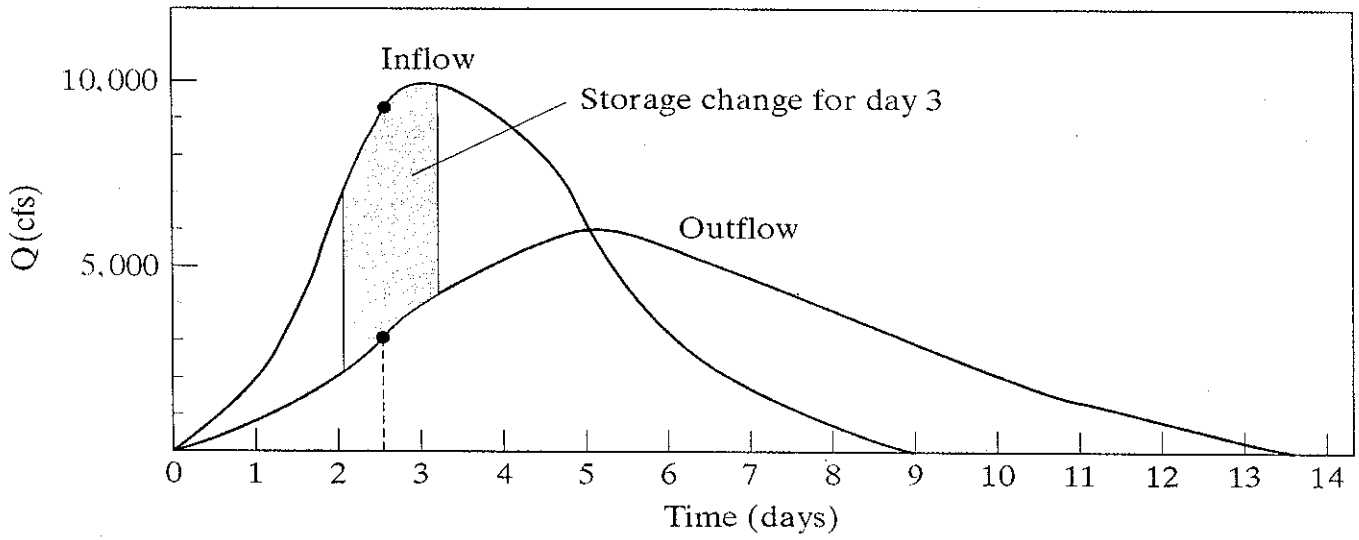

Figure E4.1(a)

Determining Storage

- Evaluate surface area at several different depths
- Use available topographic maps or GIS based DEM sources
- Outflows can be computed as function of depth for either pipes, orifices, or weirs

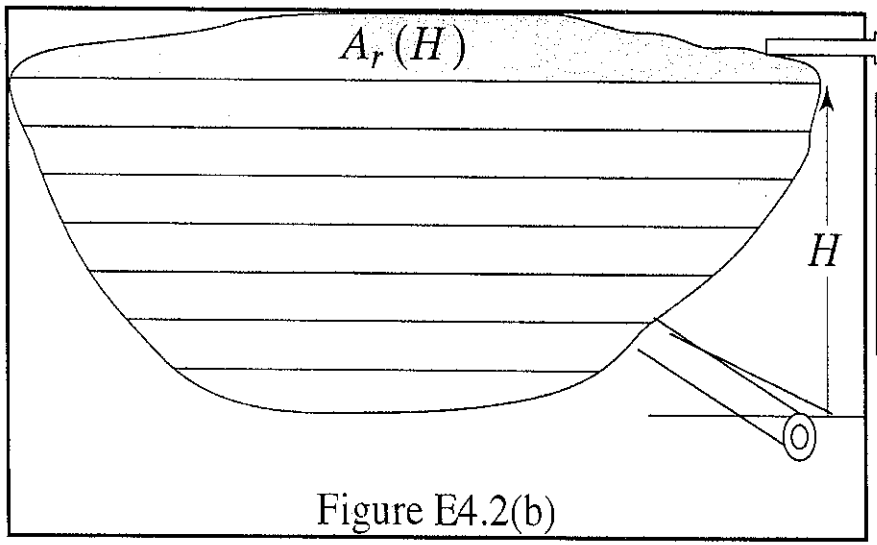

Figure E4.2(b)

$$Q = CA\sqrt{2gH} \text{ for orifice flow}$$

$$Q = CLH^{3/2} \text{ for weir flow}$$

Typical Storage -Outflow

- Plot of Storage in acre-ft vs. Outflow in cfs
- Storage is largely a function of topography
- Outflows can be computed as function of elevation for either pipes or weirs

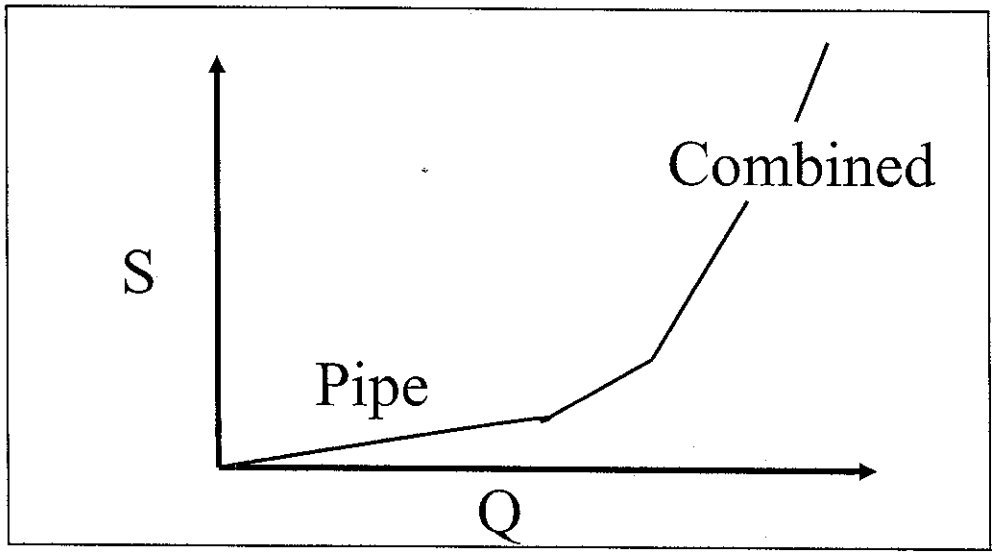

Reservoir Routing

$$I_1 + I_2 + \left(\frac{2S_1}{dt} - Q_1\right) = \left(\frac{2S_2}{dt} + Q_2\right)$$

1. **LHS of Eqn is known**
2. **Know S as fcn of Q**
3. **Solve Eqn for RHS**
4. **Solve for Q_2 from S_2**

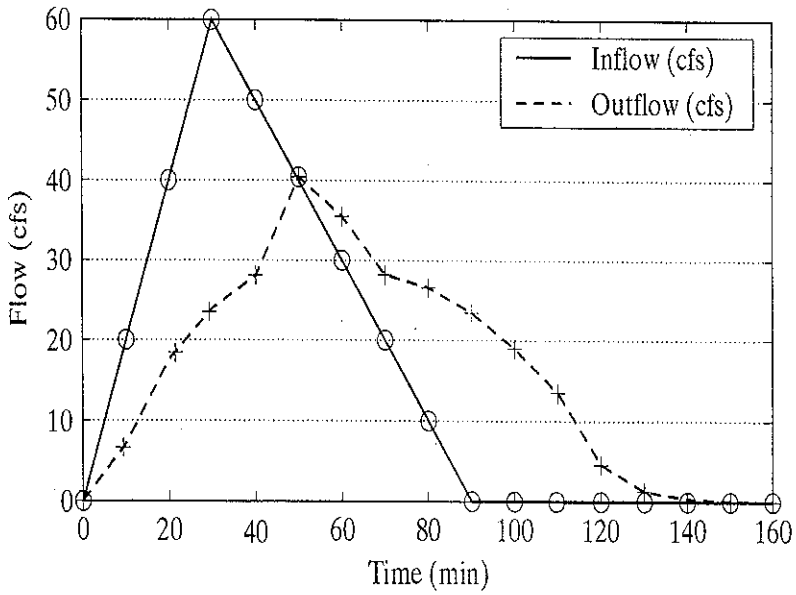

Figure E4.5(a)
Hydrographs.

Repeat each time step

Example Pond Routing

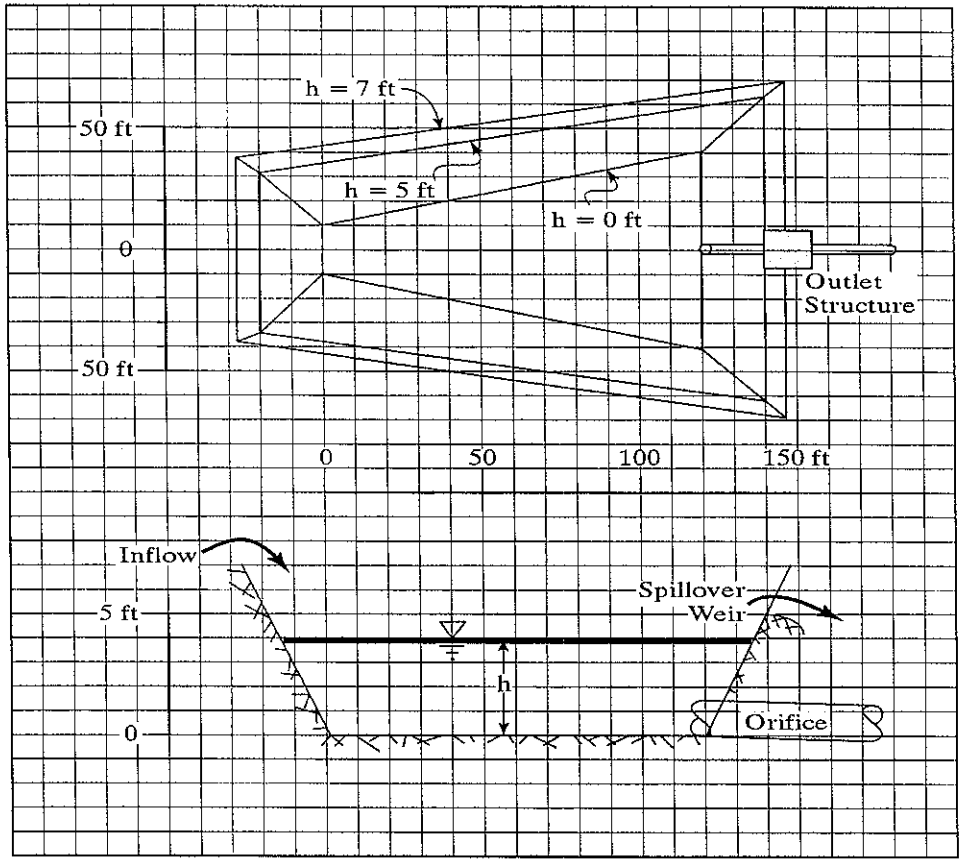

Note that outlet consists of weir and orifice.

Weir crest at h = 5.0 ft

Orifice at h = 0 ft

Area (6000 to 17,416 ft^2)

Volume ranges from 6772 to 84006 ft^3

Example Pond Routing

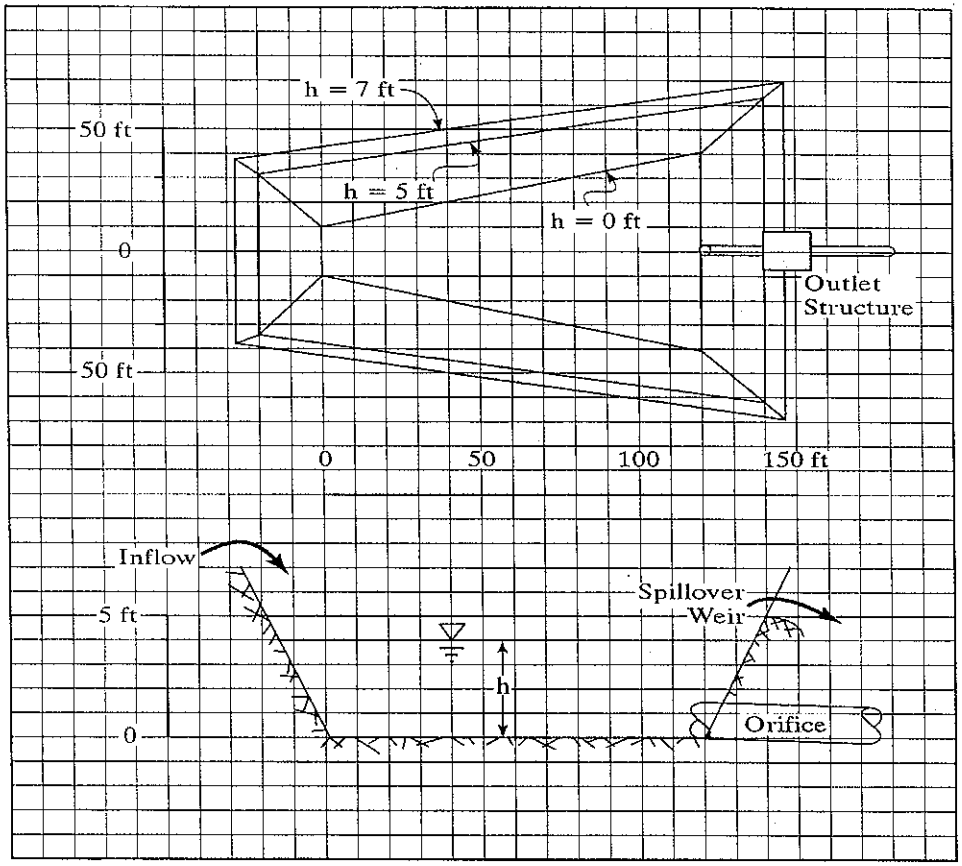

Develop Q (orifice) vs h

Develop Q (weir) vs h

Develop A and Vol vs h

Storage - Indication

***2S/dt + Q vs Q* where Q is sum of weir and orifice flow rates.**

Storage Indication

$$I_1 + I_2 + \left(\frac{2S_1}{dt} - Q_1\right) = \left(\frac{2S_2}{dt} + Q_2\right)$$

1. **LHS of Eqn is known at initial t**
2. **Know S as fcn of Q from outlet**
3. **Solve Eqn for -- $(2S_2/dt + Q_2)$**
4. **Solve for Q_2 from S_2**

Storage Indication Curve

- **Relates *Q* and storage indication, (*2S / dt + Q*)**
- **Developed from topography and outlet data**
- **Pipe flow + weir flow combine to produce Q (out)**

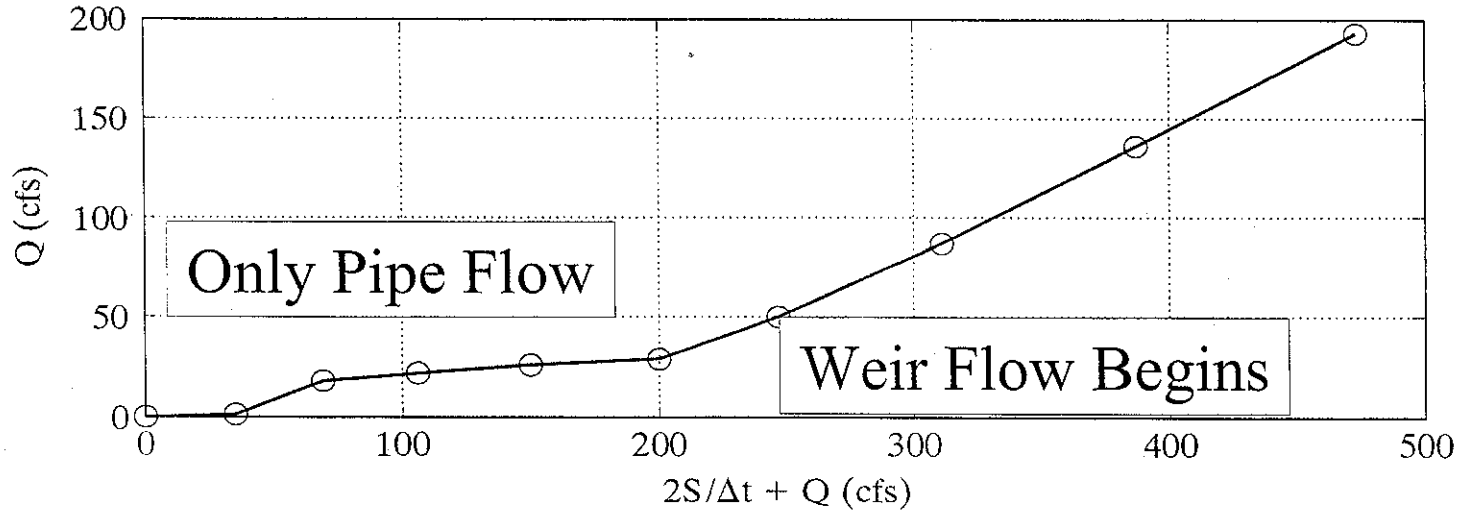

Figure E4.5(c)

Storage indication curve.

Storage Indication Inputs

height h - ft	Area 10^2 ft	Cum Vol 10^3 ft	Q total cfs	$2S/dt + Q_n$ cfs
0	6	0	0	0
1	7.5	6.8	13	35
2	9.2	15.1	18	69
3	11.0	25.3	22	106
4	13.0	37.4	26	150
5	15.1	51.5	29	200
7	17.4	84.0	159	473

Storage-Indication

Storage Indication Results

Time	I_n	$I_n + I_{n+1}$	$2S/dt - Q_n$	$(2S/dt + Q)_{n+1}$	Q_{n+1}
0	0	0	0	0	0
10	20	20	0	20	7.2
20	40	60	5.6	65.6	17.6
30	60	100	30.4	130.4	24.0
40	50	110	82.4	192.4	28.1
50	40	90	136.3	226.3	40.4
60	30	70	145.5	215.5	35.5

And so on ….

S-I Routing Results

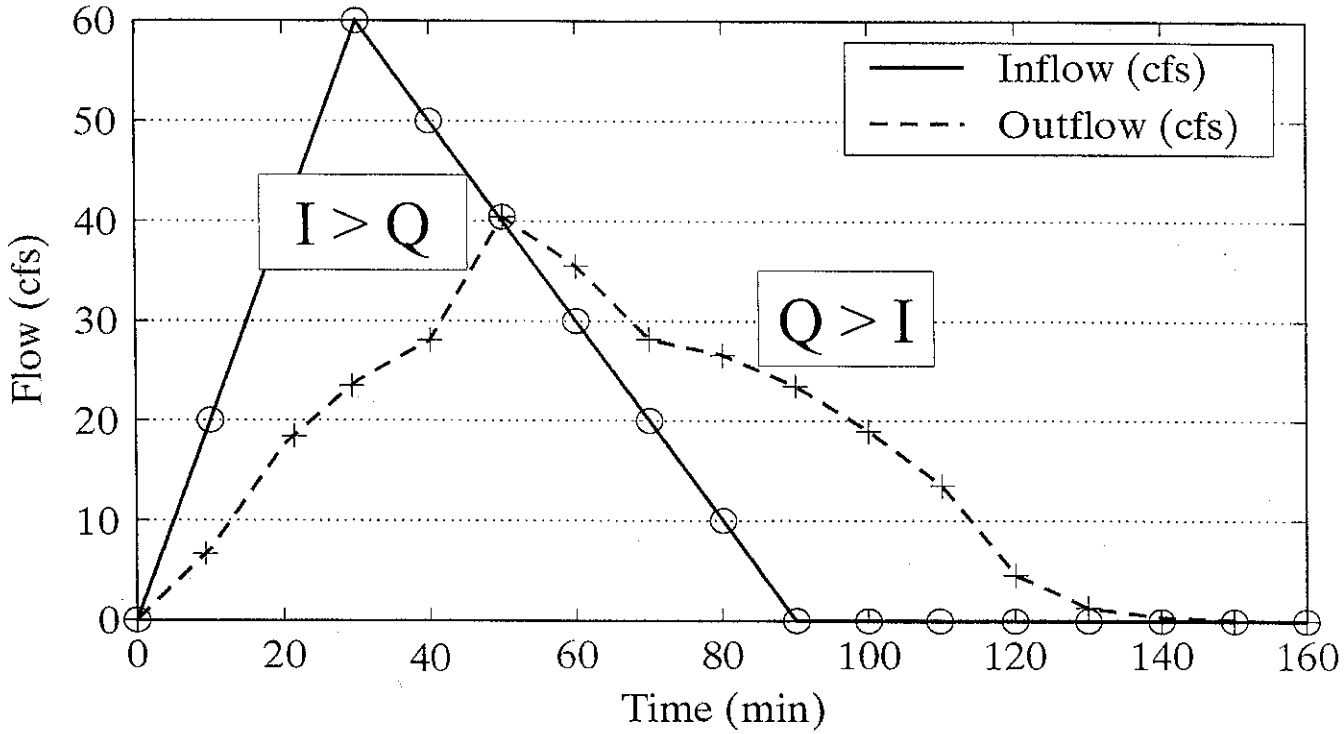

Figure E4.5(a)

Hydrographs.

S-I Routing Results

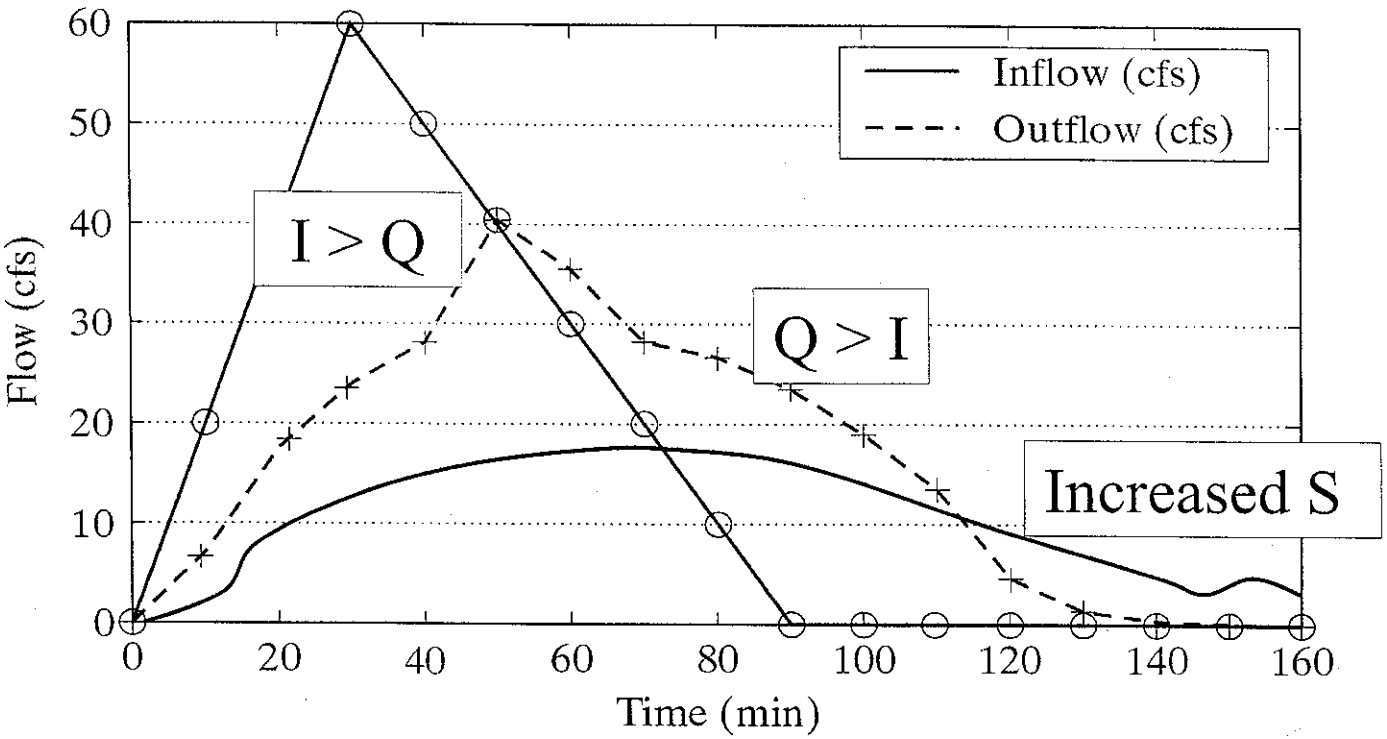

Figure E4.5(a)

Hydrographs.

Comparisons: River vs. Reservoir Routing

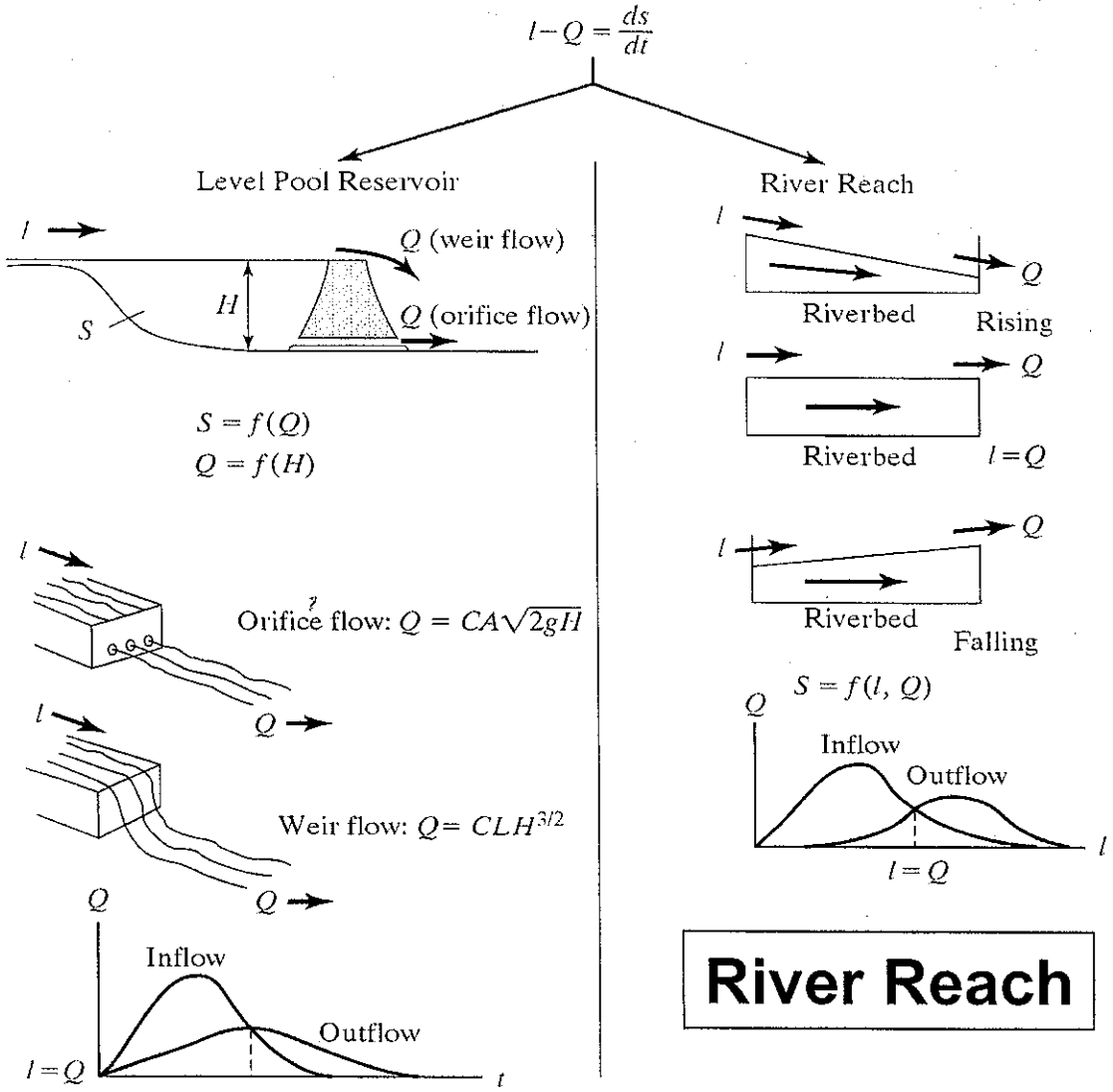

Level pool reservoir

River Reach

HAND OUT 15: Types of backwater (Chapters 5 and 6 of our syllabus).
Source: Mays, L. (2006). *"Water resources engineering."* John Wiley and Sons.

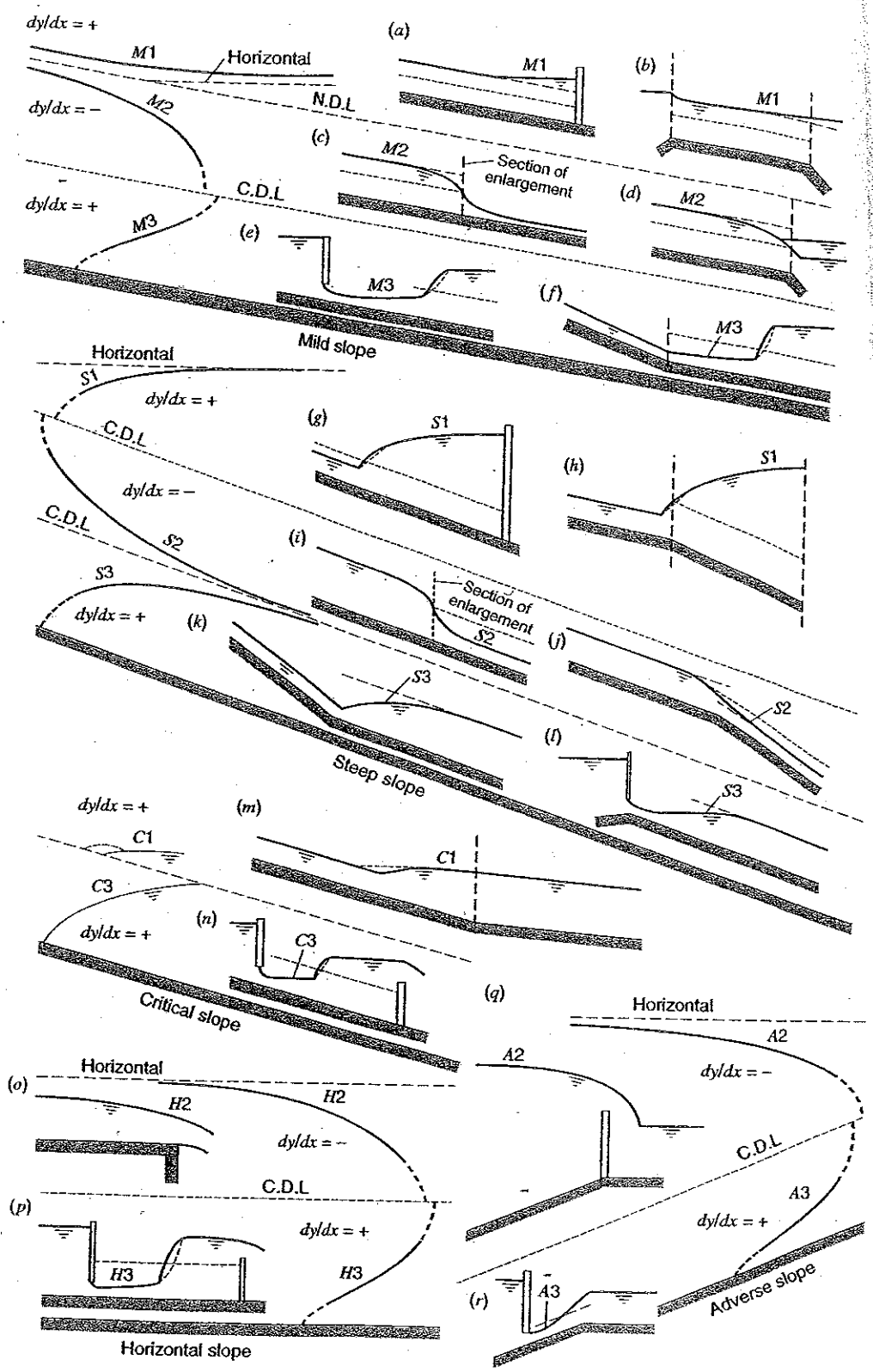

Figure 5.3.3 Flow profiles (from Chow (1959)).

HAND OUT 16: Numerical solution for backwater curves (Chapters 5 and 6 of our syllabus). Source: pages from Chow, V. T. (1959). *"Open-channel hydraulics."* Mc-Graw Hill.

BACKWATER CURVES

Gradually-varied flows

Differential equation:

$$\frac{dH}{dx} = -S_f \quad (1)$$

where: $H = \frac{U^2}{2g} + z + y$ (2)

and: $S_f = C_f \frac{U^2}{gy}$ (3)

We can discretize (1) using any of the methods we saw for $\frac{du}{dt} = -Ku$. Notice that the two equations look very similar. We can use a forward, backward, or a centered scheme. Using a centered scheme:

$$\frac{H_{j+1} - H_j}{\Delta x} = -\frac{1}{2}(S_{fj} + S_{fj+1}) \quad (4)$$

H is a function of y. S_f is also a function of y. Recall that in backwater curves our objective is to compute the variation of y with distance. The computation starts at one of the [redacted] boundaries of the cur

ve and proceeds to the other boundary. (2)

Example:

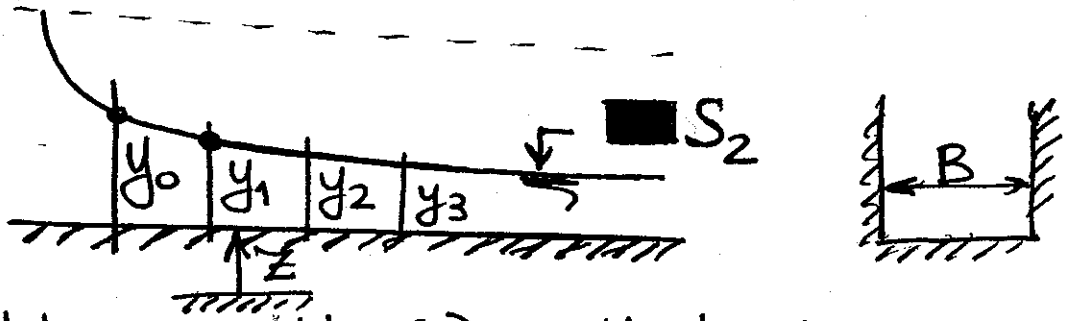

The problem with (4) is that, since $H=H(y)$ and $S_f(y)$, y is at both sides of the equal sign.

First method: We can circumvent this problem by fixing y. Say $y_0=10$ m; let's fix $y_1=9.9$ m, $y_2=9.8$ m, etc. If we know y, and the channel has a rectangular cross section, we can compute the area as: $A_0=By_0$, $A_1=By_1$, $A_2=By_2$, etc. Further, if the discharge per unit width, q_w, is known, we can compute: $U_0=\frac{q_w}{y_0}$, $U_1=\frac{q_w}{y_1}$, $U_2=\frac{q_w}{y_2}$, etc. If C_f is given, we can compute H_0, H_1, H_2, etc., and S_{f0}, S_{f1}, S_{f2}, etc.

For the first two cross sections:

$$\frac{H_1 - H_0}{\Delta x} = -\frac{1}{2}(S_{f0} + S_{f1}) \quad (5)$$

From (5), we know everything except Δx. So we can compute Δx from (5). This means that we compute the distance at which $y_1 = 9.9\,m$ occurs from $y_0 = 10\,m$. This method is called <u>explicit</u>, because we can compute Δx from known values: $\Delta x = \frac{(H_0 - H_1)2}{(S_{f0} + S_{f1})}$ (6)

We repeat the procedure between H_1 and H_2, H_2 and H_3, etc. In this way, we build the curve.

<u>Second method</u>: Equation (4) is also used. Let's denote Z the elevation of the water surface from the datum:

$$Z = z + y$$

$$H = Z + \frac{U^2}{2g} \quad (7)$$

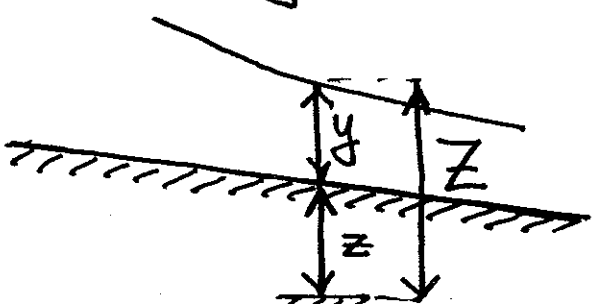

From (4):

$$H_{j+1} = H_j - \frac{1}{2}(S_{fj} + S_{fj+1})\Delta x \quad (8)$$

This method is best suited for natural channels. This method is based on trial and error procedure (iterative). Thus, it is called implicit method. Procedure:

1) We guess a value of $Z_{\blacksquare 1}$ (recall eqn. (5)) Since we know z_1, we can obtain y_1. Having y_1, we compute A_1, U_1, S_{f_1} and H_1. All these values at 0 are known because it is the initial condition. But this value of Z_1 corresponds to a given Δx that we specify. Thus, all these values give us another value of H_1^2. If H_1^2 is different from H_1^1, we need to vary our guess of $\blacksquare$ Z_1. The iteration continues until

$$\left| \frac{H_1^{m+1} - H_1^m}{H_1^{m+1}} \right| < \text{tol.}$$

Then, we need to move to another pair of cross sections and repeat the procedure.

Examples: Taken from Open-channel hydraulics, by Ven Te Chow, McGraw-Hill.

$$S_f = C_f \frac{U^2}{gy} = \frac{n^2 U^2}{[redacted] R^{4/3}}$$

Example of explicit method

TABLE 10-4. COMPUTATION OF THE FLOW PROFILE BY THE DIRECT STEP METHOD FOR EXAMPLE 10-7

$Q = 400$ cfs $\quad n = 0.025 \quad S_0 = 0.0016 \quad \alpha = 1.10 \quad y_c = 2.22$ ft $\quad y_n = 3.36$ ft

y (1)	A (2)	R (3)	$R^{2/3}$ (4)	V (5)	$\alpha V^2/2g$ (6)	E (7)	ΔE (8)	S_f (9)	$\bar{S}_f$ (10)	$S_0 - \bar{S}_f$ (11)	Δx (12)	x (13)
5.00	150.00	3.54	5.40	2.667	0.1217	5.1217	.....	0.000370				
4.80	142.08	3.43	5.17	2.819	0.1356	4.9356	0.1861	0.000433	0.000402	0.001198	155	155
4.60	134.32	3.31	4.94	2.979	0.1517	4.7517	0.1839	0.000507	0.000470	0.001130	163	318
4.40	126.72	3.19	4.70	3.156	0.1706	4.5706	0.1811	0.000598	0.000553	0.001047	173	491
4.20	119.28	3.08	4.50	3.354	0.1925	4.3925	0.1781	0.000705	0.000652	0.000948	188	679
4.00	112.00	2.96	4.25	3.572	0.2184	4.2184	0.1741	0.000850	0.000778	0.000822	212	891
3.80	104.88	2.84	4.02	3.814	0.2490	4.0490	0.1694	0.001020	0.000935	0.000665	255	1,146
3.70	101.38	2.77	3.88	3.948	0.2664	3.9664	0.0826	0.001132	0.001076	0.000524	158	1,304
3.60	97.92	2.71	3.78	4.085	0.2856	3.8856	0.0808	0.001244	0.001188	0.000412	196	1,500
3.55	96.21	2.68	3.72	4.158	0.2958	3.8458	0.0398	0.001310	0.001277	0.000323	123	1,623
3.50	94.50	2.65	3.66	4.233	0.3067	3.8067	0.0391	0.001382	0.001346	0.000254	154	1,777
3.47	93.48	2.63	3.63	4.278	0.3131	3.7831	0.0236	0.001427	0.001405	0.000195	121	1,898
3.44	92.45	2.61	3.59	4.326	0.3202	3.7602	0.0229	0.001471	0.001449	0.000151	152	2,050
3.42	91.80	2.60	3.57	4.357	0.3246	3.7446	0.0156	0.001500	0.001486	0.000114	137	2,187
3.40	91.12	2.59	3.55	4.388	0.3292	3.7292	0.0154	0.001535	0.001518	0.000082	188	2,375

TABLE 10-5. COMPUTATION OF THE FLOW PROFILE FOR EXAMPLE 10-8 BY THE DIRECT STEP METHOD

$Q = 252$ cfs $\quad n = 0.012 \quad S_0 = 0.02 \quad \alpha = 1.0 \quad y_c = 4.35$ ft $\quad y_n = 2.60$ ft

y/D	y	A	R	$R^{2/3}$	V	$\alpha V^2/2g$	E	ΔE	S_f	$\bar{S}_f$	$S_0 - \bar{S}_f$	Δx	x
0.725	4.35	21.95	1.794	2.180	11.48	2.048	6.398		0.00392				
0.70	4.20	21.13	1.777	2.154	11.93	2.211	6.411	0.013	0.00429	0.00411	0.01589	0.8	0.8
0.65	3.90	19.45	1.728	2.073	12.96	2.609	6.509	0.098	0.00525	0.00477	0.01523	6.4	7.2
0.60	3.60	17.71	1.666	1.976	14.23	3.145	6.745	0.236	0.00666	0.00596	0.01404	16.8	24.0
0.55	3.30	15.93	1.590	1.855	15.85	3.901	7.201	0.456	0.00880	0.00773	0.01227	37.2	61.2
0.50	3.00	14.13	1.500	1.717	17.85	4.947	7.947	0.746	0.01202	0.01041	0.00959	77.8	139.0
0.48	2.88	13.42	1.460	1.656	18.76	5.465	8.345	0.398	0.01378	0.01290	0.00710	56.1	195.1
0.47	2.82	13.06	1.440	1.626	19.30	5.785	8.605	0.260	0.01486	0.01432	0.00568	45.8	240.9
0.46	2.76	12.70	1.420	1.596	19.85	6.119	8.879	0.274	0.01600	0.01543	0.00457	60.0	300.9

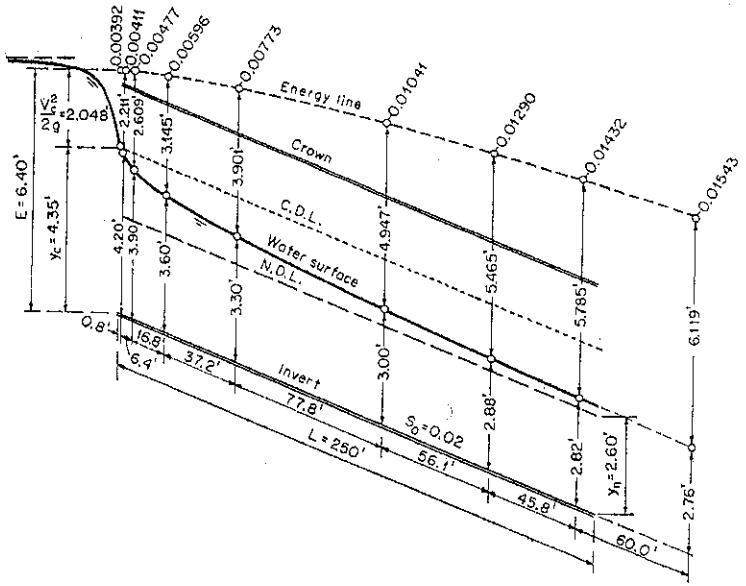

FIG. 10-7. An $S2$ flow profile computed by the direct step method.

Another example of explicit method (7)

Implicit method

(8)

Solution. The step computations are arranged in tabular form, as shown in Table 10-6. Values in each column of the table are explained as follows:

Col. 1. Section identified by station number such as "station 1 + 55." The location of the stations is fixed at the distances determined in Example 10-7 in order to compare the procedure with that of the direct step method.

Col. 2. Water-surface elevation at the station. A trial value is first entered in this column; this will be verified or rejected on the basis of the computations made in the remaining columns of the table. For the first step, this elevation must be given or assumed. Since the elevation of the dam site is 600 m.s.l. and the height of the dam is 5 ft, the first entry is 605.00 m.s.l. When the trial value in the second step has been verified, it becomes the basis for the verification of the trial value in the next step, and so on.

Col. 3. Depth of flow in ft, corresponding to the water-surface elevation in col. 2. For instance, the depth of flow at station 1 + 55 is equal to water-surface elevation minus elevation at the dam site minus (distance from the dam site times bed slope), or $605.048 - 600.000 - 155 \times 0.0016 = 4.80$ ft.

Col. 4. Water area corresponding to y in col. 3

Col. 5. Mean velocity equal to the given discharge 400 cfs divided by the water area in col. 4

Col. 6. Velocity head in ft, corresponding to the velocity in col. 5

Col. 7. Total head computed by Eq. (10-47), equal to the sum of Z in col. 2 and the velocity head in col. 6

Col. 8. Hydraulic radius in ft, corresponding to y in col. 3

Col. 9. Four-thirds power of the hydraulic radius

Col. 10. Friction slope computed by Eq. (9-8), with $n = 0.025$, V from col. 5, and $R^{4/3}$ from col. 9

Col. 11. Average friction slope through the reach between the sections in each step, approximately equal to the arithmetic mean of the friction slope just computed in col. 10 and that of the previous step

Col. 12. Length of the reach between the sections, equal to the difference in station numbers between the stations

Col. 13. Friction loss in the reach, equal to the product of the values in cols. 11 and 12.

Col. 14. Eddy loss in the reach, equal to zero

Col. 15. Elevation of the total head in ft. This is computed by Eq. (10-49), that is, by adding the values of h_f and h_e in cols. 13 and 14 to the elevation at the lower end of the reach, which is found in col. 15 of the previous reach. If the value so obtained does not agree closely with that entered in col. 7, a new trial value of the water-surface elevation is assumed, and so on, until agreement is obtained. The value that leads to agreement is the correct water-surface elevation. The computation may then proceed to the next step. The computed flow profile is practically identical with that obtained by the graphical-integration method shown in Fig. 10-3.

10-5. Computation of a Family of Flow Profiles. In previous articles methods were described for determining a single flow profile. Frequently, several flow profiles, or a family of flow profiles, are desired for various conditions of stage and discharge. An example of this type of problem is the determination of the economical height of a dam, where the initial elevation is indeterminate and, hence, a number of flow profiles may have to be computed for the same discharge with different assumed

Implicit

TABLE 10-6. COMPUTATION OF THE FLOW PROFILE FOR EXAMPLE 10-9 BY THE STANDARD STEP METHOD

$Q = 400$ cfs $\quad n = 0.025 \quad S_0 = 0.0016 \quad \alpha = 1.10 \quad h_e = 0 \quad y_c = 2.22$ ft $\quad y_n = 3.36$ ft

Station (1)	Z (2)	y (3)	A (4)	V (5)	$\alpha V^2/2g$ (6)	H (7)	R (8)	$R^{4/3}$ (9)	S_f (10)	$\bar{S}_f$ (11)	Δx (12)	h_f (13)	h_e (14)	H (15)
0 + 00	605.000	5.00	150.00	2.667	0.1217	605.122	3.54	5.40	0.000370	.....	...	.....	...	605.122
1 + 55	605.048	4.80	142.08	2.819	0.1356	605.184	3.43	5.17	0.000433	0.000402	155	0.062	0	605.184
3 + 18	605.109	4.60	134.32	2.979	0.1517	605.261	3.31	4.92	0.000507	0.000470	163	0.077	0	605.261
4 + 91	605.186	4.40	126.72	3.156	0.1706	605.357	3.19	4.70	0.000598	0.000553	173	0.096	0	605.357
6 + 79	605.286	4.20	119.28	3.354	0.1925	605.479	3.08	4.50	0.000705	0.000652	188	0.122	0	605.479
8 + 91	605.426	4.00	112.00	3.572	0.2184	605.644	2.96	4.25	0.000850	0.000778	212	0.165	0	605.644
11 + 46	605.633	3.80	104.88	3.814	0.2490	605.882	2.84	4.02	0.001020	0.000935	255	0.238	0	605.882
13 + 04	605.786	3.70	101.38	3.948	0.2664	606.052	2.77	3.88	0.001132	0.001076	158	0.170	0	606.052
15 + 00	605.999	3.60	97.92	4.085	0.2856	606.285	2.71	3.78	0.001244	0.001188	196	0.233	0	606.285
16 + 23	606.146	3.55	96.21	4.158	0.2958	606.442	2.68	3.72	0.001310	0.001277	123	0.157	0	606.442
17 + 77	606.343	3.50	94.50	4.233	0.3067	606.650	2.65	3.66	0.001382	0.001346	154	0.208	0	606.650
18 + 98	606.507	3.47	93.48	4.278	0.3131	606.820	2.63	3.63	0.001427	0.001405	121	0.170	0	606.820
20 + 50	606.720	3.44	92.45	4.326	0.3202	607.040	2.61	3.59	0.001471	0.001449	152	0.220	0	607.040
21 + 87	606.919	3.42	91.80	4.357	0.3246	607.244	2.60	3.57	0.001500	0.001486	137	0.204	0	607.244
23 + 75	607.201	3.40	91.12	4.388	0.3292	607.530	2.59	3.55	0.001535	0.001518	188	0.286	0	607.530

9

HAND OUT 17: Hydrologic routing (Chapter 6 of our syllabus). Source: Mays, L. (2006). *"Water resources engineering."* John Wiley and Sons.

Chapter 9

Reservoir and Stream Flow Routing

9.1 ROUTING

Figure 9.1.1 illustrates how stream flow increases as the *variable source area* extends into the drainage basin. The variable source area is the area of the watershed that is actually contributing flow to the stream at any point. The variable source area expands during rainfall and contracts thereafter.

Flow routing is the procedure to determine the time and magnitude of flow (i.e., the flow hydrograph) at a point on a watercourse from known or assumed hydrographs at one or more points upstream. If the flow is a flood, the procedure is specifically known as flood routing. Routing by lumped system methods is called *hydrologic (lumped) routing*, and routing by distributed systems methods is called *hydraulic (distributed) routing*.

For hydrologic routing, input $I(t)$, output $Q(t)$, and storage $S(t)$ as functions of time are related by the continuity equation (3.2.10)

$$\frac{dS}{dt} = I(t) - Q(t) \tag{9.1.1}$$

Even if an inflow hydrograph $I(t)$ is known, equation (9.1.1) cannot be solved directly to obtain the outflow hydrograph $Q(t)$, because both Q and S are unknown. A second relationship, or storage function, is required to relate S, I, and Q; coupling the storage function with the continuity equations provides a solvable combination of two equations and two unknowns.

The specific form of the storage function depends on the nature of the system being analyzed. In reservoir routing by the level pool method (Section 9.2), storage is a nonlinear function of Q, $S = f(Q)$ and the function $f(Q)$ is determined by relating reservoir storage and outflow to reservoir water level. In the Muskingum method (Section 9.3) for flow routing in channels, storage is linearly related to I and Q.

The effect of storage is to redistribute the hydrograph by shifting the centroid of the inflow hydrograph to the position of that of the outflow hydrograph in a *time of redistribution*. In very long channels, the entire flood wave also travels a considerable distance and the centroid of its hydrograph may then be shifted by a time period longer than the time of redistribution. This additional time may be considered the *time of translation*. The total time of flood movement between the centroids of the inflow and outflow hydrographs is equal to the sum of the time of redistribution and the time of translation. The process of redistribution modifies the shape of the hydrograph, while translation changes its position.

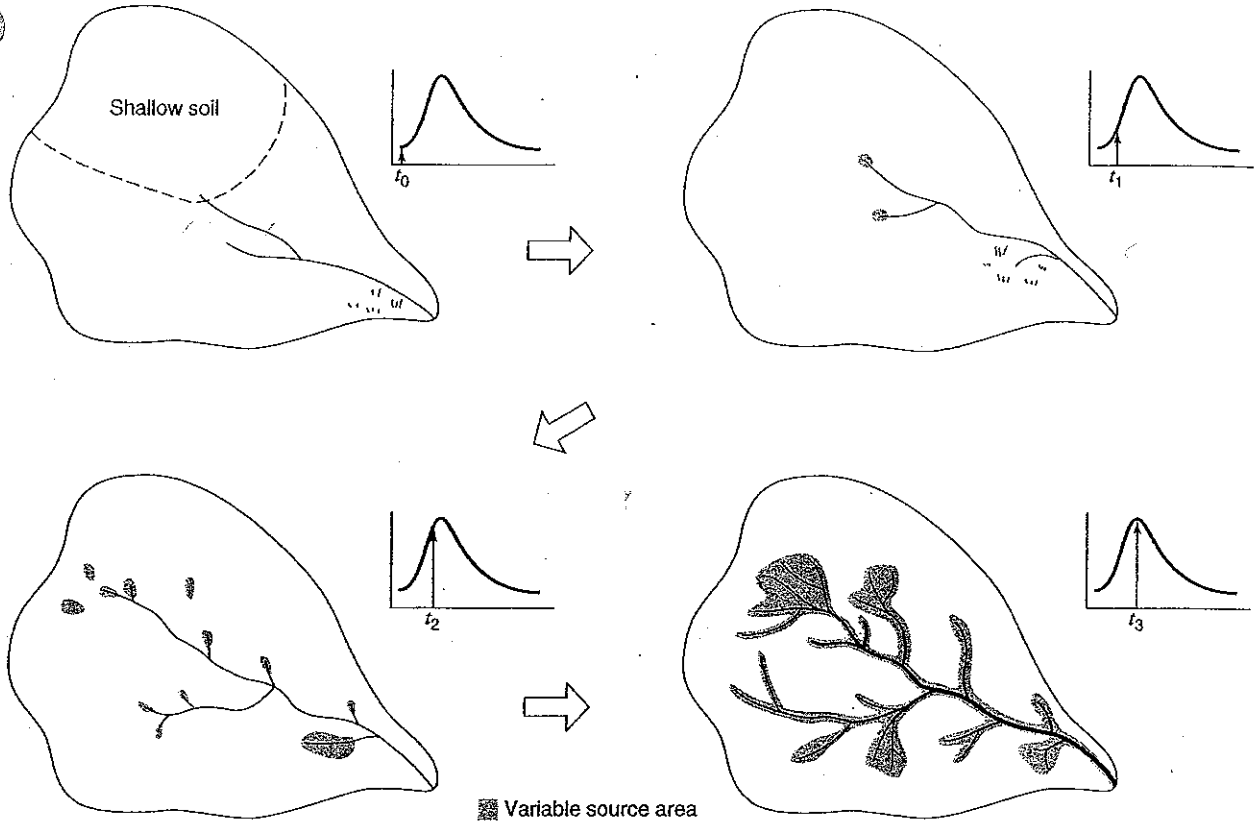

Figure 9.1.1 The small arrows in the hydrographs show how streamflow increases as the variable source extends into swamps, shallow soils, and ephemeral channels. The process reverses as streamflow declines (from Hewlett (1982)).

9.2 HYDROLOGIC RESERVOIR ROUTING

Level pool routing is a procedure for calculating the outflow hydrograph from a reservoir assuming a horizontal water surface, given its inflow hydrograph and storage-outflow characteristics. Equation (9.1.1) can be expressed in the in finite-difference form to express the change in storage over a time interval (see Figure 9.2.1) as

$$S_{j+1} - S_j = \frac{I_j + I_{j+1}}{2}\Delta t - \frac{Q_j + Q_{j+1}}{2}\Delta t \tag{9.2.1}$$

The inflow values at the beginning and end of the jth time interval are I_j and I_{j+1}, respectively, and the corresponding values of the outflow are Q_j and Q_{j+1}. The values of I_j and I_{j+1} are prespecified. The values of Q_j and S_j are known at the jth time interval from calculations for the previous time interval. Hence, equation (9.2.1) contains two unknowns, Q_{j+1} and S_{j+1}, which are isolated by multiplying (9.1.1) through by $2/\Delta t$, and rearranging the result to produce:

$$\left[\frac{2S_{j+1}}{\Delta t} + Q_{j+1}\right] = (I_j + I_{j+1}) + \left[\frac{2S_j}{\Delta t} - Q_j\right] \tag{9.2.2}$$

In order to calculate the outflow Q_{j+1}, a storage-outflow function relating $2S/\Delta t + Q$ and Q is needed. The method for developing this function using elevation-storage and elevation-outflow relationships is shown in Figure 9.2.2. The relationship between water surface elevation and reservoir storage can be derived by planimetering topographic maps or from field surveys. The elevation-discharge relation is derived from hydraulic equations relating head and discharge for

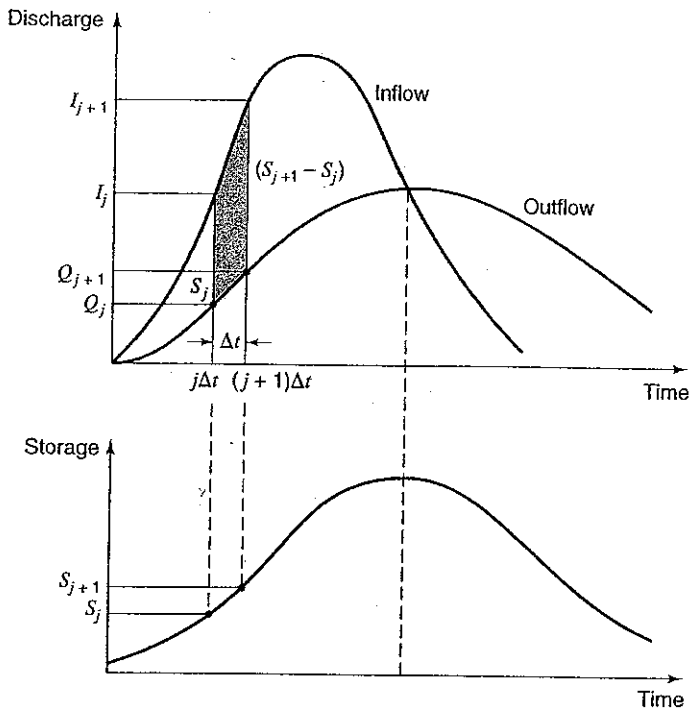

Figure 9.2.1 Change of storage during a routing period Δt.

various types of spillways and outlet works. (See Chapter 17.) The value of Δt is taken as the time interval of the inflow hydrograph. For a given value of water surface elevation, the values of storage S and discharge Q are determined (parts (*a*) and (*b*) of Figure 9.2.2), and then the value of $2S/\Delta t + Q$ is calculated and plotted on the horizontal axis of a graph with the value of the outflow Q on the vertical axis (part (*c*) of Figure 9.2.2).

In routing the flow through time interval j, all terms on the right side of equation (9.2.2) are known, and so the value of $2S_{j+1}/\Delta t + Q_{j+1}$ can be computed. The corresponding value of Q_{j+1} can be determined from the storage-outflow function $2S/\Delta t + Q$ versus Q, either graphically or by linear interpolation of tabular values. To set up the data required for the next time interval, the value of $(2S_{j+1}/\Delta t - Q_{j+1})$ is calculated using

$$\left[\frac{2S_{j+1}}{\Delta t} - Q_{j+1}\right] = \left[\frac{2S_{j+1}}{\Delta t} + Q_{j+1}\right] - 2Q_{j+1} \tag{9.2.3}$$

The computation is then repeated for subsequent routing periods.

EXAMPLE 9.2.1

Consider a 2-acre stormwater detention basin with vertical walls. The triangular inflow hydrograph increases linearly from zero to a peak of 60 cfs at 60 min and then decreases linearly to a zero discharge at 180 min. Route the inflow hydrograph through the detention basin using the head-discharge relationship for the 5-ft diameter pipe spillway in columns (1) and (2) of Table 9.2.1. The pipe is located at the bottom of the basin. Assuming the basin is initially empty, use the level pool routing procedure with a 10-min time interval to determine the maximum depth in the detention basin.

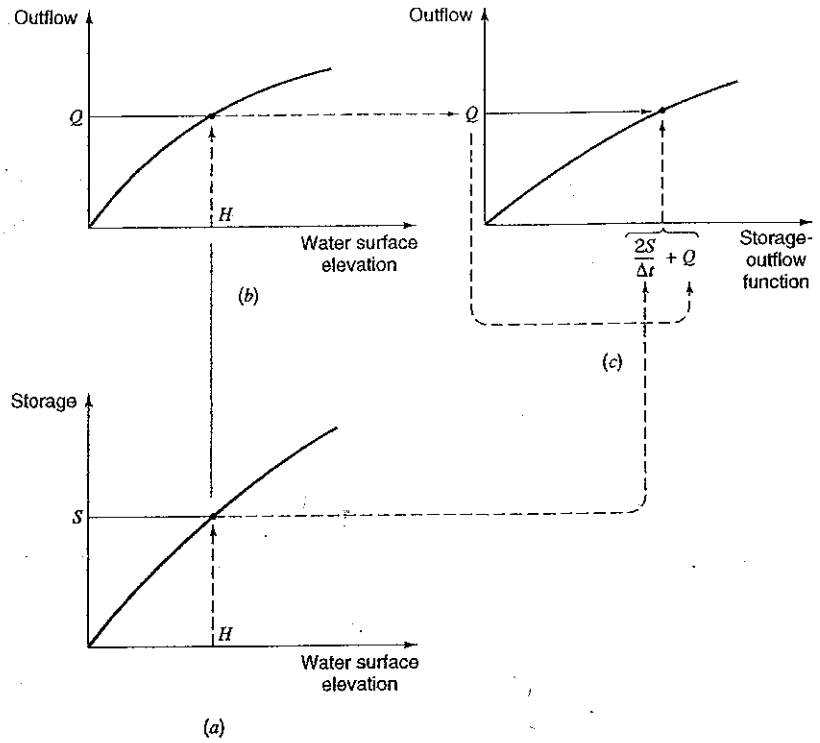

Figure 9.2.2 Development of the storage-outflow function for level pool routing on the basis of storage-elevation-outflow curves (from Chow et al. (1988)).

Table 9.2.1 Elevation-Discharge-Storage Data for Example 9.2.1

1	2	3	4
Head H (ft)	Discharge Q (cfs)	Storage S (ft^3)	$\frac{2S}{\Delta t} + Q$ (cfs)
0.0	0	0	.00
0.5	3	43,500	148.20
1.0	8	87,120	298.40
1.5	17	130,680	452.60
2.0	30	174,240	610.80
2.5	43	217,800	769.00
3.0	60	261,360	931.20
3.5	78	304,920	1094.40
4.0	97	348,480	1258.60
4.5	117	392,040	1423.80
5.0	137	435,600	1589.00

SOLUTION

The inflow hydrograph and the head-discharge (columns 1 and 3) and discharge-storage (columns 2 and 3) relationships are used to determine the routing relationship in Table 9.2.1. A routing interval of 10 min is used to determine the routing relationship $2S/\Delta t + Q$ vs. Q, which is columns 2 and 4 in Table 9.2.1. The routing computations are presented in Table 9.2.2, with the sequence of computations indicated by the arrows. These computations are carried out using equation (9.2.3). For the first time interval, $S_1 = Q_1 = 0$ because the reservoir is empty at $t = 0$; then $(2S_1/\Delta t - Q_1) = 0$. The value of the storage-outflow function at the end of the time interval is

$$\left[\frac{2S_2}{\Delta t}+Q_2\right]=(I_1+I_2)+\left[\frac{2S_1}{\Delta t}-Q_1\right]=(0+10)+0=10$$

The value of Q_2 is determined using linear interpolation, so that

$$Q_2=0+\frac{(3-0)}{(148.2-0)}(10-0)=0.2 \text{ cfs}$$

With $Q_2 = 0.2$, then $2S_2/\Delta t - Q_2$ for the next iteration is

$$\left[\frac{2S_2}{\Delta t}-Q_2\right]=\left[\frac{2S_2}{\Delta t}+Q_2\right]-2Q_2=10-2(0.2)=9.6 \text{ cfs}$$

The computation now proceeds to the next time interval. Refer to Table 9.2.1 for the remaining computations.

Table 9.2.2 Routing of Flow Through Detention Reservoir by the Level Pool Method (example 9.2.1)

Time t (min)	Inflow I_j (cfs)	$I_j + I_{j+1}$ (cfs)	$\frac{2S_j}{\Delta t} - Q_j$ (cfs)	$\frac{2S_{j+1}}{\Delta t} + Q_{j+1}$ (cfs)	Outflow (cfs)
.00	.00				.00
10.00	10.00	10.00	.00	10.00	.20
20.00	20.00	30.00	9.60	39.60	.80
30.00	30.00	50.00	37.99	87.99	1.78
40.00	40.00	70.00	84.43	154.43	3.21
50.00	50.00	90.00	148.01	238.01	5.99
60.00	60.00	110.00	226.04	336.04	10.20
70.00	55.00	115.00	315.64	430.64	15.72
80.00	50.00	105.00	399.21	504.21	21.24
90.00	45.00	95.00	461.72	556.72	25.56
100.00	40.00	85.00	505.61	590.61	28.34
110.00	35.00	75.00	533.93	608.93	29.85
120.00	30.00	65.00	549.24	614.24	30.28
130.00	25.00	55.00	553.67	608.67	29.83
140.00	20.00	45.00	549.02	594.02	28.62
150.00	15.00	35.00	536.78	571.78	26.79
160.00	10.00	25.00	518.19	543.19	24.44
170.00	5.00	15.00	494.30	509.30	21.66
180.00	.00	5.00	465.98	470.98	18.51
190.00	.00	.00	433.96	433.96	15.91
200.00	.00	.00	402.14	402.14	14.05
210.00	.00	.00	374.03	374.03	12.41
220.00	.00	.00	349.20	349.20	10.97
230.00	.00	.00	327.27	327.27	9.69
240.00	.00	.00	307.90	307.90	8.55

9.3 HYDROLOGIC RIVER ROUTING

The *Muskingum method* is a commonly used hydrologic routing method that is based upon a variable discharge-storage relationship. This method models the storage volume of flooding in a river channel by a combination of wedge and prism storage (Figure 9.3.1). During the advance of a flood wave, inflow exceeds outflow, producing a wedge of storage. During the recession, outflow exceeds inflow, resulting in a negative wedge. In addition, there is a prism of storage that is formed by a volume of constant cross-section along the length of prismatic channel.

Assuming that the cross-sectional area of the flood flow is directly proportional to the discharge at the section, the *volume of prism storage* is equal to KQ, where K is a proportionality coefficient (approximate as the travel time through the reach), and the *volume of wedge storage* is equal to $KX(I - Q)$, where X is a weighting factor having the range $0 \le X \le 0.5$. The total storage is defined as the sum of two components,

$$S = KQ + KX(I - Q) \tag{9.3.1}$$

which can be rearranged to give the storage function for the Muskingum method

$$S = K[XI + (1 - X)Q)] \tag{9.3.2}$$

and represents a linear model for routing flow in streams.

The value of X depends on the shape of the modeled wedge storage. The value of X ranges from 0 for reservoir-type storage to 0.5 for a full wedge. When $X = 0$, there is no wedge and hence no backwater; this is the case for a level-pool reservoir. In natural streams, X is between 0 and 0.3, with a mean value near 0.2. Great accuracy in determining X may not be necessary because the results of the method are relatively insensitive to the value of this parameter. The parameter K is the time of travel of the flood wave through the channel reach. For hydrologic routing, the values of K and X are assumed to be specified and constant throughout the range of flow.

The values of storage at time j and $j + 1$ can be written, respectively, as

$$S_j = K[XI_j + (1 - X)Q_j] \tag{9.3.3}$$

$$S_{j+1} = K[XI_{j+1} + (1 - X)Q_{j+1}] \tag{9.3.4}$$

Using equations (9.3.3) and (9.3.4), the change in storage over time interval Δt is

$$S_{j+1} - S_j = K\{[XI_{j+1} + (1 - X)Q_{j+1}] - [XI_j + (1 - X)Q_j]\} \tag{9.3.5}$$

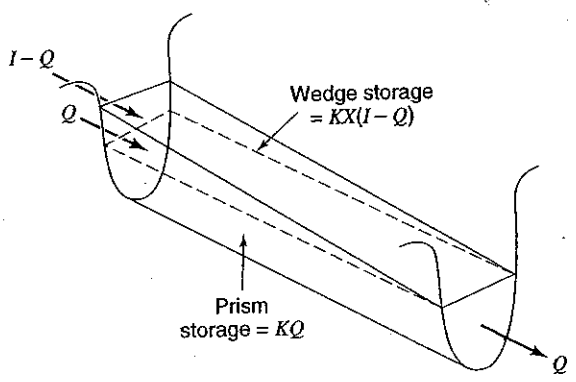

Figure 9.3.1 Prism and wedge storages in a channel reach.

The change in storage can also be expressed using equation (9.2.1). Combining equations (9.3.5) and (9.2.1) and simplifying gives

$$Q_{j+1} = C_1 I_{j+1} + C_2 I_j + C_3 Q_j \tag{9.3.6}$$

which is the routing equation for the Muskingum method, where

$$C_1 = \frac{\Delta t - 2KX}{2K(1-X) + \Delta t} \tag{9.3.7}$$

$$C_2 = \frac{\Delta t + 2KX}{2K(1-X) + \Delta t} \tag{9.3.8}$$

$$C_3 = \frac{2K(1-X) - \Delta t}{2K(1-X) + \Delta t} \tag{9.3.9}$$

Note that $C_1 + C_2 + C_3 = 1$.

The routing procedure can be repeated for several sub-reaches (N_{steps}) so that the total travel time through the reach is K. To insure that the method is computationally stable and accurate, the U.S. Army Corps of Engineers (1990) uses the following criterion to determine the number of routing reaches:

$$\frac{1}{2(1-X)} \le \frac{K}{N_{steps}\Delta t} \le \frac{1}{2X} \tag{9.3.10}$$

If observed inflow and outflow hydrographs are available for a river reach, the values of K and X can be determined. Assuming various values of X and using known values of the inflow and outflow, successive values of the numerator and denominator of the following expression for K, derived from equations (9.3.5) and (9.3.8), can be computed using

$$K = \frac{0.5\Delta t\left[(I_{j+1} + I_j) - (Q_{j+1} + Q_j)\right]}{X(I_{j+1} - I_j) + (1-X)(Q_{j+1} - Q_j)} \tag{9.3.11}$$

The computed values of the numerator (storage) and denominator (weighted discharges) are plotted for each time interval, with the numerator on the vertical axis and the denominator on the horizontal axis. This usually produces a graph in the form of a loop, as shown in Figure 9.3.2. The value of X that produces a loop closest to a single line is taken to be the correct value for the reach, and K, according to equation (9.3.11), is equal to the slope of the line. Since K is the time required for the incremental flood wave to traverse the reach, its value may also be estimated as the observed time of travel of peak flow through the reach.

EXAMPLE 9.3.1

The objective of this example is to determine K and X for the Muskingum routing method using the February 26 to March 4, 1929 data on the Tuscasawas River from Dover to Newcomerstown. This example is taken from the U.S. Army Corps of Engineers (1960) as used in Cudworth (1989). Columns 2 and 3 in Table 9.3.1 are the inflow and outflow hydrographs for the reach. The numerator and denominator of equation (9.3.11) were computed (for each time period) using four values of $X = 0$, 0.1, 0.2, and 0.3. The accumulated numerators are in column 9 and the accumulated denominators (weighted discharges) are in columns 11, 13, 15, and 17. In Figure 9.3.2, the accumulated numerator (storages) from column (9) are plotted against the corresponding accumulated denominator (weighted discharges) for each of the four X values. According to Figure 9.3.2, the best fit (linear relationship) appears to be for $X = 0.2$, which has a resulting $K = 1.0$. To perform a routing, K should equal Δt, so that if $\Delta t = 0.5$ day, as in this case, the reach should be subdivided into two equal reaches ($N_{steps} = 2$) and the value of K should be 0.5 day for each reach.

Table 9.3.1 Determination of Coefficients K and X for the Muskingum Routing Method. Tuscarawas River, Muskingum Basin, Ohio Reach from Dover to Newcomerstown, February 26 to March 4, 1929

(1) Date Δt = 0.5 day	(2) In-flow[1], ft³/s	(3) Out-flow[2], ft³/s	(4) $I_2 + I_1$, ft³/s	(5) $O_2 + O_1$, ft³/s	(6) $I_2 - I_1$, ft³/s	(7) $O_2 - O_1$, ft³/s	(8) [3]N	(9) ΣN	Values of D and ΣD for Assumed Values of X							
									$X = 0$		$X = 0.1$		$X = 0.2$		$X = 0.3$	
									[4]D (10)	ΣD (11)	D (12)	ΣD (13)	D (14)	ΣD (15)	D (16)	ΣD (17)
2-26-29 a.m.	2,200	2,000	16,700	9,000	12,300	5,000	1,900		5,000		5,700		6,500		7,200	
p.m.	14,500	7,000	42,900	18,700	13,900	4,700	6,100	1,900	4,700	5,000	5,600	5,700	6,500	6,500	7,500	7,200
2-27-29 a.m.	28,400	11,700	60,200	28,200	3,400	4,800	8,000	8,000	4,800	9,700	4,600	11,300	4,500	13,000	4,300	14,700
p.m.	31,800	16,500	61,500	40,500	–2,100	7,500	5,200	16,000	7,500	14,500	6,700	15,900	5,600	17,500	4,600	19,000
2-28-29 a.m.	29,700	24,00	55,000	53,100	–4,400	5,100	500	21,200	5,100	22,000	4,100	22,600	3,200	23,100	2,300	23,600
p.m.	25,300	29,100	45,700	57,500	–4,900	–700	–2,900	21,700	–700	27,100	–1,100	26,700	–1,500	26,300	–2,000	25,900
3-01-29 a.m.	20,400	28,400	36,700	52,200	–4,100	–4,600	–3,900	18,800	–4,600	26,400	–4,600	25,600	–4,500	24,800	–4,400	23,900
p.m.	16,300	23,800	28,900	43,200	–3,700	–4,400	–3,600	14,900	–4,400	21,800	–4,300	21,000	–4,300	20,300	–4,200	19,500
3-02-29 a.m.	12,600	19,400	21,900	34,700	–3,300	–4,100	–3,200	11,300	–4,100	17,400	–4,000	16.700	–3,900	16,000	–3,900	15,300
p.m.	9,300	15,300	16,000	26,500	–2,600	–4,100	–2,500	8,100	–4,100	13,300	–4,000	12,700	–3,800	12,100	–3,600	11,400
3-03-29 a.m.	6,700	11,200	11,700	19,400	–1,700	–3,000	–1,900	5,500	–3,000	9,200	–2,800	8,700	–2,800	8,300	–2,600	7,800
p.m.	5,000	8,200	9,100	14,600	–900	–1,800	–1,400	3,600	–1,800	6,200	–1,700	5,900	–1,600	5,500	–1,600	5,200
3-04-29 a.m.	4,100	6,400	7,700	11,600	–500	–1,200	–1,000	2,200	–1,200	4,400	–1,200	4,200	–1,100	3,900	–900	3,600
p.m.	3,600	5,200	6,000	9,800	–1,200	–600	–1,000	1,200	–600	3,200	–600	3,000	–700	2,800	–800	2,700
3-05-29 a.m.	2,400	4,600	—	—	—	—	—	200	—	2,600	—	2,400	—	2,100	—	1,900

[1]Inflow to reach was adjusted to equal volume of outflow.
[2]Outflow is the hydrograph at Newcomerstown.
[3]Numerator, N, is $\Delta t/2$, column (4) – column (5).
[4]Denominator, D, is column (7) + X[column (6) – column (7)].
Note: From plottings of column (9) versus columns (11), (13), (15), and (17), the plot giving the best fit is considered to define K and X.

$$K = \frac{\text{Numerator, } N}{\text{Denominator, } D} = \frac{0.5\Delta t\left[(I_2 + I_1) - (O_2 + O_1)\right]}{X(I_2 - I_1) + (1 - X)(O_2 - O_1)}$$

Source: Cudworth (1989).

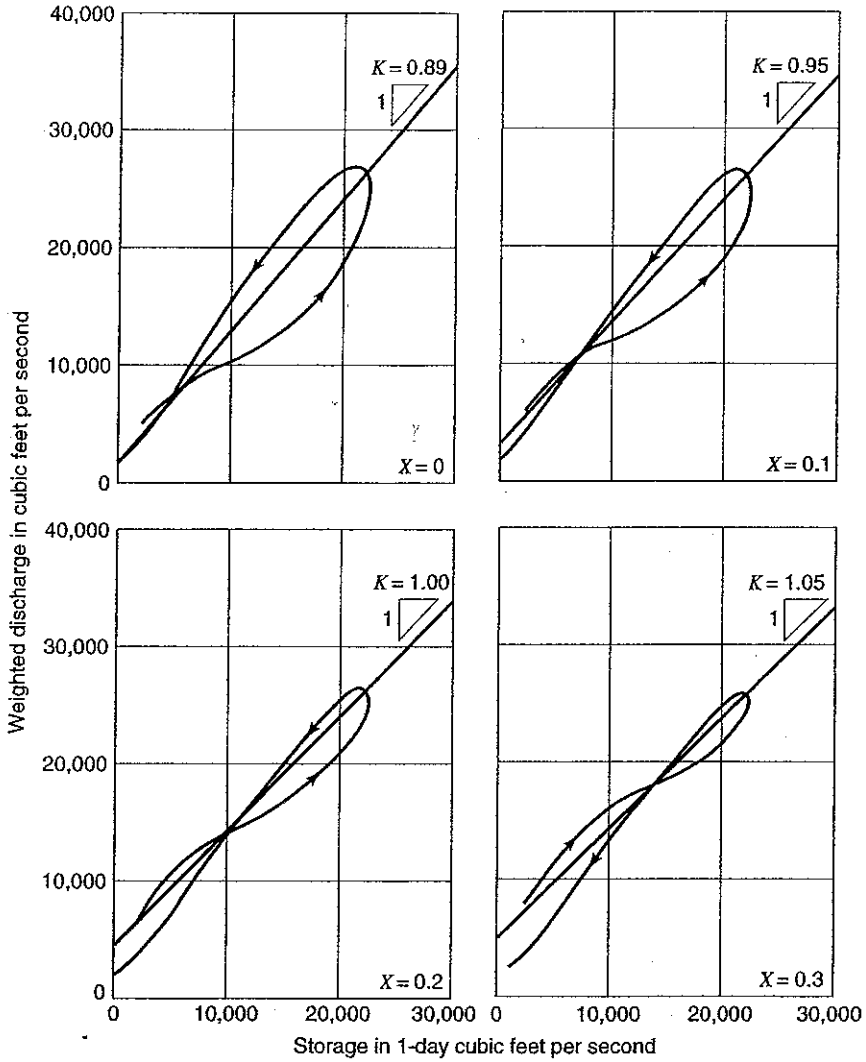

Figure 9.3.2 Typical valley storage curves.

EXAMPLE 9.3.2

Route the inflow hydrograph below using the Muskingum method; $\Delta t = 1$ hr, $X = 0.2$, $K = 0.7$ hrs.

Time (hrs)	0	1	2	3	4	5	6	7
Inflow (cfs)	0	800	2000	4200	5200	4400	3200	2500

Time (hrs)	8	9	10	11	12	13
Inflow (cfs)	2000	1500	1000	700	400	0

$$C_1 = \frac{1.0 - 2(0.7)(0.2)}{2(0.7)(1-0.2)+1.0} = 0.3396$$

$$C_2 = \frac{1.0 + 2(0.7)(0.2)}{2(0.7)(1-0.2)+1.0} = 0.6038$$

$$C_3 = \frac{2(0.7)(1-0.2) - 1.0}{2(0.7)(1-0.2)+1.0} = 0.0566$$

(Adapted from Masch (1984).)

HAND OUT 18: Hydraulic routing (Chapter 6 of our syllabus). Source: Mays, L. (2006). *"Water resources engineering."* John Wiley and Sons.

Check to see if $C_1 + C_2 + C_3 = 1$:

$0.3396 + 0.6038 + 0.0566 = 1$

Using equation (9.3.6) with $I_1 = 0$ cfs, $I_2 = 800$ cfs, and $Q_1 = 0$ cfs, compute Q_2 at $t = 1$ hr:

$$Q_2 = C_1 I_2 + C_2 I_1 + C_3 Q_1$$
$$= (0.3396)(800) + 0.6038(0) + 0.0566(0)$$
$$= 272 \text{ cfs } (7.7 \text{ m}^3/\text{s})$$

Next compute Q_3 at $t = 2$ hr:

$$Q_3 = C_1 I_3 + C_2 I_2 + C_3 Q_2$$
$$= (0.3396)(2000) + 0.6038(800) + 0.0566(272)$$
$$= 1178 \text{ cfs } (33 \text{ m}^3/\text{s})$$

The remaining computations result in

Time (hrs)	0	1	2	3	4	5	6	7
Q (cfs)	0	272	1178	2701	4455	4886	4020	3009
Time (hrs)	8	9	10	11	12	13	14	15
Q (cfs)	2359	1851	1350	918	610	276	16	1

9.4 HYDRAULIC (DISTRIBUTED) ROUTING

Distributed routing or *hydraulic routing*, also referred to as *unsteady flow routing*, is based up the one-dimensional unsteady flow equations referred to as the *Saint–Venant equations*. T hydrologic river routing and the hydrologic reservoir routing procedures presented previously a lumped procedures and compute flow rate as a function of time alone at a downstream locati Hydraulic (distributed) flow routings allow computation of the flow rate and water surface ele tion (or depth) as function of both space (location) and time. The Saint–Venant equations are p sented in Table 9.4.1 in both the *velocity-depth (nonconservation) form* and the *discharge-a (conservation) form*.

The momentum equation contains terms for the physical processes that govern the flow mom tum. These terms are: the *local acceleration term*, which describes the change in momentum d to the change in velocity over time, the *convective acceleration term*, which describes the chan in momentum due to change in velocity along the channel, the *pressure force term*, proportio to the change in the water depth along the channel, the gravity force term, proportional to the b slope S_0, and the friction force term, proportional to the friction slope S_f. The local and convecti acceleration terms represent the effect of inertial forces on the flow.

Alternative distributed flow routing models are produced by using the full continuity equati while eliminating some terms of the momentum equation (refer to Table 9.4.1). The simplest d tributed model is the *kinematic wave model*, which neglects the local acceleration, convecti acceleration, and pressure terms in the momentum equation; that is, it assumes that $S_0 = S_f$ and friction and gravity forces balance each other. The *diffusion wave model* neglects the local a convective acceleration terms but incorporates the pressure term. The *dynamic wave model* c siders all the acceleration and pressure terms in the momentum equation.

The momentum equation can also be written in forms that take into account whether the fl is steady or unsteady, and uniform or nonuniform, as illustrated in Table 9.4.1. In the continu equation, $\partial A/\partial t = 0$ for a steady flow, and the lateral inflow q is zero for a uniform flow.

Table 9.4.1 Summary of the Saint–Venant Equations*

Continuity equation

Conservation form $$\frac{\partial Q}{\partial x}+\frac{\partial A}{\partial t}=0$$

Nonconservation form $$V\frac{\partial y}{\partial x}+\frac{\partial V}{\partial x}+\frac{\partial y}{\partial t}=0$$

Momentum equation

Conservation form

$$\underbrace{\frac{1}{A}\frac{\partial Q}{\partial t}}_{\text{Local acceleration term}}+\underbrace{\frac{1}{A}\frac{\partial}{\partial x}\left(\frac{Q^2}{A}\right)}_{\text{Convective acceleration term}}+\underbrace{g\frac{\partial y}{\partial x}}_{\text{Pressure force term}}-\underbrace{g(S_0-S_f)}_{\substack{\text{Gravity force term}\\ \text{Friction force term}}}=0$$

Nonconservation form (unit with element)

$$\frac{\partial V}{\partial t}+V\frac{\partial V}{\partial x}+g\frac{\partial y}{\partial x}-g(S_0-S_f)=0$$

Kinematic wave

Diffusion wave

Dynamic wave

*Neglecting lateral inflow, wind shear, and eddy losses, and assuming $\beta = 1$.

x = longitudinal distance along the channel or river, t = time, A = cross-sectional area of flow, h = water surface elevation, S_f = friction slope, S_0 = channel bottom slope, g = acceleration due to gravity, V = velocity of flow, and y = depth of flow.

9.4.1 Unsteady Flow Equations: Continuity Equation

The *continuity equation* for an unsteady variable-density flow through a control volume can be written as in equation (3.2.1):

$$0=\frac{d}{dt}\int_{CV}\rho\, d\forall+\int_{CS}\rho\mathbf{V}\cdot\mathbf{dA} \tag{9.4.1}$$

Consider an elemental control volume of length dx in a channel. Figure 9.4.1 shows three views of the control volume: (*a*) an elevation view from the side, (*b*) a plan view from above, and (*c*) a channel cross-section. The inflow to the control volume is the sum of the flow Q entering the control volume at the upstream end of the channel and the lateral inflow q entering the control volume as a distributed flow along the side of the channel. The dimensions of q are those of flow per unit length of channel, so the rate of lateral inflow is qdx and the mass inflow rate is

$$\int_{\text{inlet}}\rho\mathbf{V}\cdot\mathbf{dA}=-\rho(Q+qdx) \tag{9.4.2}$$

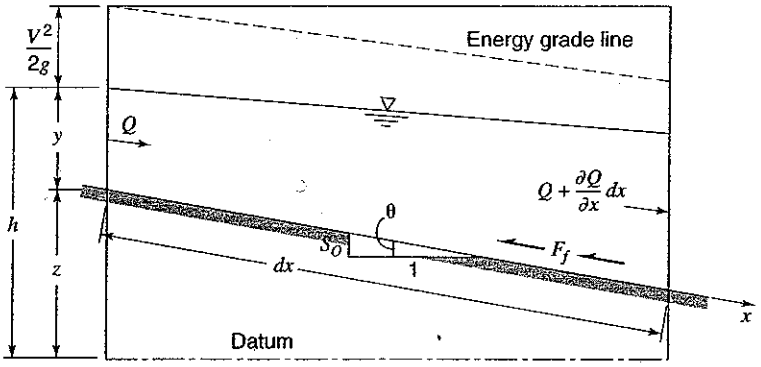

(*a*) Elevation view.

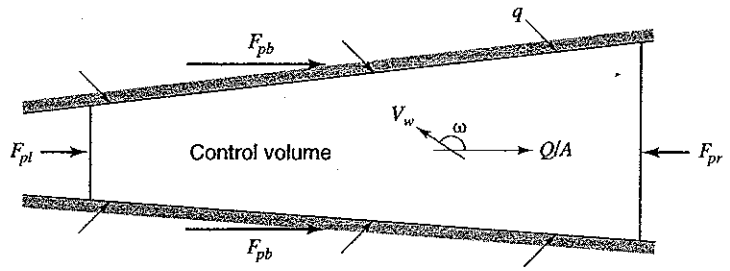

(*b*) Plan view.

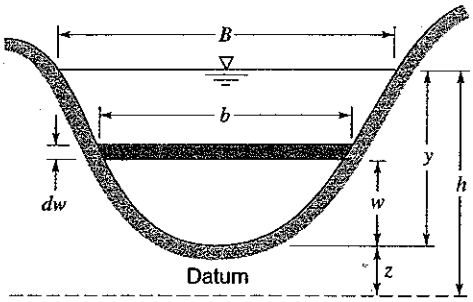

(*c*) Cross-section.

Figure 9.4.1 An elemental reach of channel for derivation of Saint–Venant equations.

This is negative because inflows are considered negative in the control volume approach (Reynolds transport theorem). The mass outflow from the control volume is

$$\int_{\text{outlet}} \rho \mathbf{V}\, \mathbf{dA} = \rho\left(Q + \frac{\partial Q}{\partial x} dx\right) \tag{9.4.3}$$

where $\partial Q/\partial x$ is the rate of change of channel flow with distance. The volume of the channel element is $A dx$, where A is the average cross-sectional area, so the rate of change of mass stored within the control volume is

$$\frac{d}{dt} \int_{CV} \rho\, d\forall = \frac{\partial(\rho A dx)}{\partial t} \tag{9.4.4}$$

where the partial derivative is used because the control volume is defined to be fixed in size (though the water level may vary within it). The net outflow of mass from the control volume is found by substituting equations (9.4.2)–(9.4.4) into (9.4.1):

$$\frac{\partial(\rho A dx)}{dt} - \rho(Q + q dx) + \rho\left(Q + \frac{\partial Q}{\partial x} dx\right) = 0 \tag{9.4.5}$$

Assuming the fluid density ρ is constant, equation (9.4.5) is simplified by dividing through by ρdx and rearranging to produce the *conservation form* of the continuity equation,

$$\frac{\partial Q}{\partial x} + \frac{\partial A}{\partial t} - q = 0 \tag{9.4.6}$$

which is applicable at a channel cross-section. This equation is valid for a *prismatic* or a *nonprismatic* channel; a prismatic channel is one in which the cross-sectional shape does not vary along the channel and the bed slope is constant.

For some methods of solving the Saint–Venant equations, the *nonconservation form* of the continuity equation is used, in which the average flow velocity V is a dependent variable, instead of Q. This form of the continuity equation can be derived for a unit width of flow within the channel, neglecting lateral inflow, as follows. For a unit width of flow, $A = y \times 1 = y$ and $Q = VA = Vy$. Substituting into equation (9.4.6) yields

$$\frac{\partial(Vy)}{\partial x} + \frac{\partial y}{\partial t} = 0 \tag{9.4.7}$$

or

$$V\frac{\partial y}{\partial x} + y\frac{\partial V}{\partial x} + \frac{\partial y}{\partial t} = 0 \tag{9.4.8}$$

9.4.2 Momentum Equation

Newton's second law is written in the form of Reynolds transport theorem as in equation (3.4.5):

$$\sum \mathbf{F} = \frac{d}{dt}\int_{CV} \mathbf{V}\rho \, d\forall + \sum_{CS} \mathbf{V}\rho\mathbf{V}\cdot\mathbf{dA} \tag{9.4.9}$$

This states that the sum of the forces applied is equal to the rate of change of momentum stored within the control volume plus the net outflow of momentum across the control surface. This equation, in the form $\Sigma F = 0$, was applied to steady uniform flow in an open channel in Chapter 5. Here, unsteady nonuniform flow is considered.

Forces. There are five forces acting on the control volume:

$$\sum F = F_g + F_f + F_e + F_p \tag{9.4.10}$$

where F_g is the *gravity force* along the channel due to the weight of the water in the control volume, F_f is the *friction force* along the bottom and sides of the control volume, F_e is the *contraction/expansion force* produced by abrupt changes in the channel cross-section, and F_p is the *unbalanced pressure force* (see Figure 9.4.1). Each of these four forces is evaluated in the following paragraphs.

Gravity. The volume of fluid in the control volume is Adx and its weight is $\rho gAdx$. For a small angle of channel inclination θ, $S_0 \approx \sin\theta$ and the gravity force is given by

$$F_g = \rho gAdx \sin\theta \approx \rho gAS_0 dx \tag{9.4.11}$$

where the channel bottom slope S_0 equals $-\partial z/\partial x$.

Friction. Frictional forces created by the shear stress along the bottom and sides of the control volume are given by $-\tau_0 P dx$, where $\tau_0 = \gamma R S_f = \rho g(A/P)S_f$ is the bed shear stress and P is the wetted perimeter. Hence the friction force is written as

$$F_f = -\rho g A S_f dx \tag{9.4.12}$$

where the friction slope S_f is derived from resistance equations such as Manning's equation.

Contraction/expansion. Abrupt contractions or expansions of the channel cause energy losses through eddy motion. Such losses are similar to minor losses in a pipe system. The magnitude of eddy losses is related to the change in velocity head $V^2/2g = (Q/A)^2/2g$ through the length of channel causing the losses. The drag forces creating these eddy losses are given by

$$F_e = -\rho g A S_e dx \tag{9.4.13}$$

where S_e is the eddy loss slope

$$S_e = \frac{K_e}{2g}\frac{\partial (Q/A)^2}{\partial x} \tag{9.4.14}$$

in which K_e is the nondimensional expansion or contraction coefficient, negative for channel expansion (where $\partial(Q/A)^2/\partial x$ is negative) and positive for channel contractions.

Pressure. Referring to Figure 9.4.1, the unbalanced pressure force is the resultant of the hydrostatic force on the each side of the control volume. Chow et al. (1988) provide a detailed derivation of the pressure force F_p as simply

$$F_p = \rho g A \frac{\partial y}{\partial x} dx \tag{9.4.15}$$

The sum of the forces in equation (9.4.10) can be expressed, after substituting equations (9.4.11), (9.4.12), (9.4.13), and (9.4.15), as

$$\Sigma F = \rho A S_0 dx - \rho g A S_f dx - \rho g A S_e dx - \rho g A \frac{\partial y}{\partial x} dx \tag{9.4.16}$$

Momentum. The two momentum terms on the right-hand side of equation (9.4.9) represent the rate of change of storage of momentum in the control volume, and the net outflow of momentum across the control surface, respectively.

Net momentum outflow. The mass inflow rate to the control volume (equation (9.4.2)) is $-\rho(Q + qdx)$, representing both stream inflow and lateral inflow. The corresponding momentum is computed by multiplying the two mass inflow rates by their respective velocity and a *momentum correction factor* β:

$$\int_{\text{inlet}} \mathbf{V}\rho\mathbf{V}\, d\mathbf{A} = -\rho\left(\beta V Q + \beta v_x q dx\right) \tag{9.4.17}$$

where $-\rho\beta VQ$ is the momentum entering from the upstream end of the channel, and $-\rho\beta v_x q dx$ is the momentum entering the main channel with the lateral inflow, which has a velocity v_x in the x direction. The term β is known as the *momentum coefficient* or *Boussinesq coefficient*; it accounts for the nonuniform distribution of velocity at a channel cross-section in computing the momentum. The value of β is given by

$$\beta = \frac{1}{V^2 A}\int v^2 dA \tag{9.4.18}$$

where v is the velocity through a small element of area dA in the channel cross-section. The value of β ranges from 1.01 for straight prismatic channels to 1.33 for river valleys with floodplains (Chow, 1959; Henderson, 1966).

The momentum leaving the control volume is

$$\int_{\text{outlet}} \mathbf{V}\rho\mathbf{V}\,\mathbf{dA} = \rho\left[\beta VQ + \frac{\partial(\beta VQ)}{\partial x}dx\right] \tag{9.4.19}$$

The net outflow of momentum across the control surface is the sum of equations (9.4.17) and (9.4.19):

$$\int_{\text{CS}} \mathbf{V}\rho\mathbf{V}d\mathbf{A} = -\rho(\beta VQ + \beta v_x q dx) + \rho\left[\beta VQ + \frac{\partial(\beta VQ)}{\partial x}dx\right]$$

$$= -\rho\left[\beta v_x q - \frac{\partial(\beta VQ)}{\partial x}\right]dx \tag{9.4.20}$$

Momentum storage. The time rate of change of momentum stored in the control volume is found by using the fact that the volume of the elemental channel is Adx, so its momentum is $\rho AdxV$, or ρQdx, and then

$$\frac{d}{dt}\int_{\text{CV}} \mathbf{V}\rho\, d\forall = \rho\frac{\partial Q}{\partial x}dx \tag{9.4.21}$$

After substituting the force terms from equation (9.4.16) and the momentum terms from equations (9.4.20) and (9.4.21) into the momentum equation (9.4.9), it reads

$$\rho gAS_0dx - \rho gAS_f dx - \rho gAS_e dx - \rho gA\frac{\partial y}{\partial x}dx = -\rho\left[\beta\, v_x q - \frac{\partial(\beta VQ)}{\partial x}\right]dx + \rho\frac{\partial Q}{\partial t}dx \tag{9.4.22}$$

Dividing through by ρdx, replacing V with Q/A, and rearranging produces the conservation form of the momentum equation:

$$\frac{\partial Q}{\partial t} + \frac{\partial(\beta Q^2/A)}{\partial t} + gA\left(\frac{\partial y}{\partial x} - S_0 + S_f + S_e\right) - \beta q v_x = 0 \tag{9.4.23}$$

The depth y in equation (9.4.23) can be replaced by the water surface elevation h, using

$$h = y + z \tag{9.4.24}$$

where z is the elevation of the channel bottom above a datum such as mean sea level. The derivative of equation (9.4.24) with respect to the longitudinal distance x along the channel is

$$\frac{\partial h}{\partial x} = \frac{\partial y}{\partial x} + \frac{\partial z}{\partial x} \tag{9.4.25}$$

but $\partial z/\partial x = -S_0$, so

$$\frac{\partial h}{\partial x} = \frac{\partial y}{\partial x} - S_0 \tag{9.4.26}$$

The momentum equation can now be expressed in terms of h by using equation (9.4.26) in (9.4.23):

$$\frac{\partial Q}{\partial t} + \frac{\partial\left(\beta\, Q^2/A\right)}{\partial x} + gA\left(\frac{\partial h}{\partial x} + S_f + S_e\right) - \beta q v_x = 0 \tag{9.4.27}$$

The Saint–Venant equations, (9.4.6) for continuity and (9.4.27) for momentum, are the governing equations for one-dimensional, unsteady flow in an open channel. The use of the terms S_f and S_e in equation (9.4.27), which represent the rate of energy loss as the flow passes through the channel, illustrates the close relationship between energy and momentum considerations in describing

the flow. Strelkoff (1969) showed that the momentum equation for the Saint–Venant equations can also be derived from energy principles, rather than by using Newton's second law as presented here.

The nonconservation form of the momentum equation can be derived in a similar manner to the nonconservation form of the continuity equation. Neglecting eddy losses, wind shear effect, and lateral inflow, the nonconservation form of the momentum equation for a unit width in the flow is

$$\frac{\partial V}{\partial t} + V\frac{\partial V}{\partial x} + g\left(\frac{\partial y}{\partial x} - S_0 + S_f\right) = 0 \tag{9.4.28}$$

9.5 KINEMATIC WAVE MODEL FOR CHANNELS

In Section 8.9, a kinematic wave overland flow runoff model was presented. This is an implicit nonlinear kinematic model that is used in the KINEROS model. This section presents a general discussion of the kinematic wave followed by brief description of the very simplest linear models, such as those found in the U.S. Army Corps of Engineers HEC-1, and the more complicated models such as the KINEROS model (Woolhiser et al., 1990).

Kinematic waves govern flow when inertial and pressure forces are not important. Dynamic waves govern flow when these forces are important, as in the movement of a large flood wave in a wide river. In a kinematic wave, the gravity and friction forces are balanced, so the flow does not accelerate appreciably.

For a kinematic wave, the energy grade line is parallel to the channel bottom and the flow is steady and uniform ($S_0 = S_f$) within the differential length, while for a dynamic wave the energy grade line and water surface elevation are not parallel to the bed, even within a differential element.

9.5.1 Kinematic Wave Equations

A *wave* is a variation in a flow, such as a change in flow rate or water surface elevation, and the *wave celerity* is the velocity with which this variation travels along the channel. The celerity depends on the type of wave being considered and may be quite different from the water velocity. For a kinematic wave the acceleration and pressure terms in the momentum equation are negligible, so the wave motion is described principally by the equation of continuity. The name kinematic is thus applicable, as *kinematics* refers to the study of motion exclusive of the influence of mass and force; in *dynamics* these quantities are included.

The kinematic wave model is defined by the following equations.

Continuity:

$$\frac{\partial Q}{\partial x} + \frac{\partial A}{\partial t} = q(x, t) \tag{9.5.1}$$

Momentum:

$$S_0 = S_f \tag{9.5.2}$$

where $q(x, t)$ is the net lateral inflow per unit length of channel.

The momentum equation can also be expressed in the form

$$A = \alpha Q^{\beta} \tag{9.5.3}$$

For example, Manning's equation written with $S_0 = S_f$ and $R = A/P$ is

$$Q = \frac{1.49 S_0^{1/2}}{nP^{2/3}} A^{5/3} \tag{9.5.4}$$

which can be solved for A as

$$A = \left(\frac{nP^{2/3}}{1.49\sqrt{S_0}} \right)^{3/5} Q^{3/5} \tag{9.5.5}$$

so $\alpha = \left[nP^{2/3} / \left(1.49\sqrt{S_0}\right) \right]^{0.6}$ and $\beta = 0.6$ in this case.

Equation (9.5.1) contains two dependent variables, A and Q, but A can be eliminated by differentiating equation (9.5.3):

$$\frac{\partial A}{\partial t} = \alpha\beta Q^{\beta-1} \left(\frac{\partial Q}{\partial t} \right) \tag{9.5.6}$$

and substituting for $\partial A/\partial t$ in equation (9.5.1) to give

$$\frac{\partial Q}{\partial x} + \alpha\beta Q^{\beta-1} \left(\frac{\partial Q}{\partial t} \right) = q \tag{9.5.7}$$

Alternatively, the momentum equation could be expressed as

$$Q = aA^B \tag{9.5.8}$$

where a and B are defined using Manning's equation. Using

$$\frac{\partial Q}{\partial x} = \frac{dQ}{dA} \frac{\partial A}{\partial x} \tag{9.5.9}$$

the governing equation is

$$\frac{\partial A}{\partial t} + \frac{dQ}{dA} \frac{\partial A}{\partial x} = q \tag{9.5.10}$$

where dQ/dA is determined by differentiating equation (9.5.8):

$$\frac{dQ}{dA} = aBA^{B-1} \tag{9.5.11}$$

and substituting in equation (9.5.10):

$$\frac{\partial A}{\partial t} = aBA^{B-1} \frac{\partial A}{\partial t} = q \tag{9.5.12}$$

The kinematic wave equation (9.5.7) has Q as the dependent variable and the kinematic wave equation (9.5.12) has A as the dependent variable. First consider equation (9.5.7), by taking the logarithm of (9.5.3):

$$\ln A = \ln\alpha + \beta \ln Q \tag{9.5.13}$$

and differentiating

$$\frac{dQ}{Q} = \frac{1}{\beta} \left(\frac{dA}{A} \right) \tag{9.5.14}$$

This defines the relationship between relative errors dA/A and dQ/Q. For Manning's equation $\beta < 1$, so that the discharge estimation error would be magnified by the ratio $1/\beta$ if A were the dependent variable instead of Q.

Next consider equation (9.5.12); by taking the logarithm of (9.5.8):

$$\ln Q = \ln a + B \ln A \tag{9.5.15}$$

$$\frac{dA}{A} = \frac{1}{B}\left(\frac{dQ}{Q}\right)$$

or

$$\frac{dQ}{Q} = B\left(\frac{dA}{A}\right) \tag{9.5.16}$$

In this case $B > 1$, so that the discharge estimation error would be decreased by B if A were the dependent variable instead of Q. In summary, if we use equation (9.5.3) as the form of the momentum equation, then Q is the dependent variable with equation (9.5.7) being the governing equation; if we use equation (9.5.8) as the form of the momentum equation, then A is the dependent variable with equation (9.5.12) being the governing equation.

9.5.2 U.S. Army Corps of Engineers HEC-1 Kinematic Wave Model for Overland Flow and Channel Routing

The HEC-1 computer program actually has two forms of the kinematic wave. The first is based upon equation (9.5.12) where an explicit finite difference form is used (refer to Figures 9.5.1 and 8.9.2):

$$\frac{\partial A}{\partial t} = \frac{A_{i+1}^{j+1} - A_{i+1}^{j}}{\Delta t} \tag{9.5.17}$$

$$\frac{\partial A}{\partial x} = \frac{A_{i+1}^{j} - A_{i}^{j}}{\Delta x} \tag{9.5.18}$$

and

$$A = \frac{A_{i+1}^{j} + A_{i}^{j}}{2} \tag{9.5.19}$$

$$q = \frac{q_{i+1}^{j+1} + q_{i+1}^{j}}{2} \tag{9.5.20}$$

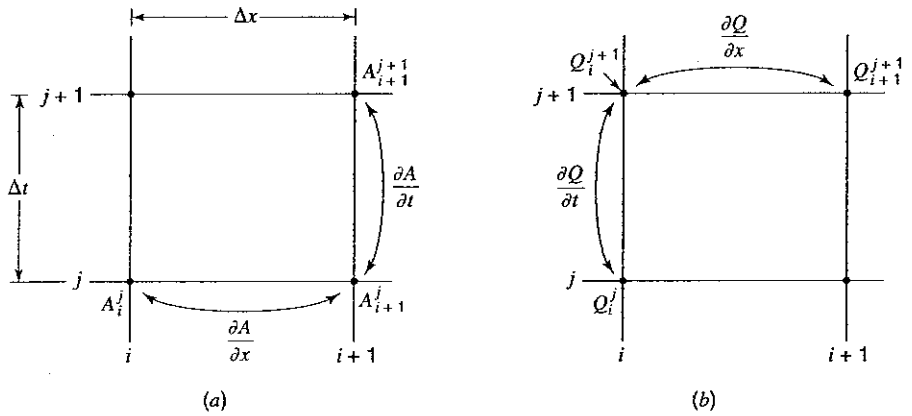

Figure 9.5.1 Finite difference forms. (*a*) HEC-1 "standard form;" (*b*) HEC-1 "conservation form."

Substituting these finite-difference approximations into equation (9.5.12) gives

$$\frac{1}{\Delta t}\left(A_{i+1}^{j+1}-A_{i+1}^{j}\right)+aB\left[\frac{A_{i+1}^{j}+A_{i}^{j}}{2}\right]^{B-1}\left[\frac{A_{i+1}^{j}-A_{i}^{j}}{\Delta x}\right]=\frac{q_{i+1}^{j+1}+q_{i+1}^{j}}{2} \tag{9.5.21}$$

The only unknown in equation (9.5.21) is A_{i+1}^{j+1}, so

$$A_{i+1}^{j+1}=A_{i+1}^{j}-aB\left(\frac{\Delta t}{\Delta x}\right)\left[\frac{A_{i+1}^{j}+A_{i}^{j}}{2}\right]^{B-1}\left(A_{i+1}^{j}-A_{i,j}\right)+\left(q_{i+1}^{j+1}+q_{i+1}^{j}\right)\frac{\Delta t}{2} \tag{9.5.22}$$

After computing A_{i+1}^{j+1} at each grid along a time line going from upstream to downstream (see Figure 8.9.2), compute the flow using equation (9.5.8):

$$Q_{i+1}^{j+1}=a\left(A_{i+1}^{j+1}\right)^{B} \tag{9.5.23}$$

The HEC-1 model uses the above kinematic wave model as long as a stability factor $R < 1$ (Alley and Smith, 1987), defined by

$$R=\frac{a}{q\Delta x}\left[\left(q\Delta t+A_{i}^{j}\right)^{B}-\left(A_{i}^{j}\right)^{B}\right] \text{ for } q>0 \tag{9.5.24a}$$

$$R=aB\left(A_{i}^{j}\right)^{B-1}\frac{\Delta t}{\Delta x} \text{ for } q=0 \tag{9.5.24b}$$

Otherwise HEC-1 uses the form of equation (9.5.1), where (see Figure 9.5.1)

$$\frac{\partial Q}{\partial x}=\frac{Q_{i+1}^{j+1}-Q_{i}^{j+1}}{\Delta x} \tag{9.5.25}$$

$$\frac{\partial A}{\partial t}=\frac{A_{i}^{j+1}-A_{i}^{j}}{\Delta t} \tag{9.5.26}$$

so

$$\frac{Q_{i+1}^{j+1}-Q_{i}^{j+1}}{\Delta x}+\frac{A_{i}^{j+1}-A_{i}^{j}}{\Delta t}=q \tag{9.5.27}$$

Solving for the only unknown Q_{i+1}^{j+1} yields

$$Q_{i+1}^{j+1}=Q_{i}^{j+1}+q\Delta x-\frac{\Delta x}{\Delta t}\left(A_{i}^{j+1}-A_{i}^{j}\right) \tag{9.5.28}$$

Then solve for A_{i+1}^{j+1} using equation (9.5.23):

$$A_{i+1}^{j+1}=\left(\frac{1}{a}Q_{i+1}^{j+1}\right)^{1/B} \tag{9.5.29}$$

The *initial condition* (values of A and Q at time 0 along the grid, referring to Figure 8.9.2) are computed assuming uniform flow or nonuniform flow for an initial discharge. The *upstream boundary* is the inflow hydrograph from which Q is obtained.

The kinematic wave schemes used in the HEC-1 model are very simplified. Chow et al. (1988) presented both linear and nonlinear kinematic wave schemes based upon the equation (9.5.7) formulation. An example of a more desirable kinematic wave formulation is that by Woolhiser et al. (1990) presented in the next subsection.

9.5.3 KINEROS Channel Flow Routing Model

The KINEROS channel routing model uses the equation (9.5.10) form of the kinematic wave equation (Woolhiser et al., 1990):

$$\frac{\partial A}{\partial t} + \frac{dQ}{dA}\frac{\partial A}{\partial x} = q(x, t) \tag{9.5.10}$$

where $q(x, t)$ is the net lateral inflow per unit length of channel. The derivatives are approximated using an implicit scheme in which the spatial and temporal derivatives are, respectively,

$$\frac{\partial A}{\partial x} = \theta\frac{A_{i+1}^{j+1} - A_i^{j+1}}{\Delta x} + (1-\theta)\frac{A_{i+1}^{j} - A_i^{j}}{\Delta x} \tag{9.5.30}$$

$$\frac{dQ}{dA}\frac{\partial A}{\partial x} = \theta\left(\frac{dQ}{dA}\right)^{j+1}\left(\frac{A_{i+1}^{j+1} - A_i^{j+1}}{\Delta x}\right) + (1-\theta)\left(\frac{dQ}{dA}\right)^{j+1}\left(\frac{A_{i+1}^{j} - A_i^{j}}{\Delta x}\right) \tag{9.5.31}$$

and

$$\frac{\partial A}{\partial t} = \frac{1}{2}\left[\frac{A_i^{j+1} - A_i^{j}}{\Delta t} + \frac{A_{i+1}^{j+1} - A_{i+1}^{j}}{\Delta t}\right] \tag{9.5.32}$$

or

$$\frac{\partial A}{\partial t} = \frac{A_i^{j+1} + A_{i+1}^{j+1} - A_i^{j} - A_{i+1}^{j}}{2\Delta t} \tag{9.5.33}$$

Substituting equations (9.5.31) and (9.5.33) into (9.5.10), we have

$$\frac{A_{i+1}^{j+1} - A_{i+1}^{j} + A_i^{j+1} - A_i^{j}}{2\Delta t} + \left\{\theta\left[\left(\frac{dQ}{dA}\right)^{j+1}\left(\frac{A_{i+1}^{j+1} - A_i^{j+1}}{\Delta x}\right)\right] + (1-\theta)\left[\left(\frac{dQ}{dA}\right)^{j+1}\left(\frac{A_{i+1}^{j} - A_i^{j}}{\Delta x}\right)\right]\right\}$$

$$= \frac{1}{2}\left(q_{i+1}^{j+1} + q_i^{j+1} + q_{i+1}^{j} + q_i^{j}\right) \tag{9.5.34}$$

The only unknown in this equation is A_{i+1}^{j+1}, which must be solved for numerically by use of an iterative scheme such as the Newton–Rhapson method (see Appendix A).

Woolhiser et al. (1990) use the following relationship between channel discharge and cross-sectional area, which embodies the kinematic wave assumption:

$$Q = \alpha R^{m-1} A \tag{9.5.35}$$

where R is the hydraulic radius and $\alpha = 1.49S^{1/2}/n$ and $m = 5/3$ for Manning's equation.

9.5.4 Kinematic Wave Celerity

Kinematic waves result from changes in Q. An increment in flow dQ can be written as

$$dQ = \frac{\partial Q}{\partial x}dx + \frac{\partial Q}{\partial t}dt \tag{9.5.36}$$

Dividing through by dx and rearranging produces:

$$\frac{\partial Q}{\partial x} + \frac{dt}{dx}\frac{\partial Q}{\partial t} = \frac{dQ}{dx} \tag{9.5.37}$$

Equations (9.5.7) and (9.5.37) are identical if

$$\frac{dQ}{dt} = q \tag{9.5.38}$$

and

$$\frac{dx}{dt} = \frac{1}{\alpha\beta Q^{\beta-1}} \tag{9.5.39}$$

Differentiating equation (9.5.3) and rearranging gives

$$\frac{dQ}{dA} = \frac{1}{\alpha\beta Q^{\beta-1}} \tag{9.5.40}$$

and by comparing equations (9.5.38) and (9.5.40), it can be seen that

$$\frac{dx}{dt} = \frac{dQ}{dA} \tag{9.5.41}$$

or

$$c_k = \frac{dx}{dt} = \frac{dQ}{dA} \tag{9.5.42}$$

where c_k is the kinematic wave celerity. This implies that an observer moving at a velocity $dx/dt = c_k$ with the flow would see the flow rate increasing at a rate of $dQ/dx = q$. If $q = 0$ the observer would see a constant discharge. Equations (9.5.38) and (9.5.42) are the *characteristic equations* for a kinematic wave, two ordinary differential equations that are mathematically equivalent to the governing continuity and momentum equations.

The kinematic wave celerity can also be expressed in terms of the depth y as

$$c_k = \frac{1}{B}\frac{dQ}{dy} \tag{9.5.43}$$

where $dA = Bdy$.

Both kinematic and dynamic wave motion are present in natural flood waves. In many cases the channel slope dominates in the momentum equation; therefore, most of a flood wave moves as a kinematic wave. Lighthill and Whitham (1955) proved that the velocity of the main part of a natural flood wave approximates that of a kinematic wave. If the other momentum terms ($\partial V/\partial t$, $V(\partial V/\partial x)$ and $(1/g)\partial y/\partial x$) are not negligible, then a dynamic wave front exists that can propagate both upstream and downstream from the main body of the flood wave.

9.6 MUSKINGUM-CUNGE MODEL

Cunge (1969) proposed a variation of the kinematic wave method based upon the Muskingum method (see Chapter 8). With the grid shown in Figure 9.6.1, the unknown discharge Q_{i+1}^{j+1} can be expressed using the Muskingum equation ($Q_{j+1} = C_1 I_{j+1} + C_2 I_j + C_3 Q_j$):

$$Q_{i+1}^{j+1} = C_1 Q_i^{j+1} + C_2 Q_i^j + C_3 Q_{i+1}^j \tag{9.6.1}$$

where $Q_{i+1}^{j+1} = Q_{j+1}$; $Q_i^{j+1} = I_{j+1}$; $Q_i^j = I_j$; and $Q_{i+1}^j = Q_j$. The Muskingum coefficients are

$$C_1 = \frac{\Delta t - 2KX}{2K(1-X) + \Delta t} \tag{9.6.2}$$

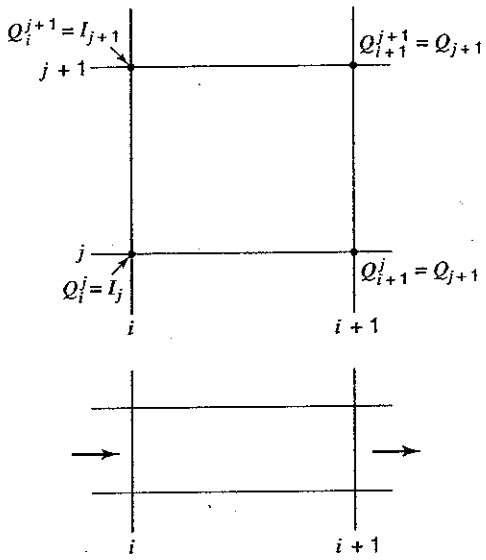

Figure 9.6.1 Finite-difference grid for Muskingum–Cunge method.

$$C_2 = \frac{\Delta t + 2KX}{2K(1-X) + \Delta t} \tag{9.6.3}$$

$$C_3 = \frac{2K(1-X) - \Delta t}{2K(1-X) + \Delta t} \tag{9.6.4}$$

Cunge (1969) showed that when K and Δt are considered constant, equation (9.6.10) is an approximate solution of the kinematic wave. He further demonstrated that (9.6.1) can be considered an approximation of a modified diffusion equation if

$$K = \frac{\Delta x}{c_k} = \frac{\Delta x}{dQ/dA} \tag{9.6.5}$$

and

$$X = \frac{1}{2}\left(1 - \frac{Q}{Bc_k S_0 \Delta x}\right) \tag{9.6.6}$$

where c_k is the celerity corresponding to Q and B, and B is the width of the water surface. The value of $\Delta x/(dQ/dA)$ in equation (9.6.5) represents the time propagation of a given discharge along a channel reach of length Δx. Numerical stability requires $0 \le x \le 1/2$. The solution procedure is basically the same as the kinematic wave.

9.7 IMPLICIT DYNAMIC WAVE MODEL

The conservation form of the Saint–Venant equations is used because this form provides the versatility required to simulate a wide range of flows from gradual long-duration flood waves in rivers to abrupt waves similar to those caused by a dam failure. The equations are developed from equations (9.4.6) and (9.4.25) as follows.

Weighted four-point finite-difference approximations given by equations (9.7.1)–(9.7.3) are used for dynamic routing with the Saint–Venant equations. The spatial derivatives $\partial Q/\partial x$ and $\partial h/\partial x$ are estimated between adjacent time lines:

$$\frac{\partial Q}{\partial x} = \theta \frac{Q_{i+1}^{j+1} - Q_i^{j+1}}{\Delta x_i} + (1-\theta)\frac{Q_{i+1}^{j} - Q_i^{j}}{\Delta x_i} \tag{9.7.1}$$

$$\frac{\partial h}{\partial x} = \theta \frac{h_{i+1}^{j+1} - h_i^{j+1}}{\Delta x_i} + (1-\theta)\frac{h_{i+1}^{j} - h_i^{j}}{\Delta x_i} \tag{9.7.2}$$

and the time derivatives are:

$$\frac{\partial (A + A_0)}{\partial t} = \frac{(A + A_0)_i^{j+1} + (A + A_0)_{i+1}^{j+1} - (A + A_0)_i^{j} - (A + A_0)_{i+1}^{j}}{2\Delta t_j} \tag{9.7.3}$$

$$\frac{\partial Q}{\partial t} = \frac{Q_i^{j+1} + Q_{i+1}^{j+1} - Q_i^{j} - Q_{i+1}^{j}}{2\Delta t_j} \tag{9.7.4}$$

The nonderivative terms, such as q and A, are estimated between adjacent time lines, using:

$$q = \theta \frac{q_i^{j+1} + q_{i+1}^{j+1}}{2} + (1-\theta)\frac{q_i^{j} + q_{i+1}^{j}}{2} = \theta \bar{q}_i^{j+1} + (1-\theta)\bar{q}_i^{j} \tag{9.7.5}$$

$$A = \theta \left[\frac{A_i^{j+1} + A_{i+1}^{j+1}}{2}\right] + (1-\theta)\left[\frac{A_i^{j} + A_{i+1}^{j}}{2}\right] = \theta \bar{A}_i^{j+1} + (1-\theta)\bar{A}_i^{j} \tag{9.7.6}$$

where $\bar{q}_i$ and $\bar{A}_i$ indicate the lateral flow and cross-sectional area averaged over the reach Δx_i.

The finite-difference form of the continuity equation is produced by substituting equations. (9.7.1), (9.7.3), and (9.7.5) into (9.4.6):

$$\theta\left(\frac{Q_{i+1}^{j+1} - Q_i^{j+1}}{\Delta x_i} - \bar{q}_i^{j+1}\right) + (1-\theta)\left(\frac{Q_{i+1}^{j} - Q_i^{j}}{\Delta x_i} - \bar{q}_i^{j}\right)$$

$$+\frac{(A + A_0)_i^{j+1} + (A + A_0)_{i+1}^{j+1} - (A + A_0)_i^{j} - (A + A_0)_{i+1}^{j}}{2\Delta t_j} = 0 \tag{9.7.7}$$

Similarly, the momentum equation (9.4.27) is written in finite-difference form as:

$$\frac{Q_i^{j+1} + Q_{i+1}^{j+1} - Q_i^{j} - Q_{i+1}^{j}}{2\Delta t_j}$$

$$+\theta\left[\frac{\left(\beta Q^2/A\right)_i^{j+1} - \left(\beta Q^2/A\right)_{i+1}^{j+1}}{\Delta x_i} + g\bar{A}_i^{j+1}\left(\frac{h_{i+1}^{j+1} - h_i^{j+1}}{\Delta x_i} + \left(\bar{S}_f\right)_i^{j+1} + \left(\bar{S}_e\right)_i^{j+1}\right) - \left(\overline{\beta q v_x}\right)_i^{j+1}\right]$$

$$+(1-\theta)\left[\frac{\left(\beta Q^2/A\right)_{i+1}^{j} - \left(\beta Q^2/A\right)_{i+1}^{j}}{\Delta x_i} + g\bar{A}_i^{j}\left(\frac{h_{i+1}^{j} - h_i^{j}}{\Delta x_i} + \left(\bar{S}_f\right)_i^{j} + \left(\bar{S}_e\right)_i^{j}\right) - \left(\overline{\beta q v_x}\right)_i^{j}\right] = 0 \tag{9.7.8}$$

The four-point finite-difference form of the continuity equation can be further modified by multiplying equation (9.7.7) by Δx_i to obtain

$$\begin{aligned}&\theta(Q_{i+1}^{j+1} - Q_i^{j+1} - \bar{q}_i^{j+1}\Delta x_i) + (1-\theta)(Q_{i+1}^{j} - Q_i^{j} - \bar{q}_i^{j}\Delta x_i)\\ &+\frac{\Delta x_i}{2\Delta t_i}\left[(A + A_0)_i^{j+1} + (A + A_0)_{i+1}^{j+1} - (A + A_0)_i^{j} - (A + A_0)_{i+1}^{j}\right] = 0\end{aligned} \tag{9.7.9}$$

Similarly, the momentum equation can be modified by multiplying by Δx_i to obtain

$$\frac{\Delta x_i}{2\Delta t_j}\left(Q_i^{j+1}+Q_{i+1}^{j+1}-Q_i^j-Q_{i+1}^j\right)$$

$$+\theta\left\{\left(\frac{\beta Q^2}{A}\right)_{i+1}^{j+1}-\left(\frac{\beta Q^2}{A}\right)_i^{j+1}+g\overline{A}_i^{j+1}\left[h_{i+1}^{j+1}-h_i^{j+1}+\left(\overline{S}_f\right)_i^{j+1}\Delta x_i+\left(\overline{S}_e\right)_i^{j+1}\Delta x_i\right]-\left(\overline{\beta q v_x}\right)_i^{j+1}\Delta x_i\right\}$$

$$+(1-\theta)\left\{\left(\frac{\beta Q^2}{A}\right)_{i+1}^{j}-\left(\frac{\beta Q^2}{A}\right)_i^{j}+g\overline{A}_i^{j}\left[h_{i+1}^{j}-h_i^{j}+\left(\overline{S}_f\right)_i^{j}\Delta x_i+\left(\overline{S}_e\right)_i^{j}\Delta x_i\right]-\left(\overline{\beta q v_x}\right)_i^{j}\Delta x_i\right\}=0 \tag{9.7.10}$$

where the average values (marked with an overbar) over a reach are defined as

$$\overline{\beta}_i=\frac{\beta_i+\beta_{i+1}}{2} \tag{9.7.11}$$

$$\overline{A}_i=\frac{A_i+A_{i+1}}{2} \tag{9.7.12}$$

$$\overline{B}_i=\frac{B_i+B_{i+1}}{2} \tag{9.7.13}$$

$$\overline{Q}_i=\frac{Q_i+Q_{i+1}}{2} \tag{9.7.14}$$

Also,

$$\overline{R}_i=\overline{A}_i/\overline{B}_i \tag{9.7.15}$$

for use in Manning's equation. Manning's equation may be solved for S_f and written in the form shown below, where the term $|Q|Q$ has magnitude Q^2 and sign positive or negative depending on whether the flow is downstream or upstream, respectively:

$$\left(\overline{S}_f\right)_i=\frac{\overline{n}_i^2|\overline{Q}_i|\overline{Q}_i}{2.208\overline{A}_i^2\overline{R}_i^{4/3}} \tag{9.7.16}$$

The minor headlosses arising from contraction and expansion of the channel are proportional to the difference between the squares of the downstream and upstream velocities, with a contraction/expansion loss coefficient K_e:

$$\left(\overline{S}_e\right)_i=\frac{\left(K_e\right)_i}{2g\Delta x_i}\left[\left(\frac{Q}{A}\right)_{i+1}^2-\left(\frac{Q}{A}\right)_i^2\right] \tag{9.7.17}$$

The terms having superscript j in equations (9.7.9) and (9.7.10) are known either from initial conditions or from a solution of the Saint–Venant equations for a previous time line. The terms g, Δx_i, β_i, K_e, C_w, and V_w are known and must be specified independently of the solution. The unknown terms are Q_i^{j+1}, Q_{i+1}^{j+1}, h_{i+1}^{j+1}, A_i^{j+1}, $A_{i+1}^{j+1}B_i^{j+1}$, and B_{i+1}^{j+1}. However, all the terms can be expressed as functions of the unknowns Q_i^{j+1}, Q_{i+1}^{j+1}, h_i^{j+1}, and h_{i+1}^{j+1}, so there are actually four unknowns. The unknowns are raised to powers other than unity, so equations (9.7.9) and (9.7.10) are nonlinear equations.

The continuity and momentum equations are considered at each of the N-1 rectangular grids shown in Figure 9.7.1, between the upstream boundary at $i = 1$ and the downstream boundary at

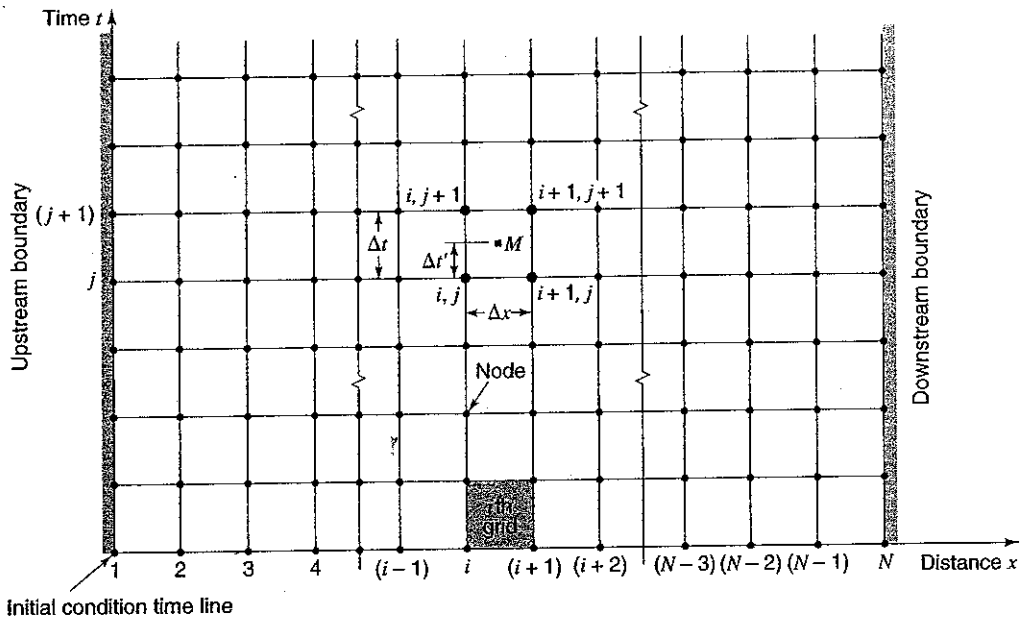

Figure 9.7.1 The x-t solution plane. The finite-difference forms of the Saint–Venant equations are solved at a discrete number of points (values of the independent variables x and t) arranged to form the rectangular grid shown. Lines parallel to the time axis represent locations along the channel, and those parallel to the distance axis represent times (from Fread (1974)).

$i = N$. This yields $2N$-2 equations. There are two unknowns at each of the N grid points (Q and h), so there are $2N$ unknowns in all. The two additional equations required to complete the solution are supplied by the upstream and downstream boundary conditions. The upstream boundary condition is usually specified as a known inflow hydrograph, while the downstream boundary condition can be specified as a known stage hydrograph, a known discharge hydrograph, or a known relationship between stage and discharge, such as a rating curve. The U.S. National Weather Service FLDWAV model (hsp.nws.noaa.gov/oh/hrl/rvmech) uses the above to describe implicit dynamic wave model formulation.

PROBLEMS

9.1.1 The storage-outflow characteristics for a reservoir are given below. Determine the storage-outflow function $2S/\Delta t + Q$ versus Q for each of the tabulated values using $\Delta t = 1.0$ hr. Plot a graph of the storage-outflow function.

Storage (106 m^3)	70	80	85	100	115
Outflow (m^3)	0	50	150	350	700

9.2.1 Route the inflow hydrograph given below through the reservoir with the storage-outflow characteristics given in problem 3.6.1 using the level pool method. Assume the reservoir has an initial storage of 70 × 106 m^3.

Time (h)	0	1	2	3	4	5	6	7	8
Inflow (m^3/s)	0	40	60	150	200	300	250	200	180

Time (h)	9	10	11	12	13	14	15	16
Inflow(m^3/s)	220	320	400	280	190	150	50	0

9.2.2 Rework problem 9.2.1 assuming the reservoir storage is initially 80 × 10^3 m^3.

9.2.3 Write a computer program to solve problems 9.2.1 and 9.2.2.

9.2.4 Rework example 9.1.1 using a 1.5-acre detention basin.

9.2.5 Rework example 9.1.1 using a triangular inflow hydrograph that increases linearly from zero to a peak of 90 cfs at 120 min and then decreases linearly to a zero discharge at 240 min. Use a 30-min routing interval.

9.2.6 Rework example 9.2.2 using $\Delta t = 2$ hrs.

9.2.7 Rework example 9.2.2 assuming $X = 0.3$ hrs.

9.3.1 Rework example 9.2.2 assuming $K = 1.4$ hr.

9.3.2 Calculate the Muskingum routing K and number of routing steps for a 1.25-mi long channel. The average cross-section dimensions for the channel are a base width of 25 ft and an average depth of 2.0 ft. Assume the channel is rectangular and has Manning's n 0.04 and a slope of 0.009 ft/ft.

9.3.3 Route the following upstream inflow hydrograph through a downstream flood control channel reach using the Muskingum method. The channel reach has a $K = 2.5$ hr and $X = 0.2$. Use a routing interval of 1 hr.

Time (h)	1	2	3	4	5	6	7
Inflow (cfs)	90	140	208	320	440	550	640
Time (h)	8	9	10	11	12	13	14
Inflow (cfs)	680	690	630	570	470	390	
Time (h)	15	16	17	18	19	20	
Inflow (cfs)	330	250	180	130	100	90	

9.3.4 Use the U.S. Army Corps of Engineers HEC-1 computer program to solve Problem 9.3.3.

REFERENCES

Alley, W. M., and P. E. Smith, Distributed Routing Rainfall-Runoff Model, Open File Report 82–344, U.S. Geological Survey, Reston, VA, 1987.

Bradley, J., *Hydraulics of Bridge Water Way*, Hydraulic Design Sevies No. 1, Federal Highway Administration. U.S. Department of Transportation, Washington, DC, 1978.

Chow, V. T., *Open Channel Hydraulics*, McGraw-Hill, New York, 1959.

Chow, V. T. (editor-in-chief), *Handbook of Applied Hydrology*, McGraw-Hill, New York, 1964.

Chow, V. T., D. R. Maidment, and L. W. Mays, *Applied Hydrology*, McGraw-Hill, New York, 1988.

Cudworth, A. G., Jr., *Flood Hydrology Manual*, U. S. Department of the Interior, Bureau of Reclamation, Denver, CO, 1989.

Cunge, J. A., "On the Subject of a Flood Propagation Method (Muskingum Method)," *Journal of Hydraulics Research*, International Association of Hydraulic Research, vol. 7, no, 2, pp. 205–230, 1969.

Fread, D. L., "Discussion of 'Implicit Flood Routing in Natural Channels,' by M. Amein and C. S. Fang," *Journal of the Hydraulics Division, ASCE*, vol. 97, no HY.7, pp. 1156–1159, 1971.

Fread, D. L., *Numerical Properties of Implicit Form-Point Finite Difference Equation of Unsteady Flow*, NOAA Technical Memorandum NWS HYDRO 18, National Weather Service, NOAA, U.S. Dept. of Commerce, Silver Spring, MD, 1974.

Fread, D. L., "Theoretical Development of Implicit Dynamic Routing Model," Dynamic Routing Service at Lower Mississippi River Forecast Center, Slidell, Louisiana, National Weather Service, NOAA, Silver Spring, MD, 1976.

Henderson, F. M., *Open Channel Flow*, Macmillan, New York, 1966.

Hewlett, J. D., *Principles of Forest Hydrology*, University of Georgia Press, Athens, GA, 1982.

Lighthill, M. J., and G. B. Whitham, "On Kinematic Waves, I: Flood Movement in Long Rivers," *Proc. Roy. Soc. London* A, vol. 229, no. 1178, pp. 281–316, 1955.

Maidment, D. R. (editor-in-chief), *Handbook of Hydrology*, McGraw-Hill, New York, 1993.

Masch, F. D., *Hydrology*, Hydraulic Engineering Circular No. 19, FHWA-10-84-15, Federal Highway Administration, U.S. Department of the Interior, McLean, VA, 1984.

Mays, L. W., and Y. K. Tung, *Hydrosystems Engineering and Management*, McGraw-Hill, New York, 1992.

McCuen, R. H., *Hydrologic Analysis and Design*, Prentice-Hall, Englewood Cliffs, NJ, 1989.

Morris, E. M., and D. A. Woolhiser, 1980, "Unsteady One-Dimensional Flow over a Plane: Partial Equilibrium and Recession Hydrographs," *Water Resources Research* 16(2): 355–360.

Mosley, M. P., and A. I. McKerchar, "Streamflow," in *Handbook of Hydrology* (edited by D. R. Maidment), McGraw-Hill, New York, 1993.

Ponce, V. M., *Engineering Hydrology: Principles and Practices*, Prentice-Hall, Englewood Cliffs, NJ, 1989.

Strahler, A. N., "Quantitative Geomorphology of Drainage Basins and Channel Networks," section 4–II in *Handbook of Applied Hydrology*, edited by V. T. Chow, pp. 4–39, 4–76, McGraw-Hill, New York, 1964.

Strelkoff, T., "Numerical Solution of Saint–Venant Equation," *Journal of the Hydraulics Division, ASCE*, vol. 96, no. HY1, pp. 223–252, 1970.

Strelkoff, T., The One-Dimensional Equations of Open-Channel Flow, *Journal of the Hydraulics Division*, American Society of Civil Engineers, vol. 95, no. Hy3, pp. 861–874, 1969.

U.S. Army Corps of Engineers, "Routing of Floods Through River Channels," *Engineer Manual*, 1110–2–1408, Washington, DC, 1960.

U.S. Army Corps of Engineers, Hydrologic Engineering Center, *HEC-1, Flood Hydrograph Package, User's Manual*, Davis, CA, 1990.

U.S. Department of Agriculture, Soil Conservation Service, "A Method for Estimating Volume and Rate of Runoff in Small Watersheds," Tech. Paper 149, Washington, DC, 1973.

U.S. Department of Agriculture, Soil Conservation Service, "Urban Hydrology for Small Watersheds," Tech. Release no. 55, Washington, DC, 1986.

U.S. Environmental Data Services, *Climate Atlas of the U.S.*, U.S. Government Printing Office, Washington, DC, pp. 43–44, 1968.

U.S. National Research Council, Committee on Opportunities in the Hydrologic Sciences, Water Science and Technology Board, *Opportunities in the Hydrologic Sciences*, National Academy Press, Washington, DC, 1991.

Viessman, W., Jr., and G. L. Lewis, *Introduction to Hydrology*, fourth edition, Harper and Row, New York, 1996.

Woolhiser, D. A., and J. A. Liggett, Unsteady, One-Dimensional Flow Over a Plane—the Rising Hydrograph, *Water Resources Research*, vol. 3(3), pp. 753–771, 1967.

Woolhiser, D. A., R. E. Smith, and D. C. Goodrich, *KINEROS, A Kinematic Runoff and Erosion Model: Documentation and User Manual*, U. S. Department of Agricultural Research Service, ARS-77, Tucson, AZ, 1990.

HAND OUT 19: Overview of hydraulic routing (Chapter 6 of our syllabus).

Overview of hydraulic routing

1) General equations

Mass: $\boxed{\frac{\partial Q}{\partial x} + \frac{\partial \Omega}{\partial t} = q}$ $\Omega \equiv A$ area

Momentum:

$$\frac{\partial Q}{\partial t} + \frac{\partial}{\partial x}\left(\beta \frac{Q^2}{\Omega}\right) + g\Omega\left(\frac{\partial y}{\partial x} + S_f + S_e\right) - \beta q v_x = 0$$

2) Approximations

a) Kinematic wave:

KW: $\frac{\partial Q}{\partial x} + \frac{\partial \Omega}{\partial t} = q$

$$S_o = S_f$$

b) "Diffusive" wave:

$$\frac{\partial Q}{\partial x} + \frac{\partial \Omega}{\partial t} = q$$

$$g\frac{\partial y}{\partial x} - g(S_o - S_f) = 0$$

3) Solutions for the KW

a) HEC-1, version a)

$$\frac{\partial \Omega}{\partial t} = \frac{\Omega_{i+1}^{j+1} - \Omega_{i+1}^{j}}{\Delta t}$$

$$\frac{\partial \Omega}{\partial x} = \frac{\Omega_{i+1}^{j} - \Omega_{i}^{j}}{\Delta x}$$

$$\Omega = \frac{\Omega_{i+1}^{j} + \Omega_{i}^{j}}{2}$$

$$q = \frac{q_{i+1}^{j+1} + q_{i+1}^{j}}{2}$$

$$\Rightarrow \boxed{\Omega_{i+1}^{j+1} = \Omega_{i+1}^{j} - \alpha B \left(\frac{\Delta t}{\Delta x}\right)\left[\frac{\Omega_{i+1}^{j} + \Omega_{i}^{j}}{2}\right]^{B-1} \times \left(\Omega_{i+1}^{j} - \Omega_{i}^{j}\right) + \left(q_{i+1}^{j+1} + q_{i+1}^{j}\right)\frac{\Delta t}{2}}$$

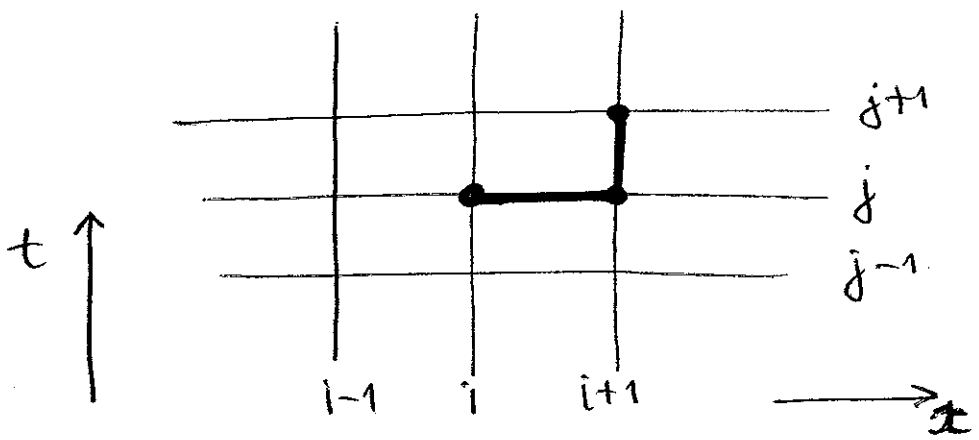

$$Q_{i+1}^{j+1} = a\left(\Omega_{i+1}^{j+1}\right)^B$$

b) HEC-1, Version b)

$$\frac{\partial Q}{\partial x} = \frac{Q_{i+1}^{j+1} - Q_i^{j+1}}{\Delta x}$$

$$\frac{\partial \Omega}{\partial t} = \frac{\Omega_i^{j+1} - A_i^j}{\Delta t}$$

$$Q_{i+1}^{j+1} = Q_i^{j+1} + q\Delta x - \frac{\Delta x}{\Delta t}\left(\Omega_i^{j+1} - \Omega_i^j\right)$$

HAND OUT 20: Overview of hydrologic and hydraulic routing (Chapter 6 of our syllabus). Source: U.S. Corps of Engineers.

Chapter 9
Streamflow and Reservoir Routing

9-1. General

a. Routing is a process used to predict the temporal and spatial variations of a flood hydrograph as it moves through a river reach or reservoir. The effects of storage and flow resistance within a river reach are reflected by changes in hydrograph shape and timing as the floodwave moves from upstream to downstream. Figure 9-1 shows the major changes that occur to a discharge hydrograph as a floodwave moves downstream.

b. In general, routing techniques may be classified into two categories: hydraulic routing, and hydrologic routing. Hydraulic routing techniques are based on the solution of the partial differential equations of unsteady open channel flow. These equations are often referred to as the St. Venant equations or the dynamic wave equations. Hydrologic routing employs the continuity equation and an analytical or an empirical relationship between storage within the reach and discharge at the outlet.

c. Flood forecasting, reservoir and channel design, floodplain studies, and watershed simulations generally utilize some form of routing. Typically, in watershed simulation studies, hydrologic routing is utilized on a reach-by-reach basis from upstream to downstream. For example, it is often necessary to obtain a discharge hydrograph at a point downstream from a location where a hydrograph has been observed or computed. For such purposes, the upstream hydrograph is routed through the reach with a hydrologic routing technique that predicts changes in hydrograph shape and timing. Local flows are then added at the downstream location to obtain the total flow hydrograph. This type of approach is adequate as long as there are no significant backwater effects or

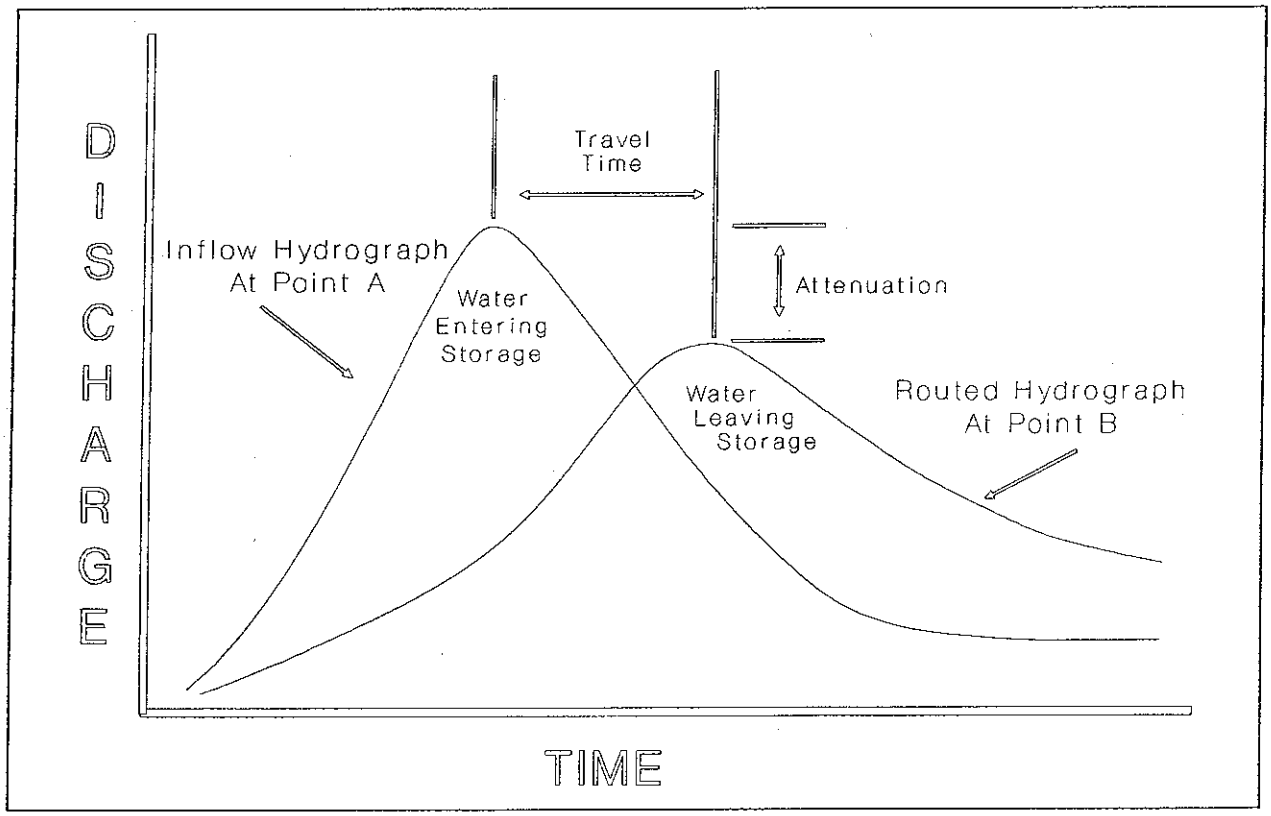

Figure 9-1. Discharge hydrograph routing effects

discontinuities in the water surface because of jumps or bores. When there are downstream controls that will have an effect on the routing process through an upstream reach, the channel configuration should be treated as one continuous system. This can only be accomplished with a hydraulic routing technique that can incorporate backwater effects as well as internal boundary conditions, such as those associated with culverts, bridges, and weirs.

d. This chapter describes several different hydraulic and hydrologic routing techniques. Assumptions, limitations, and data requirements are discussed for each. The basis for selection of a particular routing technique is reviewed, and general calibration methodologies are presented. This chapter is limited to discussions on 1-D flow routing techniques in the context of flood-runoff analysis. The focus of this chapter is on discharge (flow) rather than stage (water surface elevation). Detailed presentation of routing techniques and applications focused on stage calculations can be found in EM 1110-2-1416.

9-2. Hydraulic Routing Techniques

a. The equations of motion. The equations that describe 1-D unsteady flow in open channels, the Saint Venant equations, consist of the continuity equation, Equation 9-1, and the momentum equation, Equation 9-2. The solution of these equations defines the propagation of a floodwave with respect to distance along the channel and time.

$$A\frac{\partial V}{\partial x} + VB\frac{\partial y}{\partial x} + B\frac{\partial y}{\partial t} = q \qquad (9\text{-}1)$$

$$S_f = S_o - \frac{\partial y}{\partial x} - \frac{V}{g}\frac{\partial V}{\partial x} - \frac{1}{g}\frac{\partial V}{\partial t} \qquad (9\text{-}2)$$

where

A = cross-sectional flow area

V = average velocity of water

x = distance along channel

B = water surface width

y = depth of water

t = time

q = lateral inflow per unit length of channel

S_f = friction slope

S_o = channel bed slope

g = gravitational acceleration

Solved together with the proper boundary conditions, Equations 9-1 and 9-2 are the complete dynamic wave equations. The meaning of the various terms in the dynamic wave equations are as follows (Henderson 1966):

(1) Continuity equation.

$A\frac{\partial V}{\partial x}$ = *prism storage*

$VB\frac{\partial y}{\partial x}$ = *wedge storage*

$B\frac{\partial y}{\partial t}$ = *rate of rise*

q = *lateral inflow per unit length*

(2) Momentum equation.

S_f = *friction slope (frictional forces)*

S_o = *bed slope (gravitational effects)*

$\frac{\partial y}{\partial x}$ = *pressure differential*

$\frac{V}{g}\frac{\partial V}{\partial x}$ = *convective acceleration*

$\frac{1}{g}\frac{\partial V}{\partial t}$ = *local acceleration*

(3) Dynamic wave equations. The dynamic wave equations are considered to be the most accurate and comprehensive solution to 1-D unsteady flow problems in open channels. Nonetheless, these equations are based on specific assumptions, and therefore have limitations. The assumptions used in deriving the dynamic wave equations are as follows:

(a) Velocity is constant and the water surface is horizontal *across* any channel section.

(b) All flows are gradually varied with hydrostatic pressure prevailing at all points in the flow, such that vertical accelerations can be neglected.

(c) No lateral secondary circulation occurs.

(d) Channel boundaries are treated as fixed; therefore, no erosion or deposition occurs.

(e) Water is of uniform density, and resistance to flow can be described by empirical formulas, such as Manning's and Chezy's equation.

(f) The dynamic wave equations can be applied to a wide range of 1-D flow problems; such as, dam break floodwave routing, forecasting water surface elevations and velocities in a river system during a flood, evaluating flow conditions due to tidal fluctuations, and routing flows through irrigation and canal systems. Solution of the full equations is normally accomplished with an explicit or implicit finite difference technique. The equations are solved for incremental times (Δt) and incremental distances (Δx) along the waterway.

b. Approximations of the full equations. Depending on the relative importance of the various terms of the momentum Equation 9-2, the equation can be simplified for various applications. Approximations to the full dynamic wave equations are created by combining the continuity equation with various simplifications of the momentum equation. The most common approximations of the momentum equation are:

$$S_f = S_o - \frac{\partial y}{\partial x} - \frac{V}{g}\frac{\partial V}{\partial x} - \frac{1}{g}\frac{\partial V}{\partial t} \qquad (9\text{-}3)$$

Steady Uniform Flow
Kinematic Wave Approx.

Steady Nonuniform Flow
Diffusion Wave Approximation

Steady Nonuniform Flow
Quasi-Steady Dynamic Wave Approximation

Unsteady Nonuniform Flow
Full Dynamic Wave Equation

The use of approximations to the full equations for unsteady flow can be justified when specific terms in the momentum equation are small in comparison to the bed slope. This is best illustrated by an example taken from Henderson's book *Open Channel Flow* (1966). Henderson computed values for each of the terms on the right-hand side of the momentum equation for a steep alluvial stream:

Term:	S_o	$\frac{\partial y}{\partial x}$	$\frac{V}{g}\frac{\partial V}{\partial x}$	$\frac{1}{g}\frac{\partial V}{\partial t}$
Magnitude (ft/mi):	26	.5	.12-.25	.05

These figures relate to a very fast rising hydrograph in which the flow increased from 10,000 to 150,000 cfs and decreased again to 10,000 cfs within 24 hr. Even in this case, where changes in depth and velocity with respect to distance and time are relatively large, the last three terms are still small in comparison to the bed slope. For this type of flow situation (steep stream), an approximation of the full equations would be appropriate. For flatter slopes, the last three terms become increasingly more important.

(1) Kinematic wave approximation. Kinematic flow occurs when gravitational and frictional forces achieve a balance. In reality, a true balance between gravitational and frictional forces never occurs. However, there are flow situations in which gravitational and frictional forces approach an equilibrium. For such conditions, changes in depth and velocity with respect to time and distance are small in magnitude when compared to the bed slope of the channel. Therefore, the terms to the right of the bed slope in Equation 9-3 are assumed to be negligible. This assumption reduces the momentum equation to the following:

$$S_f = S_o \qquad (9\text{-}4)$$

Equation 9-4 essentially states that the momentum of the flow can be approximated with a uniform flow assumption as described by Manning's or Chezy's equation. Manning's equation can be written in the following form:

$$Q = \alpha A^m \qquad (9\text{-}5)$$

where α and m are related to flow geometry and surface roughness

Since the momentum equation has been reduced to a simple functional relationship between area and discharge, the movement of a floodwave is described solely by the continuity equation, written in the following form:

$$\frac{\partial A}{\partial t} + \frac{\partial Q}{\partial x} = q \tag{9-6}$$

Then by combining Equations 9-5 and 9-6, the governing kinematic wave equation is obtained as:

$$\frac{\partial A}{\partial t} + \alpha m A^{(m-1)} \frac{\partial A}{\partial x} = q \tag{9-7}$$

Because of the steady uniform flow assumptions, the kinematic wave equations do not allow for hydrograph diffusion, just simple translation of the hydrograph in time. The kinematic wave equations are usually solved by explicit or implicit finite difference techniques. Any attenuation of the peak flow that is computed using the kinematic wave equations is due to errors inherent in the finite difference solution scheme.

(a) The application of the kinematic wave equation is limited to flow conditions that do not demonstrate appreciable hydrograph attenuation. In general, the kinematic wave approximation works best when applied to steep (10 ft/mile or greater), well defined channels, where the floodwave is gradually varied.

(b) The kinematic wave approach is often applied in urban areas because the routing reaches are generally short and well defined (i.e., circular pipes, concrete lined channels, etc.).

(c) The kinematic wave equations cannot handle backwater effects since, with a kinematic model flow, disturbances can only propagate in the downstream direction. All of the terms in the momentum equation that are used to describe the propagation of the floodwave upstream (backwater effects) have been excluded.

(2) Diffusion wave approximation. Another common approximation of the full dynamic wave equations is the diffusion wave analogy. The diffusion wave model utilizes the continuity Equation 9-1 and the following simplified form of the momentum equation:

$$S_f = S_o - \frac{\partial y}{\partial x} \tag{9-8}$$

The diffusion wave model is a significant improvement over the kinematic wave model because of the inclusion of the pressure differential term in Equation 9-8. This term allows the diffusion model to describe the attenuation (diffusion effect) of the floodwave. It also allows the specification of a boundary condition at the downstream extremity of the routing reach to account for backwater effects. It does not use the inertial terms (last two terms) from Equation 9-2 and, therefore, is limited to slow to moderately rising floodwaves (Fread 1982). However, most natural floodwaves can be described with the diffusion form of the equations.

(3) Quasi-steady dynamic wave approximation. The third simplification of the full dynamic wave equations is the quasi-steady dynamic wave approximation. This model utilizes the continuity equation, Equation 9-1, and the following simplification of the momentum equation:

$$S_f = S_o - \frac{\partial y}{\partial x} - \frac{V}{g}\frac{\partial V}{\partial x} \tag{9-9}$$

In general, this simplification of the dynamic wave equations is not used in flood routing. This form of the momentum equation is more commonly used in steady flow-water surface profile computations. In the case of flood routing, the last two terms on the momentum equation are often opposite in sign and tend to counteract each other (Fread 1982). By including the convective acceleration term and not the local acceleration term, an error is introduced. This error is of greater magnitude than the error that results when both terms are excluded, as in the diffusion wave model. For steady flow-water surface profiles, the last term of the momentum equation (changes in velocity with respect to time) is assumed to be zero. However, changes in velocity with respect to distance are still very important in the calculation of steady flow-water surface profiles.

c. Data requirements. In general, the data requirements of the various hydraulic routing techniques are virtually the same. However, the amount of detail that is required for each type of data will vary depending upon the routing technique being used and the situation it is being applied to. The basic data requirements for hydraulic routing techniques are the following:

(1) Flow data (hydrographs).

(2) Channel cross sections and reach lengths.

(3) Roughness coefficients.

(4) Initial and boundary conditions.

(a) Flow data consist of discharge hydrographs from upstream locations as well as lateral inflow and tributary flow for all points along the stream.

(b) Channel cross sections are typically surveyed sections that are perpendicular to the flow lines. Key issues in selecting cross sections are the accuracy of the surveyed data and the spacing of the sections along the stream. If the routing procedure is utilized to predict stages, then the accuracy of the cross-sectional dimensions will have a direct effect on the prediction of the stage. If the cross sections are used only to route discharge hydrographs, then it is only important to ensure that the cross section is an adequate representation of the discharge versus flow area of the section. Simplified cross-sectional shapes, such as 8-point cross sections or trapezoids and rectangles, are often used to fit the discharge versus flow area of a more detailed section. Cross-sectional spacing affects the level of detail of the results as well as the accuracy of the numerical solution to the routing equations. Detailed discussions on cross-sectional spacing can be found in the reference by the Hydrologic Engineering Center (HEC) (USACE 1986).

(c) Roughness coefficients for hydraulic routing models are typically in the form of Manning's n values. Manning's coefficients have a direct impact on the travel time and amount of diffusion that will occur when routing a flood hydrograph through a channel reach. Roughness coefficients will also have a direct impact on predicted stages.

(d) All hydraulic models require that initial and boundary conditions be established before the routing can commence. Initial conditions are simply stated as the conditions at all points in the stream at the beginning of the simulation. Initial conditions are established by specifying a base flow within the channel at the start of the simulation. Channel depths and velocities can be calculated through steady-state backwater computations or a normal depth equation (e.g., Manning's equation). Boundary conditions are known relationships between discharge and time and/or discharge and stage. Hydraulic routing computations require the specification of upstream, downstream, and internal boundary conditions to solve the equations. The upstream boundary condition is the discharge (or stage) versus time relationship of the hydrograph to be routed through the reach. Downstream boundary conditions are usually established with a steady-state rating curve (discharge versus depth relationship) or through normal depth calculations (Manning's equation). Internal boundary conditions consist of lateral inflow or tributary flow hydrographs, as well as depth versus discharge relationships for hydraulic structures within the river reach.

9-3. Hydrologic Routing Techniques

Hydrologic routing employs the use of the continuity equation and either an analytical or an empirical relationship between storage within the reach and discharge at the outlet. In its simplest form, the continuity equation can be written as inflow minus outflow equals the rate of change of storage within the reach:

$$I - O = \frac{\Delta S}{\Delta t} \tag{9-10}$$

where

I = the average inflow to the reach during Δt

O = the average outflow from the reach during Δt

S = storage within the reach

a. Modified puls reservoir routing.

(1) One of the simplest routing applications is the analysis of a floodwave that passes through an unregulated reservoir (Figure 9-2a). The inflow hydrograph is known, and it is desired to compute the outflow hydrograph from the reservoir. Assuming that all gate and spillway openings are fixed, a unique relationship between storage and outflow can be developed, as shown in Figure 9-2b.

(2) The equation defining storage routing, based on the principle of conservation of mass, can be written in approximate form for a routing interval Δt. Assuming the subscripts "1" and "2" denote the beginning and end of the routing interval, the equation is written as follows:

$$\frac{O_1 + O_2}{2} = \frac{I_1 + I_2}{2} - \frac{S_2 - S_1}{\Delta t} \tag{9-11}$$

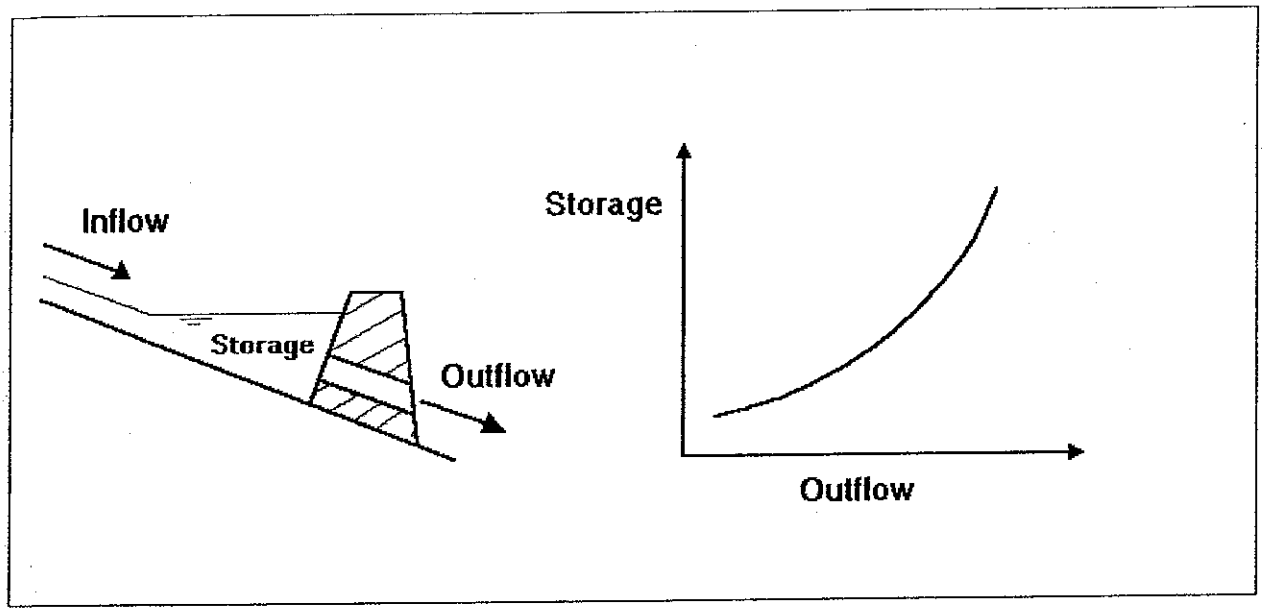

Figure 9-2. Reservoir storage routing

The known values in this equation are the inflow hydrograph and the storage and discharge at the beginning of the routing interval. The unknown values are the storage and discharge at the end of the routing interval. With two unknowns (O_2 and S_2) remaining, another relationship is required to obtain a solution. The storage-outflow relationship is normally used as the second equation. How that relationship is derived is what distinguishes various storage routing methods.

(3) For an uncontrolled reservoir, outflow and water in storage are both uniquely a function of lake elevation. The two functions can be combined to develop a storage-outflow relationship, as shown in Figure 9-3. Elevation-discharge relationships can be derived directly from hydraulic equations. Elevation-storage relationships are derived through the use of topographic maps. Elevation-area relationships are computed first, then either average end-area or conic methods are used to compute volumes.

(4) The storage-outflow relationship provides the outflow for any storage level. Starting with a nearly empty reservoir, the outflow capability would be minimal. If the inflow is less than the outflow capability, the water would flow through. During a flood, the inflow increases and eventually exceeds the outflow capability. The difference between inflow and outflow produces a change in storage. In Figure 9-4, the difference between the inflow and the outflow (on the rising side of the outflow hydrograph) represents the volume of water entering storage.

(5) As water enters storage, the outflow capability increases because the pool level increases. Therefore, the outflow increases. This increasing outflow with increasing water in storage continues until the reservoir reaches a maximum level. This will occur the moment that the outflow equals the inflow, as shown in Figure 9-4. Once the outflow becomes greater than the inflow, the storage level will begin dropping. The difference between the outflow and the inflow hydrograph on the recession side reflects water withdrawn from storage.

(6) The modified puls method applied to reservoirs consists of a repetitive solution of the continuity equation. It is assumed that the reservoir water surface remains horizontal, and therefore, outflow is a unique function of reservoir storage. The continuity equation, Equation 9-11, can be manipulated to get both of the unknown variables on the left-hand side of the equation:

$$\left(\frac{S_2}{\Delta t} + \frac{O_2}{2}\right) = \left(\frac{S_1}{\Delta t} + \frac{O_1}{2}\right) - O_1 + \frac{I_1 + I_2}{2} \qquad (9\text{-}12)$$

Since I is known for all time steps, and O_1 and S_1 are known for the first time step, the right-hand side of the equation can be calculated. The left-hand side of the equation can be solved by trial and error. This is accomplished by assuming a value for either S_2 or O_2, obtaining the corresponding value from the storage-outflow relationship, and then iterating until Equation 9-12 is satisfied.

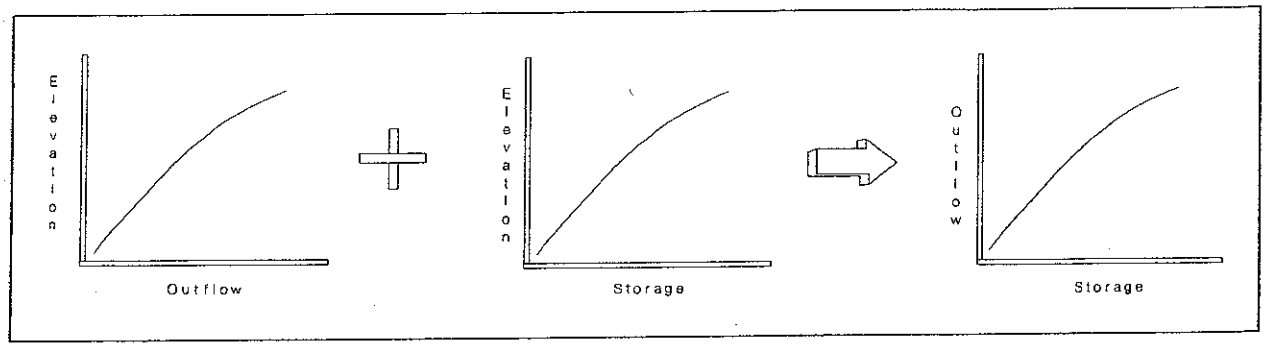

Figure 9-3. Reservoir storage-outflow curve

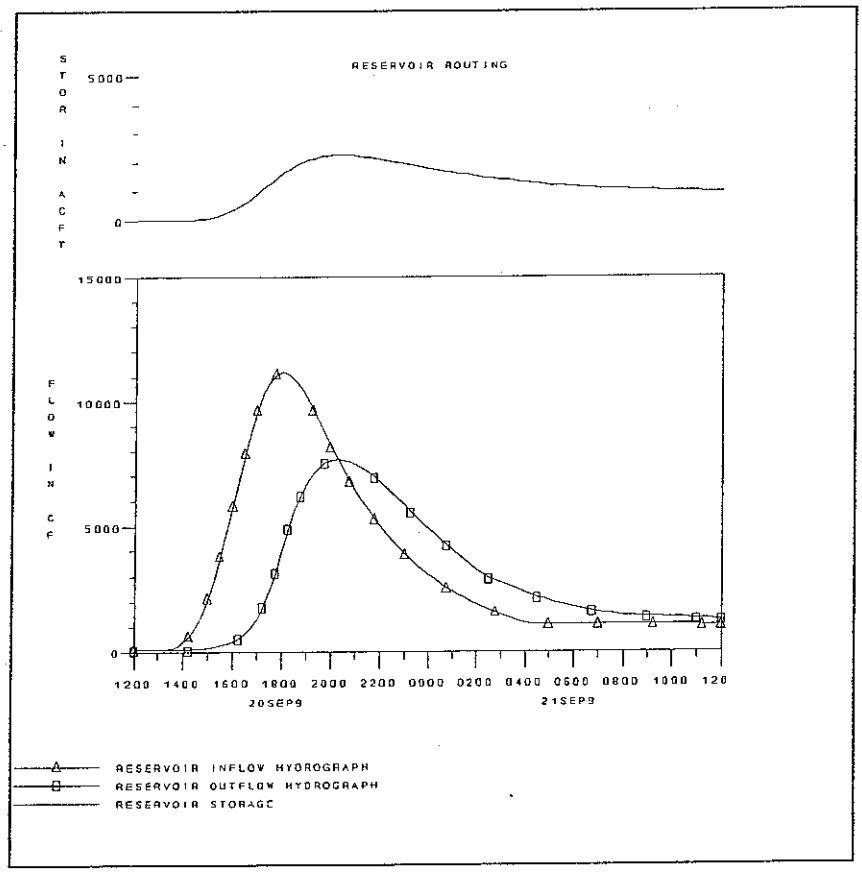

Figure 9-4. Reservoir routing example

Rather than resort to this iterative procedure, a value of Δt is selected and points on the storage-outflow curve are replotted as the "storage-indication" curve shown in Figure 9-5. This graph allows for a direct determination of the outflow (O_2) once a value of storage indication ($S_2/\Delta t + O_2/2$) has been calculated from Equation 9-12 (Viessman et al. 1977). The numerical integration of Equation 9-12 and Figure 9-5 is illustrated as an example in Table 9-1. The stepwise procedure for applying the modified puls method to reservoirs can be summarized as follows:

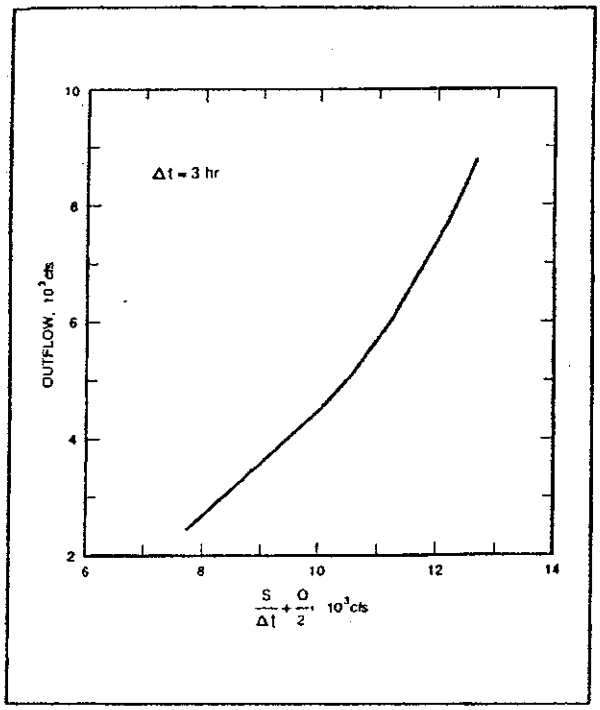

Figure 9-5. Storage-indication curve

(a) Determine a composite discharge rating curve for all of the reservoir outlet structures.

(b) Determine the reservoir storage that corresponds with each elevation on the rating curve for reservoir outflow.

(c) Select a time step and construct a storage-indication versus outflow curve $[(S/\Delta t) + (O/2)]$ versus O.

(d) Route the inflow hydrograph through the reservoir based on Equation 9-12 and the storage-indication curve.

(e) Compare the results with historical events to verify the model.

b. Modified puls channel routing. Routing in natural rivers is complicated by the fact that storage in a river reach is not a function of outflow alone. During the passing of a floodwave, the water surface in a channel is not uniform. The storage and water surface slope within a river reach, for a given outflow, is greater during the rising stages of a floodwave than during the falling (Figure 9-6). Therefore, the relationship between storage and discharge at the outlet of a channel is not a unique relationship, rather it is a looped relationship. An example storage-discharge function for a river is shown in Figure 9-7.

(1) Application of the modified puls method to rivers. To apply the modified puls method to a channel routing problem, the storage within the river reach is approximated with a series of "cascading reservoirs" (Figure 9-8). Each reservoir is assumed to have a level pool and, therefore, a unique storage-discharge relationship. The cascading reservoir approach is capable of approximating the looped storage-outflow effect when evaluating the river reach as a whole. The rising and falling floodwave is simulated with different storage levels in the cascade of reservoirs, thus producing a looped storage-outflow function for the total river reach. This is depicted graphically in Figure 9-9.

(2) Determination of the storage-outflow relationship.

(a) Determining the storage-outflow relationship for a river reach is a critical part of the modified puls procedure. In river reaches, storage-outflow relationships can be determined from one of the following:

- steady-flow profile computations,
- observed water surface profiles,
- normal-depth calculations,
- observed inflow and outflow hydrographs, and
- optimization techniques applied to observed inflow and outflow hydrographs.

(b) Steady-flow water surface profiles, computed over a range of discharges, can be used to determine storage-outflow relationships in a river reach (Figure 9-10). In this illustration, a known hydrograph at A is to be routed to location B. The storage-outflow relationship required for routing is determined by computing a series of water surface profiles, corresponding to a range of discharges. The range of discharges should encompass the range of flows that will be routed through the river reach. The storage volumes are computed by multiplying the cross-sectional area, under a specific flow profile, by the channel reach lengths. Volumes are calculated for each flow profile and then plotted against

Table 9-1
Storage Routing Calculation

(1)	(2)	(3)	(4)	(5)	(6)	(7)
Time (hr)	Inflow (cfs)	Average Inflow (cfs)	$\frac{S}{\Delta t} + \frac{O}{2}$ (cfs)	Outflow (cfs)	$\frac{S}{\Delta t}$ (cfs)	S (acre-ft)
0	3,000		8,600	3,000	7,100	1,760
		3,130				
3	3,260		8,730	3,150	7,155	1,774
		3,445				
6	3,630		9,025	3,400	7,325	1,816
		3,825				
9	4,020		9,450	3,850	7,525	1,866
		4,250				
12	4,480		9,850	4,300	7,700	1,909
.						
.						
etc.						

the corresponding discharge at the outlet. If channel or levee modifications will have an effect on the routing through the reach,modifications can be made to the cross sections, water surface profiles recalculated, and a revised storage-outflow relationship can be developed. The impacts of the channel or levee modification can be approximated by routing floods with both pre- and post-project storage-outflow relationships.

(c) Observed water surface profiles, obtained from high water marks, can be used to compute storage-outflow relationships. Sufficient stage data over a range of floods are required for this type of calculation; however, it is not likely that enough data would be available over the range of discharges needed to compute an adequate storage discharge relationship. If a few observed profiles are available, they can be used to calibrate a steady-flow water surface profile model for the channel reach of interest. Then the water surface profile model could be used to calculate the appropriate range of values to calculate the storage-outflow relationship.

(d) Normal depth associated with uniform flow does not exist in natural streams; however, the concept can be used to estimate water depth and storage in natural rivers if uniform flow conditions can reasonably be assumed. With a typical cross section, Manning's equation is solved for a range of discharges, given appropriate "n" values and an estimated slope of the energy grade line. Under the assumption of uniform flow conditions, the energy slope is considered equal to the average channel bed slope; therefore, this approach should not be applied in backwater areas.

(e) Observed inflow and outflow hydrographs can be used to compute channel storage by an inverse process of flood routing. When both inflow and outflow are known, the change in storage can be computed, and from that a storage versus outflow function can be developed. Tributary inflow, if any, must also be accounted for in this calculation. The total storage is computed from some base level storage at the beginning or end of the routing sequence.

(f) Inflow and outflow hydrographs can also be used to compute routing criteria through a process of iteration in which an initial set of routing criteria is assumed, the inflow hydrograph is routed, and the results are evaluated. The process is repeated as necessary until a suitable fit of the routed and observed hydrograph is obtained.

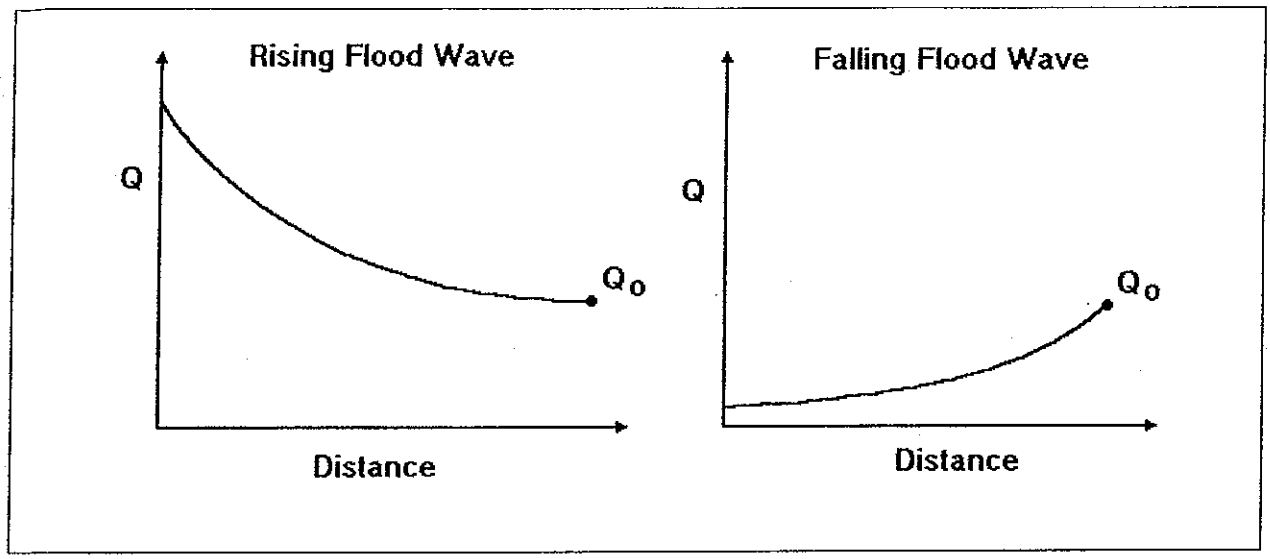

Figure 9-6. Rising and falling floodwave

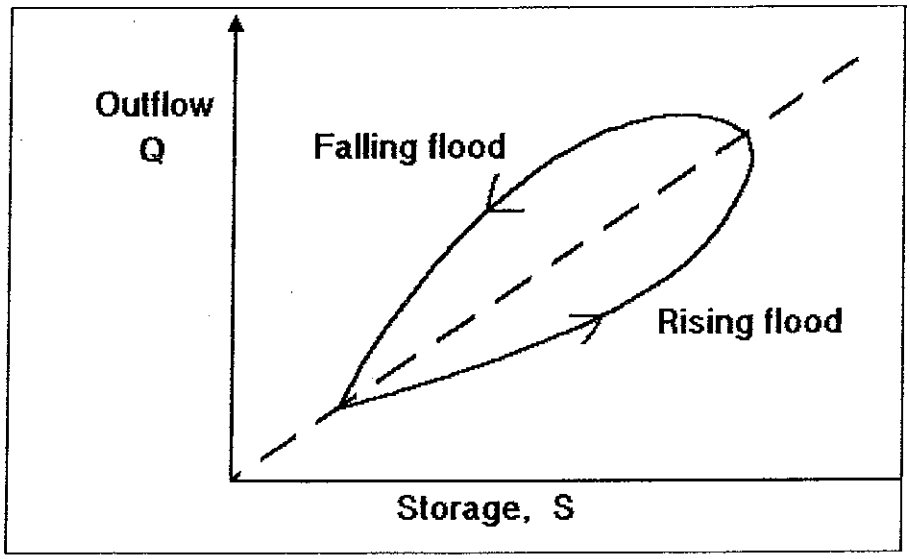

Figure 9-7. Looped storage-outflow relationship for a river reach

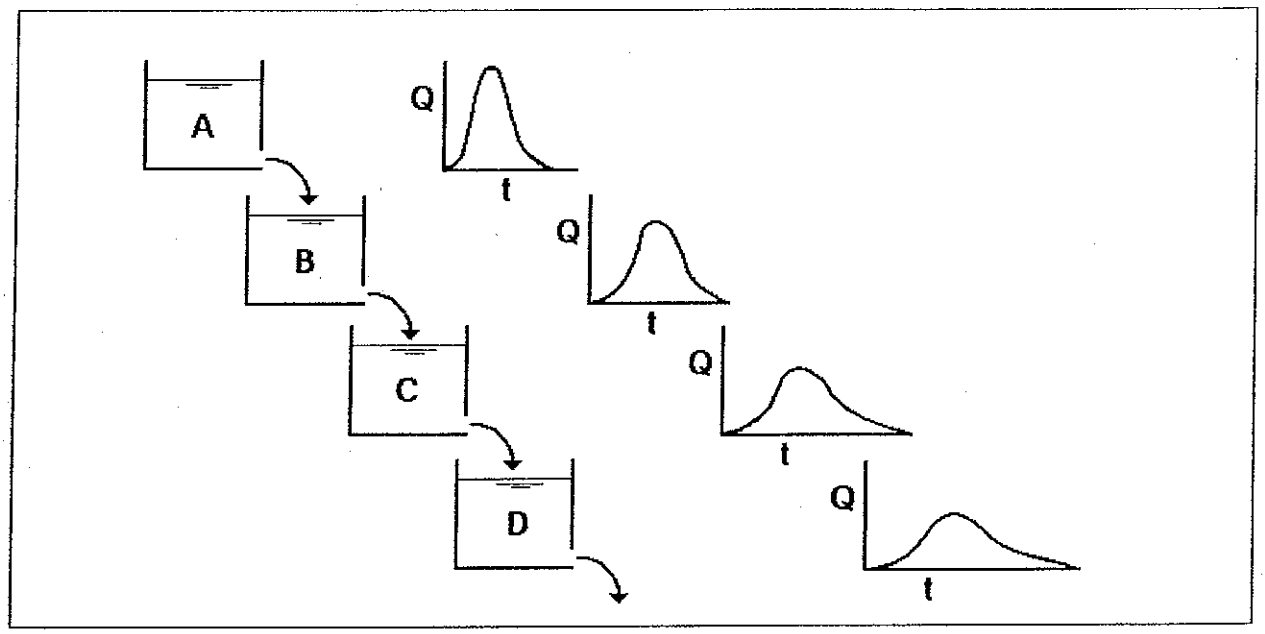

Figure 9-8. Cascade of reservoirs, depicting storage routing in a channel

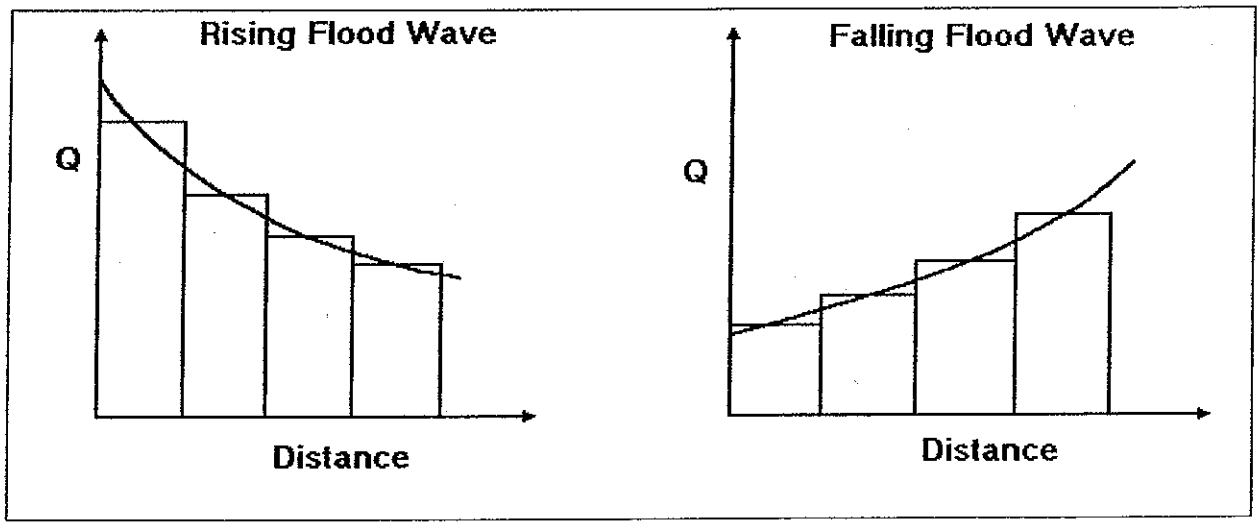

Figure 9-9. Modified puls approximation of the rising and falling floodwaves

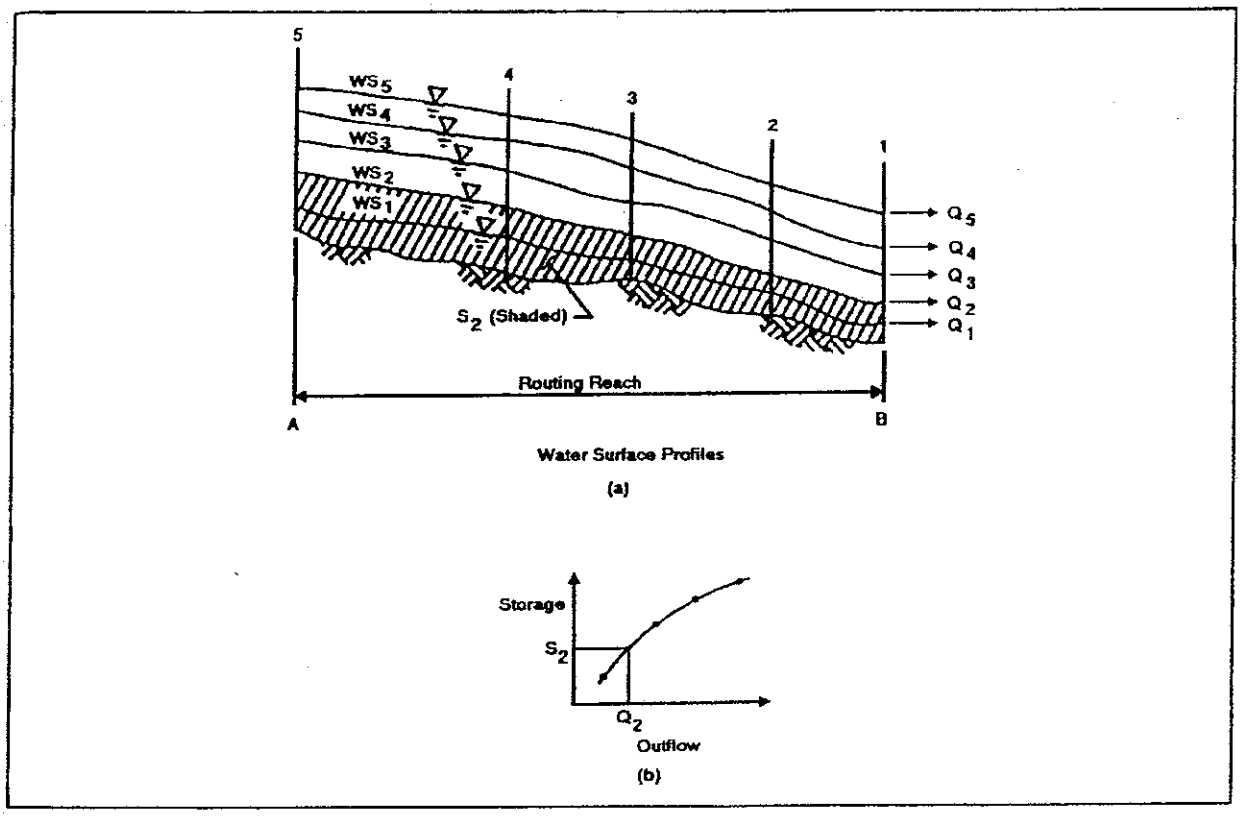

Figure 9-10. Storage-outflow relationships

(3) Determining the number of routing steps. In reservoir routing, the modified puls method is applied with one routing step. This is under the assumption that the travel time through the reservoir is smaller than the computation interval Δt. In channel routing, the travel time through the river reach is often greater than the computation interval. When this occurs, the channel must be broken down into smaller routing steps to simulate the floodwave movement and changes in hydrograph shape. The number of steps (or reach lengths) affects the attenuation of the hydrograph and should be obtained by calibration. The maximum amount of attenuation will occur when the channel routing computation is done in one step. As the number of routing steps increases, the amount of attenuation decreases. An initial estimate of the number of routing steps (NSTPS) can be obtained by dividing the total travel time (K) for the reach by the computation interval Δt.

$$K = \frac{L}{V_w}$$

$$NSTPS = \frac{K}{\Delta t} \qquad (9\text{-}13)$$

where

K = floodwave travel time through the reach

L = channel reach length

V_w = velocity of the floodwave (not average velocity)

$NSTPS$ = number of routing steps

The time interval Δt is usually determined by ensuring that there is a sufficient number of points on the rising side of the inflow hydrograph. A general rule of thumb is that the computation interval should be less than 1/5 of the time of rise (t_r) of the inflow hydrograph.

$$\Delta t \leq \frac{t_r}{5} \tag{9-14}$$

c. Muskingum method. The Muskingum method was developed to directly accommodate the looped relationship between storage and outflow that exists in rivers. With the Muskingum method, storage within a reach is visualized in two parts: prism storage and wedge storage. Prism storage is essentially the storage under the steady-flow water surface profile. Wedge storage is the additional storage under the actual water surface profile. As shown in Figure 9-11, during the rising stages of the floodwave the wedge storage is positive and added to the prism storage. During the falling stages of a floodwave, the wedge storage is negative and subtracted from the prism storage.

(1) Development of the Muskingum routing equation.

(a) Prism storage is computed as the outflow (O) times the travel time through the reach (K). Wedge storage is computed as the difference between inflow and outflow (I-O) times a weighting coefficient X and the travel time K. The coefficient K corresponds to the travel time of the floodwave through the reach. The parameter X is a dimensionless value expressing a weighting of the relative effects of inflow and outflow on the storage (S) within the reach. Thus, the Muskingum method defines the storage in the reach as a linear function of weighted inflow and outflow:

$$S = \text{prism storage} + \text{wedge storage}$$

$$S = KO + KX(I-O)$$

$$S = K\,[XI + (1-X)O] \tag{9-15}$$

where

S = total storage in the routing reach

O = rate of outflow from the routing reach

I = rate of inflow to the routing reach

K = travel time of the floodwave through the reach

X = dimensionless weighting factor, ranging from 0.0 to 0.5

(b) The quantity in the brackets of Equation 9-15 is considered an expression of weighted discharge. When $X = 0.0$, the equation reduces to $S = KO$, indicating that storage is only a function of outflow, which is equivalent to level-pool reservoir routing with storage as a linear function of outflow. When $X = 0.5$, equal weight is given to inflow and outflow, and the condition is equivalent to a uniformly progressive wave that does not attenuate. Thus, "0.0" and "0.5" are limits on the value of X, and within this range the value of X determines the degree of attenuation of the floodwave as it passes through the routing

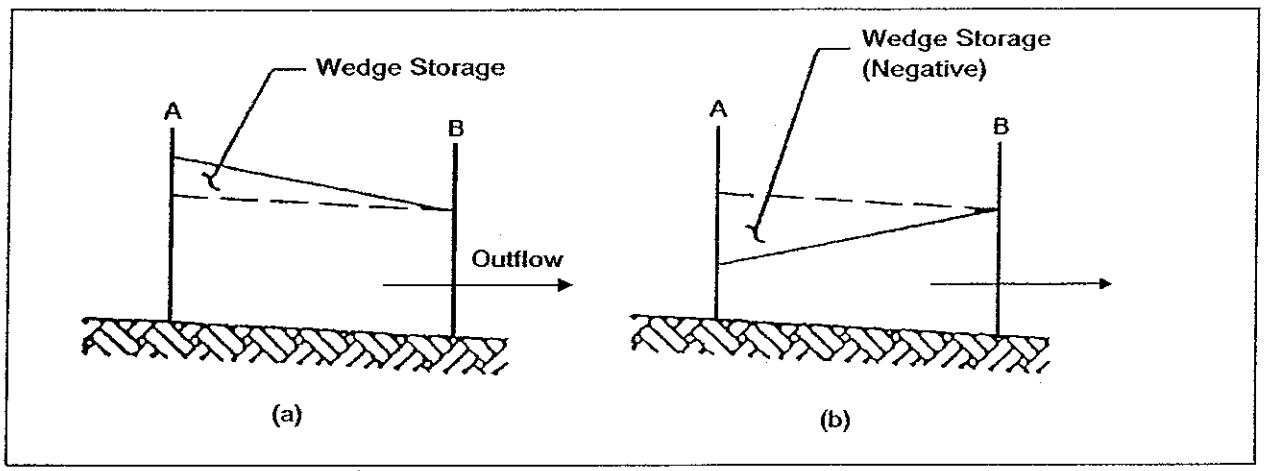

Figure 9-11. Muskingum prism and wedge storage concept

reach. A value of "0.0" produces maximum attenuation, and "0.5" produces pure translation with no attenuation.

(c) The Muskingum routing equation is obtained by combining Equation 9-15 with the continuity equation, Equation 9-11, and solving for O_2.

$$O_2 = C_1 I_2 + C_2 I_1 + C_3 O_1 \tag{9-16}$$

The subscripts 1 and 2 in this equation indicate the beginning and end, respectively, of a time interval Δt. The routing coefficients C_1, C_2, and C_3 are defined in terms of Δt, K, and X.

$$C_1 = \frac{\Delta t - 2KX}{2K(1 - X) + \Delta t} \tag{9-17}$$

$$C_2 = \frac{\Delta t + 2KX}{2K(1 - X) + \Delta t} \tag{9-18}$$

$$C_3 = \frac{2K(1 - X) - \Delta t}{2K(1 - X) + \Delta t} \tag{9-19}$$

Given an inflow hydrograph, a selected computation interval Δt, and estimates for the parameters K and X, the outflow hydrograph can be calculated.

(2) Determination of Muskingum K and X. In a gauged situation, the Muskingum K and X parameters can be calculated from observed inflow and outflow hydrographs. The travel time, K, can be estimated as the interval between similar points on the inflow and outflow hydrographs. The travel time of the routing reach can be calculated as the elapsed time between centroid of areas of the two hydrographs, between the hydrograph peaks, or between midpoints of the rising limbs. After K has been estimated, a value for X can be obtained through trial and error. Assume a value for X, and then route the inflow hydrograph with these parameters. Compare the routed hydrograph with the observed outflow hydrograph. Make adjustments to X to obtain the desired fit. Adjustments to the original estimate of K may also be necessary to obtain the best overall fit between computed and observed hydrographs. In an ungauged situation, a value for K can be estimated as the travel time of the floodwave through the routing reach. The floodwave velocity (V_w) is greater than the average velocity at a given cross section for a given discharge. The floodwave velocity can be estimated by a number of different techniques:

(a) Using Seddon's law, a floodwave velocity can be approximated from the discharge rating curve at a station whose cross section is representative of the routing reach. The slope of the discharge rating curve is equal to dQ/dy. The floodwave velocity, and therefore the travel time K, can be estimated as follows:

$$V_w = \frac{1}{B}\frac{dQ}{dy} \tag{9-20}$$

$$K = \frac{L}{V_w} \tag{9-21}$$

where

V_w = floodwave velocity, in feet/second

B = top width of the water surface

L = length of the routing reach, in feet

(b) Another means of estimating floodwave velocity is to estimate the average velocity (V) and multiply it by a ratio. The average velocity can be calculated from Manning's equation with a representative discharge and cross section for the routing reach. For various channel shapes, the floodwave velocity has been found to be a direct ratio of the average velocity.

Channel shape	Ratio V_w/V
Wide rectangular	1.67
Wide parabolic	1.44
Triangular	1.33

For natural channels, an average ratio of 1.5 is suggested. Once the wave speed has been estimated, the travel time (K) can be calculated with Equation 9-21.

(c) Estimating the Muskingum X parameter in an ungauged situation can be very difficult. X varies between 0.0 and 0.5, with 0.0 providing the maximum amount of hydrograph attenuation and 0.5 no attenuation. Experience has shown that for channels with mild slopes and flows that go out of bank, X will be closer to 0.0. For steeper streams, with well defined channels that do not have flows going out of bank, X will be closer to 0.5. Most natural channels lie somewhere in between these two limits, leaving a lot of room for "engineering judgment." One equation that can be used to estimate the Muskingum X coefficient in ungauged areas has been

developed by Cunge (1969). This equation is taken from the Muskingum-Cunge channel routing method, which is described in paragraph 9-3*e*. The equation is written as follows:

$$X = \frac{1}{2}\left(1 - \frac{Q_o}{BS_o c\Delta x}\right) \tag{9-22}$$

where

Q_o = reference flow from the inflow hydrograph

c = floodwave speed

S_o = friction slope or bed slope

B = top width of the flow area

Δx = length of the routing subreach

The choice of which flow rate to use in this equation is not completely clear. Experience has shown that a reference flow based on average values (midway between the base flow and the peak flow) is in general the most suitable choice. Reference flows based on peak flow values tend to accelerate the wave much more than it would in nature, while the converse is true if base flow reference values are used (Ponce 1983).

(3) Selection of the number of subreaches. The Muskingum equation has a constraint related to the relationship between the parameter K and the computation interval Δt. Ideally, the two should be equal, but Δt should not be less than $2KX$ to avoid negative coefficients and instabilities in the routing procedure.

$$2KX < \Delta t \leq K \tag{9-23}$$

A long routing reach should be subdivided into subreaches so that the travel time through each subreach is approximately equal to the routing interval Δt. That is:

$$Number\ of\ subreaches = \frac{K}{\Delta t}$$

This assumes that factors such as channel geometry and roughness have been taken into consideration in determining the length of the routing reach and the travel time K.

d. Working R&D routing procedure. The Working R&D procedure is a storage routing technique that accommodates the nonlinear nature of floodwave movement in natural channels. The method is useful in situations where the use of a variable K (reach travel time) would assist in obtaining accurate answers. A nonlinear storage-outflow relationship indicates that a variable K is necessary. The method is also useful in situations wherein the horizontal reservoir surface assumption of the modified puls procedure is not applicable, such as normally occurs in natural channels.

(1) The working R&D procedure could be termed "Muskingum with a variable K" or "modified puls with wedge storage." For a straight line storage-discharge (weighted discharge) relation, the procedure is the same solution as the Muskingum method. For $X = 0$, the procedure is identical to Modified Puls.

(2) The basis for the procedure derives from the concept of a "working discharge," which is a hypothetical steady flow that would result in the same natural channel storage that occurs with the passage of a floodwave. Figure 9-12 illustrates this concept.

where

I = reach inflow

O = reach outflow

D = working value discharge or simply working discharge

(3) The wedge storage (WS) may be computed in the following two ways: As in the Muskingum technique where X is a weighting factor and K is reach travel time:

$$WS = KX\,(I-O) \tag{9-24}$$

or using the working discharge (D) concept:

$$WS = K\,(D-O) \tag{9-25}$$

equating and solving for O:

$$K\,(D-O) = KX\,(I-O) \tag{9-26}$$

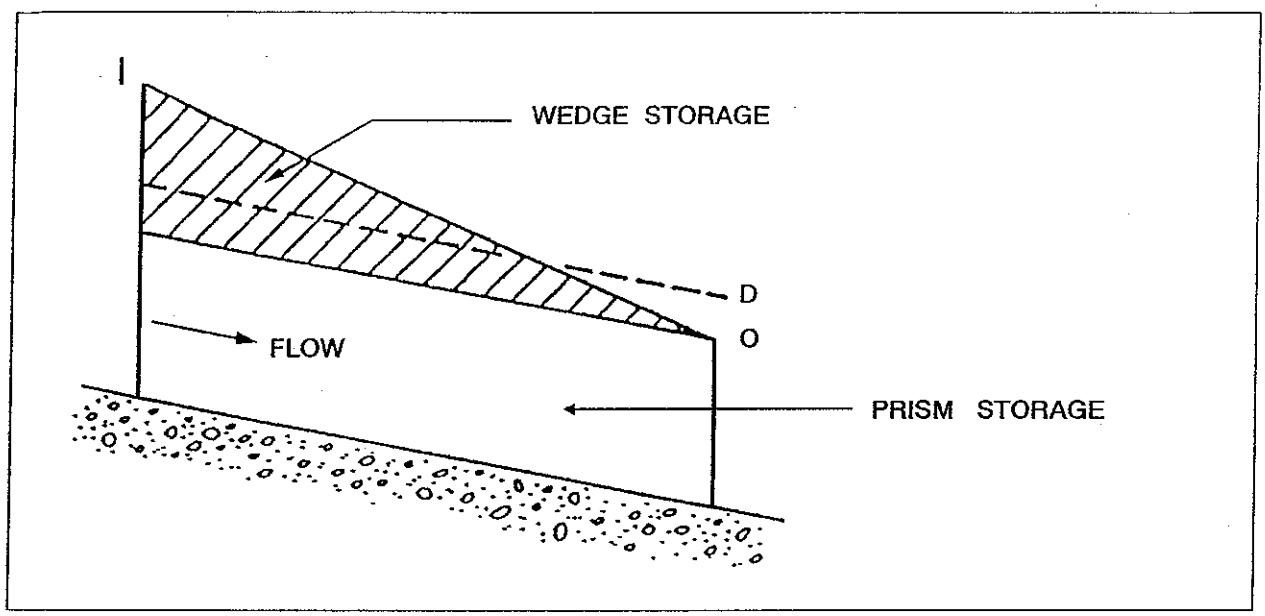

Figure 9-12. Illustration of the "working discharge" concept

or

$$O = D - \frac{X}{1-X}(I-D) \tag{9-27}$$

The continuity equation may be approximated by:

$$\frac{S_2 - S_1}{\Delta t} = 0.5\,(I_1 + I_2) - 0.5\,(O_1 + O_2) \tag{9-28}$$

where

S = storage

Δt = time increment

Substituting Equation 9-27 into 9-28 and appending the appropriate subscripts to denote beginning and end of period and performing the appropriate algebra yields:

$$0.5\Delta t(I_1 + I_2) + [S_1(1 - X) - 0.5D_1\Delta t] = [S_2(1 - X) + 0.5D_2\Delta t] \tag{9-29}$$

Let

$$R = S\,(1 - X) + 0.5D\Delta t \tag{9-30}$$

where R is termed the "working value of storage" or simply working storage and represents an index of the true natural storage. Equation 9-29 may therefore be written:

$$R_2 = R_1 + 0.5\Delta t\,(I_1 + I_2) - D_1\Delta t \tag{9-31}$$

transposing Δt results in the equation used in routing computations:

$$\frac{R_2}{\Delta t} = \frac{R_1}{\Delta t} + 0.5\,(I_1 + I_2) - D_1 \tag{9-32}$$

The form of the relationship for R (working discharge) is analogous to storage indication in the modified puls procedure. $R_2/\Delta t$ may be computed from information known at the beginning of a routing interval. The outflow at the end of the routing interval may then be determined from a

rating curve of working storage versus working discharge. The cycle is then repeated stepping forward in time.

(4) The solution scheme using this concept requires development of a rating curve of working storage versus working discharge as stated above. The following column headings are helpful in developing the function when storage-outflow data are available.

1	2	3
Storage (S)	$\frac{S}{\Delta t}(1-X)$	*Working Discharge* (D)

4	5
$\frac{D}{2}$	$\frac{S}{\Delta t}(1-X) + \frac{D}{2}$

(5) Column 2 of the tabulation is obtained from column 1 by using an appropriate conversion factor and appropriate X. The conversion factor of 1 acre-ft/hour = 12.1 cfs is useful in this regard. Column 5 is the sum of columns 2 and 4. Column 3 is plotted against column 5 on cartesian coordinate paper and a curve drawn through the plotted points. This represents the working discharge-working outflow rating curve. An example curve is shown in Figure 9-13.

(6) The routing of a hydrograph can be performed as the one shown in Table 9-2. The procedure, in narrative form is:

- Conditions known at time 1: I_1, O_1, D_1, and $R_1/\Delta t$.
- At time 2, only I_2 is known, therefore:

$$\frac{R_2}{\Delta t} = \frac{R_1}{\Delta t} + 0.5\,(I_1 + I_2) - D_1$$

- Enter working storage, working discharge function, and read out D_2.
- Calculate O_2 as follows:

$$O_2 = D_2 - \frac{X}{1-X}(I_2 - D_2)$$

- Repeat process until finished.

e. Muskingum-Cunge channel routing. The Muskingum-Cunge channel routing technique is a nonlinear coefficient method that accounts for hydrograph diffusion based on physical channel properties and the inflowing hydrograph. The advantages of this method over other hydrologic techniques are the parameters of the model are more physically based; the method has been shown to compare well against the full unsteady flow equations over a wide range of flow situations (Ponce 1983 and Brunner 1989); and the solution is independent of the user-specified computation interval. The major limitations of the Muskingum-Cunge technique are that it cannot account for backwater effects, and the method begins to diverge from the full unsteady flow solution when very rapidly rising hydrographs are routed through flat channel sections.

(1) Development of equations.

(a) The basic formulation of the equations is derived from the continuity Equation 9-33 and the diffusion form of the momentum Equation 9-34:

$$\frac{\partial A}{\partial t} + \frac{\partial Q}{\partial x} = q_l \tag{9-33}$$

$$S_f = S_o - \frac{\partial Y}{\partial x} \tag{9-34}$$

(b) By combining Equations 9-33 and 9-34 and linearizing, the following convective diffusion equation is formulated (Miller and Cunge 1975):

$$\frac{\partial Q}{\partial t} + c\frac{\partial Q}{\partial x} = \mu\frac{\partial^2 Q}{\partial x^2} + cq_L \tag{9-35}$$

where

Q = discharge, in cubic feet per second

A = flow area, in square feet

t = time, in seconds

x = distance along the channel, in feet

Y = depth of flow, in feet

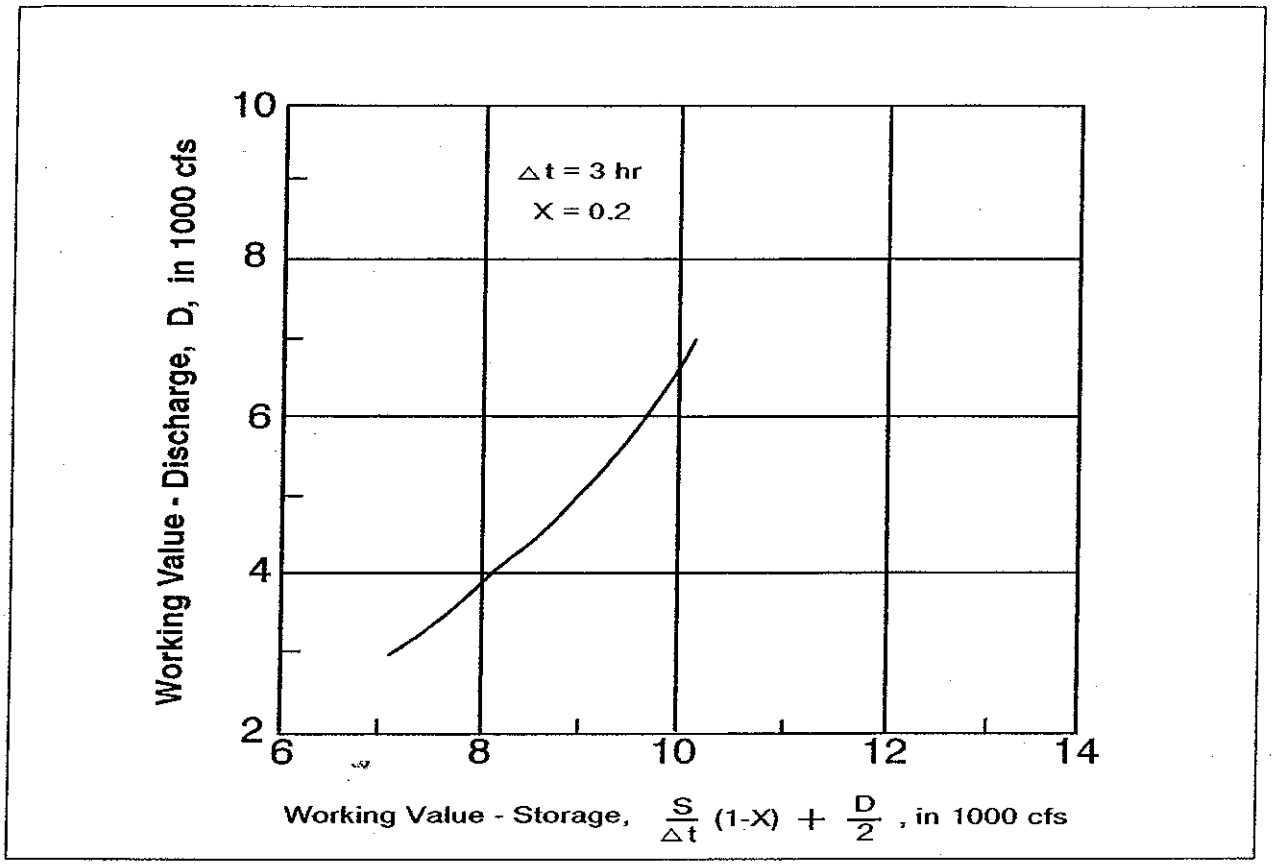

Figure 9-13. Rating curve for working R&D routing

q_L = lateral inflow per unit of channel length

S_f = friction slope

S_o = bed slope

c = the wave celerity in the x direction as defined below

The wave celerity (c) and the hydraulic diffusivity (μ) are expressed as follows:

$$c = \frac{dQ}{dA} \tag{9-36}$$

$$\mu = \frac{Q}{2BS_o} \tag{9-37}$$

where B is the top width of the water surface. The convective diffusion Equation 9-35 is the basis for the Muskingum-Cunge method.

(c) In the original Muskingum formulation, with lateral inflow, the continuity Equation 9-33) is discretized on the x-t plane (Figure 9-14) to yield:

$$Q_{j-1}^{n-1} = C_1 Q_j^n + C_2 Q_j^{n-1} + C_3 Q_{j-1}^n + C_4 Q_L \tag{9-38}$$

It is assumed that the storage in the reach is expressed as the classical Muskingum storage:

$$S = K\,[XI + (1-X)O] \tag{9-39}$$

Table 9-2
Working R&D Routing Example

Time hr	Inflow cfs	Average Inflow cfs	$\frac{K}{\Delta t} + 0.5(I_1 + I_2) - D_1$ cfs	D cfs	O cfs
	3,000		7,100	3,000	3,000
		3,130			
3	3,260		7,230	3,100	3,060
		3,445			
6	3,630		7,575	3,300	3,220
		3,825			
9	4,020		8,100	3,800	3,745
		4,250			
12	4,480		8,550	4,400	4,420

where

S = channel storage

K = cell travel time (seconds)

X = weighting factor

I = inflow

O = outflow

Therefore, the coefficients can be expressed as follows:

$$C_1 = \frac{\frac{\Delta t}{K} + 2X}{\frac{\Delta t}{K} + 2(1 - X)}$$

$$C_2 = \frac{\frac{\Delta t}{K} - 2X}{\frac{\Delta t}{K} + 2(1 - X)}$$

$$C_3 = \frac{2(1 - X) - \frac{\Delta t}{K}}{\frac{\Delta t}{K} + 2(1 - X)}$$

$$Q_L = q_L \Delta X$$

$$C_4 = \frac{2(\frac{\Delta t}{K})}{\frac{\Delta t}{K} + 2(1 - X)}$$

(d) In the Muskingum equation the amount of diffusion is based on the value of X, which varies between 0.0 and 0.5. The Muskingum X parameter is not directly related to physical channel properties. The diffusion obtained with the Muskingum technique is a function of how the equation is solved and is therefore considered numerical diffusion rather than physical. Cunge evaluated the diffusion that is produced in the Muskingum equation and analytically solved for the following diffusion coefficient:

$$\mu_n = c\ \Delta x \left(\frac{1}{2} - X \right) \tag{9-40}$$

In the Muskingum-Cunge formulation, the amount of diffusion is controlled by forcing the numerical diffusion to match the physical diffusion of the convective diffusion Equation 9-35. This is accomplished by setting Equations 9-37 and 9-40 equal to each other. The Muskingum-Cunge equation is therefore considered an approximation of the convective diffusion Equation 9-35. As a result, the parameters K and X are expressed as follows (Cunge 1969 and Ponce and Yevjevich 1978):

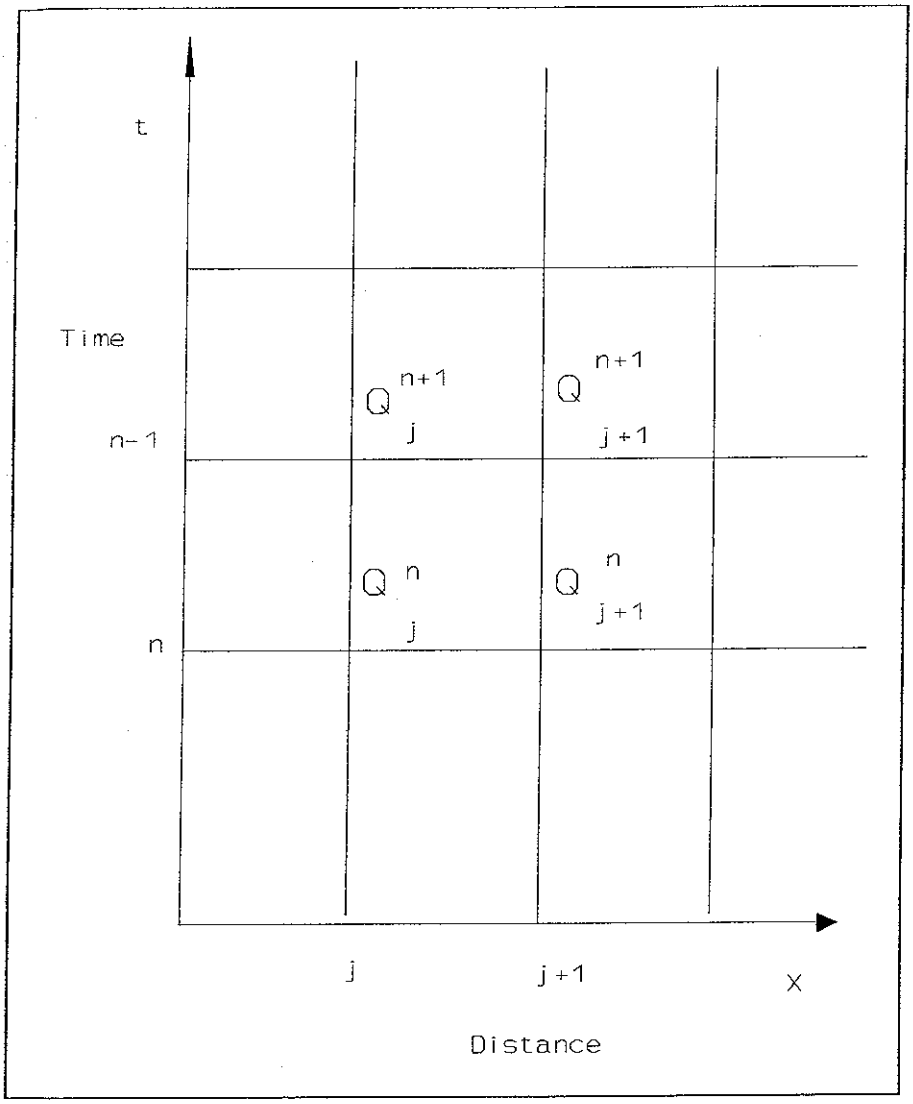

Figure 9-14. Discretization of the continuity equation on x-t plane

$$K = \frac{\Delta X}{c} \tag{9-41}$$

$$X = \frac{1}{2}\left(1 - \frac{Q}{BS_o c\Delta x}\right) \tag{9-42}$$

(2) Solution of the equations.

(a) The method is nonlinear in that the flow hydraulics (Q, B, c), and therefore the routing coefficients (C_1, C_2, C_3, and C_4) are recalculated for every Δx distance step and Δt time step. An iterative four-point averaging scheme is used to solve for c, B, and Q. This process has been described in detail by Ponce (1986).

(b) Values for Δt and Δx are chosen for accuracy and stability. First, Δt should be evaluated by looking at the following three criteria and selecting the smallest value: (1) the user-defined computation interval, (2) the time of rise of the inflow hydrograph divided by 20 ($^{Tr}/_{20}$), and (3) the travel time through the channel reach. Once Δt is chosen, Δx is defined as follows:

$$\Delta x = c\Delta t \tag{9-43}$$

but Δx must also meet the following criteria to preserve consistency in the method (Ponce 1983):

$$\Delta x < \frac{1}{2}\left(c\Delta t + \frac{Q_o}{BS_o c}\right) \tag{9-44}$$

where Q_o is the reference flow and Q_B is the baseflow taken from the inflow hydrograph as:

$$Q_o = Q_B + 0.50\ (Q_{peak} - Q_B)$$

(3) Data requirements.

(a) Data for the Muskingum-Cunge method consist of the following:

- Representative channel cross section.
- Reach length, L.
- Manning roughness coefficients, n (for main channel and overbanks).
- Friction slope (S_f) or channel bed slope (S_o).

(b) The method can be used with a simple cross section (i.e., trapezoid, rectangle, square, triangle, or circular pipe) or a more detailed cross section (i.e., cross sections with a left overbank, main channel, and a right overbank). The cross section is assumed to be representative of the entire routing reach. If this assumption is not adequate, the routing reach should be broken up into smaller subreaches with representative cross sections for each. Reach lengths are measured directly from topographic maps. Roughness coefficients (Manning's n) must be estimated for main channels as well as overbank areas. If information is available to estimate an approximate energy grade line slope (friction slope, S_f), that slope should be used instead of the bed slope. If no information is available to estimate the slope of the energy grade line, the channel bed slope should be used.

(4) Advantages and limitations. The Muskingum-Cunge routing technique is considered to be a nonlinear coefficient method that accounts for hydrograph diffusion based on physical channel properties and the inflowing hydrograph. The advantages of this method over other hydrologic techniques are: the parameters of the model are physically based, and therefore this method will make for a good ungauged routing technique; several studies have shown that the method compares very well with the full unsteady flow equations over a wide range of flow conditions (Ponce 1983 and Brunner 1989); and the solution is independent of the user-specified computation interval. The major limitations of the Muskingum-Cunge technique are that the method can not account for backwater effects, and the method begins to diverge from the complete unsteady flow solution when very rapidly rising hydrographs (i.e., less than 2 hr) are routed through flat channel sections (i.e., channel slopes less than 1 ft/mile). For hydrographs with longer rise times (T_r), the method can be used for channel reaches with slopes less than 1 ft/mile.

9-4. Applicability of Routing Techniques

a. Selecting the appropriate routing method. With such a wide range of hydraulic and hydrologic routing techniques, selecting the appropriate routing method for each specific problem is not clearly defined. However, certain thought processes and some general guidelines can be used to narrow the choices, and ultimately the selection of an appropriate method can be made.

b. Hydrologic routing method. Typically, in rainfall-runoff analyses, hydrologic routing procedures are utilized on a reach-by-reach basis from upstream to downstream. In general, the main goal of the rainfall-runoff study is to calculate discharge hydrographs at several locations in the watershed. In the absence of significant backwater effects, the hydrologic routing models offer the advantages of simplicity, ease of use, and computational efficiency. Also, the accuracy of hydrologic methods in calculating discharge hydrographs is normally well within the range of acceptable values. It should be remembered, however, that insignificant backwater effects alone do not always justify the use of a hydrologic method. There are many other factors that must be considered when deciding if a hydrologic model will be appropriate, or if it is necessary to use a more detailed hydraulic model.

c. Hydraulic routing method. The full unsteady flow equations have the capability to simulate the widest range of flow situations and channel characteristics. Hydraulic models, in general, are more physically based since they only have one parameter (the roughness coefficient) to estimate or calibrate. Roughness coefficients can be estimated with some degree of accuracy from inspection of the waterway, which makes the hydraulic methods more applicable to ungauged situations.

d. Evaluating the routing method. There are several factors that should be considered when evaluating which routing method is the most appropriate for a given

situation. The following is a list of the major factors that should be considered in this selection process:

(1) Backwater effects. Backwater effects can be produced by tidal fluctuations, significant tributary inflows, dams, bridges, culverts, and channel constrictions. A floodwave that is subjected to the influences of backwater will be attenuated and delayed in time. Of the hydrologic methods discussed previously, only the modified puls method is capable of incorporating the effects of backwater into the solution. This is accomplished by calculating a storage-discharge relationship that has the effects of backwater included in the relationship. Storage-discharge relationships can be determined from steady flow-water surface profile calculations, observed water surface profiles, normal depth calculations, and observed inflow and outflow hydrographs. All of these techniques, except the normal depth calculations, are capable of including the effects of backwater into the storage-discharge relationship. Of the hydraulic methods discussed in this chapter, only the kinematic wave technique is not capable of accounting for the influences of backwater on the floodwave. This is due to the fact that the kinematic wave equations are based on uniform flow assumptions and a normal depth downstream boundary condition.

(2) Floodplains. When the flood hydrograph reaches a magnitude that is greater than the channels carrying capacity, water flows out into the overbank areas. Depending on the characteristics of the overbanks, the flow can be slowed greatly, and often ponding of water can occur. The effects of the floodplains on the floodwave can be very significant. The factors that are important in evaluating to what extent the floodplain will impact the hydrograph are the width of the floodplain, the slope of the floodplain in the lateral direction, and the resistance to flow due to vegetation in the floodplain. To analyze the transition from main channel to overbank flows, the modeling technique must account for varying conveyance between the main channel and the overbank areas. For 1-D flow models, this is normally accomplished by calculating the hydraulic properties of the main channel and the overbank areas separately, then combining them to formulate a composite set of hydraulic relationships. This can be accomplished in all of the routing methods discussed previously except for the Muskingum method. The Muskingum method is a linear routing technique that uses coefficients to account for hydrograph timing and diffusion. These coefficients are usually held constant during the routing of a given floodwave. While these coefficients can be calibrated to match the peak flow and timing of a specific flood magnitude, they can not be used to model a range of floods that may remain in bank or go out of bank. When modeling floods through extremely flat and wide floodplains, the assumption of 1-D flow in itself may be inadequate. For this flow condition, velocities in the lateral direction (across the floodplain) may be just as predominant as those in the longitudinal direction (down the channel). When this occurs, a two-dimensional (2-D) flow model would give a more accurate representation of the physical processes. This subject is beyond the scope of this chapter. For more information on this topic, the reader is referred to EM 1110-2-1416.

(3) Channel slope and hydrograph characteristics. The slope of the channel will not only affect the velocity of the floodwave, but it can also affect the amount of attenuation that will occur during the routing process. Steep channel slopes accelerate the floodwave, while mild channel slopes are prone to slower velocities and greater amounts of hydrograph attenuation. Of all the routing methods presented in this chapter, only the complete unsteady flow equations are capable of routing floodwaves through channels that range from steep to extremely flat slopes. As the channel slopes become flatter, many of the methods begin to break down. For the simplified hydraulic methods, the terms in the momentum equation that were excluded become more important in magnitude as the channel slope is decreased. Because of this, the range of applicable channel slopes decreases with the number of terms excluded from the momentum equation. As a rule of thumb, the kinematic wave equations should only be applied to relatively steep channels (10 ft/mile or greater). Since the diffusion wave approximation includes the pressure differential term in the momentum equation, it is applicable to a wider range of slopes than the kinematic wave equations. The diffusion wave technique can be used to route slow rising floodwaves through extremely flat slopes. However, rapidly rising floodwaves should be limited to mild to steep channel slopes (approximately 1 ft/mile or greater). This limitation is due to the fact that the acceleration terms in the momentum equation increase in magnitude as the time of rise of the inflowing hydrograph is decreased. Since the diffusion wave method does not include these acceleration terms, routing rapidly rising hydrographs through flat channel slopes can result in errors in the amount of diffusion that will occur. While "rules of thumb" for channel slopes can be established, it should be realized that it is the combination of channel slope and the time of rise of the inflow hydrograph together that will determine if a method is applicable or not.

(a) Ponce and Yevjevich (1978) established a numerical criteria for the applicability of hydraulic routing

techniques. According to Ponce, the error due to the use of the kinematic wave model (error in hydrograph peak accumulated after an elapsed time equal to the hydrograph duration) is within 5 percent, provided the following inequality is satisfied:

$$\frac{TS_o u_o}{d_o} \geq 171 \tag{9-45}$$

where

T = hydrograph duration, in seconds

S_o = friction slope or bed slope

u_o = reference mean velocity

d_o = reference flow depth

When applying Equation 9-45 to check the validity of using the kinematic wave model, the reference values should correspond as closely as possible to the average flow conditions of the hydrograph to be routed.

(b) The error due to the use of the diffusion wave model is within 5 percent, provided the following inequality is satisfied:

$$TS_o\left(\frac{g}{d_o}\right)^{1/2} \geq 30 \tag{9-46}$$

where g = acceleration of gravity. For instance, assume S_o = 0.001, u_o = 3 ft/s, and d_o = 10 ft. The kinematic wave model will apply for hydrographs of duration larger than 6.59 days. Likewise, the diffusion wave model will apply for hydrographs of duration larger than 0.19 days.

(c) Of the hydrologic methods, the Muskingum-Cunge method is applicable to the widest range of channel slopes and inflowing hydrographs. This is due to the fact that the Muskingum-Cunge technique is an approximation of the diffusion wave equations, and therefore can be applied to channel slopes of a similar range in magnitude. The other hydrologic techniques use an approximate relationship in place of the momentum equation. Experience has shown that these techniques should not be applied to channels with slopes less than 2 ft/mi. However, if there is gauged data available, some of the parameters of the hydrologic methods can be calibrated to produce the desired attenuation effects that occur in very flat streams.

(4) Flow networks. In a dendritic stream system, if the tributary flows or the main channel flows do not cause significant backwater at the confluence of the two streams, any of the hydraulic or hydrologic routing methods can be applied. If significant backwater does occur at the confluence of two streams, then the hydraulic methods that can account for backwater (full unsteady flow and diffusion wave) should be applied. For full networks, where the flow divides and possibly changes direction during the event, only the full unsteady flow equations and the diffusion wave equations can be applied.

(5) Subcritical and supercritical flow. During a flood event, a stream may experience transitions between subcritical and supercritical flow regimes. If the supercritical flow reaches are long, or if it is important to calculate an accurate stage within the supercritical reach, the transitions between subcritical and supercritical flow should be treated as internal boundary conditions and the supercritical flow reach as a separate routing section. This is normally accomplished with hydraulic routing methods that have specific routines to handle supercritical flow. In general, none of the hydrologic methods have knowledge about the flow regime (supercritical or subcritical), since hydrologic methods are only concerned with flows and not stages. If the supercritical flow reaches are short, they will not have a noticeable impact on the discharge hydrograph. Therefore, when it is only important to calculate the discharge hydrograph, and not stages, hydrologic routing methods can be used for reaches with small sections of supercritical flow.

(6) Observed data. In general, if observed data are not available, the routing methods that are more physically based are preferred and will be easier to apply. When gauged data are available, all of the methods should be calibrated to match observed flows and/or stages as best as possible. The hydraulic methods, as well as the Muskingum-Cunge technique, are considered physically based in the sense that they only have one parameter (roughness coefficient) that must be estimated or calibrated. The other hydrologic methods may have more than one parameter to be estimated or calibrated. Many of these parameters, such as the Muskingum X and the number of subreaches (NSTPS), are not related directly to physical aspects of the channel and inflowing hydrograph. Because of this, these methods are generally not used in ungauged situations. The final choice of a routing model is also influenced by other factors, such as the required accuracy, the type and availability of data, the type of information desired (flow hydrographs, stages, velocities, etc.), and the familiarity and experience of the user with a given method. The modeler must take all of these factors

into consideration when selecting an appropriate routing technique for a specific problem. Table 9-3 contains a list of some of the factors discussed previously, along with some guidance as to which routing methods are appropriate and which are not. This table should be used as guidance in selecting an appropriate method for routing discharge hydrographs. By no means is this table all inclusive.

Table 9-3
Selecting the Appropriate Channel Routing Technique

Factors to consider in the selection of a routing technique.	Methods that are appropriate for this specific factor.	Methods that are not appropriate for this factor.
1. No observed hydrograph data available for calibration.	* Full Dynamic Wave * Diffusion Wave * Kinematic Wave * Muskingum-Cunge	* Modified Puls * Muskingum * Working R&D
2. Significant backwater that will influence discharge hydrograph.	* Full Dynamic Wave * Diffusion Wave * Modified Puls * Working R&D	* Kinematic Wave * Muskingum * Muskingum-Cunge
3. Flood wave will go out of bank into the flood plains.	* All hydraulic and hydrologic methods that calculate hydraulic properties of main channel separate from overbanks.	* Muskingum
4. Channel slope > 10 ft/mile and $\frac{TS_o u_o}{d_o} \geq 171$	* All methods presented	* None
5. Channel slopes from 10 to 2 ft/mile and $\frac{TS_o u_o}{d_o} < 171$	* Full Dynamic Wave * Diffusion Wave * Muskingum-Cunge * Modified Puls * Muskingum * Working R&D	* Kinematic Wave
6. Channel slope < 2 ft/mile and $TS_o\left(\frac{g}{d_o}\right)^{1/2} \geq 30$	* Full Dynamic Wave * Diffusion Wave * Muskingum-Cunge	* Kinematic Wave * Modified Puls * Muskingum * Working R&D
7. Channel slope < 2 ft/mile and $TS_o\left(\frac{g}{d_o}\right)^{1/2} < 30$	* Full Dynamic Wave	* All others

HAND OUT 21: Kinematic wave (Chapter 6 of our syllabus). Sources: Altinakar, M., and Graf, W. (1998). *"Fluvial Hydraulics."* John Wiley and Sons

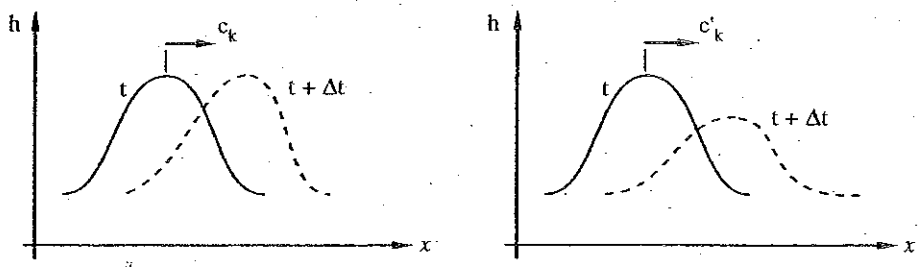

a) *onde cinématique* b) *onde diffusive*

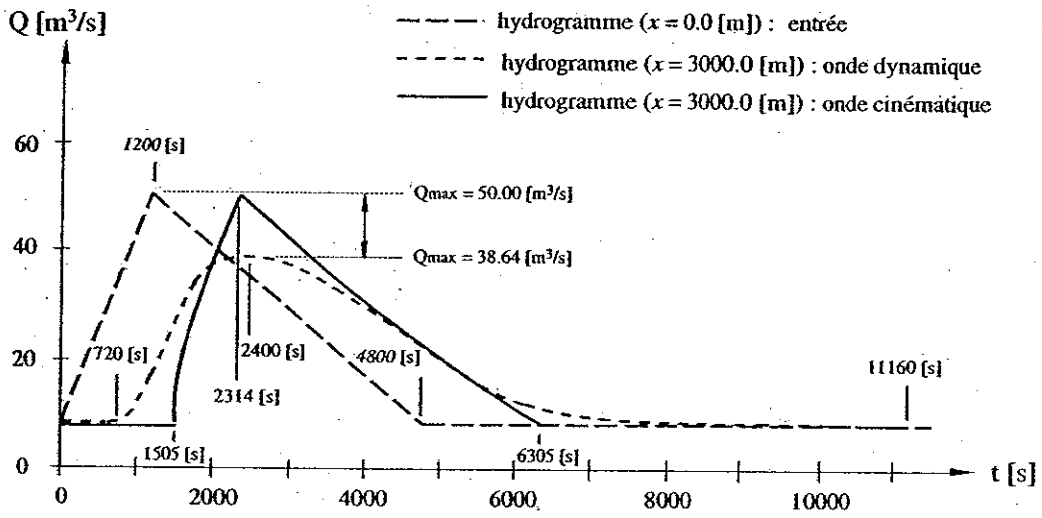

Fig. Ex.5.C.3
Comparaison des hydrogrammes : onde cinématique et onde dynamique.

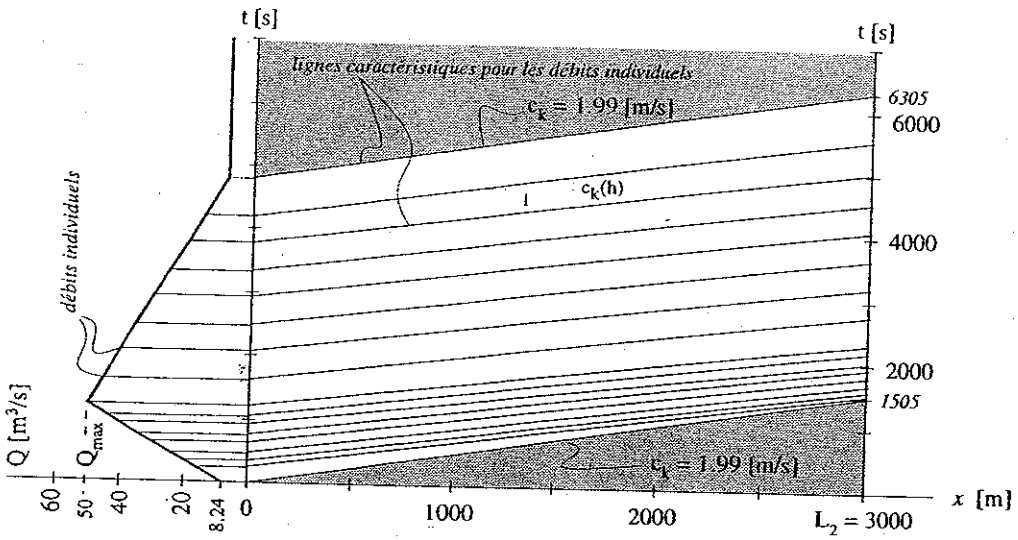
t [s]
t [s]
lignes caractéristiques pour les débits individuels
$c_k = 1.99$ [m/s]
6305
6000
$c_k(h)$
débits individuels
4000
2000
1505
Q [m³/s]
Q_{max} = 50
$c_k = 1.99$ [m/s]
60
50
40
20
8.24
0
1000
2000
$L_2 = 3000$
x [m]

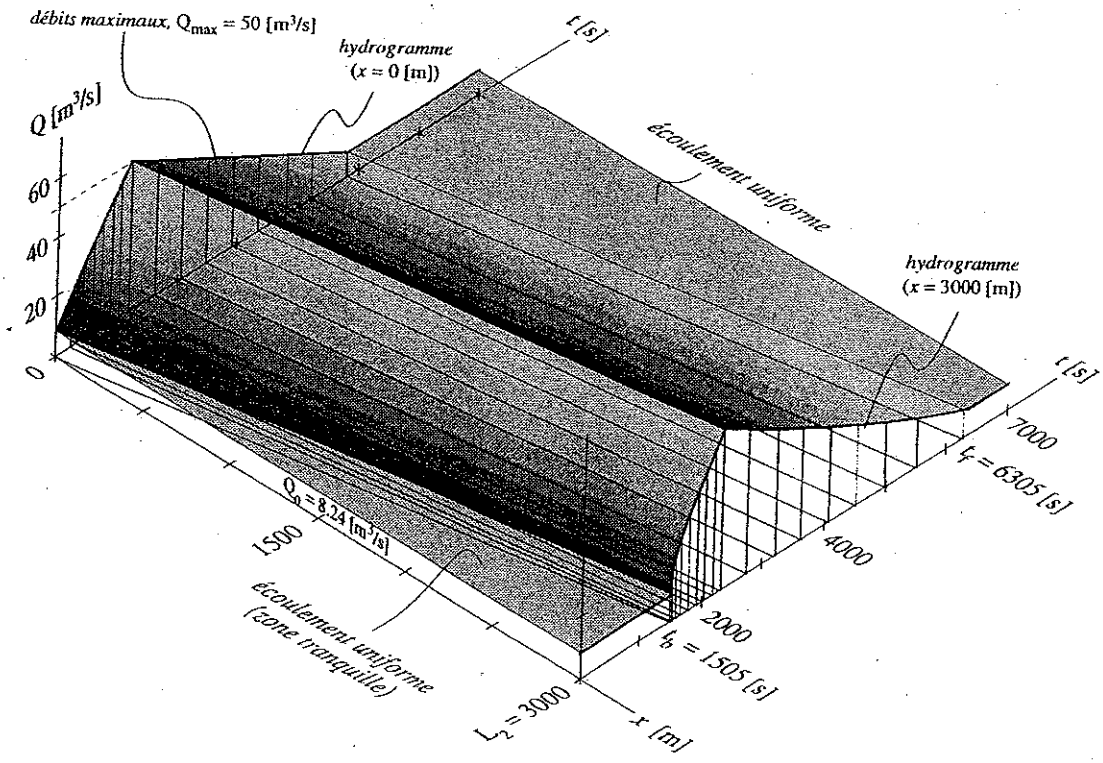
débits maximaux, Q_{max} = 50 [m³/s]
hydrogramme
(x = 0 [m])
t [s]
Q [m³/s]
écoulement uniforme
hydrogramme
(x = 3000 [m])
60
40
20
0
t [s]
7000
t_f = 6305 [s]
Q_0 = 8.24 [m³/s]
1500
4000
2000
t_0 = 1505 [s]
écoulement uniforme
(zone tranquille)
L_2 = 3000
x [m]

HAND OUT 22: Continuous source of a pollutant (Chapter 7 of our syllabus). Sources: Altinakar, M., and Graf, W. (1998). *"Fluvial Hydraulics."* John Wiley and Sons, and Koutitas, C. G. (1983). "Elements of computational hydraulics." Pentech Press, UK.

In the absence of velocity, $\vec{V} = 0$, eq. 8.35 becomes evidently eq. 8.32.

2° For one-dimensional convection-diffusion in the x-direction, in a channel with a weak velocity, $u \equiv U$, being uniformly distributed over the flow depth, the above equation, eq. 8.35, can be written as :

$$C(x,t) = \frac{\mathcal{M}_1}{\sqrt{4\pi\,\varepsilon_m t}} \exp\left[-\frac{(x-Ut)^2}{4\,\varepsilon_m t}\right] \tag{8.36}$$

where C is the average concentration in a section, S, of the channel.

The total mass of the substance, M_0, introduced instantaneously and uniformly over the section, S, defines :

$$\mathcal{M}_1 = \frac{M_0}{S} = \int_{-\infty}^{+\infty} C(x,t)\,dx = \int_{-\infty}^{+\infty} C(x,0)\,dx \tag{8.27a}$$

3° All remarks made for pure diffusion (see sect. 8.2.1) remain valid; the velocity of translation, u or U, is taken into account by coordinate transformation, $x' = x - ut$ or $x' = x - Ut$ (see Fig. 8.3 and Fig. 8.6).

The mass, M_0, displaces itself with the velocity of translation, U, and at the same time it spreads out according to the normal curve (see Fig. 8.6). The maximum concentration, C_{max}, is propagated with the velocity and it decreases with time.

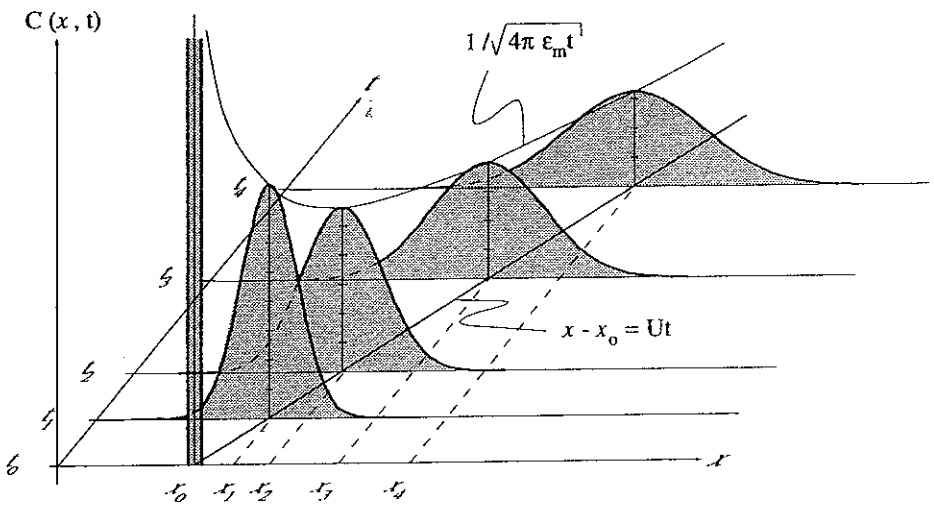

Fig. 8.6 Evolution of the concentration, $C(x,t)$, for a mass, M_0, injected instantaneously at $x = x_o$ into a medium in motion, U.

8.3.2 Continuous Source

1° Considered will be the one-dimensional convection-diffusion in a medium moving with a non-zero velocity, $\vec{V}(u,0,0) \neq 0$.

At a certain station, $x = 0$, an average concentration is introduced in a continuous and constant way, $C_o = Cte$.

The average velocity, U, being weak (without distribution over the flow depth) transports the average concentration, C, and diffusion takes place at the same time.

2° The solution to the one-dimensional convection-diffusion equation (see eq. 8.6b) is (see *Daily* et *Harleman*, 1966, p. 434) given by :

$$C(x,t) = \frac{C_o}{2}\left[\exp\left(\frac{Ux}{\varepsilon_m}\right) erfc\left(\frac{x+Ut}{\sqrt{4\,\varepsilon_m t}}\right) + erfc\left(\frac{x-Ut}{\sqrt{4\,\varepsilon_m t}}\right)\right] \qquad (8.37)$$

In the absence of velocity, U = 0, eq. 8.37 becomes evidently eq. 8.33.

The evolution of the concentration, C(*x*,t), is shown at Fig. 8.7. Note that the concentration of the value $C_o/2$ displaces itself with the velocity of the flow, U.

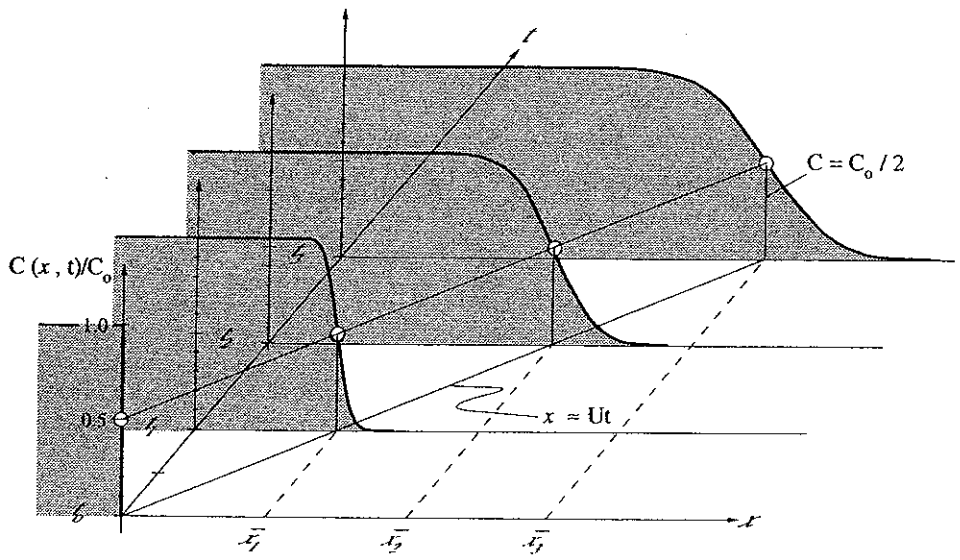

Fig. 8.7 Evolution of the concentration, C(*x*,t), for a concentration, C_o, introduced continuously into a flow with an average velocity, U.

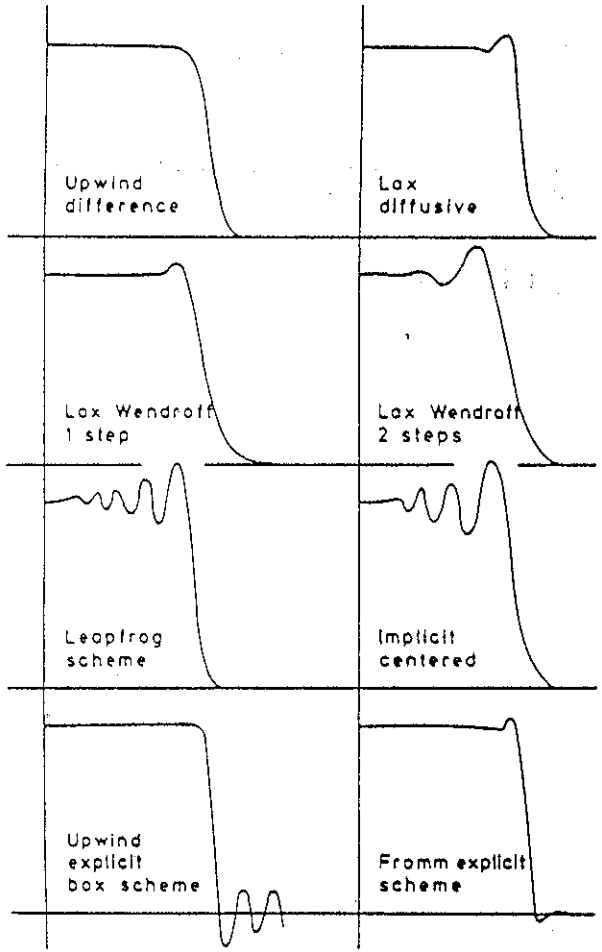

Fig. 3.1 1-D advection equation. Solutions by various finite difference schemes

$+1$, at a point i, j of the flow domain, has the form

$$c_{ij}^{n+1} = c_{ij}^{n} - \frac{(\Delta t)u}{2\Delta x}(c_{i+1j}^{n} - c_{i-1j}^{n}) - \frac{(\Delta t)v}{2\Delta y}(c_{ij+1}^{n} - c_{ij-1}^{n}) + \frac{(\Delta t)D_x}{\Delta x^2}(c_{i+1j}^{n} - 2c_{ij}^{n} + c_{i-1j}^{n}) + \frac{(\Delta t)D_y}{\Delta y^2}(c_{ij+1}^{n} - 2c_{ij}^{n} + c_{ij-1}^{n}) \quad (3.22)$$

(It should be noted that centered differences for pure advection are unstable and the diffusion part of the operator is necessary to suppress instability.) The explicit scheme is very easily programmable but the time step Δt is limited by the known stability criteria. The use of implicit finite differences for both parts of the operators $u\,\partial c/\partial x$, $D\,\partial^2 c/\partial x^2$ lead to an algebraic system in IM × JM unknowns (where IM, JM are the maximum values of the indices I, J along x, y respectively). The fully implicit scheme leads to the inductive relation

$$\frac{c_{ij}^{n+1} - c_{ij}^{n}}{\Delta t} = -u\left(\frac{c_{i+1j}^{n+1} - c_{i-1j}^{n+1}}{2\Delta x}\right) - v\left(\frac{c_{ij+1}^{n+1} - c_{ij-1}^{n+1}}{2\Delta y}\right) + \frac{D_x(c_{i+1j}^{n+1} - 2c_{ij}^{n+1} + c_{i-1j}^{n+1})}{\Delta x^2} + \frac{D_y(c_{ij+1}^{n+1} - 2c_{ij}^{n+1} + c_{ij+1}^{n+1})}{\Delta y^2} \quad (3.23)$$

In order to avoid the large computational volume required for the fully implicit scheme (retaining at the same time the qualifications of the implicitness) it is preferable to apply the ADI technique (Alternating Directions Implicit). According to this method the solution advances from time level n to $n+1$ using an implicit scheme along y and explicit along x, while alternately from $n+1$ to $n+2$, using an implicit scheme along x and explicit along y. The inductive formula takes the forms:

$$c_{ij}^{n+1} = c_{ij}^{n} - \frac{u\Delta t}{2\Delta x}(c_{i+1j}^{n} - c_{i-1j}^{n}) - \frac{v\Delta t}{2\Delta y}(c_{ij+1}^{n+1} - c_{ij-1}^{n+1}) + \frac{(\Delta t)D_x}{\Delta x^2}(c_{i+1j}^{n} - 2c_{ij}^{n} + c_{i-1j}^{n}) + \frac{(\Delta t)D_y}{\Delta y^2}(c_{ij+1}^{n+\frac{1}{2}} - 2c_{ij}^{n+\frac{1}{2}} + c_{ij-1}^{n+\frac{1}{2}}) \quad (3.24)$$

$$c_{ij}^{n+2} = c_{ij}^{n+1} - \frac{u\Delta t}{2\Delta x}(c_{i+1j}^{n+2} - c_{i-1j}^{n+2}) - \frac{v\Delta t}{2\Delta y}(c_{ij+1}^{n+1} - c_{ij-1}^{n+1}) + \frac{(\Delta t)D_x}{\Delta x^2}(c_{i+1j}^{n+\frac{1}{2}} - 2c_{ij}^{n+\frac{1}{2}} + c_{i-1j}^{n+\frac{1}{2}}) + \frac{(\Delta t)D_y}{\Delta y^2}(c_{ij+1}^{n+1} - 2c_{ij}^{n+1} + c_{ij-1}^{n+1}) \quad (3.25)$$

This technique leads to the solution of IM algebraic systems in JM unknowns when advancing from n to $n+1$ and to the solution of JM

HAND OUT 23: Numerical schemes to solve the advection and diffusion equations (Chapter 7 of our syllabus).

SCHEMES

1) UPWIND:

$$\frac{C_i^{j+1} - C_i^j}{\Delta t} = -U \frac{(C_i^j - C_{i-1}^j)}{\Delta x}$$

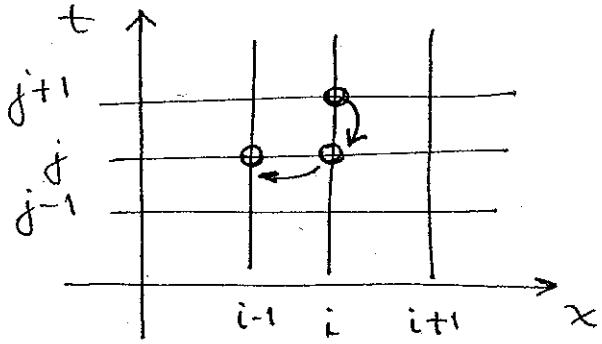

$$\Rightarrow \boxed{C_i^{j+1} = C_i^j \left[1 - U \frac{\Delta t}{\Delta x}\right] + \frac{\Delta t}{\Delta x} U C_{i-1}^j}$$

2) LEAP FROG

$$\frac{C_i^{j+1} - C_i^{j-1}}{2\Delta t} = -U \frac{(C_{i+1}^j - C_{i-1}^j)}{2\Delta x}$$

$$\boxed{C_i^{j+1} = -\frac{\Delta t}{\Delta x} U (C_{i+1}^j - C_{i-1}^j) + C_i^{j-1}}$$

3) LAX

$$\frac{C_i^{j+1} - \frac{(C_{i+1}^j + C_{i-1}^j)}{2}}{\Delta t} = -\frac{U}{2\Delta x}(C_{i+1}^j - C_{i-1}^j)$$

4) DIFFUSION:

$$\frac{C_i^{j+1} - C_i^j}{\Delta t} = D \left[\frac{C_{i+1}^j - 2C_i^j + C_{i-1}^j}{\Delta x^2}\right]$$

$$C_i^{j+1} = C_i^j \left[1 - 2\mathcal{D}\right] + \mathcal{D}\left[C_{i+1}^j + C_{i-1}^j\right]$$

where $\mathcal{D} = D\dfrac{\Delta t}{\Delta x^2}$